PHASE-TRAFFICKING METHODS IN NATURAL PRODUCTS, MODULATORS OF ORGANIC ANION TRANSPORTING POLYPEPTIDES FROM *ROLLINIA EMARGINATA*, AND PREGNANE AND CARDIAC GLYCOSIDES FROM *ASCLEPIAS SPP*.

BY

JUAN JOSE ARAYA BARRANTES

Submitted to the graduate degree program in Medicinal Chemistry and the Graduate Faculty of the University of Kansas in partial fulfillment of the requirements for the degree of Doctor of Philosophy.

_____

Chair

_____

_____

_____

_____

Committee members

Date Defended: _____

The Dissertation Committee for Juan Jose Araya Barrantes

certifies that this is the approved version of the following dissertation:

PHASE-TRAFFICKING METHODS IN NATURAL PRODUCTS, MODULATORS OF ORGANIC ANION TRANSPORTING POLYPEPTIDES FROM *ROLLINIA EMARGINATA*, AND PREGNANE AND CARDIAC GLYCOSIDES FROM *ASCLEPIAS SPP.*

_____

Chair

_____

_____

_____

_____

Committee members

Date approved:_____

ABSTRACT

Phase-Trafficking Methods in Natural Products, Modulators of Organic Anion Transporting Polypeptides from *Rollinia emarginata*, and Pregnane and Cardiac Glycosides from *Asclepias spp.*

Juan J. Araya Barrantes, Ph. D.

The University of Kansas, 2012

For decades, chemists and medicinal chemists have found in nature the source of inspiration for drug discovery and development. This work describes several aspects of the interaction between the fields of natural products and medicinal chemistry, from isolation and characterization of bioactive molecules to semi-synthetic analogs preparation.

A new phase-trafficking approach for acidic, basic, and neutral compounds separation from organic plant extracts was developed, validated and successfully applied to crude plant extracts. This new method could be applied to natural extracts of diverse origin in order to generate better quality samples for initial bioassays. Furthermore, this new catch-and-release methodology allowed the isolation and identification of three compounds new to the literature from the extensively studied ginger rhizomes.

Using a more traditional bioassay guided fractionation, we have identified six small-molecules from *Rollinia emarginata* that modulate organic anion transporting polypeptide´s (OATPs) function. The results of this study show that diverse plant materials are a promising source for the isolation of OATP modulating compounds, and that a bioassay-guided approach can be used

to efficiently identify selective OATP modulators. In addition, a ^{1}H NMR-based metabolomic approach was used as a dereplication tool to study the effect of aqueous green tea extracts on OATP1B1-mediated uptake of estrone-3-sulfate. Our findings suggested that not only the gallate catechins were important for the observed uptake inhibition, but also compounds theogalline and 3-*p*-cumaroyl quinic acid could have been involved.

A screening against breast cancer cell line Hs578T was conducted with ten plant species from the Asclepiadaceae family and, based on our findings, three plants were selected for detailed investigation: *Asclepias verticillata*, *Asclepias syriaca*, and *Asclepias sullivantii*. As a result, a total of 46 compounds were isolated and identified, half of which represented novel structures. The isolates showed a wide variety of structures including pregnane and cardiac glycosides, pentacyclic triterpenes, glycosylated flavonoids and lignans, among others. Furthermore, a group of cardiac glycosides were found to have strong cytotoxicity selected breast cancer cell lines.

Finally, using a semi-synthetic approach, cardiac glycoside analogs with modifications in the butenolide ring were pursued in order to better understand their SAR. Starting from the commercially available *trans*-aldosterone, the cardiac glycoside core was built up using a microwave-promoted allylic oxidation using SeO_2 (Riley oxidation). In addition, a microwave-promoted Miyaura-Suzuki cross-coupling was utilized to obtain the desired 17β-aryl analogs.

ACKNOWLEDGEMENTS

During my time at the University of Kansas, I have been blessed with the support of my mentors, coworkers, friends, and family; without them this work would never have been possible. First, I would like to thank Professor Barbarara Timmermann who has been an extraordinary doctoral research advisor throughout these years. She has been a constant source of guidance and encouragement and I am immeasurably grateful. I am also greatly thankful to the faculty of the department of Medicinal Chemistry and Chemistry at the University of Kansas who have shown to me the wonderful world of Medicinal Chemistry. Professor Thomas Prisinzano, in particular, had opened the doors of his laboratory where I have been able to learn the "tweaks and tricks" of organic synthesis. I would like to give special thanks to Professor Lester Mitscher as I was tremendously fortunate to work on one of his many brilliant research ideas. I also thank Professors Barbara Timmermann, Lester Mitscher, Thomas Prisinzano, Bruno Hagenbuch, and Kelly Kindscher for graciously serving as members of my oral examination committee.

I thank Dr. David VanderVelde (now at California Institute of Technology), Dr. Justin Douglas, and Mrs. Sarah Neuenswander from the Nuclear Magnetic Resonance facilities for providing an outstanding service and always offering a helping hand. Also, I would like to thank Dr. Todd Williams and the personnel at the Mass Spectrometry Laboratory as well as Dr. Victor Day from the X-Ray Crystallography Laboratory for their invaluable help in my research work. I have to thank Dr. Peter McDonald from the High-Throughput Screening Laboratory for conducting all the cytotoxicity assays and providing me great insight into the cellular-based

bioassays. Last but not least, I need to thank Jane Buttenhoff, Norma Henley, William Orth, Stuart Mills, Grace Hutchins, and Revellia Rasmussen in the Department of Medicinal Chemistry for dealing with all administrative issues related with this project.

The members in the groups of Professors Timmermann and Prisinzano as well as my fellow graduate students have helped and inspired me in my studies. Especially, I thank Dr. Huaping Zhang for his mentorship and guidance during my research.

Financial support is has been provided by the National Institutes of Health (NIH) ICBG grant 5 UO1 TW000316, NCCAM/ODS grant 1R21AT004182-01A2; University of Kansas Center for Research project 2506014-910/099; and the Kansas Bioscience Authority (KBA) and Center for Heartland Plant Innovations (HPI) grant IND0061464. Also, I personally thank the Fulbright-LASPAU fellowship and the University of Costa Rica for partially supporting my studies.

Finally, I need to give my gratitude to my family and friends. My parents, far away in Costa Rica, have taught me values that helped me succeed including perseverance and responsibility. My friends in Lawrence became family away from home; their support was vital during this journey. I also whish to thank my wife and best friend, Angie, for her love, patience, and support who gave up everything to join me in this adventure and the last five years have been undoubtedly the best time of our lives as we were blessed with the arrival of our beloved son, Jose Pablo.

To Angie and Jose Pablo

TABLE OF CONTENTS

LIST OF FIGURES

CHAPTER 1

CHAPTER 2

CHAPTER 4

LIST OF TABLES

CHAPTER 1

CHAPTER 2

CHAPTER 3

CHAPTER 4

LIST OF COMPOUNDS

CHAPTER 2

CHAPTER 3

CHAPTER 4

CHAPTER 5

ABBREVIATIONS

Ac_2O	Acetic anhydride
AUC	Area under the curve
BuLi	*n*-Butyl lithium
BuOH	*n*-Butanol
CC	Column chromatography
CCC	Counter current chromatography
CBD	Convention on biological diversity
CoA	Coenzyme A
DAHP	D-Arabino-heptulosonic acid 7-phosphate
DMAAP	Dimethylallyl diphosphate
DMAP	4-Dimethylaminopyridine
E3S	Estrone-3-sulfate
E17β	Estradiol-17β-glucuronide
EC	Epicatechin
ECG	Epicatechin gallate
EGC	Epigallocatechin
EGCG	Epigallocatechin gallate
EtOAc	Ethyl acetate
ESIMS	Electron spray ionization mass spectrometry

HMG-CoA	β-Hydroxy-β-methylglutaryl coenzyme A
HPLC	High-pressure liquid chromatography
HRMS	High-resolution mass spectrometry
HTS	High-Throughput Screening
IPP	Isopentenyl diphosphate
IR	Infra Red
KHMDS	Potassium bis(trimethylsilyl)amide
K_m	Apparent substrate affinity
LDA	Lithium Diisopropyl Amide
MeOH	Methanol
MW	Microwave
MS	Mass Spectrometry
NADPH	Nicotinamide adenine dinucleotide phosphate
NCE	New chemical entity
NF-κB	Nuclear factor kappa B
NMR	Nuclear Magnetic Resonance
OATPs	Organic Anion Transporting Polypeptides
PEP	Phosphoenol Pyruvate
PhNTf2	N-Phenylbis(trifluoromethanesulfonimide)
R_f	Retention factor
R_t	Retention time
RT	Room temperature

SEC	Size-Exclusion Chromatography
SLC	Solute carrier class
SLCO	Solute carrier organic anion transporter
SPE	Solid-phase Extraction
SSR	Solid-supported reagents
THF	Terahydrofurane
TIC+	Total ion current positive mode
TLC	Thin-layer chromatography
TMSCl	Trimethylsilylchloride
TMSOTf	Trimethylsilyl trifluoromethanesulfonate
TNF	Tumor necrosis factor
UV-Vis	Ultra violet-visible
V_{max}	Maximal rate of transport

1. INTRODUCTION

1.1. Relevance of natural products in medicinal chemistry

Nature has provided humanity with a large number of medicines for the treatment and prevention of multiple diseases. In fact, medicinal plants have been used since ancient times to treat ailments in traditional medicine systems like Chinese Materia Medica (1100 BCE) and Indian Ayurveda (1000 BCE).[1] According to data from the World Health Organization, in some Asian and African countries as much as 90% of the population still rely on traditional medicine in primary healthcare.[2] In the US, more than 40% of the population has reported the use complementary or alternative medicine at least once.[2] Furthermore, the global herbal supplements and remedies market is forecasted to reach US$ 93.15 billion by 2015 despite the recent world's economical recession.[3] Therefore, it is not surprising that natural products have impacted directly or indirectly over 50% of the new chemical entities (NCEs) developed over the past four decades (Figure 1-1). Interestingly, this figure increases to 70% if only anti-infective agents are taken into consideration and 80% corresponds to anti-cancer agents alone.[4, 5]

The history of medicinal chemistry and drug discovery are closely related to the purification of active principles from medicinal plants. Prior to the 1800s, remedies were prepared mostly from whole plants and no pure entities or drugs were available with the exception of some minerals. However, at the beginning of the 19th century, many theorists started clamoring for a switch to pure substances instead of the highly variable quality of extracts and tinctures used to that date.[1] Probably the most famous examples are the opium poppy and morphine (Figure 1-2). Opium poppy (*Papaver somniferum* L.) has been used for millennia as a sedative, however it was not until 1814 when Jean-Francois Derosne in France and Friedrich Sertürner in Germany independently reported the isolation of its active component, morphine.[6] After the isolation of

morphine, it took more than 100 years to fully elucidate its structure,[7, 8] 30 additional years to confirm the structure by synthesis,[9] and an additional 20 years until the discovery of the opioid receptors in the brain and the endogenous opioids called endorphins.[10, 11] Throughout the years, medicinal chemists have learned many lessons from morphine. For instance, the contemporary concept of pharmacophore can be recognized in the simpler analogs developed by reducing the complexity of morphine, showing that only a portion of the morphine molecule is required for its biological activity. Many of those analogs and derivatives are widely used in medicine today (Figure 1-3).[1]

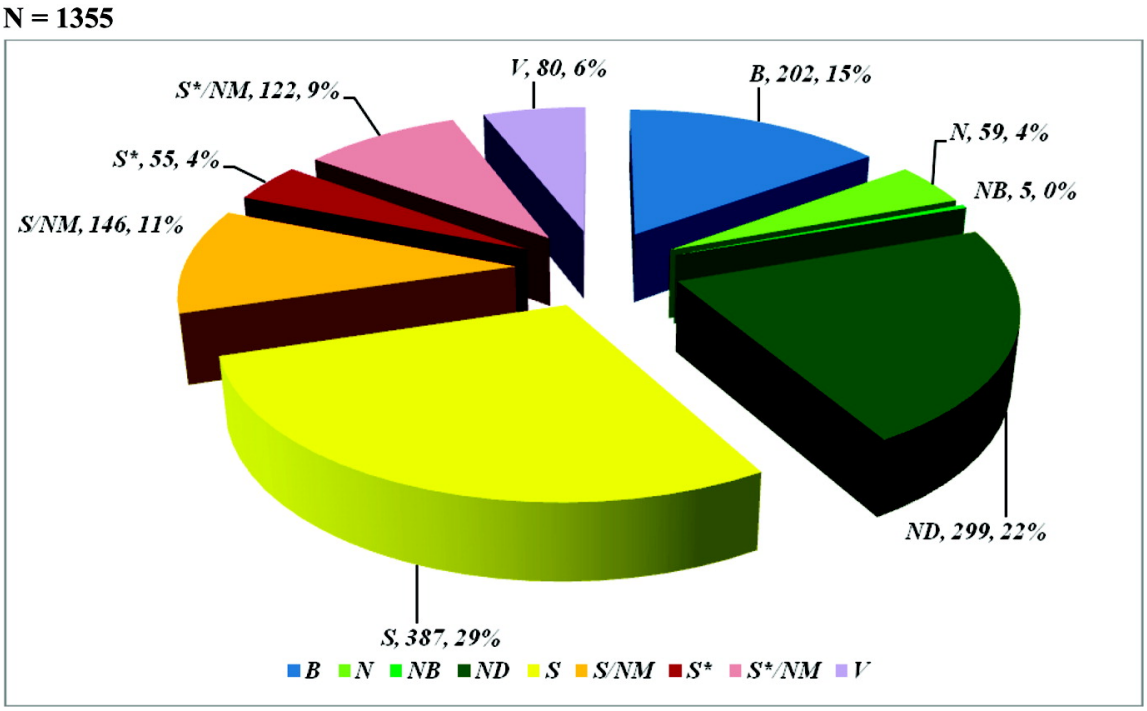

Figure 1-1 All new approved drugs 01/1981–10/2010 by category

B: Biological N: unmodified natural product, ND: modified natural product, NB: natural product "botanical", S: synthetic compound, S* and S*/NM: synthetic compound with natural product pharmacophore, S/NM: synthetic compound showing competitive inhibition of the natural product substrate. (Reprinted with permission from Cragg and Newman[12] Copyright 2012 American Chemical Society.)

In addition to morphine, countless examples of medicinally useful natural products could be cited here ranging from anticancer agents like taxol and vinblanstine to the lipid-lowering agent mevastatin. It is clear that natural products research has had a significant impact on medicinal chemistry.[13] As accurately described by Carter[14] "natural products that are discovered as leads in screening may well serve as the starting point for medicinal chemistry programs aimed at enhancing their biological profiles".

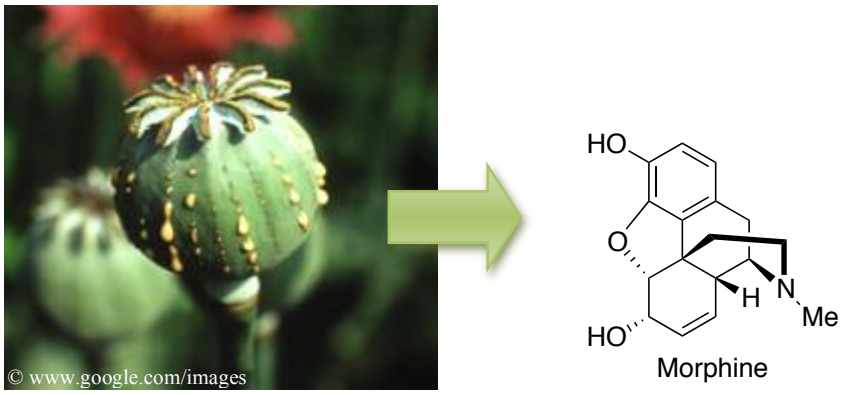

Figure 1-2 The opium poppy (left) and structure of morphine (right)

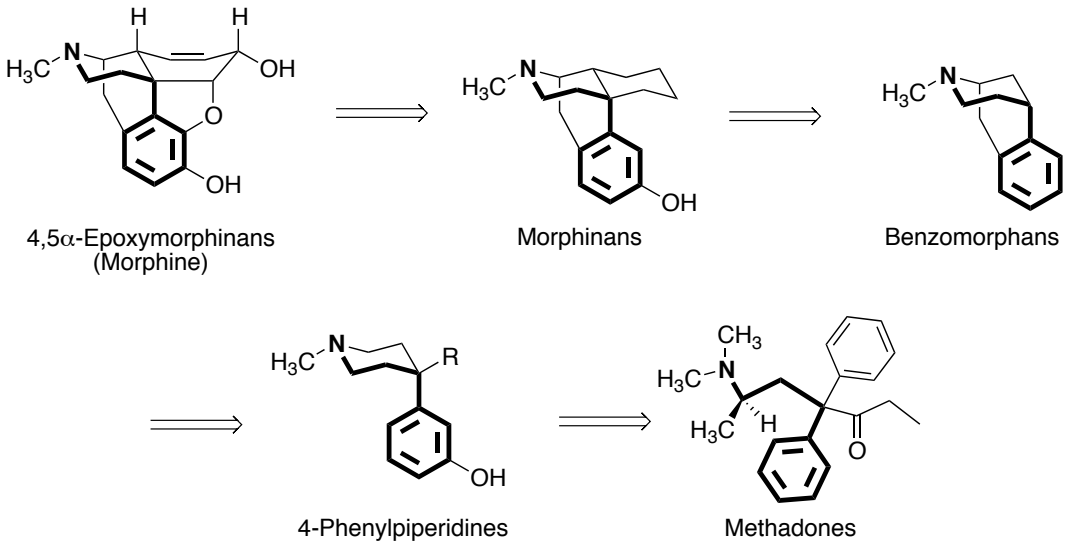

Figure 1-3 Examples of drug classes derived from morphine by rational structural modifications showing the pharmacophore with bolded atoms

1.2. Natural products-based drug lead discovery

As previously mentioned, nature has been and continues to be one of the best sources of biologically active compounds. In fact, only a small portion of the World's biodiversity has been explored for biological activity. For example, plants are probably the most studied organisms to date, and it is estimated that only 5-15% of the approximately 300,000 species have been systematically investigated from their chemical and pharmacological perspective.[15, 16] Furthermore, reinvestigation of previously studied plants using modern techniques, continues to produce new bioactive metabolites.[17, 18]

There are several characteristics that make natural products so attractive for drug discovery including their chemical complexity and diversity and their high biological target selectivity and specificity. However, natural compounds present less desirable characteristics as they are usually present in small quantities in the producing organism, have poor drug-likeness, and show difficult synthetic accessibility.[19] Despite the unquestionable importance of natural products as sources of new drugs and leads, natural-products based research and discovery (R&D) programs in many big pharmaceutical industries have been significantly reduced or shutdown replacing it with combinatorial chemistry-based drug discovery programs.[19] Hence, there are important issues that must be addressed for a successful drug discovery campaign based on natural products of plant origin (Figure 1-4) and those are listed in the following sections.[17]

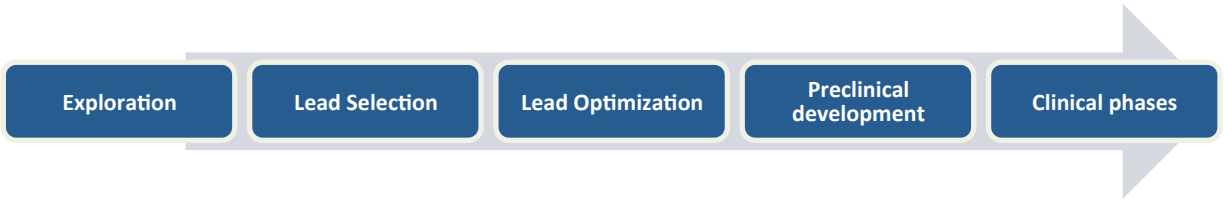

Figure 1-4 The drug discovery process workflow

1.2.1. Biomass procurement: selection, collection, and identification

The first step in any natural products-based drug discovery program is to choose and obtain the plant material. Therefore, proper sample selection using ethnopharmacologic, chemotaxonomic, and geographic criteria is fundamental.[20, 21] In addition, detailed information about the sample collection must be recorded including identification of the organism to the species level by a taxonomist, its geographical location, collection date, and a deposit of voucher specimen in a recognized herbarium as reference material.[22] This information is very important for scaling-up purposes as secondary metabolites tend to vary geographically and seasonally, even within samples of the same species.[17] In summary, a careful selection, collection, and identification can provide a reliable source of biomass in order to guarantee access to a potential lead structure for medicinal chemistry modifications, target validation, and *in vivo* studies.

Finally, after the Rio de Janeiro Convention on Biological Diversity (CBD) in 1992 and other documents like the US National Cancer Institute's Letter of Collection, biomass collections now require provisions for the country of origin to be equitably compensated for the use and commercialization of its biomass.[23, 24] In addition, the permits for access, collection, and export in developing countries are usually difficult to obtain. Finally, ethnopharmacological and traditional knowledge of indigenous people in the use of medicinal plants must be recognized and rewarded in case of an economical benefit and commercialization.[25, 26]

1.2.2. Extraction

Extraction methods strongly depend on the nature of the sample and the targeted compound or compounds. Typically, an extraction protocol involves the drying and grinding of plant material

followed by extraction with a solvent or mixture of solvents. The solvent choice should consider the polarity and solubility of the targeted compound or compounds. Also, several extraction methods are available including maceration at room temperature, boiling, soxhlet, supercritical fluid extraction, sublimation, and steam distillation. The choice of extraction method depends, among others, on the stability, desired purity, quantity, and physical and chemical properties of the targeted compounds.[17] In addition, tannins and complex carbohydrates should be removed early in the process either by classic liquid/liquid partition or solid-phase extraction using polyamide in order to avoid interference with *in vitro* assay systems.[27]

1.2.3. Screening

Bioassays use a biological system to detect properties of a sample that can be a pure compound or a complex mixture. They could involve *in vivo* systems (whole organism), *ex vivo* systems (isolated tissues or organs) as *in vitro* systems (cultured cells). *In vitro* systems are by far the most popular choice for initial screening assays due to their low cost, high speed, and throughput formatting. The biological assay of natural products is often not a simple task, especially during the initial separation stages. A number of variables need to be considered when conducting biological testing of natural products, including the selection of a suitable solvent that can dissolve or suspend the sample but which does not interfere with the assay, acidic or basic nature of the samples, positive and negative controls, and sensitivity of the assay to detect components in a very low concentration. In the last few decades, advances in high throughput screening (HTS) have impacted natural products research due to the miniaturization and automation of the bioassay process as well as the development of robust, specific, and more sensitive assays.[17]

1.2.4. Bioassay-guided fractionation and isolation

The isolation of the bioactive components from a complex extract obtained from plant material is not an easy task, especially if the active constituent is present in very low amounts. Consequently, there is not a single separation technique that can be applied, instead a number of fractionation steps are available and each depends on the characteristics of a given extract or fraction. Initially, the crude extract is separated into various fractions containing simpler mixtures of compounds with similar polarity or molecular size. Fractionation then relies on methods like liquid/liquid partition, column chromatography (CC), size-exclusion chromatography (SEC), solid-phase extraction (SPE), and others.[17] Subsequently, more selective purification steps typically follow and are done in a smaller scale and using better resolution techniques such as medium pressure column chromatography, reverse- and normal-phase automatic flash chromatography, and high-pressure liquid chromatography (HPLC).[17] Despite the technique or techniques used during the fractionation and purification processes of a given extract, a reliable bioassay allows the following of desired activity throughout the separation steps to the pure bioactive compounds.

1.2.5. Dereplication

Dereplication comprises the identification, partial or total, of a natural product without its separation from the original matrix. By this method, the novelty of structures present in a biologically active extract can be assessed, hence giving valuable information to move forward during an investigation project.[28] A successful dereplication strategy can increase the screening throughput and enhance the number of novel compounds identified. Several strategies to achieve

this goal have been applied using modern separation and spectroscopic technologies such as hyphenated techniques and multivariate analysis.[17] The earlier includes techniques like HPLC-MS, HPLC-NMR, GC-MS, and other variants that combine the use of powerful separation equipment with an informative spectroscopic tool.[29, 30] The multivariate analysis involves a metabolomic approach that aims to analyze the whole initial or partially purified crude mixtures by means of a statistical comparison of complex spectroscopic data to reveal the presence of relevant metabolites.

1.2.6. Structure elucidation

The structure elucidation of natural products depends strongly on modern spectroscopic and spectrometric methods including high-field nuclear magnetic resonance (NMR) and high-resolution mass spectrometry (HRMS). Often these techniques give enough information to unambiguously assign the structure of a new compound, however ultraviolet-visible (UV-Vis), infrared spectroscopy (IR), and physical properties like melting point and optical rotation corroborate and support a proposed structure. In addition, X-ray crystallography is a powerful technique when crystallization of the sample to a good quality crystal is possible.[31]

1.3. Secondary metabolism in plants

Proteins, carbohydrates, fats, and nucleic acids are often called "the molecules of life" because they are common to most life forms on our planet. Hence, such molecules are collectively described as primary metabolites and they are result of primary metabolism. In contrast, there are metabolic routes and compounds that have a much more limited distribution in nature and are often genus- or family-specific. These types of specialized compounds are called secondary metabolites and they represent most of the pharmacologically active natural products. Usually, secondary metabolites are derived from a selected number of biogenetic routes that are shared by many organisms. Some of the relevant biological routes for the compounds isolated in the present study are described next.[32, 33]

1.3.1. The shikimate pathway

The shikimate pathway (Figure 1-5) is employed only by microorganisms and plants and produces aromatic compounds. Shikimic acid is the main intermediate in the pathway and was originally isolated from plants of *Illicium* genus (Japanese "shikimi"). The phenylpropane unit produced by this route is the basic building block found in many natural products like cinnamic acids, coumarins, lignans, and flavonoids. Furthermore, shikimic acid is currently the starting material for the synthesis of the antiviral agent oseltamivir (Tamiflu®), first line drug against avian influenza, and its main source is the star anise (*Illicium verum*).[32, 33]

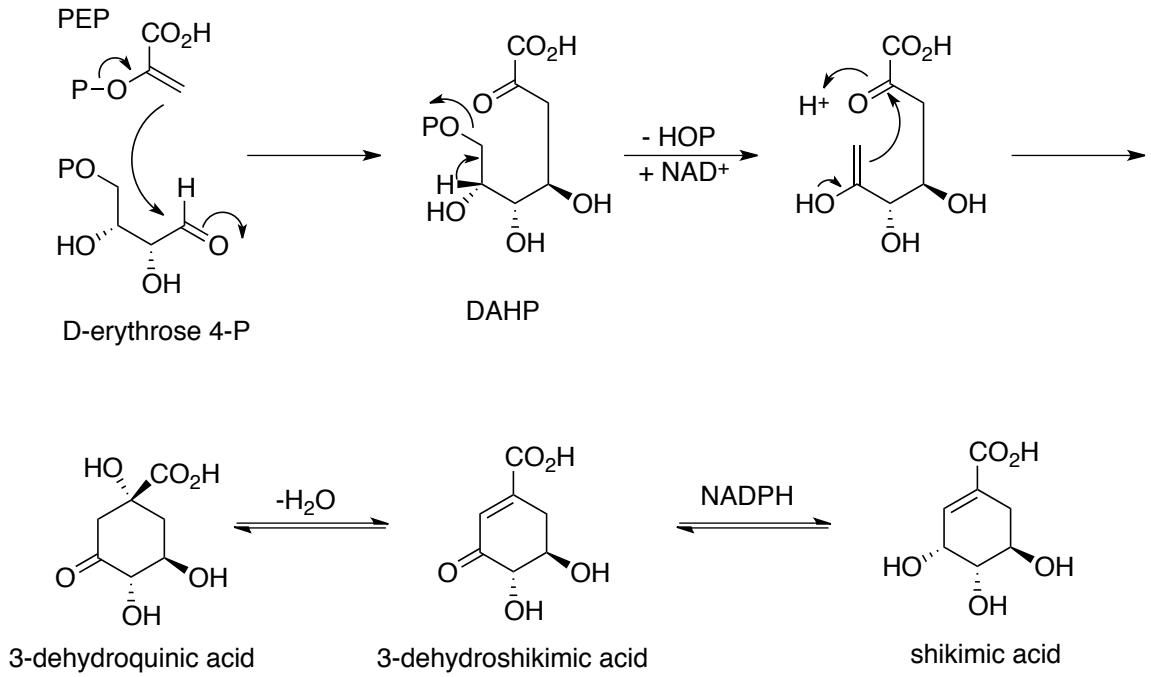

Figure 1-5 Biosynthesis of shikimic acid from phosphoenol pyruvate (PEP) and D-erythrose 4-phosphate (DAHP: D-arabino-heptulosonic acid 7-phosphate)

1.3.2. The mevalonate and the methylerythriol phosphate pathways

Terpenoids are probably one of the largest and most structurally diverse group of natural products. They are derived from five carbon units called "isoprene units" and joined together in diverse numbers and fashions. The terpenoids are classified according to the number of isoprene units present in their structures as hemiterpenes (1 unit), monoterpenes (2 units), sesquiterpenes (3 units), diterpenes (4 units), sesterterpenes (5 units), triterpenes (6 units), tetraterpenes (8 units), and polyterpenes (*n* units). The basic reactive isoprenic units in the terpenoids biosynthetic pathway are dimethylallyl diphosphate (DMAPP) and isopentenyl diphosphate (IPP) which are produced in the mevalonate (Figure 1-6) or the deoxyxylulose phosphate (Figure 1-7) pathways.[32, 33]

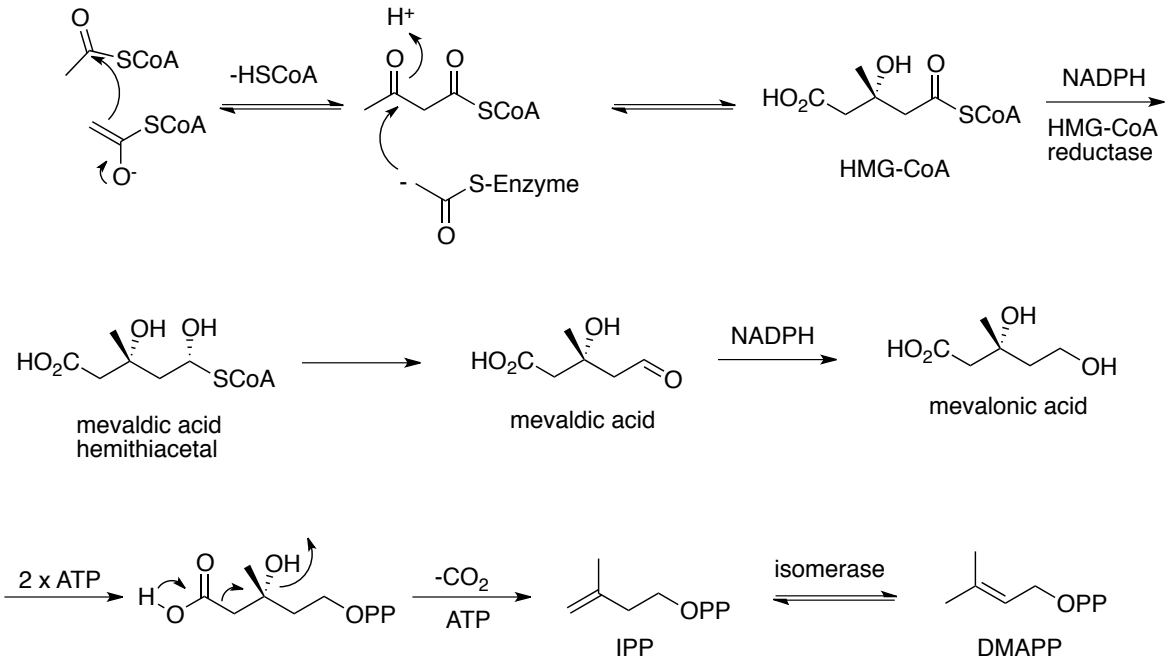

Figure 1-6 Biosynthesis of dimethylallyl diphosphate (DMAPP) in the mevalonate pathway (HMG-CoA: β-hydroxy-β-methylglutaryl coenzyme A, IPP: isopentyl diphosphate)

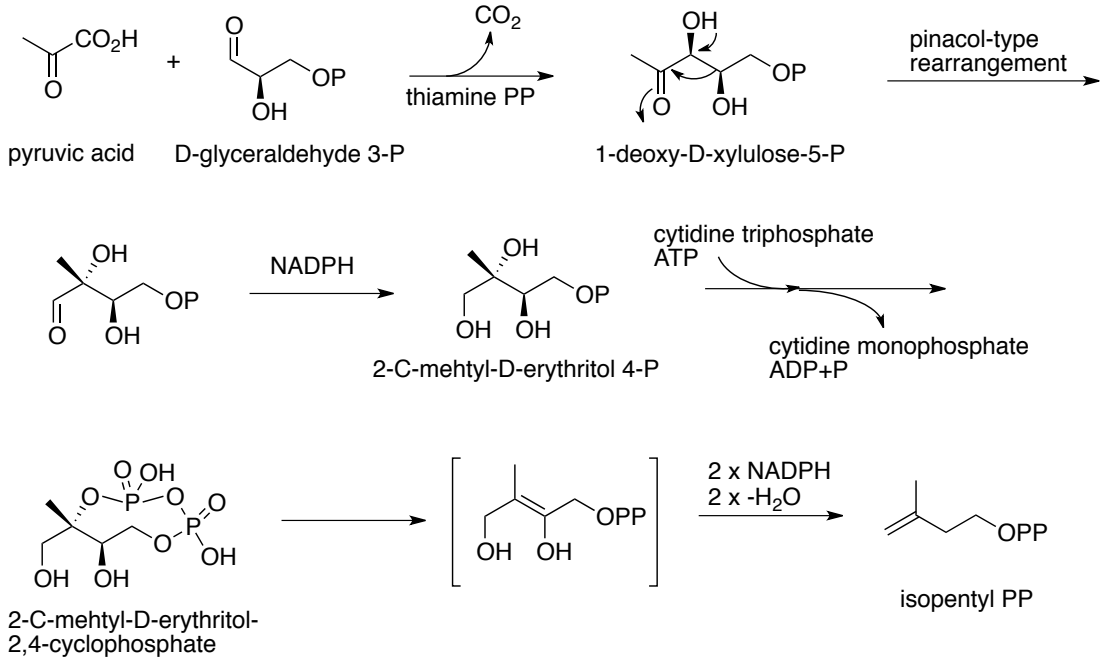

Figure 1-7 Biosynthesis of dimethylallyl diphosphate (DMAPP) in the deoxyxylulose phosphate pathway (IPP: isopentyl diphosphate)

1.3.3. The acetate pathway

The polymerization of acetate units and subsequent modifications give origin to a wide variety of compounds ranging from simple fatty acids to complex polyketides. Nature utilizes a series of Claisen-type reactions between acetyl-CoA or malonyl-CoA units to form poly-β-keto chains that can follow different biosynthetic routes (Figure 1-8). The polyketides constitute a large and diverse class of natural products that include simple phenols, anthraquinones, flavonoids (Figure 1-9), flavonones, chalcones, macrolides, and polyethers. Cannabinoids from *Cannabis sativa*, the anticancer doxorubicin and antibiotic erythromycin are some representative examples of medicinal-relevant acetate-pathway derived metabolites.[32, 33]

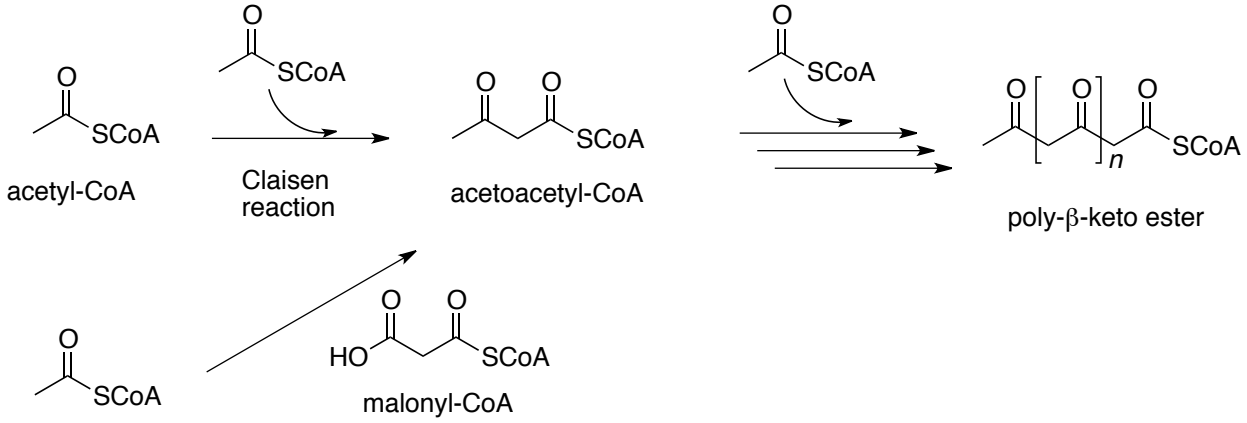

Figure 1-8 Basic polymerization reaction in the acetate pathway

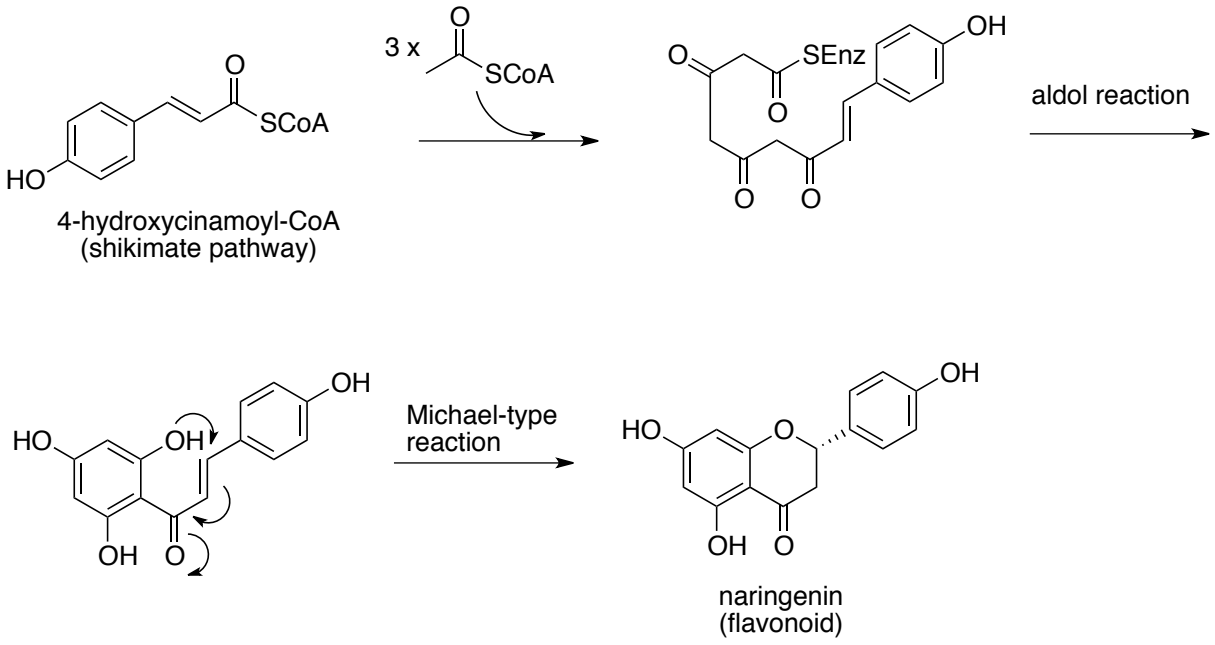

Figure 1-9 Biosynthesis of flavonoids: a shikimate-acetate mixed pathway

Cardiac glycosides are biosynthetically derived form the mevalonate and the acetate pathways (Section 1.4.1) and this important group of bioactive natural products will be discussed in detail in the following sections because a number of cytotoxic cardiac glycosides were isolated as part of this work from the *Asclepias* species (Chapter 4). Therefore, an extended background about this type of compounds is offered next.

1.4. Cardiac glycosides

Cardiac glycosides have been used during decades to increase heart force contractions.[34] This group of compounds was initially identified from the poisonous foxglove (*Digitalis purpurea* L.) plant, however a wide variety of structures showing similar pharmacological properties have been identified from other plant species (Table 1-1) and from toads of the *Buffo* species as well. Structurally, cardiac glycosides comprise a steroidal core with an unsaturated lactone ring at the 17-position and often posses a sugar moiety at the 3-position (Figure 1-10). Unlike steroidal hormones, cardiac glycosides are characterized by the *cis*-*cis* fusion of A/B and C/D rings, but *trans*-*cis* stereochemistry can be found in compounds from the Asclepiadaceae plant family (Figure 1-11). In addition, the lactone ring at the 17-position can be a γ-butenolide or α-pyrone ring, giving origin to two major subgroups called cardenolides and bufadienolides respectively (Figure 1-10).[32]

Table 1-1 Plant sources of cardiac glycosides*

Family	Genera	Main cardenolides
Apocynaceae	*Nerium, Acakanthera, Strophantus, Thevetia, Cerbera*	Oleandrin, neriin, neriantin, odoroside A and B, ouabain, cymarin, sarmentocymarin, periplocymarin, K-strophantin, thevetin
Asclepiadaceae	*Calotropis, Asclepias, Periploca, Xysmalobium, Gomphocarpus, Pregularia, Leptadenia*	Periplocin, strophantidin, strophantidol, nigrescin, uzarin, gomphoside, calotropin, calctin, vorucharin, uscharin, 2"-oxovurscharin
Brassicaceae	*Cheiranthus*	Chiroide A, cheirotoxin
Celastraceae	*Euonymus*	Eunoside, euobioside, euomonoside
Fabaceae	*Coronilla*	Alloglaucotoxin, corotoxin, coroglaucin
Moraceae	*Antiaria*	Antiarin
Scrophulariacae	*Digitalis*	Digitoxin, gitoxin, gitalin, digoxin, F-gitoin, digitonin, lantanoside A-C
Crassulaceae	*Kalanchoe, Tylecodon, Cotyledon, Bryophyllum*	Lancetoxin A-B, kalanchoside, bryotoxin A-C, bryophyllin B, cotiledoside, tyledoside A-D
Iridaceae	*Moraea, Homeria*	Scillirosidin and bovogenin A derivatives
Liliaceae	*Convalaria, Urginea, Bowiea*	Scillarene A-B, scilliroside, scillarenia, scillia-cinoside, scilligaucoside, proscillaridin A
Melianthaceae	*Melianthus, Bersama*	Melianthusigenin, bersenogenin, berscillogenin
Ranunculaceae	*Helleborus, Adonis*	Helleborein, helleborin, hellebrin, helebrigenin, adonidin, adonin, cymarin, cymarin, adonitoxin
Santalaceae	*Thesium*	Thesiuside

* Adapted from Newman *et al.*[35] and Mijatovic *et al.*[36]

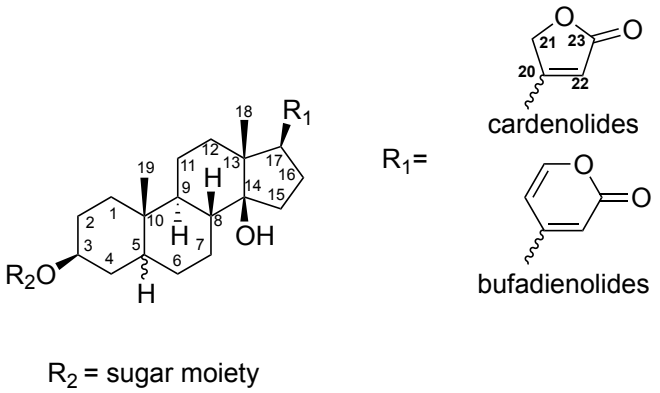

Figure 1-10 General structures of cardenolides and bufadienolides

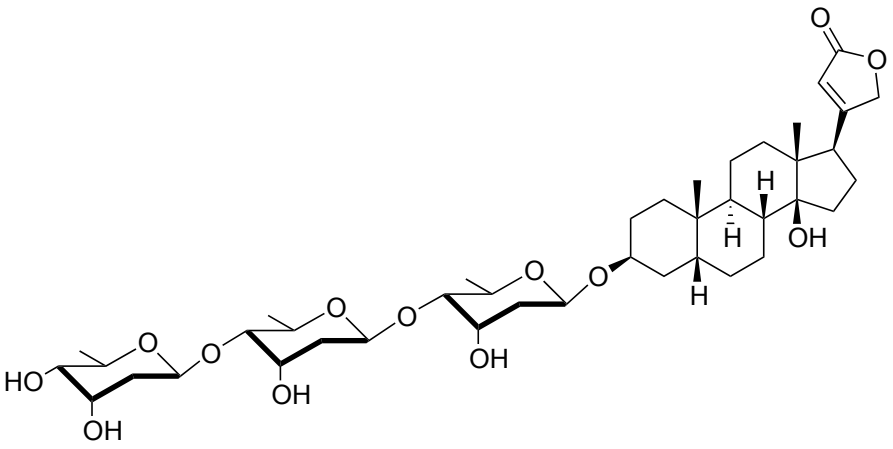

Digitoxin

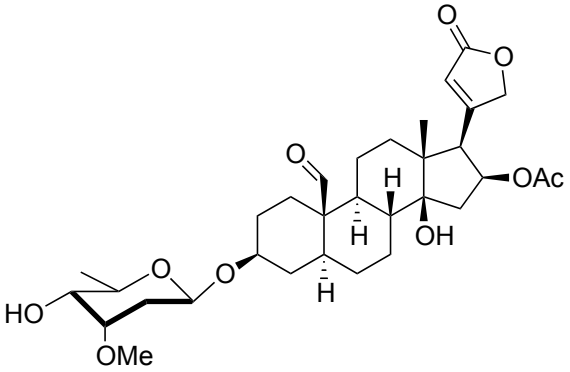

Oleandrin

Figure 1-11 Structures of digitoxin and oleandrin

1.4.1. Biosynthesis of cardiac glycosides

Cardiac glycosides are biosynthesized from cholesterol by a series of steps including shortening of the side-chain to a two-carbon α-mehtylketone group, hydroxylation and epimerization reactions, and incorporation of two or three carbons to form cardenolides or bufadienolides respectively (Figure 1-12).[32] Therefore, it is considered that pregnanes are intermediates in this biosynthetic pathway. In fact, a large number of plant steroids have been described including progesterone.[37]

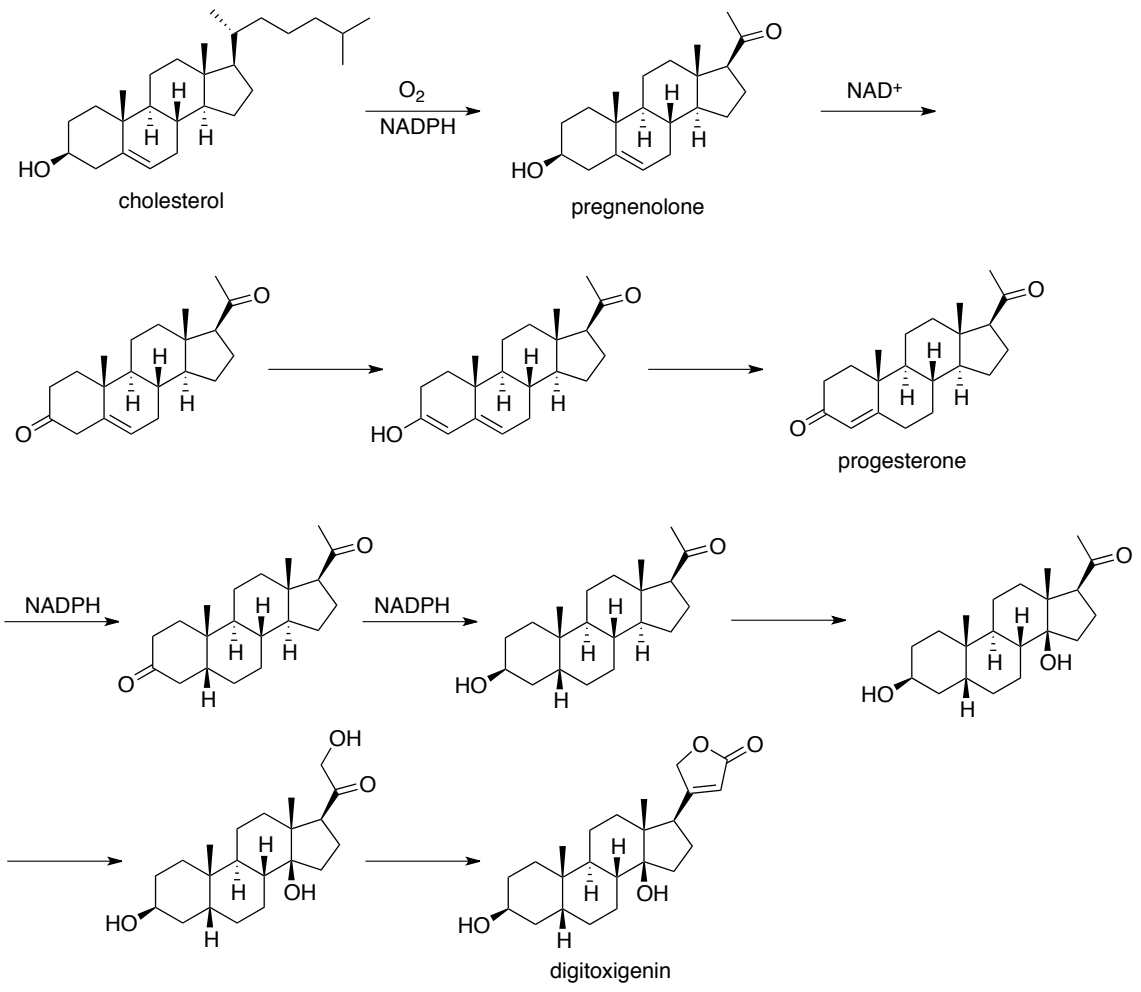

Figure 1-12 Proposed biosynthetic pathway of cardiac glycosides

1.4.2. Biological activity of cardiac glycosides

The mechanism of action of cardiac glycosides was discovered by Schatzmann and colleagues in 1965 as specific inhibitors of the Na^+,K^+-ATPase.[38] The Na^+,K^+-ATPase is a ubiquitous membrane protein responsible for keeping the cellular membrane potential by actively transporting two potassium ions into and three sodium ions out of the cell using energy from ATP hydrolysis. The increasing of the force in the cardiac muscle contraction is produced when inhibition of the Na^+,K^+-ATPase by the cardiac glycosides raises the level of sodium ions in cardiac myocites. As a result the activity of the Na^+,Ca^{2+} exchanger is reduced and the intracellular concentration of Ca^{2+} is increased leading to a higher contraction (positive ionotropic effect).[39] In recent years, studies have shown that Na^+,K^+-ATPase is not only a membrane transporter but also a signal transducer that is triggered upon binding of cardiac steroids (Figure 1-13). The multiple downstream signals have implications in the regulation of cell growth,[40] cell motility,[41] and apoptosis.[42] Furthermore, endogenous cardiotonic steroids have been discovered as a novel group of hormones and the biological processes that they regulate are being actively investigated; some include regulation of renal sodium transport, arterial pressure, cell growth, differentiation, apoptosis and fibrosis, modulation of immunity and carbohydrate metabolism, and control of various central nervous functions including behavior.[43, 44]

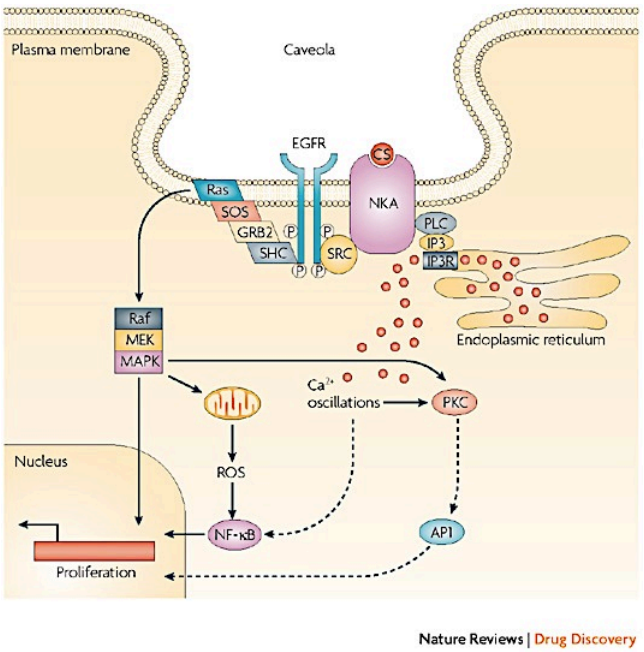

Figure 1-13 Signal transduction role of the Na^+,K^+-ATPase (Reproduced with permission from Prassas and Diamanis[45] Copyright 2012 Nature Reviews Drug Discovery.)

1.4.3. The Na^+,K^+-ATPase

The Na^+,K^+-ATPase belongs to the P-type family of cation pumps. The X-ray crystal structure at 3.5 Å resolution has been published (Protein Data Bank number 3A3Y).[46] Structurally, the Na^+,K^+-ATPase is an oligomer composed of at least two subunits: α and β. The α-subunit bears binding sites for Na^+, K^+, Mg^{2+}, ATP, and a highly conserved cardiac glycoside binding site. In addition the α-subunit also contains regulatory sites modulated by phosphorylation. Meanwhile, the β-subunit has a regulatory chaperone-like activity facilitating the recruitment of the α-subunit to the plasma membrane and for the occlusion of potassium ions. There are four α- and three β-subunit isoforms identified and all possible combinations lead to catalytically competent enzymes. In addition, a third subunit type, the FXYD regulatory transmembrane protein family, can be associated with functional Na^+,K^+-ATPase in certain cell types.[47] The most common

oligomer is α1β1, which is expressed widely unlike other combinations that are more restricted to certain tissues. Interestingly, the subunit α4 is exclusively expressed in testes and spermatozoids and it has recently been postulated as a viable target for male contraception drug development.[48, 49]

The Na^+,K^+-ATPase has a conserved binding site for cardiac glycosides. These types of compounds inhibit the pump activity by interacting with the cellular surface binding "groove" composed of multiple functional groups in the α-subunit mainly (Figure 1-14).[50] Several groups have published studies on the binding mode of cardiac glycosides to the Na^+,K^+-ATPase.[51-54]

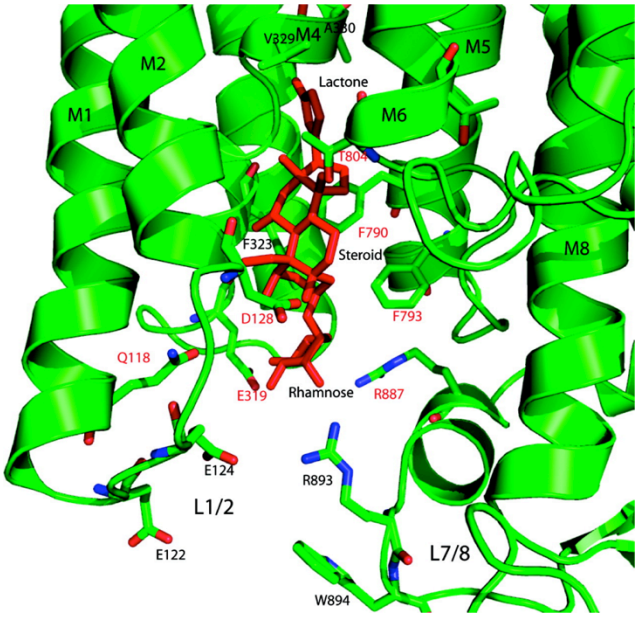

Figure 1-14 The Na^+,K^+-ATPase binding site for cardiotonic steroids. Ouabain is shown in skeletal formula (Reproduced with permission from Cornelius and Mahmmooud[54] Copyright 2012 American Chemical Society.)

1.4.4. Cytotoxic properties of cardiac glycosides

Cytotoxic properties of cardiac glycosides were reported more than four decades ago.[55] However, the narrow therapeutic window shown by these agents has been considered an impossible hurdle to overcome. Nevertheless, after Stenkvist *et al.*[56-58] observed a reduced mortality and more benign morphology on breast cancer patients taking digitalis compared to control, the interest for the potential anticancer applications of this type of compounds started to grow. In fact, it is now established that cardiac glycosides can induce apoptosis and inhibit growth of cancer cell lines.[39, 59-62] The *in vitro* and *in vivo* antiproliferative effect of cardenolides, bufadienolides, and semi-synthetic derivatives have been demonstrated against several cancer cell lines including breast, ovarian, prostate, melanoma, lung, leukemia, neuroblastoma, renal adenocarcinoma, lymphoma, and hepatocellular cancer cell lines.[63-69] Although the mechanism of action of this type of compound has not been elucidated, there are several hypotheses that are summarized in the Table 1-2.

As mentioned in the previous section, the signaling pathways triggered by the Na^+,K^+-ATPase upon binding of cardiac glycosides have just started to be understood, but it is clear that the signaling cascades have not the same final responses in cancer when compared to normal cells. Consequently, a differential expression and activity of the Na^+,K^+-ATPase subunits in tumor cells compared with normal cells has been postulated. In fact, expression profiles of the subunits of Na^+,K^+-ATPase have been demonstrated in bladder, gastric, colorectal and non-small-cell lung cancer cell lines.[43, 45]

Table 1-2 Proposed cytotoxicity mechanisms-of-action for cardiac glycosides

Entry	Mechanism
1	Alterations in the homeostasis of K^+, Na^+ and Ca^{2+}
2	Inhibition of TNF/NF-κB pathway[70]
3	Alteration of gene expression profiles[71]
4	Increased level of p21[72]
5	Alterations in membrane fluidity[72]
6	Increased expression of FasL[73]
7	Increased production of ROS[74, 75]
8	Increased regulation of DR4 and DR5[70]
9	Inhibition of glycolysis[76]
10	Inhibition of topoisomerase II[77]

Despite the increased number of scientists investigating in this field, only one new drug candidate has reached clinical trials: the semi-synthetic derivate UNBS1450 obtained from the plant *Calotropis procera* (Figure 1-15).[78] The regulatory role of UNBS1450 for several signaling pathways involving proliferation and cell death has been recently reported.[79, 80] In addition, a hot-water extract of *Nerium oleander*, Anvirzel™, was advanced to Phase I clinical trials in the US for cancer treatment, however no response was found.[81] In addition, the ouabain analog rostufuroxin (PST 2238) is currently undergoing Phase II trials as an antihypertensive agent.[82, 83] Finally, the classic cardiac glycoside digoxin is currently in Phase II clinical trials for prostate cancer.[84, 85]

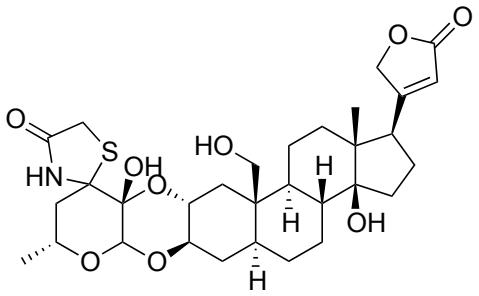

UNBS1450

Figure 1-15 Structure of UNBS1450 currently in phase I clinical trials

1.4.5. Structure-activity relationships of cardiac glycosides

The relationship between the structure of cardiac glycosides and their inhibition of the Na^+,K^+-ATPase has been described in detailed.[86] However, the structural features that trigger the signaling cascade without affecting the pumping function of the Na^+,K^+-ATPase are not equally clear. The sugar moiety of the classic cardenolides has been studied by neoglycorandomization and glycorandomization, showing that reduction of the potential cardiotoxicity and enhancement of cytotoxicity toward malignant cells is, indeed, possible (Figure 1-16).[87-89] Although modifications to the steroidal core have not been explored as exhaustively as the sugar moiety, useful information has been published in the last few decades and it is summarized in Figure 1-17.[90]

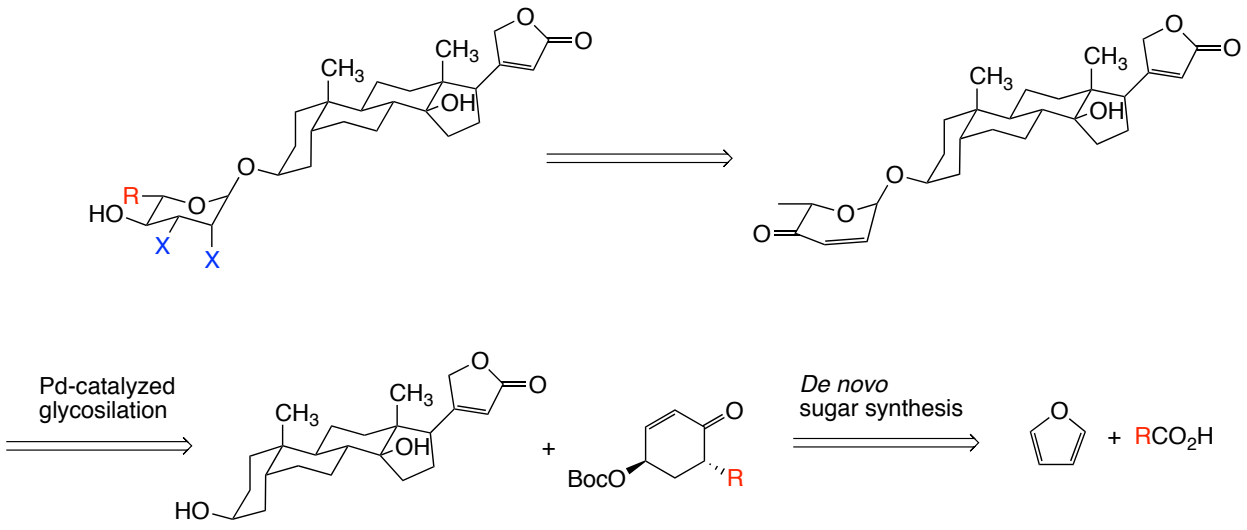

Figure 1-16 Glycorandomization approach for cardiac glycoside SAR studies

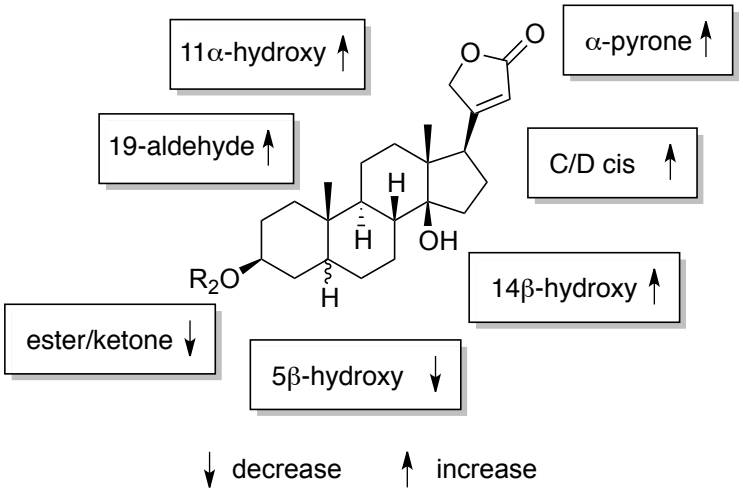

Figure 1-17 General SAR of cytotoxic properties of cardiac glycosides

Finally, one project described in this dissertation work involves the identification of natural products as modulators of organic anion transporting polypeptides (OATPs). Consequently, the last few sections of this chapter will be devoted to introduce the structure, function, and importance of these transporters.

1.5. Organic anion transporting polypeptides (OATPs)

Organic anion transporting polypeptides (OATPs) are membrane transport proteins that belong to the solute carrier (SLC) superfamily and are classified within the solute carrier organic anion transporter family (SLCO). OATPs mediate the active cellular influx of a variety of amphipatic compounds including bile salts, steroid conjugates, thyroid hormones, anionic oligopeptides, and several drugs and other xenobiotics. OATPs are selectively expressed in apical and basolateral membranes of polarized cells in the liver, kidney, intestine, and blood-brain barrier.[91] Absorption and distribution of drugs that are substrates of OATPs expressed in the intestinal enterocytes and the hepatocytes can be affected directly by OATP modulators. Furthermore, specific-tissue expression of OATPs can also affect the distribution of drugs due to interactions with these transporters. In fact, inhibition of OATPs can lead, at least partially, to drug-drug and food-drug interactions.[92-94] More recently, altered expression of certain OATPs in cancer cells has been linked with resistance in some types of cancers.[95, 96]

1.5.1. Structure of OATPs

OATPs are transmembrane proteins that can contain 643-722 amino acids. Hydrophathy analysis has predicted that this type of proteins should contain 12 transmembrane domains, however no experimental evidence exists supporting this prediction (Figure 1-18). Although the

OATP-mediated transport mechanism is not completely understood, it seems to be dependent of sodium, chloride and potassium gradients, membrane potential and ATP levels.[91, 97]

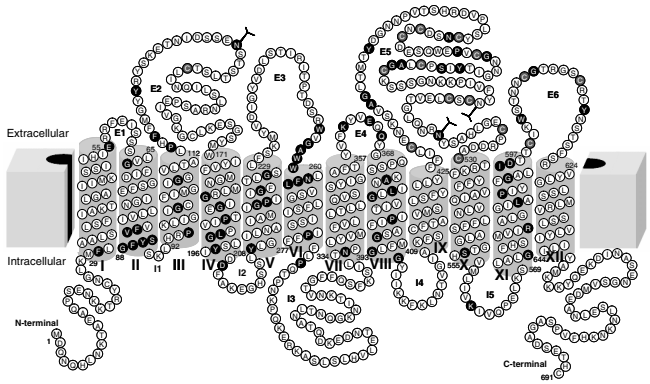

Figure 1-18 Predicted model of human OATP1B1 showing twelve transmembrane domains (Reproduced from Hagenbuch, B. and Gui, C.[91] with permission. Copyright 2008 Informa UK Ltda.)

1.5.2. Modulation of OATPs

Despite the importance of regulation and study of OATPs, only a few examples of specific modulators of OATPs have been identified to date. Recently, Gui *et al.* have developed a HTS-based method to identify specific modulators (OATP1B1 or OATP1B3) allowing use of synthetic chemical libraries to search for small-molecules that interact with the OATPs function.[98] However, this HTS-method is limited and failed to identify modulators for OATP1B1. In addition, plant sources can be another source of potential OATPs modulators. In fact, herbal extracts used in dietary supplements have been found to affect transport by OATP1B1, OATP1B3[99] and by OATP2B1[100] and the interactions between OATPs and fruit juices are well-documented.[101-104] Also, interactions of OATP1B1 with flavonoids have been shown.[105] Modulators of specific isoforms of the OATPs could be used as probes to investigate specific functions of these transporters.

2. APPLICATION OF PHASE-TRAFFICKING METHODS TO NATURAL PRODUCT ISOLATION

2.1. Introduction

In 1963, R.B. Merrifield revolutionized peptide synthesis by introducing solid-phase reagents. This brilliantly simple idea allowed the use of reagents in excess and simplified purification, leading to higher yields and fast isolation.[106] Subsequent elaboration using combinatorial techniques have led to peptide compound libraries of thousands of compounds. Since then, an impressive number of inventive modifications have been introduced in a wide range of fields in academic and industrial laboratories.[107, 108] Particularly, organic chemists have taken advantage of specific interactions between small organic molecules and solid-supported reagents (SSR) to achieve quick reactions and purification of desired non-peptide products applying creative phase-switching strategies.[109] Furthermore, the isolation process using solid-phase protocols only involves simple operations of filtration and solvent removal that are suitable for automation and high throughput applications, and has found particular value in combinatorial chemistry laboratories.[110] Despite the multiple advantages of SSR for isolation of small synthetic organic molecules, this method has yet to find application in resolving complex natural product extracts. Ion-exchange resins have long been used for purification of particular classes of natural products (i.e. quinine[111, 112]) at a scale only occasionally used in fractionation schemes. Few examples of applications to natural products research include recovery and concentration of thiamine from rice bran extract,[113] isolation of alkaloids from *Lindelofia achusoides*[114] and *Aconitum septentrionale*,[115] simultaneous determination of phenolics and alkaloids in methanolic extracts of *Gentisia* species,[116] and selective adsorption of tea polyphenols.[117] Generally, the use of exchange resins as column chromatography components in labor-intensive schemes is a common feature in these reports.

As mentioned in the previous chapter (Section 1.2), the initial biological activity evaluation of crude extracts shows multiple disadvantages that can lead to false-positive and false-negative outcomes in both biochemical and cellular screenings, thus reducing the rate of success and increasing cost.[19] In order to address these difficulties, improved fractionation methods have been developed, including pre-treatments to reduce tannins,[27] automated fractionation,[118] single or multiple solid-phase extraction (SPE),[119, 120] counter current chromatography (CCC),[121] preparative high pressure liquid chromatography (HPLC) and elaborate applications of complex and costly devices. These methods require either a substantial investment or lengthy and tedious protocols in the laboratory, preventing their implementation, especially in remote regions of current bioprospecting interest. Consequently, the need for applications that can generate samples in a convenient and rapid manner with suitable quality for initial bioassay is of great current interest. Such a method should not only increase the relative concentration of potentially active compounds, but also reduce interference from other components in the initial mixture. Also, some additional desirable features would include speed, low cost, be environmentally benign, not labor-intensive, and be adaptable to field bioprospecting conditions. To address these needs, we designed and optimized a phase-switching application that takes advantage of weak ion exchange resins for a simultaneous rapid recovery of neutral, basic, and acidic components from crude organic plant extracts.[122]

2.2. Method development

Normally, the acid-base character of natural products has allowed selective isolation of compounds based upon their functional groups by using pH manipulation in liquid-liquid partition protocols. However, these more tedious, time consuming, and solvent demanding conventional solution-phase chemistries can be replaced in principle with simultaneous catch-and-release methodologies using immobilized reagents for natural product extract resolution as is now commonly done in combinatorial chemistry laboratories for synthetic compounds.[123] In our study, the appropriate resins were kept separated from one another by the use of porous bags dipped simultaneously in the stirred plant extracts. As illustrated in Figure 2-1, groups of acidic and basic compounds can be selectively trapped using an appropriate ion-exchange resin, leaving behind the neutral compounds in solution so that they can each be recovered by simple evaporation. Those operations can, in principle, be adapted to field conditions, far away from the home laboratory during bioprospecting activities.

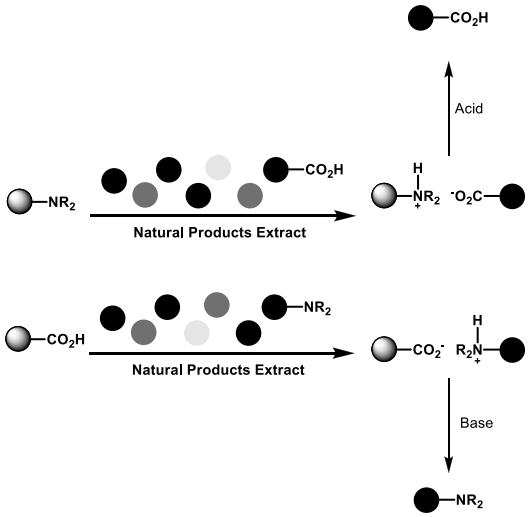

Figure 2-1 Catch-and-release principle of selective separation using ion-exchange resins. In the first phase the acidic and basic resins are kept spatially separated by employing porous bags. In the second phase the resin bags are withdrawn and separately eluted with appropriate solvents

Since spatially separated resins do not interfere with each other's functions,[124] weakly basic and weakly acidic resins can be confined into separate "packets" followed by their joint immersion into a solution of an organic plant extract allowing for partitioning of its components based upon their acid-base characteristics.[124] In order to work out the conditions necessary to accomplish this and, in order to validate our method, an "artificial extract" was prepared by mixing known amounts of neutral, basic, and acidic model compounds (quinine, 3,4,5-trimethoxybenzoic acid, and methyl 3,4,5-trimethoxybenzoate respectively; Figure 2-2) and this mixture was subjected to the separation scheme shown in Figure 2-3 using the polyacrylic-divinylbenzene resins Dowex® MAC-3 (carboxylic acid functional group) and Dowex® Marathon® WBA (dimethylamino functional group). These resins were chosen after preliminary experimentation with a variety of resins because of their large exchange capacities, stability over a wide pH range, and relative ease of regeneration for repeated use.[125, 126]

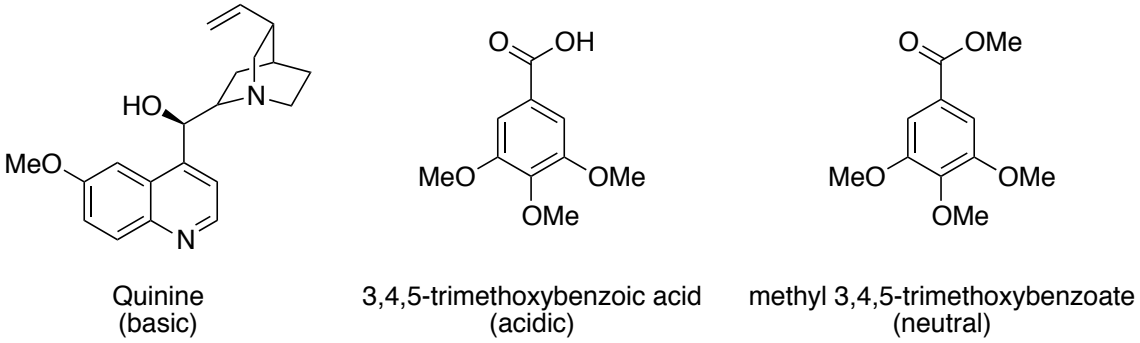

Quinine (basic) | 3,4,5-trimethoxybenzoic acid (acidic) | methyl 3,4,5-trimethoxybenzoate (neutral)

Figure 2-2 Structures of quinine, 3,4,5-trimethoxybenzoic acid, and methyl 3,4,5-trimethoxybenzoate

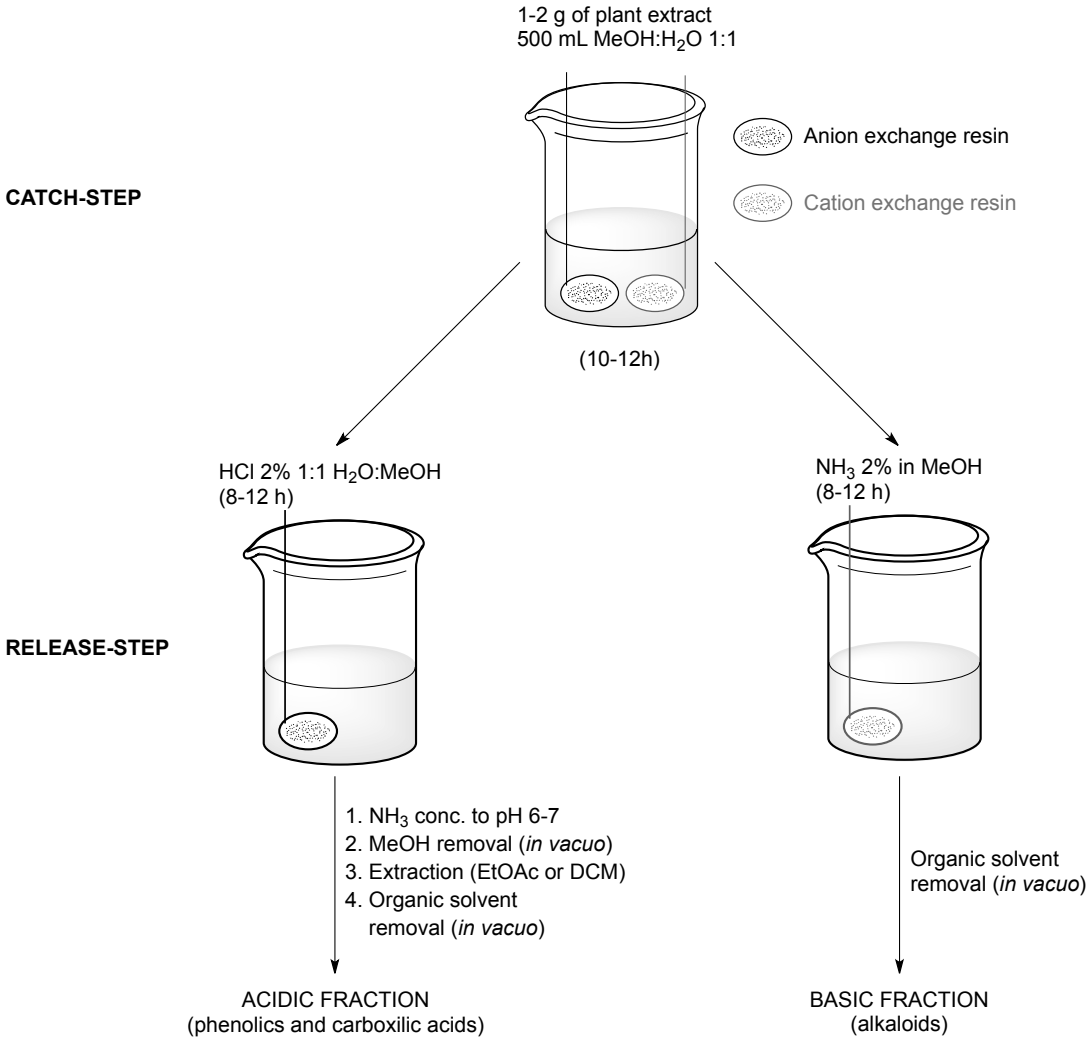

Figure 2-3 General catch-and-release protocol scheme. The neutral components remain in the original methanol-water solution and are recovered by evaporation

The resins were packed into the tea-filter bag and cleaned according to the manufacturer's guidelines prior to conducting the experiment. The adsorption of model compounds was followed by HPLC during a 24 hour period (Figure 2-4). Complete sequestration (ca. 98%) of acidic and basic compounds from the extract solution (1-2 g in 500 mL of MeOH:H_2O 1:1 v/v) was achieved in 8-12 hours; meanwhile, non-specific adsorption to the resins of neutral

compounds was 14% in the same period using a resin-to-sample ratio of 200:1. A simple saturation experiment showed that a resin-to-sample ratio smaller than 50:1 failed to achieve complete adsorption in a 12 hour period (Figure 2-5). Finally, a change to a water and methanol solvent mixture revealed 1:1 (v/v) as the optimum solvent ratio to use during the trapping step, showing the best balance of solubilization and polarity while reducing the non-selective adsorption of neutral compounds into resins, but still promoting the rapid "switch" of acidic and basic organic compounds from solution onto the respective solid phases.

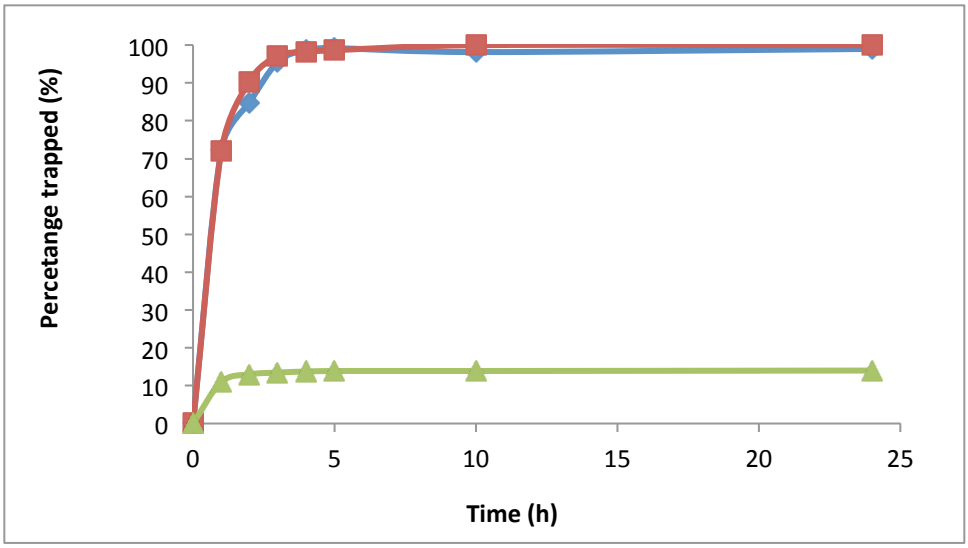

Figure 2-4 Basic (blue diamonds), acidic (red squares), and neutral (green triangles) model compound sequestration into solid phase in a 24-hour period

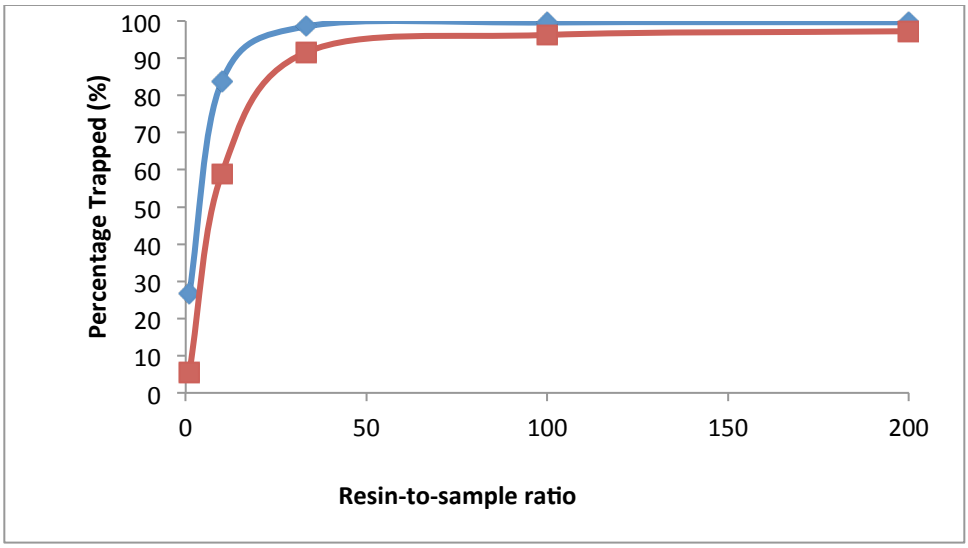

Figure 2-5 Saturation curves for 12-hour period adsorption of basic (blue diamonds) and acidic (red squares) compounds

After removal of the loaded resins from the processed solution, the neutral fraction was simply recovered by removal of solvents under reduced pressure. Acidic and basic fractions were released from the corresponding resins by dipping the bags separately in basic and acid solutions respectively under optimized conditions. Model compounds in the tested samples were recovered in 75%, 91% and 98% yields for neutral, basic, and acidic fractions respectively. In addition, the recovered compounds were highly pure based upon HPLC traces (Figure 2-6). These results demonstrated that the desired selective separation could be achieved with the proposed methodology. Small quantities of the neutral compounds adhered to the resins, presumably due to their lipophilic polymeric backbone. If desired, these compounds could be recovered more completely by washing the resins with pure solvent before release of the ionic contents. The method thus clearly worked efficiently and the next step was to challenge it with a real plant extract to show its practical use and validate the method. With the optimized protocol in hand,

the plant extracts of *Skytanthus acutus* Meyen (Apocynaceae) and *Camellia sinensis* L. (Kuntze) (Theaceae) were next subjected to similar separation steps.

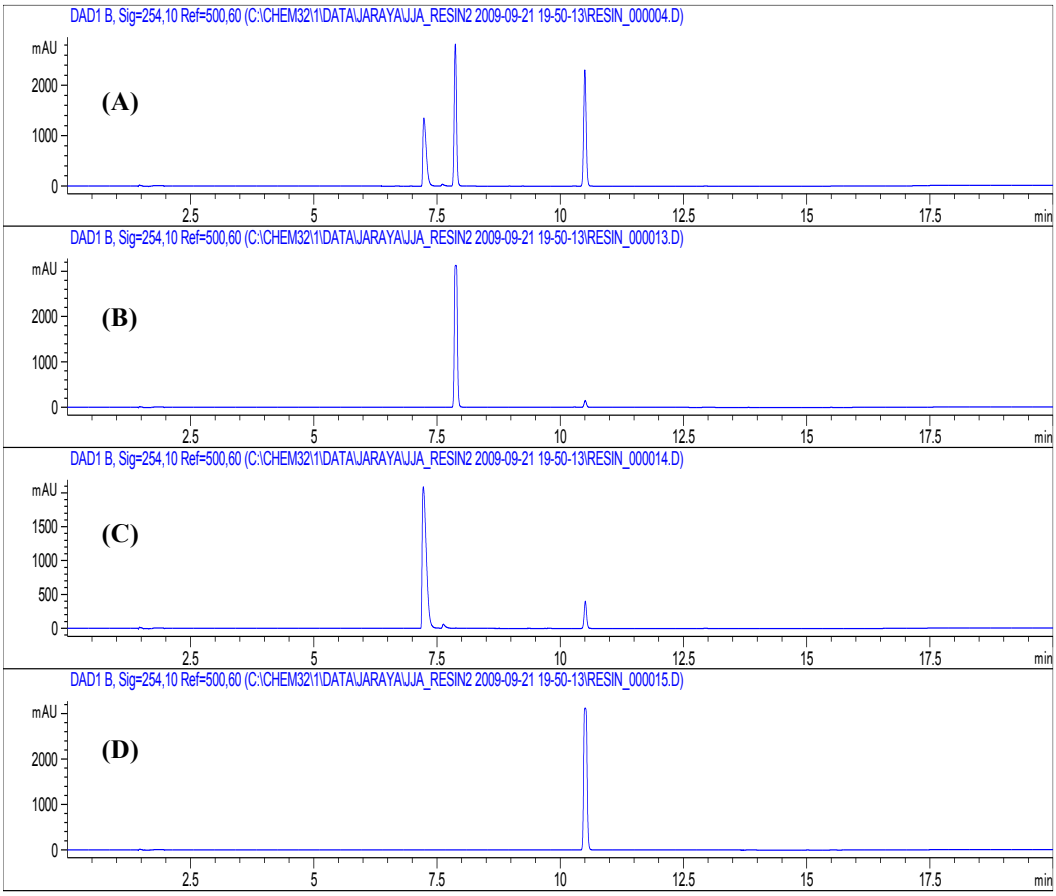

Figure 2-6 HPLC profile of artificial mixture (A) and recovered fractions: acidic (B), basic (C), and neutral (D)

Plant alkaloids exhibit a wide range of potent pharmacological activities and are considered very important for drug discovery purposes.[127] Therefore, generation of alkaloid-enriched fractions from plant extracts is very valuable for initial biological screening. In addition, removal of alkaloids from the plant extract can allow for the evaluation of different type of bioactivities due to other components possibly masked by the activity of the alkaloids in the original extract.

The South American plant *S. acutus* was used as an alkaloid-containing model plant to test and validate our new method in much more complex mixtures. First, the main monoterpene alkaloid present in the methanolic extract of *S. acutus*, skytanthine (**2.1**, Figure 2-7), was isolated and purified using a traditional isolation scheme as described in the literature.[128] The structure and purity of skytanthine were confirmed by spectroscopic methods namely, ^{1}H, ^{13}C, and 2D NMR as well as HRMS. The organic extract of *S. acutus* was then submitted to the solid-phase separation scheme. Skytanthine was successfully removed from the solution and selectively recovered in the basic fraction as shown in the LCMS traces in Figure 2-8. Skytanthine lacks a suitable UV chromophore but is readily detected in the total ion current LCMS traces. From this it is clear that skytanthine, as expected, concentrated in the acidic resin and was extracted therefrom. In addition, the recovered basic fraction was comparable with the mixture obtained more laboriously by applying a traditional liquid-liquid extraction, by means of LCMS traces (Figure 2-6) and the yield of the alkaloid-rich fraction from the extract (6.1% compared with 5.4% by the traditional partition) was somewhat superior using the new method.

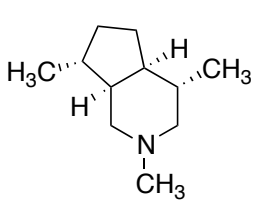

Skytanthine (**2.1**)

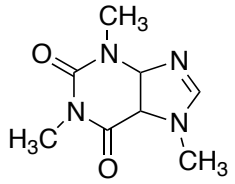

Caffeine (**2.2**)

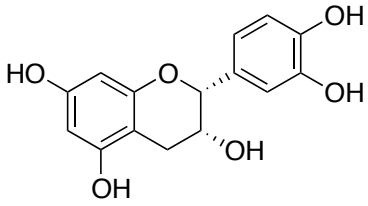

EC (**2.3**)

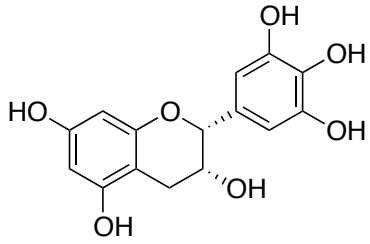

EGC (**2.4**)

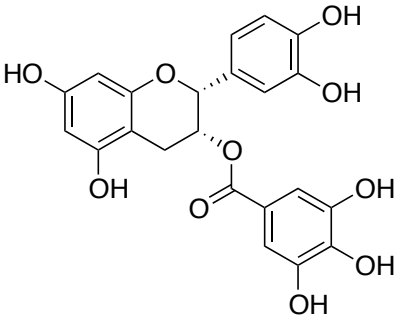

ECG (**2.5**)

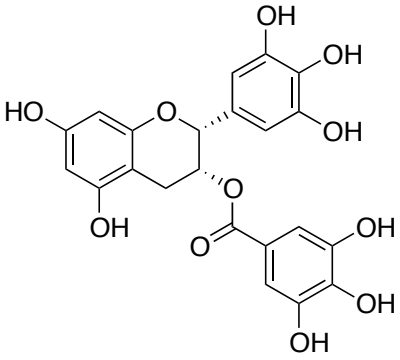

EGCG (**2.6**)

Figure 2-7 Structures of recovered compounds using catch-and-release approach from *S. acutus* (**2.1**) and *C. sinensis* (**2.2-2.6**)

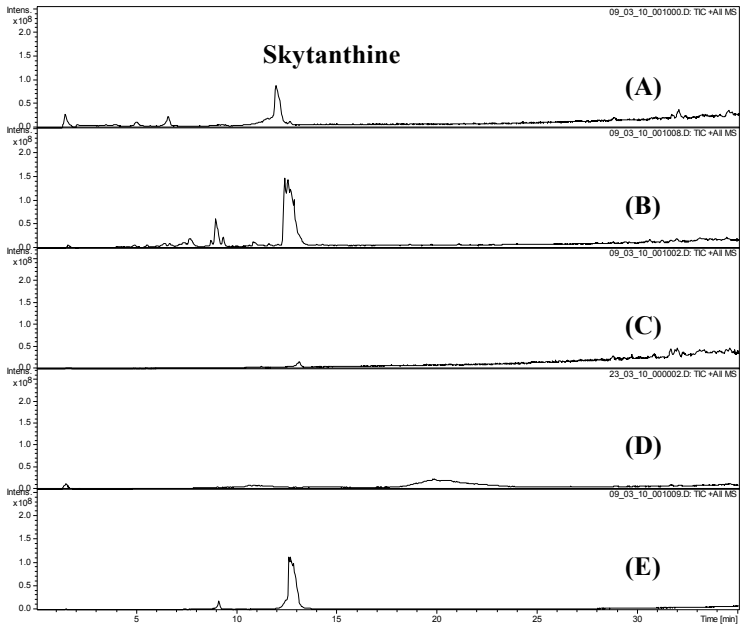

Figure 2-8 HPLC-MS^n (TIC+) traces of *S. acutus* extract (A), basic (B), acidic (C), and neutral fractions (D), and skytanthine (E)

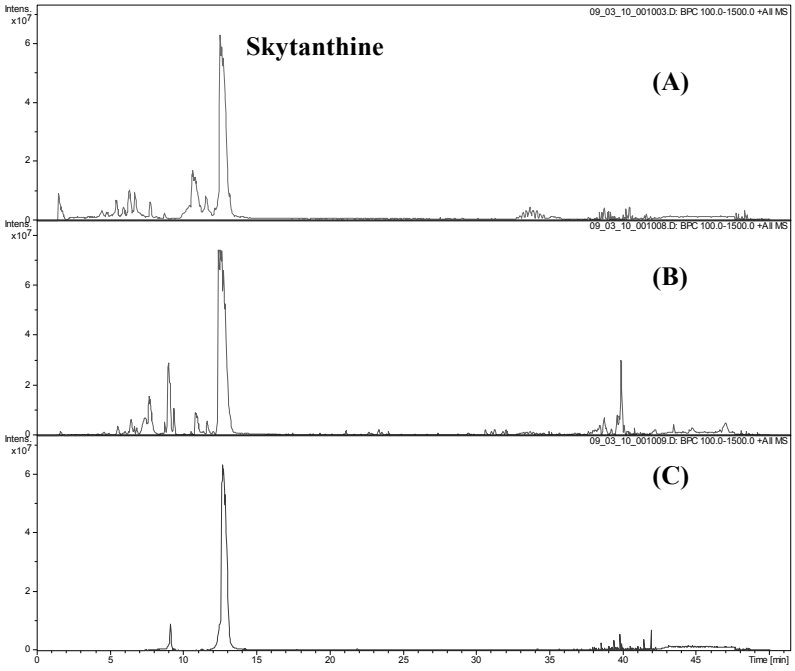

Figure 2-9 HPLC-MS^n (TIC+) traces of *S. acutus* basic extracts using the new solid-phase method (A), or traditional extraction method (B), and skytanthine (C)

Plant phenolics are a large group of natural products that exhibit a number of useful biological activities and are widely distributed in the plant kingdom, including most of the food plants in the human diet.[129] Green tea catechins have been extensively investigated in the last two decades for their biological activities.[130-133] Also, green tea is probably the most consumed beverage worldwide.[134] As green tea contains a significant percentage of the purine alkaloid caffeine this species is particularly suitable for the validation of our resin-based separation method. After applying the separation scheme to the green tea organic extract, catechins were analyzed by HPLC. Adsorption of the four main catechins (EC: epicatechin, **2.3**; EGC: epigallocatechin, **2.4**; ECG: epicatechin gallate, **2.5**; and EGCG: epigallocatechin gallate, **2.6**) and caffeine (**2.2**) (Figure 2-7) was followed using HPLC as shown in Figure 2-10. Phenolics were rapidly sequestered from solution in 6 hours, however only 50% of the caffeine was removed from the solution in the same time period. Not surprisingly, the gallate-containing catechins (ECG and EGCG) were adsorbed more rapidly and to a greater extent than the non-gallate containing counterparts due to their greater acidity. In order to minimize the oxidation of catechins during the recovery stage, the original procedure was slightly modified by using an ultrasound bath for 30 min. three times with portions of acidic solution, instead of leaving the sample in the shaker overnight. The resulting catechin-rich fraction (acidic fraction, 26% yield) clearly showed the presence of four main catechin peaks in the HPLC trace (Figure 2-10) but only minor amounts of caffeine. Meanwhile, caffeine was now incompletely removed by the acidic resin. The recovered yield (4.4%) was lower, however, when compared with traditional method (5.5%). In this case, yields of both acidic and basic fractions were comparable with traditional liquid/liquid partition extraction for caffeine ($CHCl_3$ layer, 5.5%) and catechins (EtOAc layer, 30%) by means of HPLC traces.

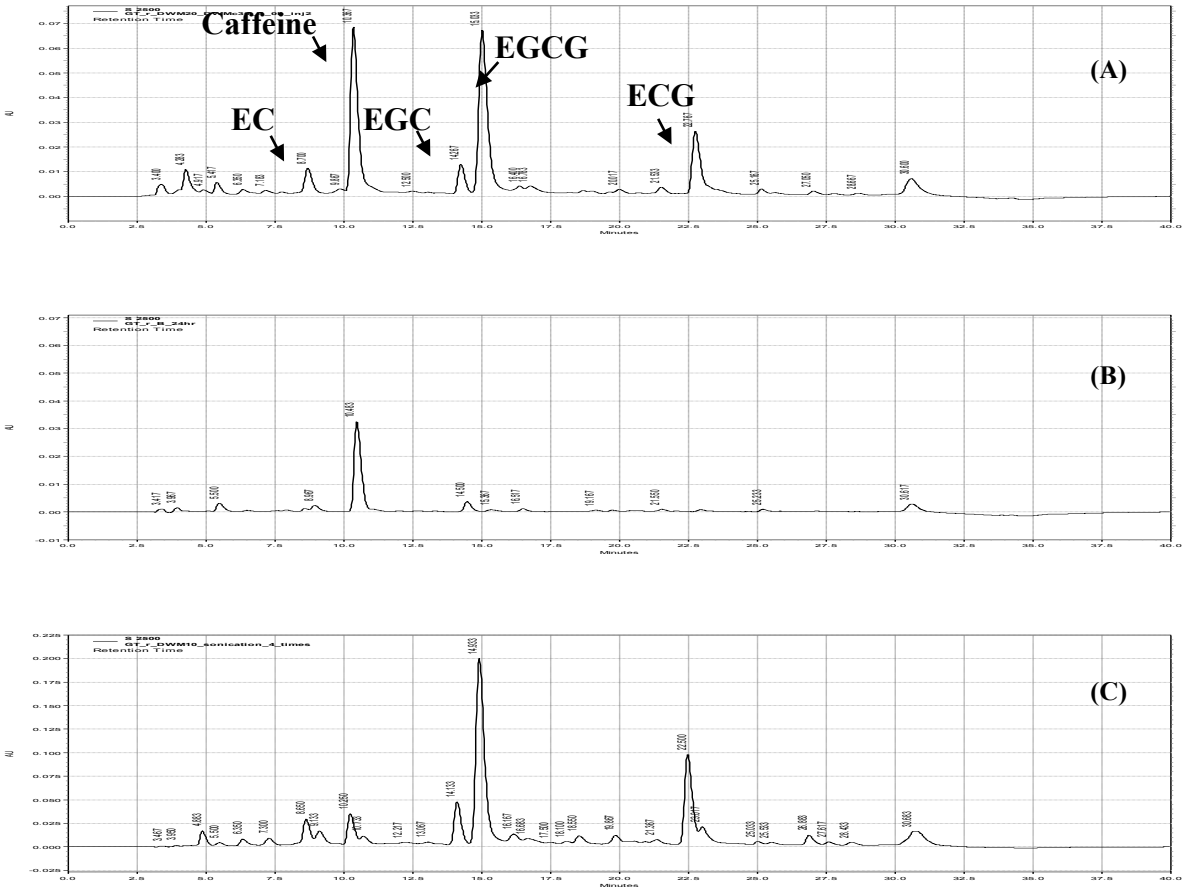

Figure 2-10 HPLC-UV (278 nm) traces of green tea extract (A), basic fraction (B), and acidic fraction (C). The peak assignment is based on co-chromatography using standard compounds

2.3. Method application: zingerines from *Zingiber officinale* Roscoe

As described in the previous section, our catch-and-release methodology showed very encouraging results in resolving an artificial mixture of compounds and model plant extracts. Hence, in order to expand the scope of our separation procedure, a ginger extract was prepared and subjected to a similar separation method, with the goal of purifying its phenolic compounds, gingerols and shogaols (Figure 2-11) from the neutral essential oils, a task that typically requires a large-scale normal-phase column chromatography that consumes large quantities of dichloromethane and acetone. Unlike green tea phenolics, gingerols and shogaols only contain one acidic phenolic group; consequently they are less polar and less water-soluble which represented a good prospect to test our new methodology.

Ginger, *Zingiber officinale* Roscoe (Zingiberaceae), is used worldwide not only as a spice in food, but also in various traditional systems of medicine against different ailments such as arthritis, rheumatism, infectious diseases, and vomiting.[135, 136] The chemistry of ginger has been extensively investigated with over 100 compounds identified in both fresh and dried samples.[137, 138] Ginger's numerous biological activities have been attributed mainly to the gingerols and shogaols, the major pungent principles found in both fresh and dried ginger rhizomes.[139, 140]

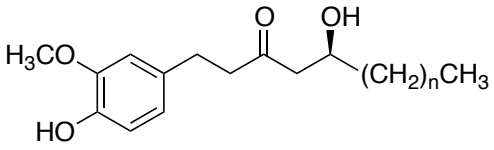

[6]-gingerol, n=4
[8]-gingerol, n=6
[10]-gingerol, n=8

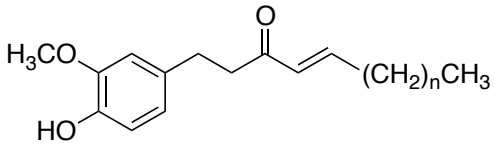

[6]-shogaol, n=4
[8]-shogaol, n=6
[10]-shogaol, n=8

Figure 2-11 Representative structure of gingerols and shogaols

A methanolic extract of ginger rhizomes was submitted to our separation scheme (Figure 2-3). As expected, the basic resin trapped the phenolic compounds, including the main constituents including gingerols and shogaols (Figure 2-12). Interestingly, the analysis of LCMS traces of the basic fraction revealed the presence of several compounds with odd molecular weight values, which prompted us to investigate further the nature of these components because, to our knowledge, no nitrogen-containing basic metabolites have been previously reported from ginger. After scaling up the separation procedure, we were able to isolate and identify three new nitrogenous compounds from ginger that were named [6]-, [8]-, and [10]-zingerines, as they are 5-(6-amino-9*H*-purin-9-yl) analogs of [6]-, [8]-, and [10]-gingerols respectively (Figure 2-13). Although reported in a small number of microbial and marine products, secondary metabolites that contain a purine ring attached to a non-carbohydrate carbon skeleton are very rare in higher plants.[141, 142]

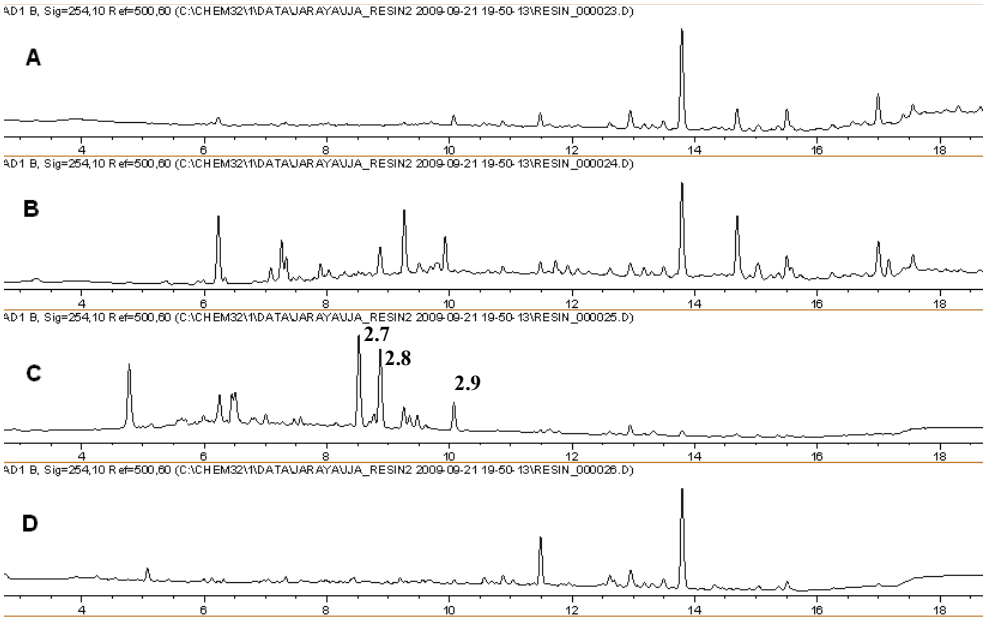

Figure 2-12 HPLC-UV (254 nm) traces of (A) methanolic extract, (B) acidic fraction, (C) basic fraction, and (D) neutral fraction obtained from ginger dried rhizome

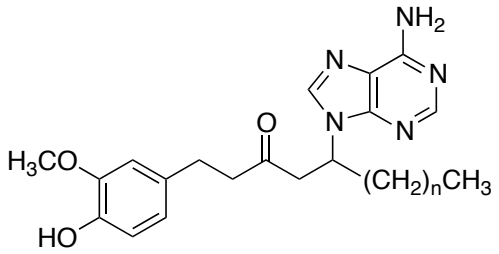

[6]-zingerine, n=4 (**2.7**)
[8]-zingerine, n=6 (**2.8**)
[10]-zingerine, n=8 (**2.9**)

Figure 2-13 Structure of [6]-, [8]-, and [10]-zingerines **(2.7-2.9)**

2.3.1. Structure elucidation

Initially, our small-scale separation protocol allowed for the isolation of the main compound **2.7** from the basic fraction after two additional purification steps: column chromatography on Sephadex LH-20 followed by semi-preparative reverse phase HPLC. The HRMS *m/z* 412.2362 $[M+H]^+$ (calc. for $C_{22}H_{30}N_5O_2$ 412.2349) was consistent with the presence of five nitrogen atoms in the molecular formula. The ESIMS/MS showed the neutral loss of *m/z* 276.2, leaving the stable charged purine fragment of *m/z* 136.1 (Figure 2-14). Furthermore, the structure of **2.7** was deduced based on analyses of the ^{1}H, ^{13}C NMR, ^{1}H ^{1}H-COSY, HSQC and HMBC spectra and supported by IR and UV spectra. First, the splitting pattern and coupling constants of the aromatic protons in the ^{1}H NMR δ_H 6.63 (d, *J*=2.0 Hz, H-2'), 6.59 (d, *J*=8.0 Hz, H-5') and 6.44 (dd, J=8.0, 2.2 Hz, H-6') were consistent with a 1,2,4-trisubstituted benzene ring system and the corresponding aromatic carbons δ_C 133.7 (C-1'), 113.0 (C-2'), 148.9 (C-3'), 145.8 (C-4'), 116.2 (C-5') and 121.6 (C-6') were readily assigned with the assistance of correlations observed in the HSQC and HMBC spectra (Figure 2-15). Second, the attachments of the methoxy group δ_H 3.76 (s, 3'-OCH_3) to C-3' and methylene group δ_H 2.67 (m, H-1) to C-1' were established based on the

correlations observed in the HMBC spectrum. Third, the chemical shift of aromatic carbon C-4' (*s*, δ_C 145.8) suggested that this position was oxygenated. Analogous to [6]-gingerol, two spin systems corresponding to a decanyl chain were identified in compound **2.7** based on ^{1}H ^{1}H-COSY, HSQC and HMBC spectra, showing two distinctive structural features: a ketone group δ_C 209.6 (s, C-3) and a methine proton δ_H 4.91 (m, H-5). Finally, with only two proton signals left δ_H 8.16 (brs, H-4") and 8.12 (brs, H-8"), five nitrogen atoms, and five carbon signals δ_C 153.4 (C-2"), 150.6 (C-4"), 120.4 (C-5"), 157.3 (C-6"), and 142.6 (C-8"); the presence of an adenine ring was proposed and supported by ESIMS/MS fragmentation and HMBC spectra. Furthermore, adenine substitution at the C-5 position explained satisfactorily the shift to lower filed of H-5 (m, δ_H 4.91) when compared with the corresponding signal of [6]-gingerol.[143] In addition, the structure was confirmed by synthesis (*vide infra*). After scaling-up the separation protocol, compounds **2.8** and **2.9** were isolated showing similar fragmentation patterns in the ESIMS/MS, almost identical low field signals in ^{1}H- and ^{13}C NMR spectra (Table 2-1), and differing from compound **2.7** only in the number of methylene groups in the aliphatic region. Accordingly, their structures **2.8** and **2.9** were assigned relative to that previously described for compound **2.7**.

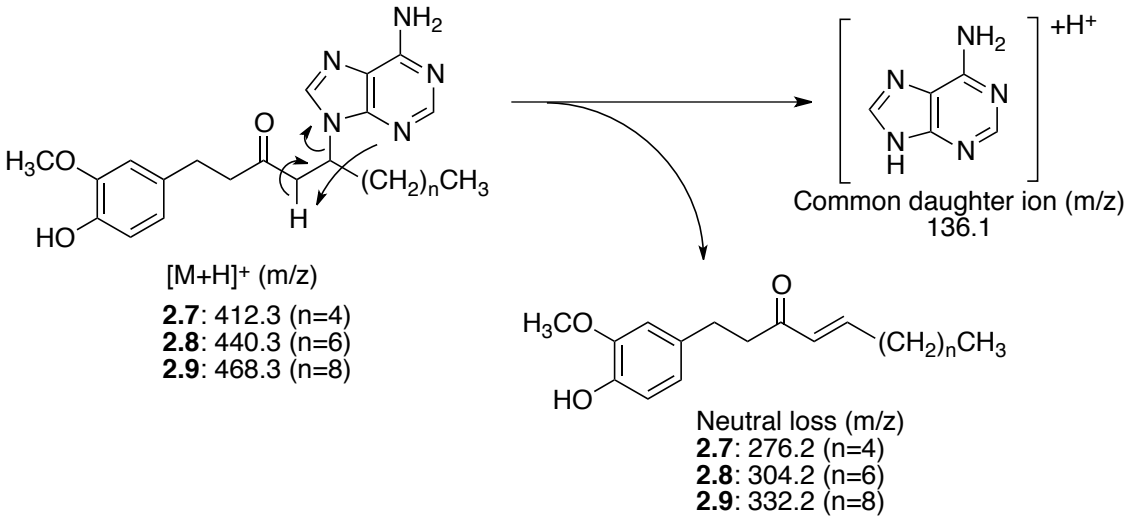

Figure 2-14 Proposed fragmentation of [6]-, [8]-, and [10]-zingerines (**2.7-2.9**)

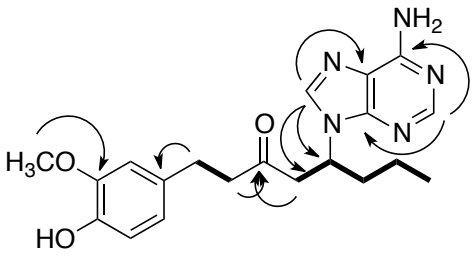

Figure 2-15 Selected COSY (thick bonds) and HMBC (arrows) correlations observed for [6]-zingerine (**2.7**)

Although purine is the most widely distributed *N*-heterocyclic ring in nature, purine-containing plant secondary metabolites are not commonly found.[142] Simple purine alkaloids, like caffeine or theanine, have a limited taxonomic distribution in the plant kingdom and a purine ring attached to a non-carbohydrate carbon skeleton, as in the case of compounds **2.7-2.9**, is an unusual structural feature. Among the limited reports of this class of natural products are the cucurbitane

triterpenoids isolated from *Cucurbita pepo cv dayangua*,[141] alachalasine F-G from the fungus *Podospora vesticola*,[144] and a limited number of examples from marine sponges.[145-147]

Compounds **2.7-2.9** have not been previously reported in the literature and they represent the first basic nitrogen-containing secondary metabolites in ginger.[148] We named this group of compounds zingerines, as they are 5-(6-amino-9*H*-purin-9-yl) analogs of the commonly found gingerols. Compounds **2.7-2.9** were detected in the original extract prior to any purification step using targeted LCMS analysis as well as in two extracts prepared from additional commercial samples of ginger rizhomes (Figure 2-16). The results showed a strong evidence that the three new compounds were not likely to be artifacts of the new isolation process. Interestingly, the isolation of zingerines using classic liquid/liquid methodology was unsuccessful presumably due to the acidic phenolic group they contain that makes these compounds amphoteric and thus soluble in the aqueous phase under basic conditions. Probably, the amphoteric behavior of the zingerines coupled with their strong adsorption on silica gel are the two main reasons that have prevented their isolation and identification in the previous phytochemical studies of ginger.

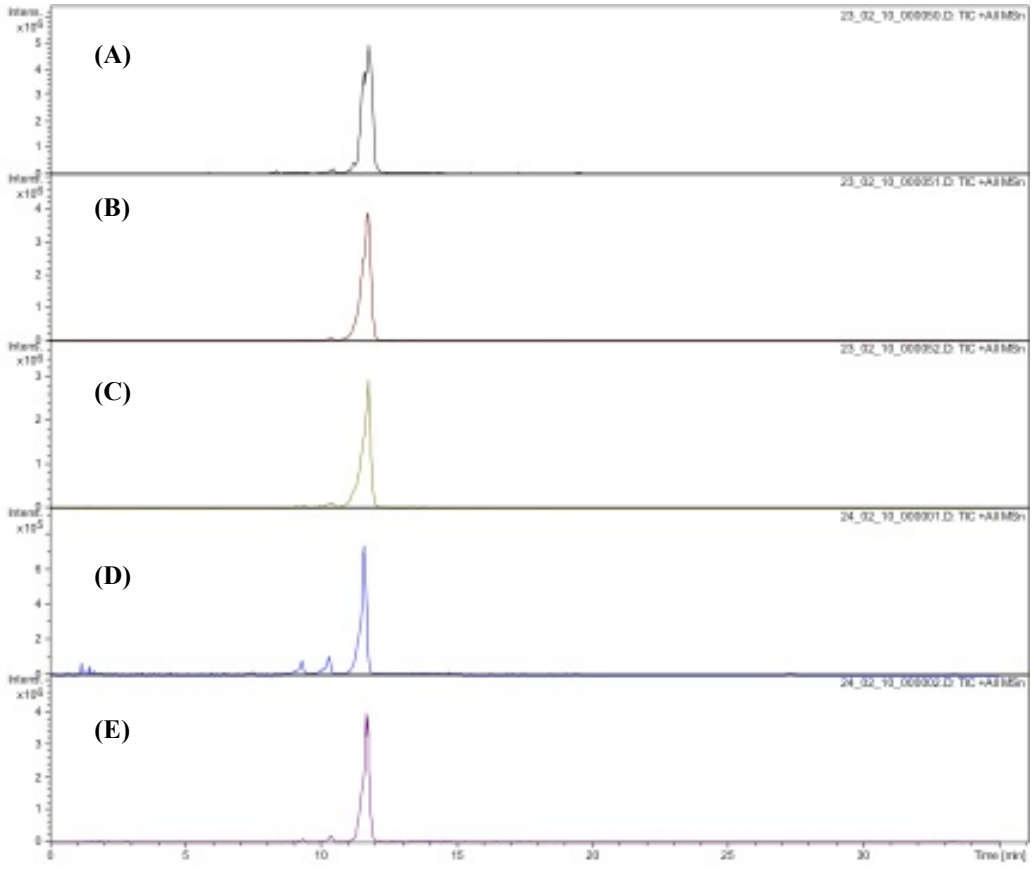

Figure 2-16 Targeted LCMS traces TIC+ MS^3(m/z 412 to 136.1i) of (A) zingerines-rich fraction, (B) basic fraction, (C) methanolic ginger extract lot #E99/03/B8, (D) methanolic ginger extract lot #E99/01/B8, and methanolic ginger extract lot #E94/01/B8

The presence of zingerines in the dried ginger rhizome extract could in theory arise from a Michael-type reaction between shogaols, dehydration products of gingerols during drying of ginger rizhome, and adenine. To explore the feasibility of such a reaction, we dissolved an equimolar mixture of [6]-shogaol and adenine in a mixture of 1:1 MeOH:H_2O and stirred the reaction mixture during 72 h at room temperature. The formation of [6]-zingerine was only detected by means of LCMS analysis, but not using UV detection, suggesting that only minute quantities of the compound are produced under those conditions. As expected, basic and acidic

catalysis increased the yield of the desired product. Using basic conditions, the reaction was scaled-up to 90 mg of [6]-shogaol and 45.2 mg (1.2 eq.) of adenine under agitation for 72 h at room temperature to obtain compound **2.7** in 36% isolated yield. Similarly, [8]-shogaol (50 mg) and [10]-shogaol (50 mg) were subjected to identical reaction conditions thereupon we obtained compounds **2.8** and **2.9** in 28% and 30% isolated yield, respectively (Figure 2-17). The synthetically obtained products were identical to the ones isolated from ginger plant material by means of ^{1}H- and ^{13}C-NMR spectra and HPLC traces (Figure 2-18). This confirmed the proposed structures of the zingerines. In addition, both natural and synthetic samples were optically inactive demonstrating that the compounds were racemic mixtures. This was confirmed by means of chiral HPLC resolution of both synthetic and natural [6]-zingerine, showing two peaks with 1:1 area under the curve (AUC) ratio (Figure 2-19). Although natural [6]-zingerine was not optically active, an enzymatic origin cannot be ruled out definitively because of the possible operation of a retro Michael/Michael type reaction equilibrium leading to racemization under experimental conditions. Furthermore, identification of biosynthetic genes and their enzymatic products responsible for the origin of zingerines would definitely exclude an artificial genesis. Although gingerols are present in relatively high quantities in ginger rhizome, we were unable to detect free adenine in the initial extract or basic fraction using LCMS analysis.

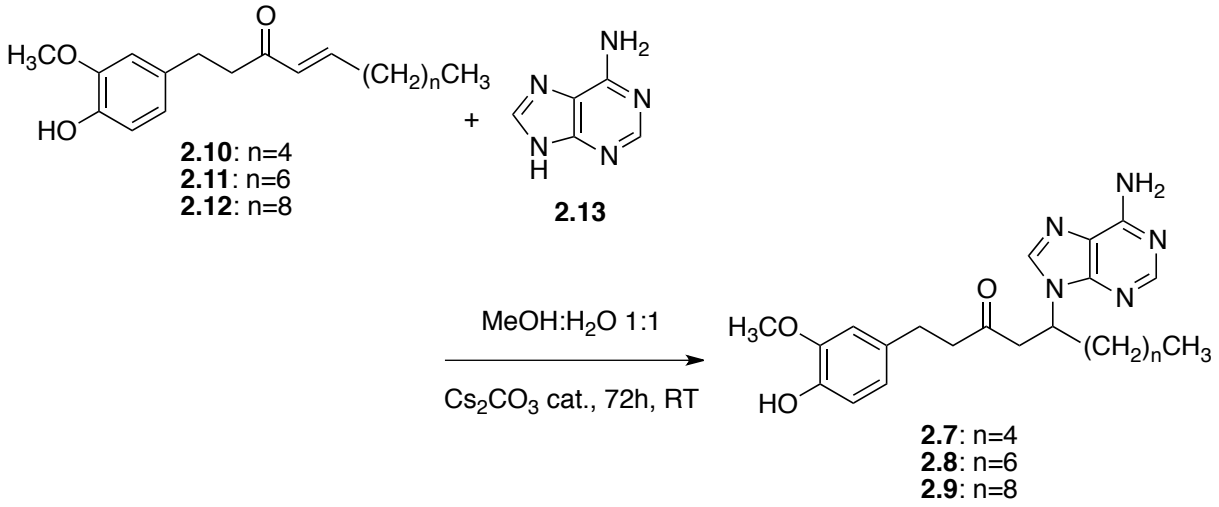

Figure. 2-17 Synthesis of [6]-, [8]-, and [10]-zingerines (**2.7-2.9**)

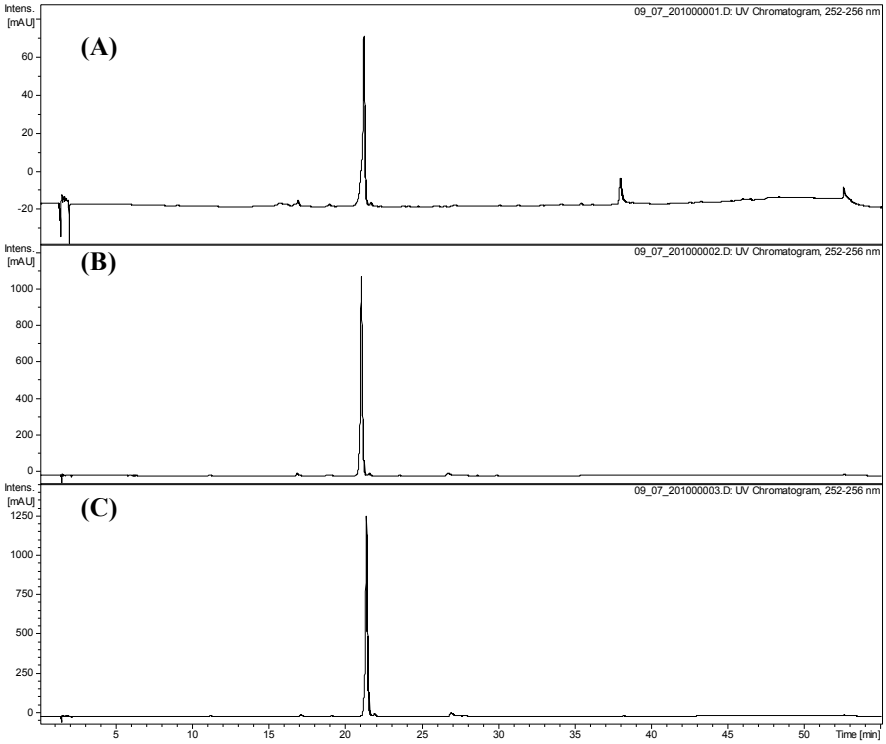

Figure 2-18 HPLC trace of [6]-zingerine **(2.7**) (A) isolated from ginger rhizome, (B) obtained by synthesis, (C) co-chromatography of both samples under the same conditions

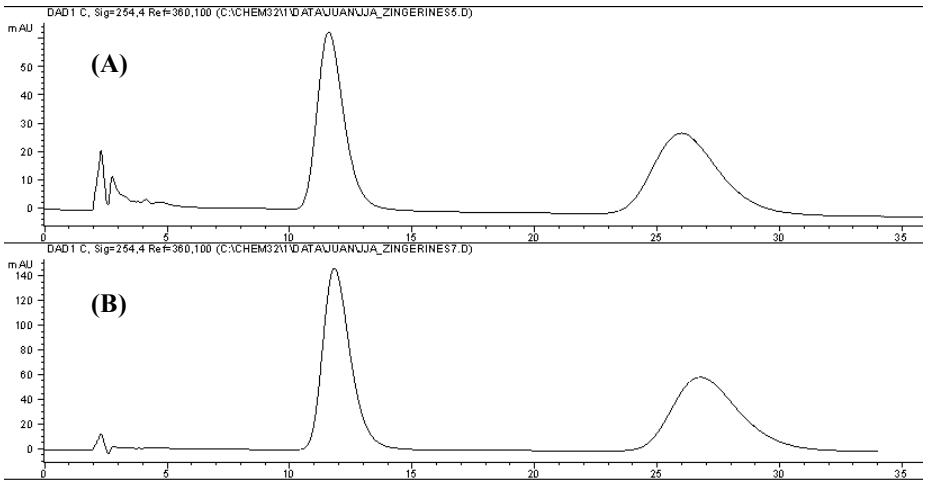

Figure. 2-19 HPLC chiral resolution of [6]-zingerine **(2.7**) (A) isolated from ginger rhizome and (B) obtained by synthesis

2.4. Conclusions

In summary, a new phase-trafficking approach for the separation of acidic, basic, and neutral compounds from organic plant extracts was developed, validated and successfully applied not only to artificial mixtures of model compounds, but also to crude plant extracts. Furthermore, this new catch-and-release methodology allowed for the isolation and identification of three compounds new to the literature from the most extensively studied ginger rhizomes. The new compounds contain an adenine group attached to the gingerol-type carbon skeleton, an unusual structural feature in higher plants. We envision that this new method could be applied more widely to natural extracts of diverse origin in order to generate better quality samples for initial bioassays. This novel approach offers multiple advantages over traditional extraction methods, as it is not labor intensive, makes use of only small quantities of "green" solvents, solid-supported reagents can be recycled, are inexpensive and can be easily adapted to field conditions for bioprospecting activities.

This work was published in two separated papers:

- Araya, J.J.; Montenegro, G.; Mitscher, L.A.; Timmermann, B.N. Application of Phase-Trafficking Methods to Natural Products Research. *J. Nat. Prod.* **2010**, *73*(9), 1568-1572
- Araya, J.J.; Zhang, H.; Prisinzano, T.E.; Mitscher, L.A.; Timmermann, B.N. Identification of Unprecedented Purine-Containing Compounds, the Zingerines, from Ginger Rhizomes (*Zingiber officinale* Roscoe) using a Phase-Trafficking Approach. *Phytochemistry*. **2011**, *72*, 935-941

2.5. Experimental data

2.5.1. General procedures

^{1}H, ^{13}C NMR, and 2D spectra were recorded with a Bruker DRX-400 instrument (400 MHz and 100 MHz, respectively) or a Bruker Avance AV-III 500 instrument with a dual carbon/proton cryoprobe (500 MHz and 125 MHz, respectively). The samples were dissolved in the appropriate deuterated solvent ($CDCl_3$, CD_3OD, C_5D_5N) and the shifts were expressed in parts per million (ppm) relative to residual corresponding protonated solvent as an internal standard. Abbreviations are: s, singlet; d, doublet; t, triplet; q, quartet; br, broad. Infrared spectra were recorded with a Thermo Nicolet Avatar 380 FT-IR spectrometer and are expressed in wave numbers (cm^{-1}). Melting points were determined using an OptiMelt automatic melting point apparatus and are uncorrected. High resolution mass spectra were collected using a LCT Premier Waters Corp. spectrometer. Optical rotations were measured with a Rudolph RS Autopol IV automatic polarimeter. UV-Vis measurements were conducted with a Varian Cary 50 UV-Vis spectrophotometer. Agitations of samples were performed with a New Brunswick Scientific Excella E1 Platform Shaker. Semi-preparative HPLC was conducted using an Agilent 1200 HPLC system with a Phenomenex Luna C18 column (5μm, 250×10 mm), flow rate of 4.5 mL/min (approx. 160 bar), injection volume of 50 μL (ca. 10 mg sample), and UV detection using diode array. Preparative HPLC separations were done using an Agilent 1100 HPLC system with a Phenomenex Luna C18 (5 μm, 250×21.4 mm), flow rate of 30 mL/min (approx. 60 bar), injection volume of 800 μL (ca. 100 mg sample), and UV detection using diode array. Chiral HPLC analysis was performed using a Chiralcel OD-H column (No. ODHOCD-LH013) purchased from Chiral Technologies Inc. (West Chester, PA) in an Agilent 1100 system and the

solvent system used was isocratic hexanes:isopropanol 70:30 (v/v), the flow rate was 0.9 mL/min, the injection volume was 25 μL, and UV detection at 254 nm. Flash chromatography was performed using Sorbent Technologies silica gel (20-40 μm or 12-24 μm) with the noted eluent system. Other separations were conducting using Sephadex LH-20 and MCI-gel column chromatography with the noted eluent system. Automatic flash chromatography was performed using a Teledyne Isco CombiFlash system and pre-packed Gold silica gel column (normal and reverse phase) with the indicated solvent system. All other solvents were used without further purification or drying procedures unless otherwise noted. Reaction flasks were oven or flame-dried and cooled under vacuum then purged with argon; all reactions were conducted under argon unless otherwise noted. Where indicated, microwave heating was applied using a Biotage microwave reactor.

The following resins and pure compounds were purchased from Sigma-Aldrich (St. Louis, MO): Dowex™ Marthon™ WBA Anion-Exchange resin (Batch # 13004PC); Dowex™ MAC-3 ion exchange resin (Batch # 13228TD); Quinine anhydrous (Lot code1375702); 3,4,5-trimethoxybenzoic acid 99% (Batch # 05529MH); Methyl 3,4,5/trimethoxybenzoate 98% (Lot S29247-308). Aromatreu® Finum tea filters were purchased from www.cheftools.com.

2.5.2. Plant Material

Aerial parts of *S. acutus* were collected and identified by G. Montenegro, L. Iturriaga and L. Gonzalez on December 16, 1995, in Caldera, Chile (26 55'S; 70 67' W). A voucher specimen has been deposited in the herbarium of the Pontificia Universidad Catolica, Santiago, Chile (coll. No. 0458). *Camellia sinensis* biomass was provided by the Royal Estates Tea Company, a

Division of Thomas J. Lipton, Co.(Englewood Cliffs, NJ). The green tea blend was labeled "Green Research Standard". Dry powdered ginger rhizomes (150 kg) were purchased from Naturex (South Hackensack, NJ) Lot. # E99/03/B8**.**

2.5.3. Plant extraction and isolation

S. acutus and *C. sinensis* biomass were extracted exhaustively with mixtures of MeOH and CH_2Cl_2 (1:1, v/v), then the organic solvents were removed under vacuum to afford the crude organic extract. Each crude extract (2.5 g) was submitted to the general-catch-and-release procedure and the resulting fractions were analyzed by LCMS. In addition, a portion of *S. acutus* extract (10 g) was suspended in water and HCl 10% was added dropwise to pH<4, then extracted three times with CH_2Cl_2. The aqueous layer was then neutralized with NH_3 conc. to pH>9 and extracted again with CH_2Cl_2. The resulting alkaloid extract (540 mg, 5.4%) was separated using silica gel SPE (Phenomenex, 20mm) washed with methanol (100 mL) and followed by methanol 5% NH_3 to obtain the crude skytanthine (**2.1**) that was finally purified by recrystallization (CH_2Cl_2:Hexanes/ 1:1, m.p. 134.6-135.8°C). The structure was confirmed by ^{1}H NMR, ^{13}C - NMR, two-dimensional NMR experiments, IR, UV, and HRMS. The data were in agreement with those previously reported in the literature.[128] Finally, for comparison purposes, the green tea extract (2.5 g) was suspended in water and extracted successively with $CHCl_3$ and EtOAc to generate caffeine- and catechin-rich fractions respectively.

Dried ginger rizhome (40 kg) was subjected to a first extraction using CH_2Cl_2 (130 L) twice during 48 h. Removal of the organic solvent under reduced pressure afforded 1.7 kg of CH_2Cl_2 extract (4.3 %). The remaining plant material was then subjected to a second extraction using

MeOH (130 L) twice during 48h. After concentration under reduced pressure, 1.2 kg of MeOH extract residue was obtained (3.0 %). In the same way, two smaller samples (100 g) of ginger powder obtained from the same company (Lots # E99/01/B8 and #E94/01/B8) were extracted sequentially with CH_2Cl_2 (500 mL) and MeOH (500 mL) to afford CH_2Cl_2 and methanolic extract respectively.

2.5.4. General catch-and-release procedure

A total of 2.5 g of plant organic extract were suspended in 500 mL of MeOH:H_2O (1:1 v/v). Pre-washed tea bags each containing 20 g of Dowex® Marathon® WBA anion exchange resin or 20 g of Dowex® MAC-3 cation exchange resin were dipped into the solution and left shaking at 25 rpm overnight (8-10 hours). Tea bags were then removed and washed with MeOH twice, then submitted to recovery conditions. Anion exchange resin was immersed into 500 mL of HCl 2% (v/v in MeOH:H_2O 1:1) and left overnight under agitation (25 rpm); then the HCl was neutralized with NH_4OH to pH 6-7, the MeOH removed under reduced pressure, and the aqueous phase extracted three times with EtOAc or CH_2Cl_2. Removal of the separated organic extract afforded the phenolic/acidic fraction upon evaporation. Cation exchange resin was immersed into 500 mL of NH_3 2% (v/v in MeOH) and left overnight under agitation and the resulting solution was concentrated under reduce pressure to afford the alkaloidal fraction. The original working solution was also concentrated under reduced pressure to yield the neutral fraction.

2.5.5. Artificial extract preparation and separation

Approximately 100 mg of each of the model compounds (quinine, 3,4,5-trimethoxybenzoic acid, and methyl 3,4,5-trimethoxybenzoate) were weighed with an analytical balance, dissolved

in 500.0 mL of a mixture of MeOH and H_2O 1:1 and submitted to the general catch-and-release procedure. During the first 6 hours, every hour a 1.00 mL sample was taken and analyzed using HPLC, then additional aliquots were taken after 10 and 24 hours. Concentrations were determined by interpolation from a calibration curve prepared for each compound by appropriate dilution of a mother solution of 20 mg/mL to final concentrations of 0.1 to 1.0 mg/mL.

2.5.6. HPLC/MS^n analyses

The on-line HPLC/MS^n analyses of extracts and fractions were performed using an Agilent 1200 Series liquid chromatography system coupled to the Agilent IonTrap LCMS 6310 mass spectrometer. The positive ion ESI-MS experimental conditions were as follows: HV capillary voltage, 3.5 kV; drying temperature, 350°C; drying gas, 12.0 L/min; nebulizer, 15 psi; and capillary exit voltage, 124.8V. The Frag Ampl was set to 1.0V and the smart fragmentation function was used (Smart Frag Ampl was 30-200%). HPLC separations were done using an Agilent Eclipse XDB-C18 column (5μm, 4.6×150 mm) and the flow rate was 1.0 mL/min (approx. 80 bar). The mobile phase for *S. acutus* samples consisted of a linear gradient of acetonitrile and water from 10:90 (v/v) (t=0 min) to 100:0 (t=25 min), then 100:0 until (t=30 min), and finally 10:90 during 10 min (t=40 min) for recovery. In contrast, the mobile phase gradient program for *C. sinensis* samples was acetonitrile and 5mM formic acid 5:95 (v/v) (t=0 min), 15:85 (t=15 min), 100:0 (t=35 min) and wash for 5 minutes, and finally recovery to 5:95 (t=50 min). All samples were dissolved in the mobile phase to a concentration of 1.0 mg/mL and filtered using 13 mm filters with 0.45 μm PTFE membranes (VWR). The injection volume was 25 μL.

Targeted analysis of zingerines was programmed as follows: (a) for [6]-zingerine, isolation and fragmentation of ions *m/z* 411-413, then isolation and detection of ion *m/z* 136.1; (b) for [8]-zingerine, isolation and fragmentation of ions *m/z* 439-441, then isolation and detection of ion *m/z* 136.1; (c) for [10**]-**zingerine, isolation and fragmentation of ions *m/z* 467-469, then isolation and detection of ion *m/z* 136.1. The HPLC separations were done using an Agilent Eclipse XDB-C18 column (5μm, 4.6×150 mm) and the flow rate was 1.0 mL/min (approx. 80 bar). The mobile phase was a linear gradient of acetonitrile and water from 25:75 (v/v) (t=0 min) to 35:65 (t=5 min), then 55:45 (t=15 min), 100:0 (t=25 min), and finally recovery to 25:75 (t=35 min).

2.5.7. Scale-up catch-and-release procedure

The ginger rhizome was initially extracted with CH_2Cl_2, and then with methanol. The methanolic rhizome extract (100 g) was suspended in 2 L of MeOH:H_2O 1:1 mixture (v/v). A total of 200 g of prewashed Dowex MAC-3 resin was added to the mixture and left stirring overnight. The resin was then filtered off, washed several times with pure MeOH (until the filtrate was clear) and the resin was finally left overnight stirring in 2 L of NH_3 2% in MeOH. The resin was filtered off, and filtrate concentrated under reduced pressure to afford 1.9 g of basic fraction residue (1.9 %).

2.5.8. Isolation of zingerines

The basic fractions from the general catch-and-release protocol were then separated by Sephadex LH-20 column chromatography (100 g) using MeOH as eluent to give 80 fractions (10 mL each) that were combined into 7 fractions (A-G) according to RP-TLC using MeOH:H_2O 4:1 (v/v) as solvent system. Fraction F (210 mg) was then purified using semipreparative HPLC with

a linear gradient program of acetonitrile and water from 25:75 (v/v) (t=0 min) to 35:65 (t=5 min), then 55:45 (t=15 min), 100:0 (t=25 min), and finally recovery to 25:75 (t=35 min). Compound **2.7** (18.2 mg, t_R =14.7 min), compound **2.8** (5.2 mg, t_R = 19.1 min), and compound **2.9** (4.8 mg, t_R = 22.5 min) were obtained after removal of the mobile phase under reduce pressure.

2.5.9. Large scale isolation of shogaols

Pure [6]-, [8]-, and [10]-shogaol were isolated as described previously and the structures of the shogaols were confirmed by spectroscopic methods.[143, 149] Briefly, the CH_2Cl_2 extract was submitted to a silica gel column chromatography using hexanes with increasing amounts of acetone as solvent system. Shogaol-enriched fractions were obtained by TLC comparison (Hexanes:acetone 9:1 v/v as solvent system) with authentic samples and submitted to preparative HPLC using mixtures of ACN and H_2O as eluent.

2.5.10. General synthesis of zingerines

A mixture of shogaol (0.33 mmol) and adenine (0.40 mmol, 1.2 eq.) and Cs_2CO_3 (5 mg) in MeOH:H_2O 1:1 (15 mL) was stirred at room temperature for 72 h. Then, organic solvent was removed under reduced pressure and filtration, the reaction mixtures were purified by semi preparative HPLC to afford the corresponding zingerines. Accordingly, [6]-zingerine (42.7 mg), [8]-zingerine (19.4 mg), and [10]-zingerine (19.4 mg) were obtained in 36%, 28%, and 30% yields, respectively.

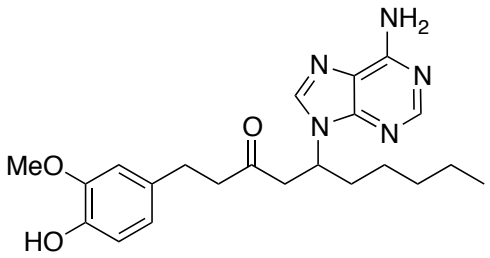

2.7

[6]-Zingerine (2.7) 5-(6-Amino-9*H*-purin-9-yl)-1-(4-hydroxy-3-methoxyphenyl)decan-3-one; pale yellow oil; $[\alpha]^{D}_{25}$=-0.004 (c. 0.03, MeOH); UV (MeOH, c=0.5 mM) λ_{max} nm: 208, 262; IR ν cm^{-1}: 3326 (N-H), 3153 (N-H), 1711 (conj. >C=O), 1514 (C=C); ^{1}H NMR(CD_3OD, 500 MHz) see Table 2-2; ^{13}C NMR (CD_3OD, 133 MHz) see Table 2-1; ESIMS *m/z* 412.3 $[M+H]^+$; ESIMS/MS *m/z* 136.1 [M+H-276.2]; HRMS *m/z* 412.2362 $[M+H]^+$ (calc. for $C_{22}H_{30}N_5O_2$ 412.2349).

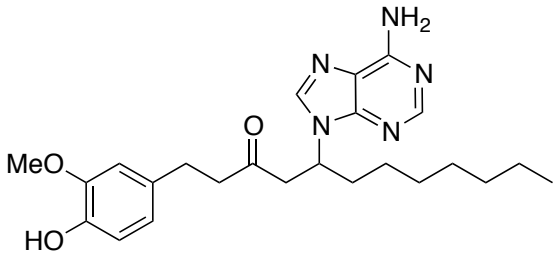

2.8

[8]-Zingerine (2.8). 5-(6-Amino-9*H*-purin-9-yl)-1-(4-hydroxy-3-methoxyphenyl)dodecan-3-one; pale yellow oil; $[\alpha]^{D}_{25}$=-0.002 (c. 0.02, MeOH); UV (MeOH, c=0.5 mM) λ_{max} nm: 208, 262; IR ν cm^{-1}: 3325 (N-H), 3153 (N-H), 1713 (conj. >C=O), 1513 (C=C); ^{1}H NMR(CD_3OD, 500 MHz) see Table 2-2; ^{13}C NMR (CD_3OD, 133 MHz) see Table 2-1; ESIMS *m/z* 440.3 $[M+H]^+$; ESIMS/MS *m/z* 136.1 [M+H-304.2]; HRMS *m/z* 440.2695 $[M+H]^+$ (calc. for $C_{24}H_{34}N_5O_3$ 440.2662).

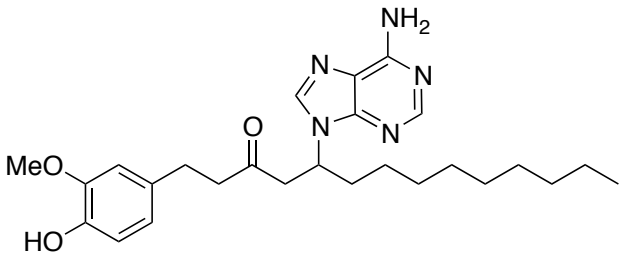

2.9

[10]-Zingerine (2.9) 5-(6-Amino-9*H*-purin-9-yl)-1-(4-hydroxy-3-methoxyphenyl)tetradecan-3-one; pale yellow oil; $[\alpha]^{D}_{25}$= -0.001 (c. 0.02 MeOH); UV (MeOH, c=0.5 mM) λ_{max} nm: 208, 262; IR ν cm^{-1}: 3326 (N-H), 3152 (N-H), 1710 (conj. >C=O), 1513 (C=C); ^{1}H NMR(CD_3OD, 500 MHz) and ^{13}C NMR (CD_3OD, 133 MHz) see Table 5.1; ESIMS *m/z* 468.3 $[M+H]^+$; ESIMS/MS *m/z* 136.1 [M+H-332.2]; HRMS *m/z* 468.2921 $[M+H]^+$ (calc. for $C_{26}H_{38}N_5O_3$ 468.2975)

Table 2-1 ^{13}C-NMR Spectroscopic data (500 MHz, CD_3OD) for [6]-, [8]-, and [9]-zingerines (**2.7-2.9**)

Atom	**2.7**	**2.8**	**2.9**
	δ_C	δ_C	δ_C
1	30.4, CH_2	30.4, CH_2	30.4, CH_2
2	45.7, CH_2	45.7, CH_2	45.7, CH_2
3	209.6, C	209.6, C	209.6, CH
4a 4b	47.7, CH_2	47.8, CH_2	47.8, CH_2
5	54.0, CH	54.0, CH	54.0, CH
6a 6b	35.1, CH_2	35.1, CH_2	35.1, CH_2
7a 7b	32.3, CH_2	32.9, CH_2	33.2, CH_2
8	26.8, CH_2	30.2, CH_2	30.6, CH_2
9	23.5, CH_2	30.1, CH_2	30.5, CH_2
10	14.3, CH_3	27.1, CH_2	30.5, CH_2
11		23.7, CH_2	30.0, CH_2
12		14.5, CH_3	27.1, CH_2
13			23.8, CH_2
14			14.6, CH_3
1'	133.7, C	133.7, C	133.7, C
2'	113.0, CH	113.0, CH	113.0, CH
3'	148.9, C	148.9, C	148.9, C
4'	145.8, C	145.9, C	145.9, C
5'	116.2, CH	116.2, CH	116.2, CH
6'	121.6, CH	121.6, CH	121.7, CH
2''	153.4, C	153.5, C	153.5, C
4''	150.6, CH	150.7, CH	150.7, CH
5''	120.4, C	120.4, C	120.5, C
6''	157.3, C	157.4, C	157.4, C
8''	142.6, CH	142.7, CH	142.6, CH
3'-OMe	56.4, CH_3	56.4, CH_3	56.4, CH_3

Table 2-2 ^{1}H-NMR Spectroscopic data (500 MHz, CD_3OD) for [6]-, [8]-, and [9]-zingerines (**2.7-2.9**)

Atom	**2.7**	**2.8**	**2.9**
	δ_H (*J* in Hz)	δ_H (*J* in Hz)	δ_H (*J* in Hz)
1	2.67, m	2.68, m	2.67, m
2	2.67, m	2.68, m	2.67, m
4a	3.39, dd (17.6, 8.8)	3.40, dd (17.8, 8.9)	3.39, dd (17.9, 8.7)
4b	3.05, dd (17.6, 4.7)	3.05, dd (17.8, 4.8)	3.05, dd (17.9, 4.9)
5	4.91, m	4.92, m	4.92, m
6a	1.82, m	1.80, m	1.80, m
6b	2.08, m	2.08, m	2.08, m
7a	0.98, m	1.24, m	1.24, m
7b	1.20, m		
8	1.20, m	1.24, m	1.24, m
9	1.20, m	1.24, m	1.24, m
10	0.81, t (6.9)	1.24, m	1.24, m
11		1.24, m	1.24, m
12		0.84, t (7.0)	1.24, m
13			1.24, m
14			0.87, t (7.0)
2'	6.63, d (2.0)	6.63, d (1.8)	6.63, d (1.9)
5'	6.59, d (8.0)	6.59, d (7.9)	6.59, d (7.9)
6'	6.44, dd (8.0, 2.0)	6.45, dd (7.9, 1.8)	6.45, dd (7.9, 1.9)
4''	8.16, br s	8.16, br s	8.16, br s
8''	8.12, br s	8.12, br s	8.12, br s
3'-OMe	3.76, s	3.76, s	3.76, s

3. BIOASSAY-GUIDED ISOLATION OF MODULATORS OF ORGANIC ANION TRANSPORTING POLYPEPTIDES (OATPs)

3.1. Introduction

Organic anion transporting polypeptides (OATPs) comprise a super-family of sodium-dependent transporters that mediate cellular uptake of many endogenous and exogenous substances. The liver-specific OATP1B1 and OATP1B3 are known to be responsible for uptake of numerous drugs (Table 3-1) and inhibition of these transporters can potentially lead to drug-drug interactions or food-drug interactions.[150, 151] Furthermore, OATP modulators can be useful pharmacologic probes.

Table 3-1 Substrates of OATP1B1 and OATP1B3 uptake activity.

OATP1B1	OATP1B3
Atrovastatin, atrasentan, bosetan, cerivastatin, enalapril, fluvastatin, methotrexate, olmesartan, pivastatin, pravastatin, rifampicin, rosuvastatin, valsartan	Digoxin, docetaxel, enalapril, fexofenadine, fluvastatin, methotrexate, olmesartan, ouabain, paclitaxel, pitavastatin, rifampicin, rosuvastatin, valsartan

The main goal of this project was to identify natural product modulators of OATP1B1 and OATP1B3 using a bioassay-guided fractionation with a functional transport assay using two radioactive-labeled substrates namely, estrone-3-sulfate and estradiol-17β-glucuronide. As previously mentioned, plants are potential sources of OATP modulators. For instance, herbal extracts used in dietary supplements have been found to affect transport by OATPs and several pure secondary metabolites from plants have been shown to interact with OATPs.[100-104] Hence, extracts and fractions obtained from South American plants were screened for effects on OATP1B1- and OATP1B3-mediated uptake of the two-model substrates estradiol-17β-

glucuronide (E17β) and estrone-3-sulfate (E3S). Several plant species, including *Rollinia emarginata* Schlecht (Annonaceae), showed interesting results, which warranted further investigation. The stem bark of this South American species is used in combination with *Ilex paraguayensis* St Hilaire (Aquifoliaceae) (common name: hierba mate), to treat migraine and as a relaxant. Antiprotozoal and antifeedant properties have been reported for this species as well.[152, 153]

This investigation represents the first bioassay-guided isolation strategy for identification of OATP modulators.[154] The biological evaluation of the isolates included in this chapter was conducted by Dr. M. Roth in Dr. B. Hagenbuch's laboratory at the University of Kansas Medical Center.

3.2. Modulators of OATP1B1 and OATP1B3 from *Rollinia emarginata*

From the organic extract of *R. emarginata*, six substrate-specific or transporter-specific modulators of OATPs were isolated and identified: the pentacyclic triterpenes ursolic acid (**3.1**) and oleanolic acid (**3.2**), the diterpene β-sitosterol (**3.3**), the monoterpene ester 8-*trans*-*p*-coumaroyloxy-α-terpineol (**3.4**), and the querecetin-glycosides rutin (**3.5**) and quercetin 3-*O*-α-L-arabinopyranosyl (1→2) α-L-rhamnopyranoside (**3.6**) (Figure 3-1). As illustrated in Figure 3-2, a classic partition scheme was followed and, based on the observed biological activity, the attention focused on hexanes and BuOH fractions which allowed for a directed isolation of pure compounds.

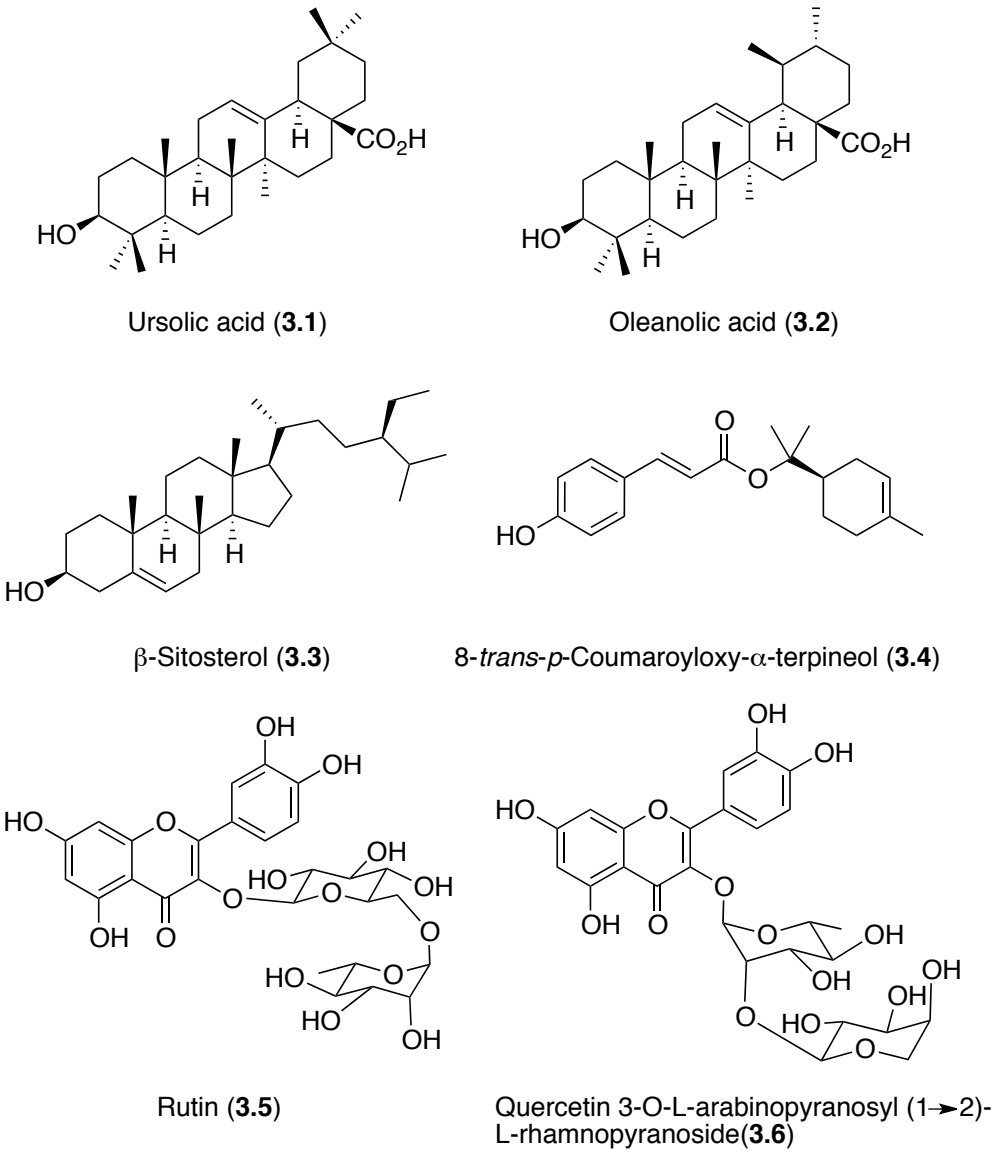

Figure 3-1 Modulators of OATP1B1 and OATP1B3 from *R. emarginata*

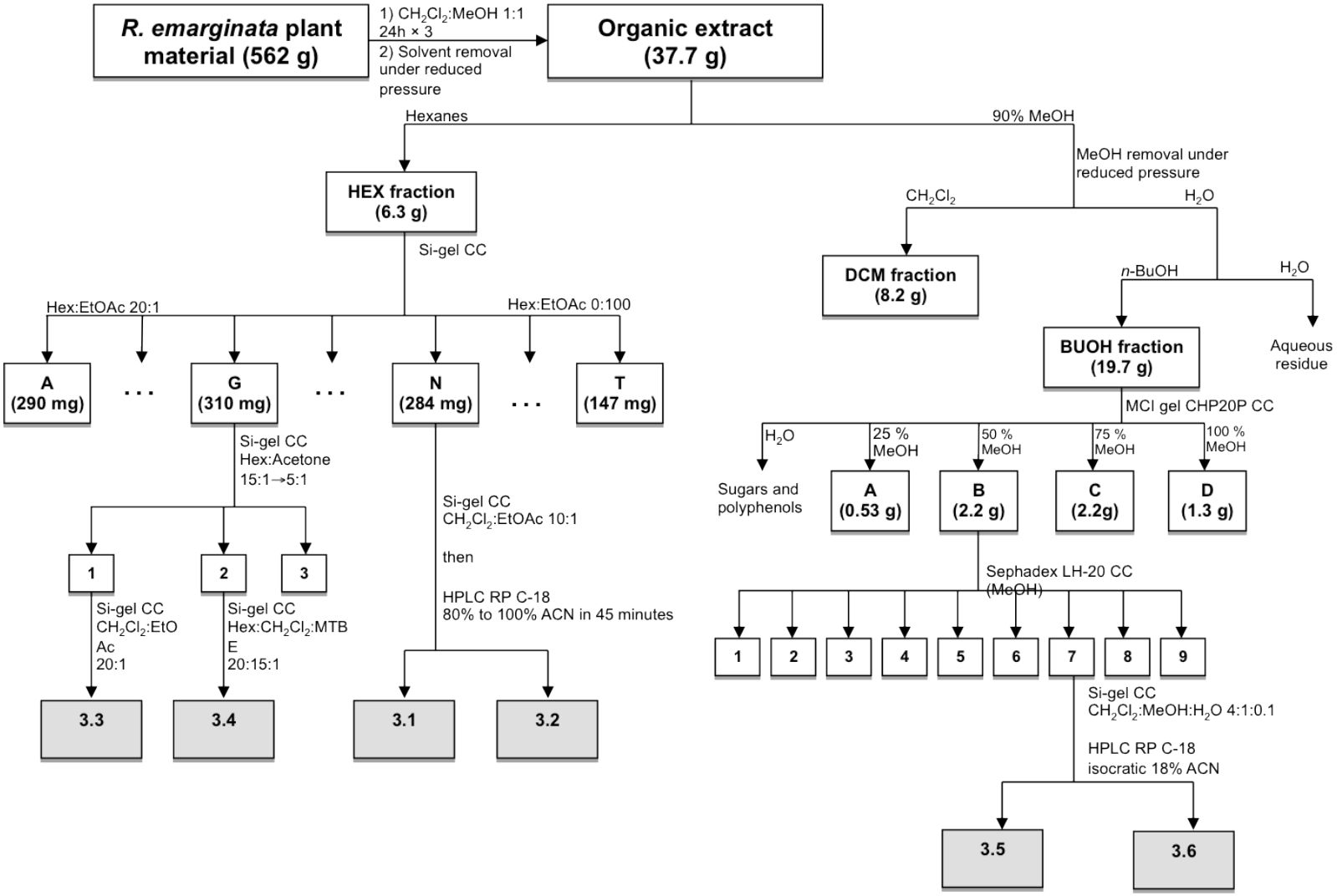

Figure 3-2 Bioassay-guided fractionation of *R. emarginata*

During the bioassay-guided isolation, each separation step was followed by functional assays performed in triplicate on 96-well plates using aliquots of the original fractions solubilized in DMSO. Two model substrates, E17β (OATP1B1: K_m = 5.4 μM; OATP1B3: K_m = 15.8 μM) and E3S (OATP1B1 high affinity component: K_m = 0.22 μM; OATP1B3: K_m = 58 μM) were used to identify substrate-dependent effects on transport.[155, 156] Fractions were co-incubated with wild-type or OATP-expressing cells with uptake buffer containing 0.03 μg/ml plant extracts or fractions and 0.1 μM E17β or 1 μM E3S for 5 minutes at 37˚C. Fractions showing promising results were further fractionated (Figure 3-3). The initial extract inhibited uptake of both substrates by both transporters; however, the hexane (HEX) and butanol (BUOH) fractions both showed preferential inhibition of OATP1B1-mediated transport of E17βG. From the HEX fraction, four known compounds (**3.1**-**3.4**) were isolated and characterized. These compounds were identified using spectroscopic data and compared with literature data.[157-159] Ursolic acid (**3.1**), oleanolic acid (**3.2**), and 8-*trans*-*p*-coumaroyloxy-α-terpineol (**3.4**) inhibited OATP1B1 transport of E17β by more than 50% while having a minimal effect on OATP1B1 transport of E3S (Figure 3-3). Interestingly, the butanol subfraction B strongly stimulated uptake of E3S by OATP1B3, while inhibiting uptake of E17βG by both OATPs. Purification of components of fraction BuOH-B revealed the presence of two known glycosylated flavonoids rutin (**3.5**) and quercetin 3-*O*-α-L-arabinopyranosyl (1→2) α-L-rhamnopyranoside (**3.6**).[159, 160] After testing, it was shown that **3.6** was the responsible for the observed activity.

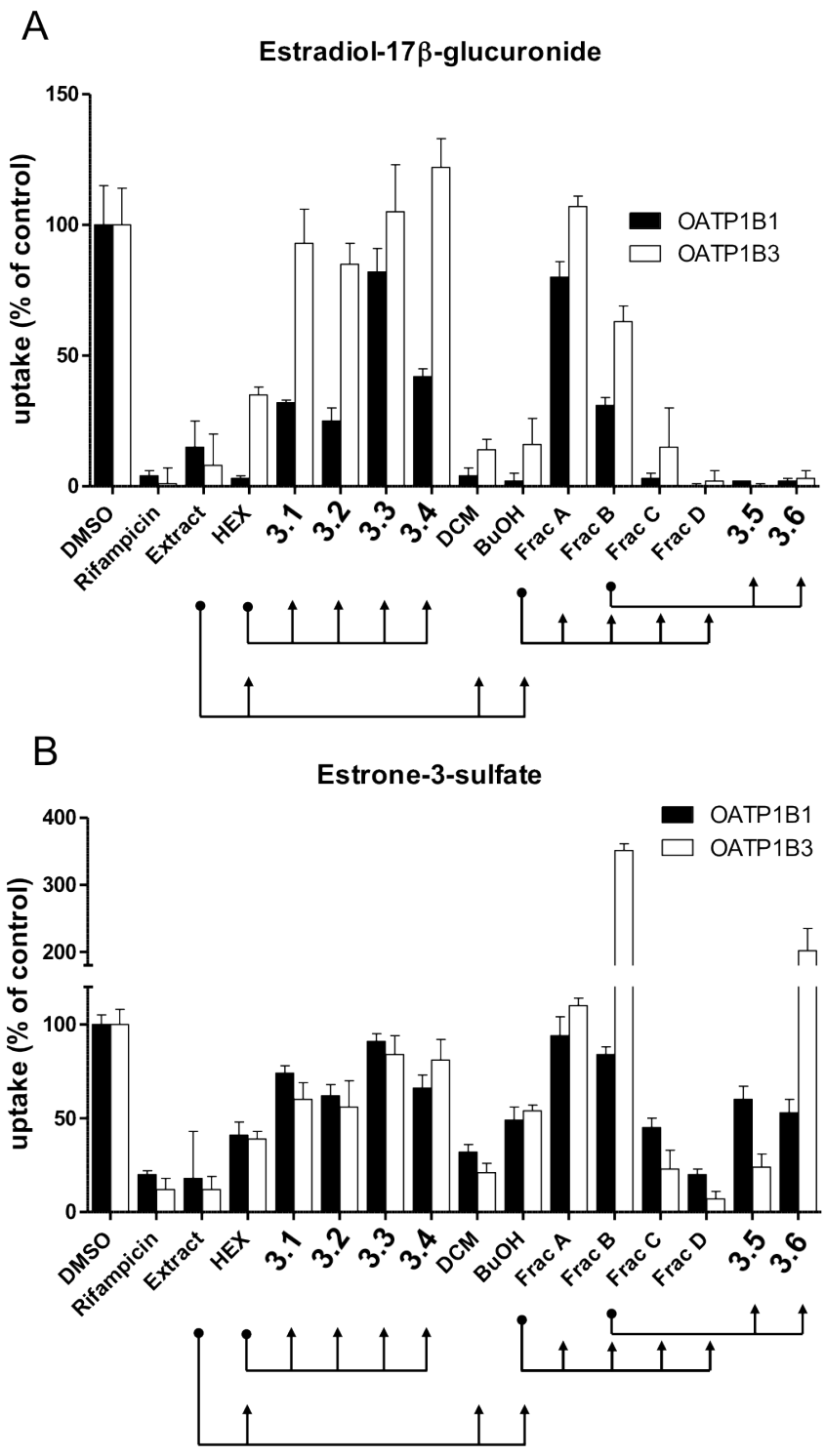

Figure 3-3 Effect of *R. emarginata* extract and its fractions on OATP1B1- and OATP1B3-mediated uptake of (A) E17β and (B) E3S

The ability of ursolic acid (**3.1**), oleanolic acid (**3.2**), and 8-*trans-p*-coumaroyloxy-α-terpineol (**3.4**) to modulate the OATP1B1- and OATP1B3-mediated transport of 0.1 μM E17β or E3S was measured for 20 seconds at 37˚C. All three compounds significantly inhibited uptake of E17β by OATP1B1 ($p < 0.001$), while having no effect on uptake by OATP1B3 (Figure 3-4). Unfortunately, β-sitosterol (**3.3**) could not be characterized in detail due to its very low solubility in DMSO. 8-*trans-p*-Coumaroyloxy-α-terpineol (**3.4**) had a similar effect on the uptake of E3S, inhibiting OATP1B1- but not OATP1B3-mediated transport. However, uptake of E3S by both transporters was inhibited to an equal extent by ursolic acid (**3.1**) and oleanolic acid (**3.2**). Inhibition of E17βG transport by OATP1B1 was further studied with a concentration dependency. Ursolic acid (**3.1**) and oleanolic acid (**3.2**) inhibited uptake of E17β with IC_{50} values of 15.3 μM and 4.2 μM, respectively (Figure 3-5). Although the structure of ursolic acid (**3.1**) and oleanolic acid (**3.2**) are closely related, the inhibition of substrate uptake by the OATPs was not identical showing an interesting structure-activity relationship. In principle, other commercially available pentacyclic triterpenes (i.e. betulinic acid) could be used to further investigate the interaction of this type of compound with the OATPs. In addition, these pentacyclic triterpenes commonly found in edible and medicinal plants like prunes, plums, rosemary, and basil have been investigated as chemopreventive agents for cancer and other diseases.[161-163] The role of OATP modulation by ursolic acid and oleanolic acid in any of these reported indications or potential food-drug interaction remains to be determined. 8-*trans-p*-Coumaroyloxy-α-terpineol (**3.4**) was found to be the weakest inhibitor; therefore, the full plateau of inhibition could not be determined due to its limited solubility.

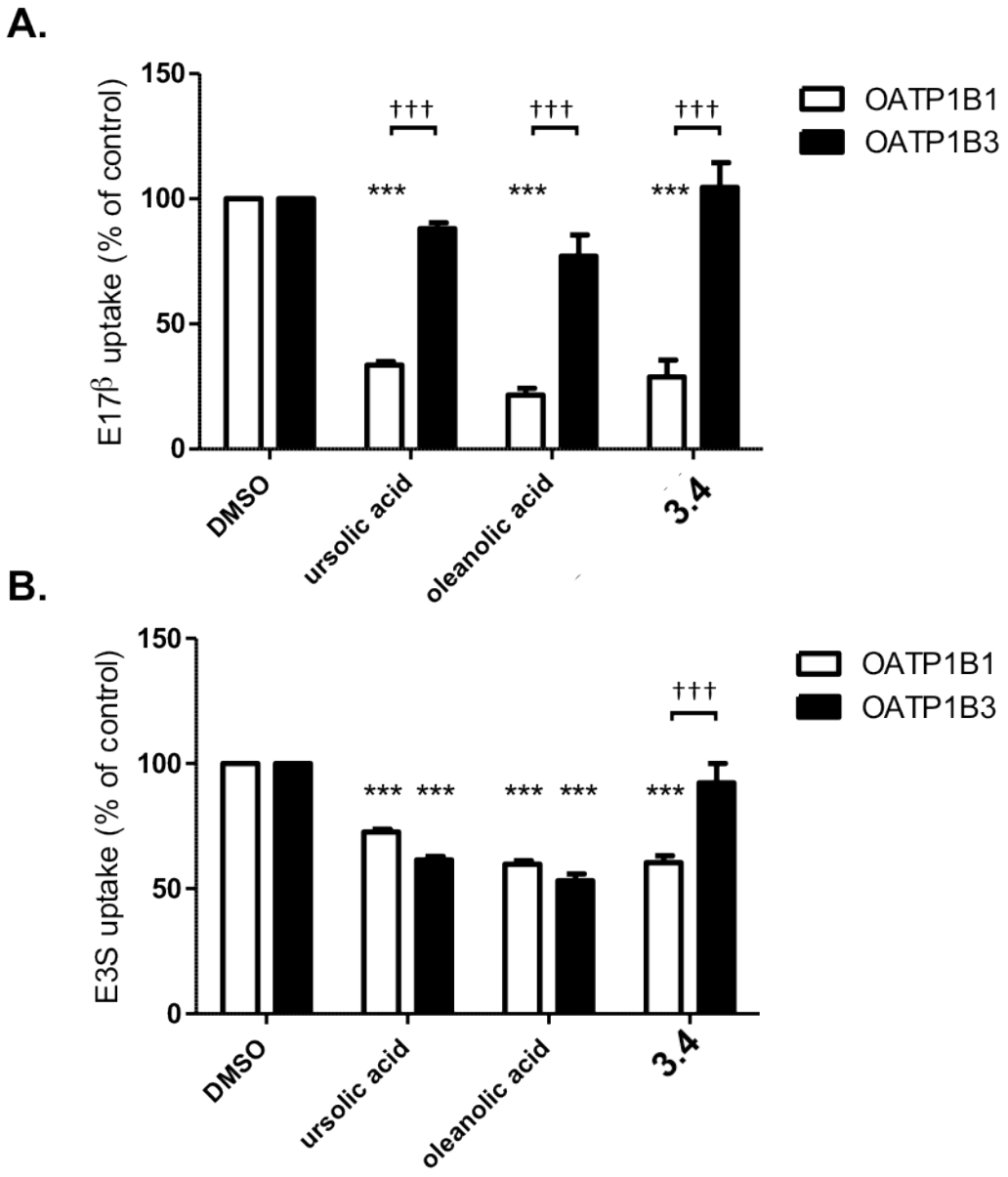

Figure 3-4 Effect of ursolic acid (**3.1**), oleanolic acid (**3.2**), and 8-*trans-p*-coumaroyloxy-α-terpineol (**3.4**) on OATP-mediated uptake

*** P < 0.001 from the vehicle control), (††† P < 0.001 between OATP1B1 and OATP1B3

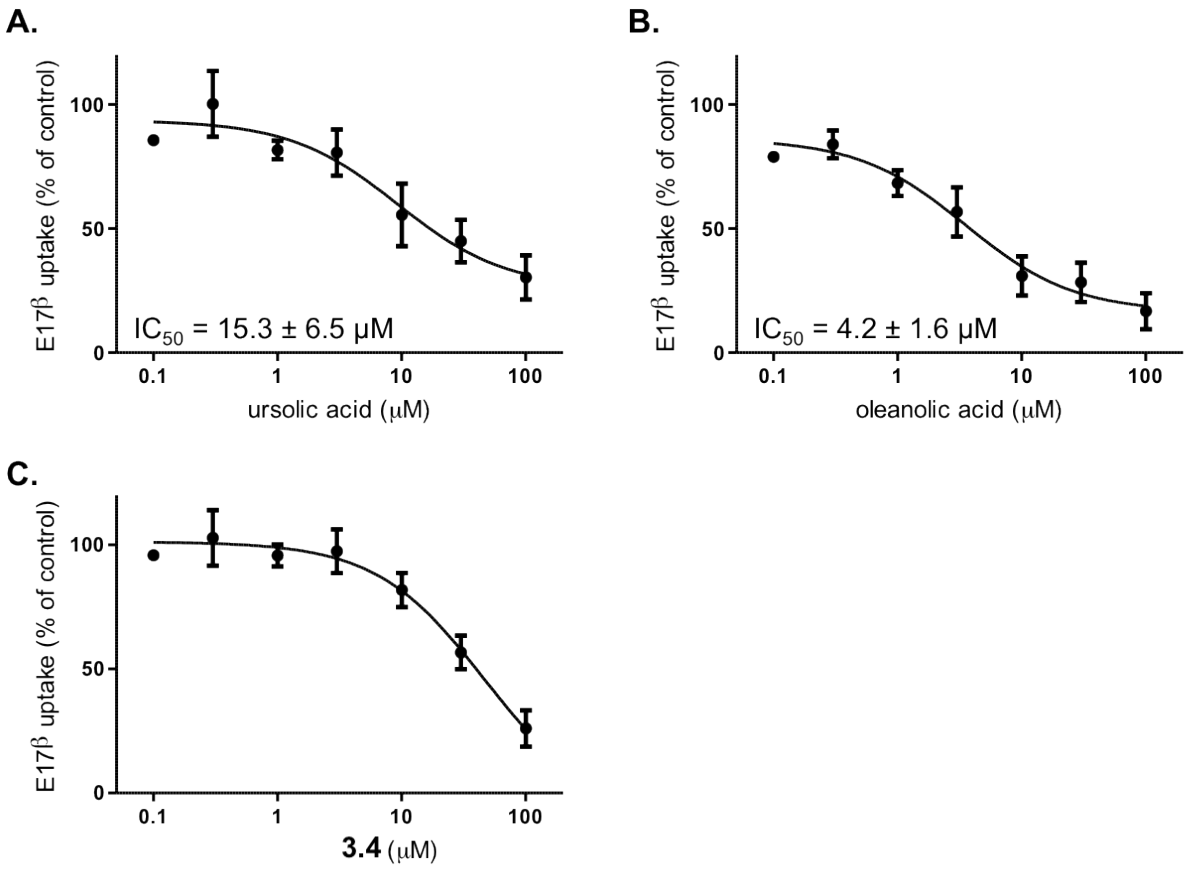

Figure 3-5 Concentration-dependent effect of ursolic acid (**3.1**), oleanolic acid (**3.2**), and 8-*trans-p*-coumaroyloxy-α-terpineol (**3.4**) on OATP1B1-mediated uptake of E17β

Kinetic analysis of E17G and E3S uptake was performed in the presence of each interacting compound or the vehicle control, and results are shown in Table 3-2. The affinity of E17βG for OATP1B1 was slightly decreased by each of the four substrates tested. The maximal rate of transport (V_{max}) was not changed by ursolic acid (**3.1**) or 8-*trans-p*-coumaroyloxy-α-terpineol (**3.4**), but was somewhat decreased by both oleanolic acid (**3.2**) and quercetin 3-*O*-α-L-arabinopyranosyl (1→2) α-L-rhamnopyranoside (**3.6**) indicating that none of the observed changes reached statistical significance. In initial experiments, ursolic acid (**3.1**), oleanolic acid

(**3.2**), and 8-*trans*-*p*-coumaroyloxy-α-terpineol (**3.4**) did not alter the low-affinity, high-capacity component of OATP1B1-mediated transport of estrone-3-sulfate; therefore only the high-affinity component was studied. As for E17β transport, all four compounds caused small but non-significant decreases in substrate affinity, although none altered the maximal rate of transport.

Quercetin-3-*O*-α-L-arabinopyranosyl-(1→2)-α-L-rhamnopyranoside (**3.6**) showed a very interesting behavior by stimulating the uptake of E3S by OATP1B3, while inhibiting the uptake of the same substrate by OATP1B1. Hence, to further investigate the substrate-dependent effects of **3.6**, uptake of 0.1 μM E17β or E3S by OATP1B1 and OATP1B3 was measured for 20 seconds at 37˚C in the presence of increasing concentrations of **3.6**. Uptake of E17β was inhibited by **3.6** to a similar extent for both transporters (Figure 3-6). OATP1B1-mediated uptake of E3S was inhibited to a lesser extent (IC_{50} = 130 μM). The stimulation of OATP1B3-mediated uptake of E3S was also concentration dependent, with an EC_{50} of 6.8 μM. At concentrations higher than 100 μM, the effect of **3.6** on E3S decreased, although it remained stimulatory to the highest tested concentration of 1 mM. Quercetin-3-*O*-α-L-arabinopyranosyl-(1→2)-α-L-rhamnopyranoside (**3.6**), however, significantly altered the kinetic parameters of OATP1B3-mediated transport of both model substrates, as illustrated in Figure 3-7. OATP1B3-mediated E17β uptake was inhibited in a non-competitive manner. Inclusion of 25 μM (squares) or 75 μM (triangles) of **3.6** in the uptake media decreased the maximal rate of transport (V_{max}) from 280 ± 45 to 188 ± 40 (not statistically significant) and 83 ± 9 pmol/mg*min ($p < 0.05$), respectively. Quercetin-3-*O*-α-L-arabinopyranosyl-(1→2)-α-L-rhamnopyranoside (**3.6**) had no effect on the apparent affinity (K_m) for E17β (16 ± 9, 17 ± 5, and 18 ± 9 μM, respectively). Uptake of E3S by

OATP1B3 was measured in the presence of 50 μM of **3.6** or 1% DMSO. As was the case with E17βG, the V_{max} was decreased, from 2.12 ± 0.34 to 1.07 ± 0.05 nmol/mg*min ($p < 0.05$). However, the K_m was also decreased nearly 10-fold, from 93 ± 38 μM to 15 ± 3 μM ($p < 0.005$). This explains the stimulation of transport seen at low E3S concentrations despite the decrease in V_{max}. Further investigation of this effect on OATP1B3 revealed that the maximal rate of transport (V_{max}) was reduced for both substrates (Figure 3-7). The apparent substrate affinity (K_m) for E17βG was unchanged, causing inhibition of transport at all concentrations studied. In contrast, the affinity for E3S was increased 10-fold, leading to stimulation of transport at low substrate concentrations, and inhibition of transport at high substrate concentrations.

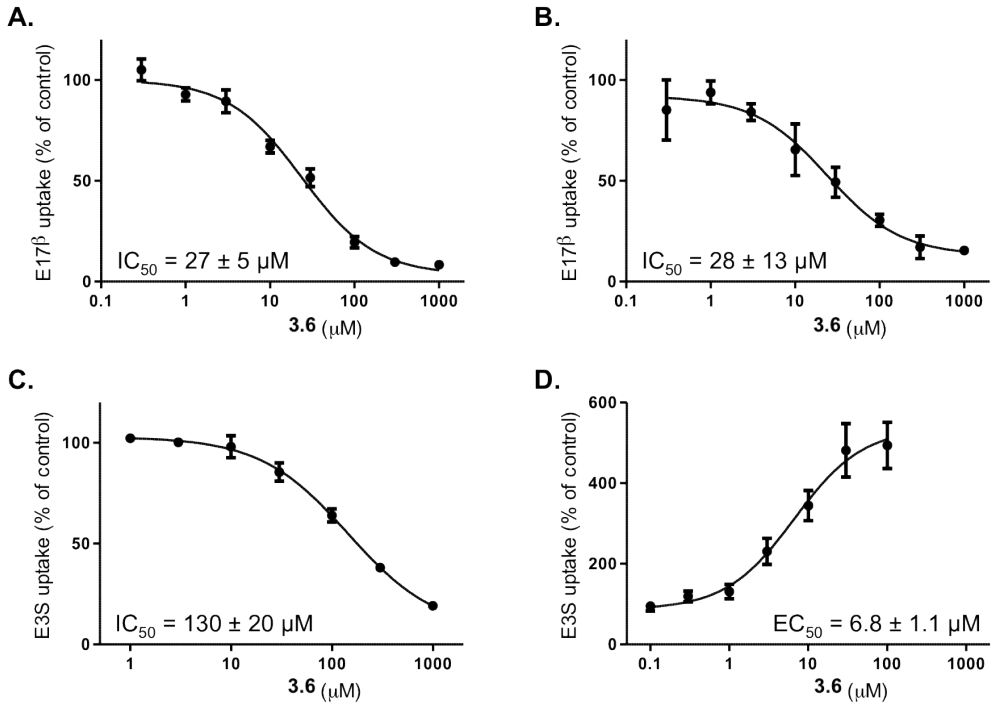

Figure 3-6 Concentration-dependent effect of quercetin-3-*O*-α-L-arabinopyranosyl-(1→2)-α-L-rhamnopyranoside (**3.6**) on OATP-mediated uptake of E17β and E3S. OATP1B1 (**A**, **C**) or OATP1B3 (**C**, **D**)

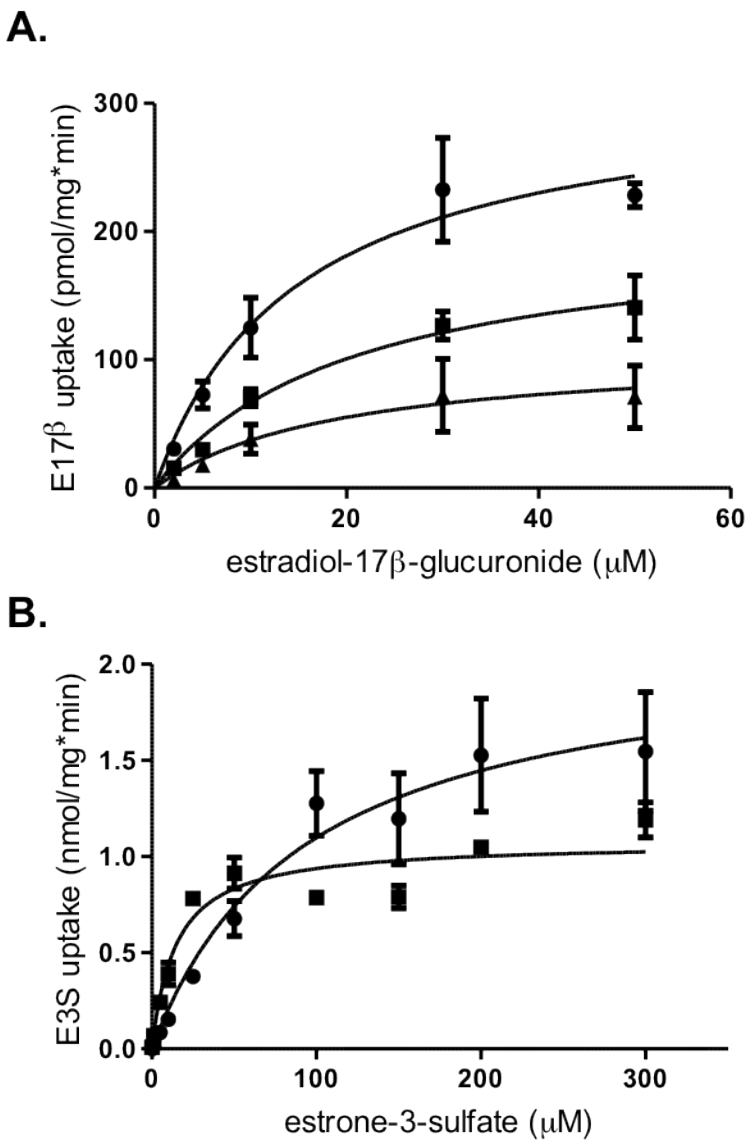

Figure 3-7 Effect of **3.6** on OATP1B3-mediated transport. **A.** Cells were incubated with increasing concentrations of E17β in the presence of 25 μM (squares) or 75 μM (triangles) **3.6**, or the vehicle control (0.5% DMSO, circles) under initial linear rate conditions. **B.** Cells were incubated with increasing concentrations of E3S in the presence of 50 μM **3.6** (squares) or the vehicle control (circles) under initial linear rate conditions

The function of transporters can be inhibited or stimulated by a number of mechanisms. However, allosteric interaction and competitive inhibition seem to best fit the observed substrate-dependent and OATP-subtype specific effects for the isolates. There is evidence that OATPs have multiple binding sites, therefore a compound may behave differently in two different OATP isoforms with different binding sites. This competitive inhibition would be expected to decrease affinity for the substrate that shares a binding site, while not affecting the V_{max}. As relatively weak inhibitors, ursolic acid (**3.1**), oleanolic acid (**3.2**), and 8-*trans-p*-coumaroyloxy-α-terpineol (**3.4**) did not show a statistically significant effect on the kinetic parameters of OATP1B1- or OATP1B3-mediated uptake, suggesting that if they are substrates, they have very low-affinity. These three compounds may bind to a portion of OATP1B1 or OATP1B3, sterically hindering either the binding or the translocation of substrates. In the case of quercetin-3-*O*-α-L-arabinopyranosyl-(1→2)-α-L-rhamnopyranoside (**3.6**), this binding could also cause a conformational change in OATP1B3 that increases the affinity of the transporter for E3S while not affecting the E17β binding site.

Interestingly, although **3.6** stimulated transport of E3S, the structurally similar **3.5** did not show the same effect. Both compounds share the same flavonoid core (quercetin), however the identity and connectivity of the sugars in the moiety are different. The three-dimensional minimized-energy conformations of **3.5** (red) and **3.6** (blue) (Figure 3-8) were calculated and aligned using SYBYL. Clearly, despite the similarity in the carbon-skeletons, the sugar moieties have very different conformations and the relative orientation of the aromatic B-ring with respect to the flavonoid core plane differs significantly in both structures. Glycosylated flavonoids are distributed in higher plants ubiquitously, and many of the fruits and vegetables in our diet

contain large amounts of this type of compounds. Flavonoids are better known for their antioxidant activity and they are part of many herbal supplements sold over-the-counter. Consequently, flavonoid-rich herbals or foods can potentially lead to interactions with drugs that are taken up by OATP1B1 or OATP1B3.

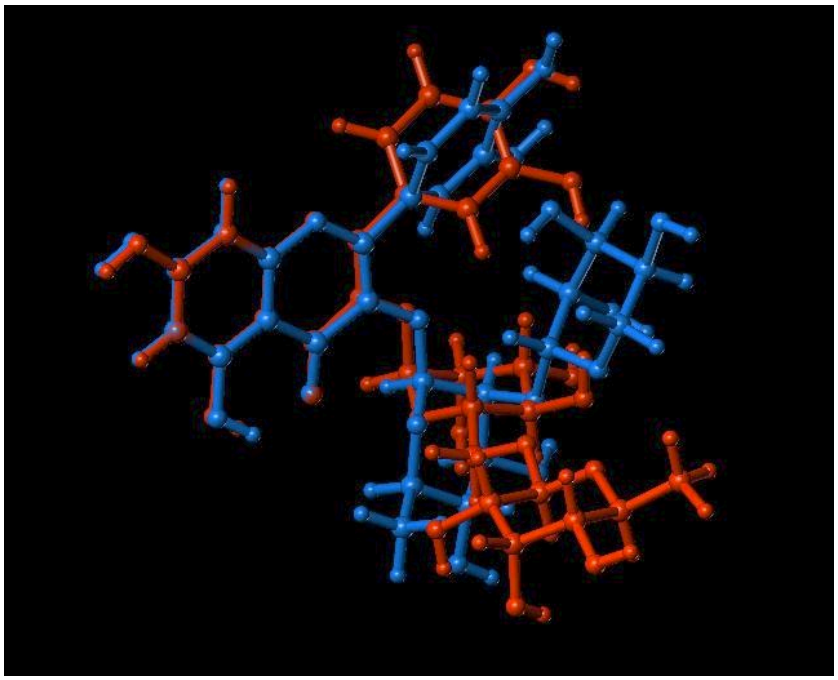

Figure 3-8 Conformation of rutin (**3.5,** blue) and quercetin-3-*O*-α-L-arabinopyranosyl-(1→2)-α-L-rhamnopyranoside (**3.6**, red) after MM2 energy minimization protocol using SYBYL

This work represents the first successful bioassay-guided isolation campaign for OATP modulator identification from a plant source. We have been able to show that such an approach is possible (proof-of-concept) and can be further applied to other OATPs in order to identify molecules with interesting effects on this type of transporters.

Table 3-2 Kinetics of OATP-mediated transport in the absence and presence of modulators

OATP1B1			
Substrate	Inhibitor	K_m (μM)	V_{max} (pmol/mg protein/min)
E17βG	None	7 ± 1	175 ± 11
	3.1	20 ± 11	217 ± 60
	3.2	13 ± 3	117 ± 10
	3.4	36 ± 19	258 ± 86
	3.6	15 ± 6	92 ± 18
E3S[1]	None	0.5 ± 0.1	96 ± 10
	3.1	0.8 ± 0.1	105 ± 8
	3.2	0.7 ± 0.1	85 ± 5
	3.4	1.3 ± 0.3	102 ± 10
	3.6	0.8 ± 0.2	93 ± 8
OATP1B3			
Substrate	Inhibitor	K_m (μM)	V_{max} (pmol/mg protein/min)
E17βG	None	16 ± 9	280 ± 45
	3.1	n/a	n/a
	3.2	n/a	n/a
	3.4	n/a	n/a
	3.6 (25 μM)	17 ± 5	188 ± 40
	3.6 (75 μM)	18 ± 9	83 ± 9*
E3S	None	93 ± 38	2120 ± 340
	3.1	---	---
	3.2	---	---
	3.4	n/a	n/a
	3.6 (50 μM)	15 ± 3**	1070 ± 50

All inhibitors were used at 100 μM unless indicated. [1]High affinity component; * = $p < 0.05$; ** = $p < 0.005$; n/a = no significant inhibition of 0.1 μM substrate by 100 μM inhibitor; --- = no apparent inhibition at the concentrations required to determine kinetics

3.3. Green tea modulation of OATPs: NMR-based metabolomics as a dereplication tool

Green tea is probably one of the most popular beverages worldwide and its consumption is associated with multiple health benefits.[164] Catechins, the major metabolites present in green tea, are believed to be responsible for most of the biological activities attributed to this beverage. Particularly, liver-related disease risks can be reduced by green tea consumption as described by a number of clinical and *in vitro* studies.[165-167] Intriguingly, most of the *in vitro* studies are preformed with the purified catechins, especially epigallocatechin gallate (EGCG), even when the bioavailability of this type of compounds is extremely low as they are highly metabolized before they can reach the bloodstream.[168] Although valuable information can be obtained from *in vitro* studies with the purified green tea catechins, it is an over-simplified model when compared with whole green tea extracts. Like other herbals, infused green tea contains hundreds of compounds and their role in the biological activity is not well understood. In fact, other components besides EGCG present in green tea have been shown to alter the catechin absorption and disposition.[169] Conversely, working with green tea extracts can be very challenging and multivariate analysis tools are needed in order to cope with the complexity of the mixtures. For instance, a multivariate-approach allowed to assess the quality of 200 kinds of tea using ^{1}H NMR.[170] Also, GC-MS and ^{1}H NMR-based metabolomics investigation of human urine revealed a more comprehensive picture of the metabolic changes suffered after the ingestion of green tea.[171]

For this project, our objective was to use NMR-based metabolomics as a dereplication tool to identify compounds present in aqueous extracts of several commercial green teas responsible for inhibition of OATP1B1-mediated E3S uptake. Previous work in our research group has

demonstrated the effects of individual green tea catechins over OATPs. ECG and EGCG were shown to inhibit the uptake of E3S by OATP1B1.[99] The aqueous green tea extracts were prepared using hot water as is done for regular tea infusions. A total of 35 commercial samples of green tea (Table 3-3, Experimental data) were analyzed using ^{1}H NMR (500 MHz, DMSO-d_6) (Figure 3-9).

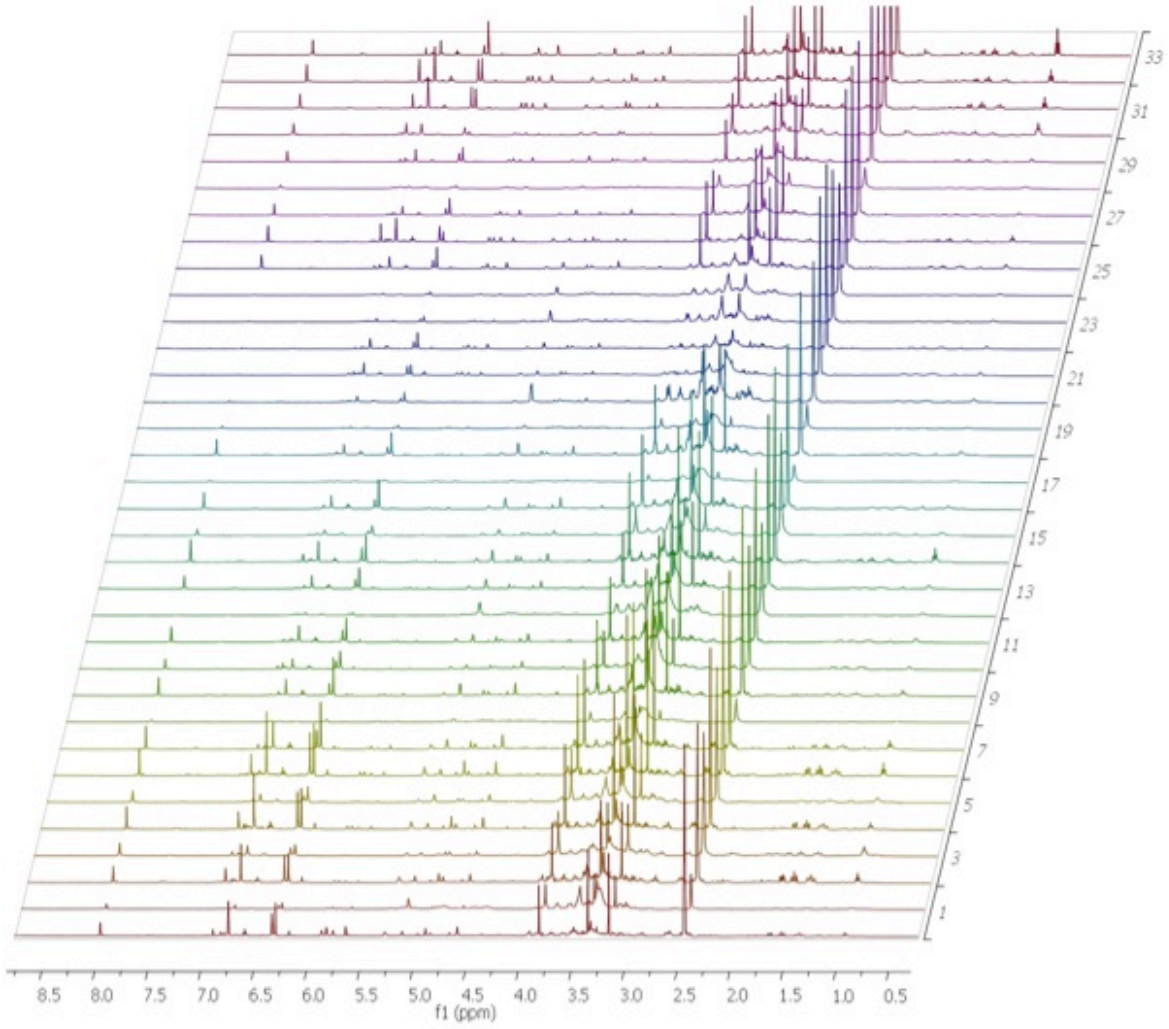

Figure 3-9 Stacked ^{1}H NMR spectra of commercial green tea samples

The ^{1}H NMR signals of the main catechins as well as those of caffeine were assigned in the complex mixture using purified catechins, 2D NMR experiments, and literature data as illustrated in Figure 3-10 (see Table 3-2, Experimental Section).[172] In addition, using the residual peak from DMSO-d_6 as internal standard, the catechins as well as caffeine were quantified as described by Pierens *et al*.[173] For validation purposes, caffeine concentration in the samples was also determined by standard HPLC analysis and compared with the results obtained by NMR (Figure 3-11).

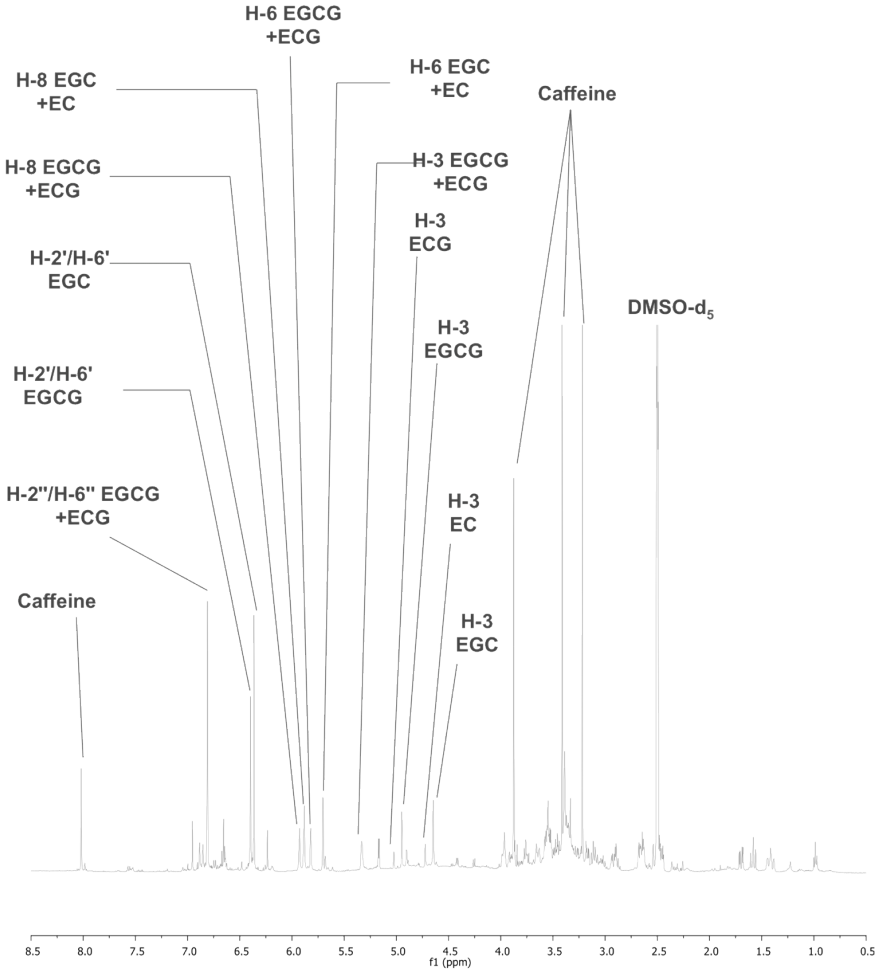

Figure 3-10 ^{1}H NMR Signal assignment of catechins and caffeine (EC: epicatechin, EGC: epigallocatechin, ECG: epicatechingallate, EGCG: epigallocatechingallate)

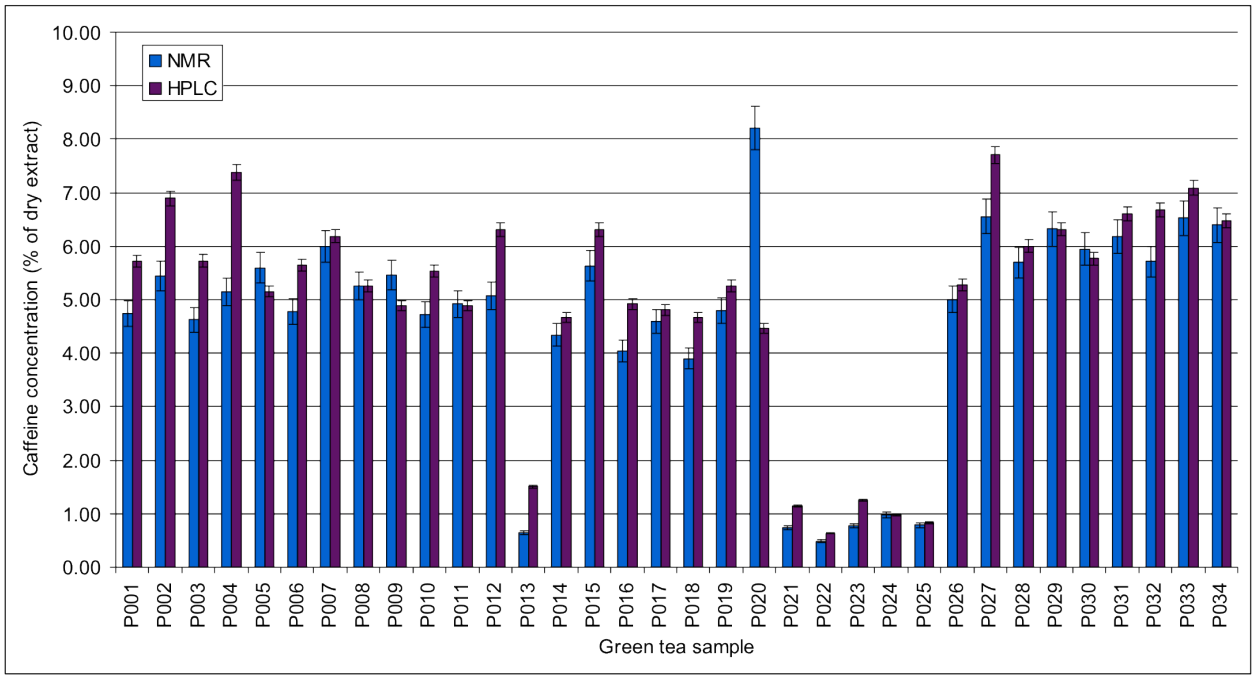

Figure 3-11 Caffeine concentration calculated using NMR- and HPLC-based methods

The green tea extracts' ability to inhibit the OATP1B1-mediated uptake of E3S was evaluated as described previously. As shown in Figure 3-12, significant variations were observed among the analyzed samples that can not be readily explained neither by simple visual inspection of the NMR data nor by the EGCG concentration in the samples. If the EGCG concentration in the samples is plotted against the inhibition of OATP1B1-mediated E3S uptake, a negative relationship is observed with a very poor correlation (R^2=0.18), suggesting that other variables may be contributing to the measured biological activity (Figure 3-13).

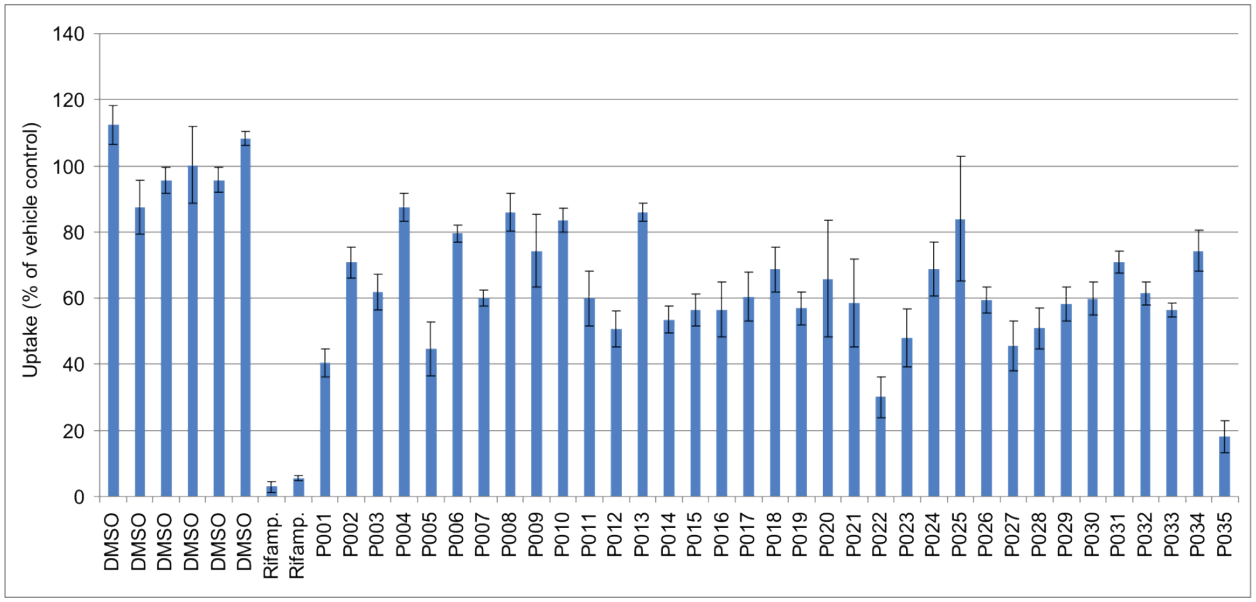

Figure 3-12 OATP1B1 uptake inhibition of E3S by commercial green tea sample extracts.

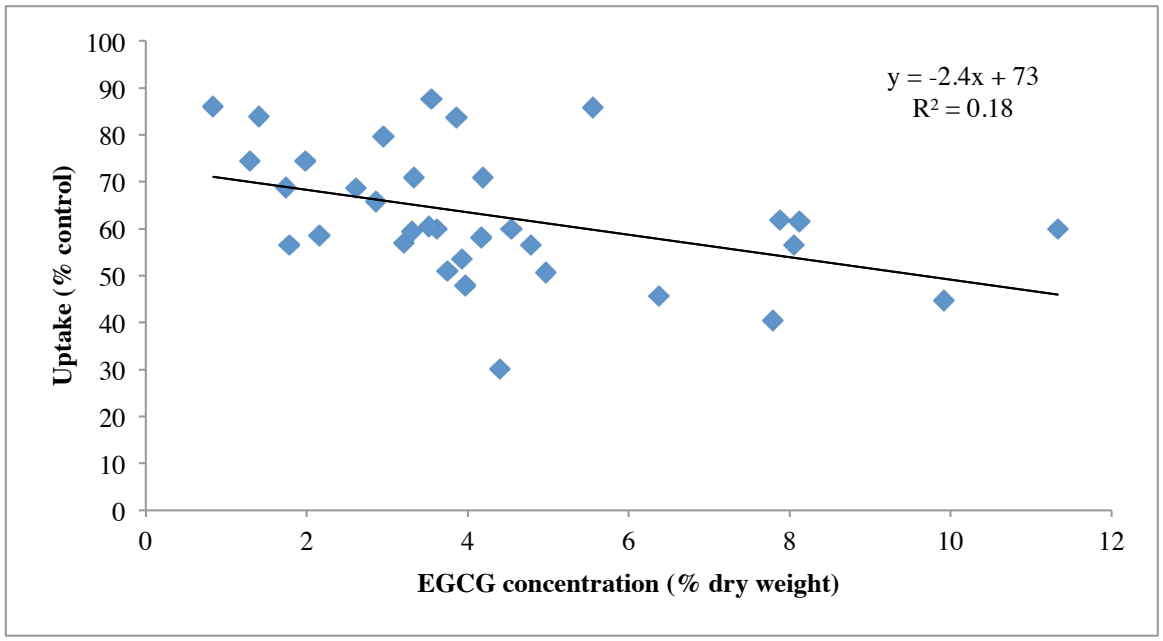

Figure 3-13 OATP1B1-mediated E3S uptake inhibition by commercial green tea samples vs. calculated EGCG concentration

In order to analyze the entire data set, a multivariate analysis protocol was conducted following three steps including data acquisition, data cleaning and transformation (bucketing), and multivariate analysis (Figure 3-14). In the case of the green tea ^{1}H NMR data set, the NMR spectra were transformed into data amenable for statistical analysis by dividing it into small regions containing integral and chemical shift information (*bucketing*). The resulting data matrix was then analyzed using the multivariate partial least squares (PLS). The goal of the multivariate analysis was to reduce the number of variables by linear combination of the original buckets (spectral regions). Finally, the new variables provided information about the regions of the NMR spectrum that were important in order to explain the samples' variability and the relationship with the observed property (uptake inhibition).

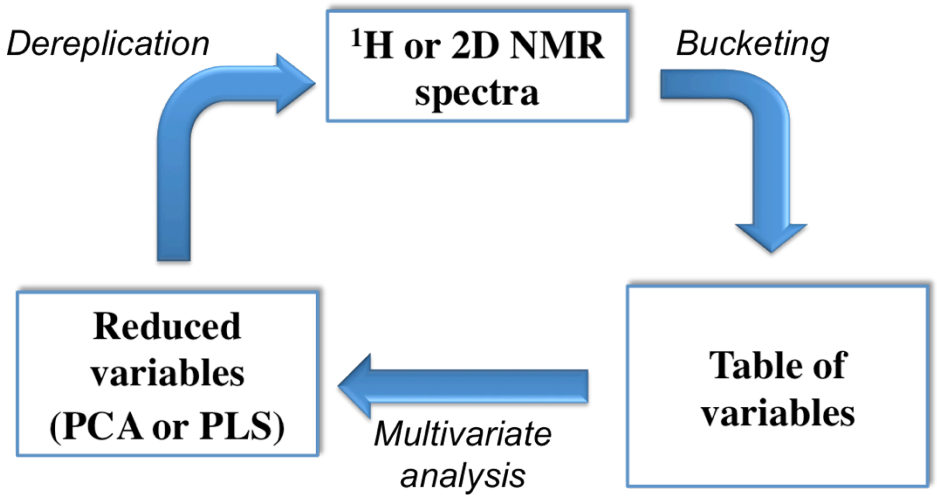

Figure 3-14 Flow chart showing the steps in a NMR-based metabolomics analysis

First, each ^{1}H NMR spectrum was aligned using the solvent residual peak and the bucketing was done using the software AMIX (Bruker) that allowed importing NMR spectra directly from

TopSpin (Bruker) acquisition interface. The resulting data matrix (34 samples × 400 buckets = 13,600 data points) and the OATP1B1-mediated E3S uptake inhibition were fed into the statistical software SIMCA P+. Next, a PLS analysis was performed which, unlike principal component analysis (PCA), correlates the NMR bucketing data (matrix) with the OATP1B1 uptake inhibition (vector). Two new combined variables (t_1 and t_2) were generated and the distribution map of the samples in the new statistical space is shown in Figure 3-15. The variable t_1 showed a good correlation with the uptake inhibition values (Figure 3-16). Samples with lower percentage of inhibition (more active) had negative t_1 values and samples with higher percentage of inhibition (less active) had positive t_1 values. The loading plot of variable t_1 (Figure 3-16) showed the statistical weights associated with each spectral region or bucket. Negative loading values corresponded with regions in the spectrum that are important for stronger inhibition of OATP1B1-mediated E3S uptake (lower percentage of uptake inhibition). With those regions identified in the spectrum, a more careful analysis of the NMR data can be performed using 2D NMR experiments, model compounds, and literature data. As expected, the statistical model allowed us to identify signals corresponding to the catechins EGCG and ECG as relevant for stronger uptake inhibition. Interestingly, a number of signals in the spectrum not related with catechins were also identified. As shown in Figure 3-18, the 2D NMR experiment DQFCOSY allowed identification of spin systems associated with *p*-substituted cinnamic-type fragment and polyoxygenated cyclohexene-type structure. The first fragment was identified based on the observed *trans*- and *para*- coupling constants and the chemical shift suggested a carbonyl-conjugated system. The CH_2-CH-CH-CH-CH_2 sequence in the cyclohexane fragment was readily identified from the DQFCOSY experiment, however the cyclic structure was suggested based on the large geminal coupling observed for the menthylene groups. Based on these

fragments, the compounds *p*-coumaroyl quinic acid and theogalline were proposed as both compounds are known to occur in green tea and the ^{1}H NMR signals are consistent with those reported in the literature. Although these minor components of green tea were not isolated and evaluated as inhibitors of OATP1B1-mediated uptake of E3S to validate the previous hypothesis, we demonstrated that a metabolomic analysis could be applied for analysis of complex natural products mixtures as a dereplication tool. In fact, only in recent years the potential of metabolomic analysis of crude extracts has been recognized and more applications are expected to appear in a near future.[174]

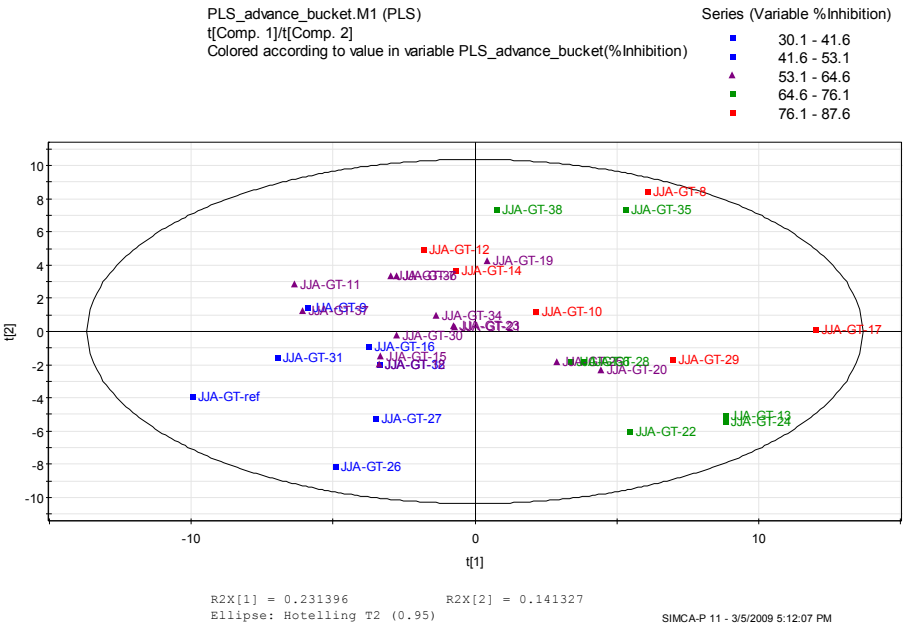

Figure 3-15 PLS t_1/t_2 score plot of the model for the green tea samples effect on OATP1B1 mediated E3S uptake

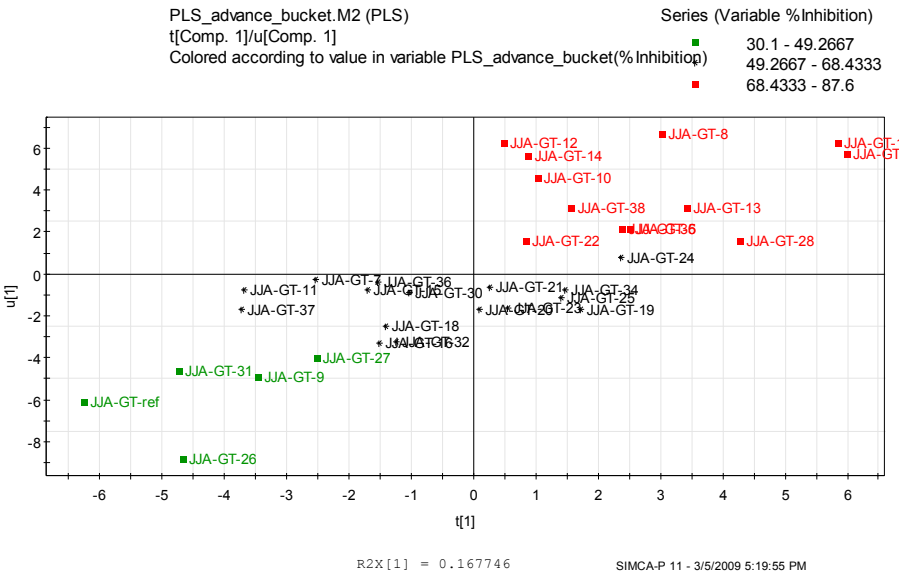

Figure 3-16 PLS t_1/u_1 score plot of the model for the green tea effect on OATP1B1-mediated E3S uptake.

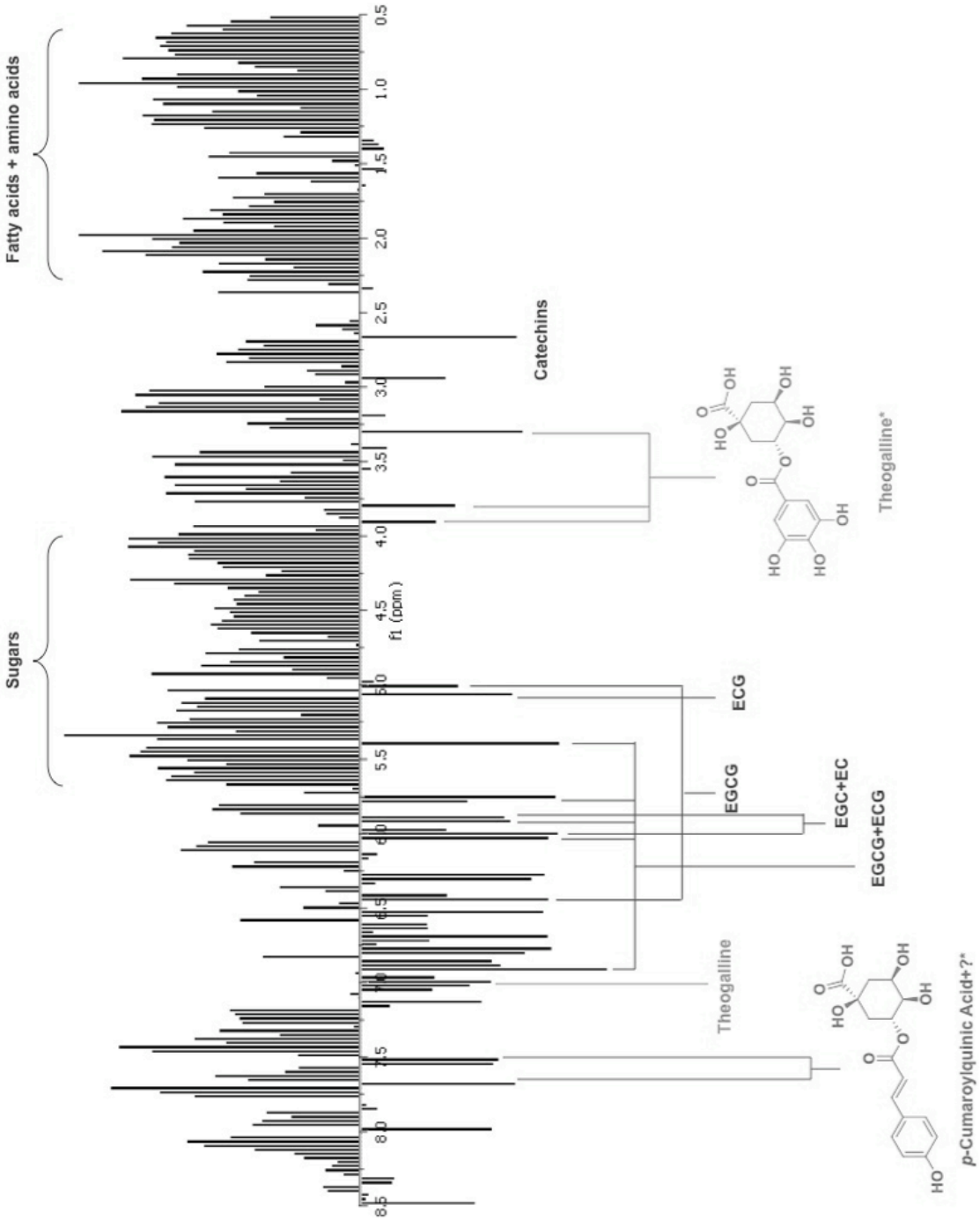

Figure 3-17 Loading plot of PLS analysis and suggested compounds

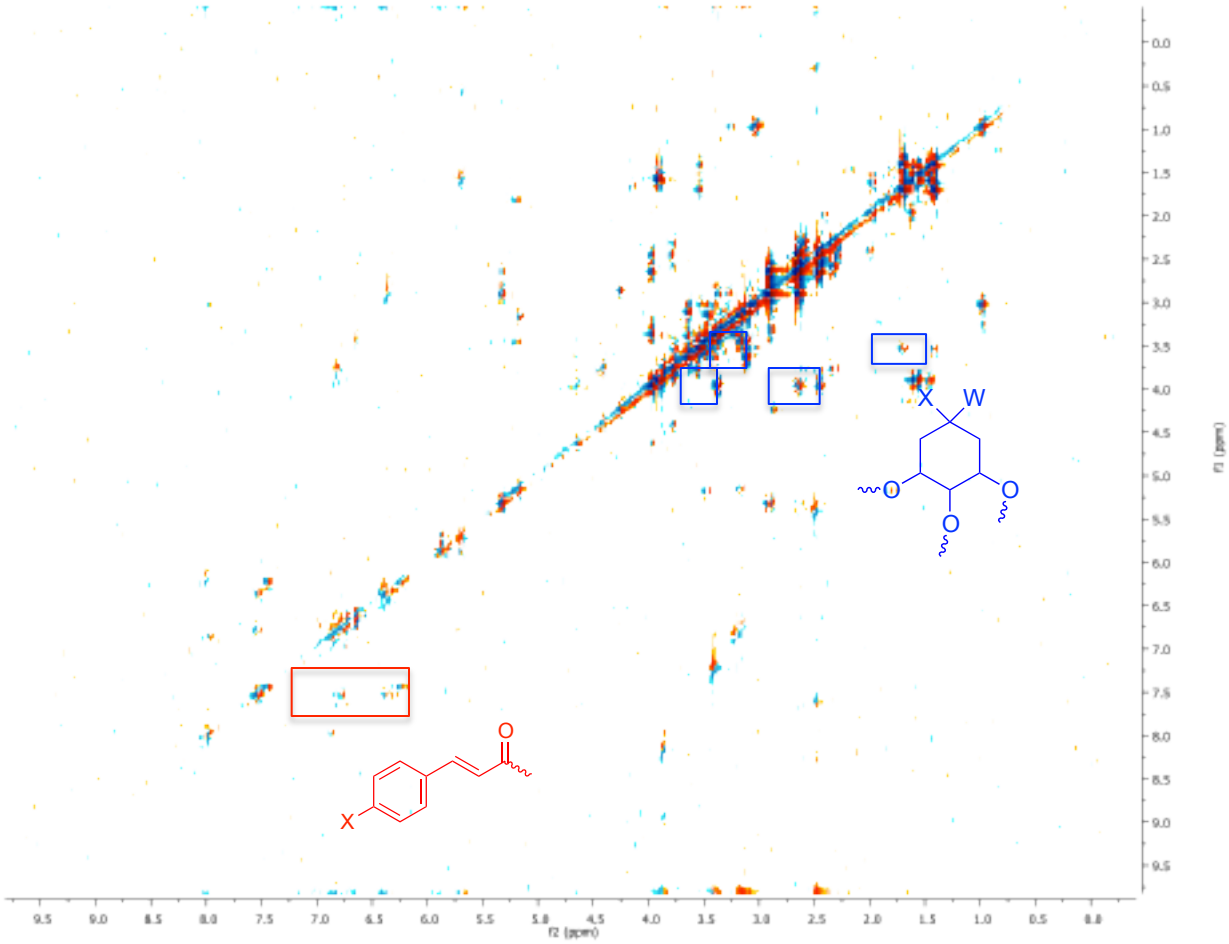

Figure 3-18 DQFCOSY spectrum for green tea sample P001

3.4. Conclusions

In conclusion, we have identified four natural products that modulate OATP function. Ursolic acid, oleanolic acid, and 8-*trans*-*p*-coumaroyloxy-α-terpineol, inhibit estradiol-17β-glucuronide uptake by OATP1B1 but not by OATP1B3, while ursolic acid and oleanolic acid inhibit estrone-3-sulfate uptake by both transporters. Quercetin 3-*O*-α-L-arabinopyranosyl(1→2) α-L-rhamnopyranoside (**3.6**) inhibits transport by OATP1B1, but has substrate-dependent effects on OATP1B3, non-competitively inhibiting uptake of both substrates at high substrate concentrations, but stimulating estrone-3-sulfate uptake at low substrate concentrations by increasing affinity. The results of this study show that diverse plant materials are a promising source for the isolation of OATP modulating compounds, and that a bioassay-guided approach can be used to efficiently identify selective OATP modulators. This work resulted in the following publication:

- Roth, M.; Araya, J.J.; Timmermann, B.N.; Hagenbuch, B. Isolation of modulators of the liver specific Organic Anion Transporting Polypeptides (OATPs) 1B1 and 1B3 from *Rollinia emarginata* Schlecht (Annonaceae). *J. Pharmacol. Exp. Ther*. 2011. 339(*2*), 624-632

In addition, a metabolomic approach was used as a dereplication tool to study the effect of aqueous green tea extracts on OATP1B1-mediated uptake of estrone-3-sulfate. The partial least squares (PLS) multivariate analysis of the ^{1}H NMR data collected for the aqueous green tea extracts suggested that not only the gallate catechins were important for the observed uptake inhibition, but also the minor compounds theogalline and 3-*p*-cumaroyl quinic acid.

3.5.Experimental data

3.5.1. General

See section 2.5.1. for additional general experimental data. [^{3}H]Estrone-3-sulfate (54.3 Ci/mmol) and [^{3}H]estradiol-17β-glucuronide (41.8 Ci/mmol) were purchased from PerkinElmer Life and Analytical Sciences (Boston, MA). Unlabeled estrone-3-sulfate, estradiol-17β-glucuronide, and rifampicin were purchased from Sigma-Aldrich (St. Louis, MO). MeOD, Pyr-d_5, and DMSO-d_6 were purchased from Cambridge Isotopes Inc.

3.5.2. Plant materials

Above-ground plant material of *Rollinia emarginata* was collected and identified in February 1999 in Argentina by R. Fortunato & A. Cabral (INTA) collection # ARP 613. LAT: 25°14'0"5 South LON:57°57'0"0 West. RN 86, 2Km NE of Patino, Department Primavera, Province Formosa.

Commercially available samples of green tea (N=34) were purchased from different grocery stores and detailed information (brand, lot number, expiration date, etc.) is presented in the Table 3-2.

3.5.3. Plant Extraction and Isolation

Dried and ground plant material (562 g) of *R. emarginata* was extracted with methanol (MeOH) and dichloromethane (CH_2Cl_2) mixture (1:1, v/v) three times for 24 hour periods at room temperature. Organic solvents were removed *in vacuo* at 35°C; the residue was suspended in MeOH:H_2O (9:1, v/v) and partitioned with hexanes (HEX fraction). After removal of MeOH,

the aqueous layer was extracted successively with CH_2Cl_2 (CH_2Cl_2 fraction) and butanol (BUOH fraction). The HEX fraction was then subjected to silica gel column chromatography (Si-Gel CC) (32-64 μm, 36x460 mm) and eluted with a gradient of hexanes-ethyl acetate (EtOAc) (20:1 to 0:100, v/v) to afford 20 subfractions (A to T), which were combined according to TLC analysis. Subfraction HEX-G (310 mg) was submitted to Si-Gel CC (12-26 μm, 36×230 mm) using a gradient of hexanes and acetone (15:1 to 5:1, v/v) to obtain three subfractions (G1-G3). Subfraction HEX-G1 (205 mg) was purified using Si-Gel CC (CH_2Cl_2:EtOAc, 20:1, v/v) to afford **3.3** (120 mg).Subfraction HEX-G2 was purified with Si-Gel CC (12-16 μm, 20×460 mm) using hexanes, CH_2Cl_2 and methyl *tert*-butyl ether (20:15:1, v/v/v) as mobile phase to yield **3.4** (10.4 mg). Also, subfraction HEX-N (284 mg) was separated using Si-gel CC (32-64μm, 36×230 mm) and CH_2Cl_2-EtOAc (10:1, v/v) as a solvent system to yield a mixture of **3.1** and **3.2** (103 mg) which was resolved by means of semipreparative HPLC (reverse phase C-18, 10×250 mm, 5μm, solvent A: acetonitrile, solvent B :water, gradient: 80%A to 100%A in 45 minutes). Fraction BUOH (19.7 g) was subject to MCI-Gel CHP20P CC (65×350 mm) and eluted with various mixtures of water and MeOH (100:0, 25:75, 50:50,75:25, 0:100; v/v) to afford four fractions (A-D). Subfraction BUOH-B (2.2g) was submitted to Sephadex LH-20 CC with MeOH as a mobile phase and a total of 180 fractions (7.5 mL each) were collected and combined into nine fractions (1-9) after TLC analysis. Pigments present in fraction BUOH-B7 (530 mg) were removed with a small Si-gel plug using CH_2Cl_2:MeOH:H_2O (4:1:0.1, v/v/v) as eluent to obtain a mixture of **3.5** and **3.6** (450 mg). A portion of this mixture (40 mg) was purified using semi preparative HPLC (reverse phase C-18, 10×250 mm, 5μm, solvent A: acetonitrile, solvent B: water, isocratic 18%A) to afford **3.5** (24 mg) and **3.6** (6.2 mg). The structures of isolated

compounds were established by one and two dimension NMR experiments and compared with those in literature; IR, UV, and HRMS were also in agreement with the proposed structures.

The 35 commercial green tea samples (c.a. 5 g) were extracted with 10 mL H_2O (70°C, 10 min). The extracts were concentrated *in vacuo* and dried overnight at 30°C in a vacuum oven.

3.5.4. Cell Culture

Chinese Hamster Ovary (CHO) cells stably transfected with OATP1B1 and OATP1B3 were seeded on 24- or 96-well plates and grown to visual confluency (48 to 72 hours). When confluent, medium was exchanged for non-selective medium containing 5 mM sodium butyrate, to non-specifically induce gene expression. Uptake experiments were performed 24 hours after induction.[155]

3.5.5. Transport Assays

Cells were washed three times with pre-warmed uptake buffer (116.4 mM NaCl, 5.3 mM KCl, 1 mM NaH_2PO_4, 0.8 mM $MgSO_4$, 5.5 mM D-glucose and 20 mM Hepes, pH adjusted to 7.4 with Trizma base). Cells were then incubated with pre-warmed uptake buffer containing the radiolabeled substrate. To stop uptake, the substrate solution was aspirated and the cells were washed four times with ice-cold uptake buffer. Cells were lysed with 1% Triton X-100 in phosphate buffered saline; lysate was used for liquid scintillation counting and protein determination using the BCA assay.[155]

3.5.6. Calculation and Statistics

All calculations were performed using Prism, (GraphPad Software Inc., La Jolla, CA). Determination of IC_{50} values and kinetic parameters was performed within the initial linear period of uptake (20 seconds). Statistical significance was determined with 2-way ANOVA followed by Bonferroni post-test or two-tailed paired t-test.

3.5.7. Quantitative NMR experiments

Each green tea extract (10.0 mg) was dissolved in 0.60 mL of DMSO-d_6. NMR experiments were performed in a Bruker AVIII 500 instrument with a dual C/H cryoprobe. The number of scans for each NMR spectrum was 32 and a delay time of 10 sec. was used to ensure full magnetization recovery. A standard solution of caffeine in DMSO-d_6 was used to calibrate the residual peak of DMSO-d_5 and use it as internal reference as described by Pierens *et al*.[173]

3.5.8. HPLC analyses

Analyses of samples were carried out using a Knauer SmartLine 5000 with a 4.6 × 250 mm *IRIS Technologies, L.L.C* IProSIL 120-5 C_{18} AQ 5.0 column at room temperature. The mobile phase consisted of (A) 0.05% TFA (B) ACN. The gradient was linear from 10 to 25% B in 25 min, 100% B in 10 min, and recovery to original conditions in 15 min. UV absorption was recorded at 278 nm.

3.5.9. Multivariate analysis

Data acquisition, processing, and management of the NMR spectra were carried out using the TopSpin 2.1 software program (Bruker). Bucketing was performed using AMIX (Bruker)

software using the SmartBucketing protocol option. Tables were exported to SIMCA P+ software and a PLS analysis was conducted.

Table 3-3 Commercial green tea samples coding information

Sample code	Brand	Type	Lot./Exp./Other
P001	Lipton	Green	
P002		Green	
P003		Green	
P004		Green	
P005		Green	
P006	La lucky brand	Green, organic	No information
P007	Ineeka/Himalayan	Green, organic	8151
P008	Numi	Green, organic	B807
P009	Equal exchange	Green, organic	No information
P010	Yogi Tea	Green, organic	No information
P011	Equal Exchange	Ceylon Green	P208069
P012	Stash	Green	No information
P013	Bigleow	Green	63919PJ81
P014	EDEN	Green, organic	8249141
P015	Best Choice	Green, organic	61470-0107-WB
P016	Twinings of London	Green	J4280578-171
P017	Bigelow	Green, decaffeinated	646094MK8
P018	Lipton	Green	SQ3 1526
P019	Tazo	Green	L01APR2008 2712
P020	Clelestial Seasonings	Green	29Jul10C
P021	Uncle Lee's Tea	Green	20121118
P022	HyVee	Green	Nov2010 AA
P023	Kroger	Green	May28 2010
P024	Salada	Green	May23 2010
P025	Salada	Green, decaffeinated	Dec17 2010
P026	Twinings of Lodon	Green, decaffeinated	01665577
P027	Lipton	Green, decaffeinated	1138
P028	Celestial Seasonings	Green, decaffeinated	02Oct10C
P029	HyVee	Green, decaffeinated	Nov2010AA
P030	Stash	Green and white	10/03/2011
P031	Private Selection	White	02/12/2011
P032	Uncle Lees' Tea	White	2013 01 08
P033	Salada	White	42 B8204
P034	Twinings of London	Oolong	01953497

Table 3-4 ^{1}H NMR-based concentration (as percentage of dry weight) of the main catechins and caffeine present in the commercial green tea samples

Sample code	EGCG	ECG	EGC	EC	Caffeine
P001	7.79	2.35	7.85	2.39	4.74
P002	3.33	0.69	5.54	1.52	5.44
P003	7.88	1.79	5.03	1.55	4.63
P004	3.55	1.81	3.14	0.85	5.15
P005	9.92	2.29	6.17	1.92	5.60
P006	2.95	0.61	4.87	1.34	4.79
P007	11.33	2.22	7.06	1.89	6.00
P008	5.55	0.85	6.96	1.74	5.26
P009	1.30	0.41	4.36	1.02	5.46
P010	3.86	0.64	7.10	1.80	4.73
P011	3.62	0.45	6.08	1.88	4.92
P012	4.97	1.38	5.99	2.03	5.08
P013	0.84	0.27	1.27	0.59	0.64
P014	3.92	1.08	5.02	1.77	4.34
P015	4.79	1.03	4.53	1.33	5.63
P016	1.78	0.44	3.83	1.02	4.04
P017	3.52	0.76	6.28	1.79	4.59
P018	2.61	0.60	4.33	1.25	3.90
P019	3.21	0.74	5.34	1.54	4.81
P020	2.86	0.81	8.62	2.27	8.21
P021	2.16	0.41	3.04	0.96	0.73
P022	4.40	1.19	3.18	1.08	0.49
P023	3.97	1.05	5.66	1.60	0.77
P024	1.74	0.38	2.73	0.67	0.98
P025	1.41	0.18	2.56	0.60	0.79
P026	3.30	0.52	5.32	1.43	5.01
P027	6.37	3.35	2.53	2.16	6.56
P028	3.75	1.04	6.10	1.54	5.70
P029	4.17	1.75	7.93	4.42	6.32
P030	4.54	0.87	5.32	1.21	5.95
P031	4.19	0.82	1.17	0.69	6.18
P032	8.12	1.84	4.91	1.58	5.72
P033	8.05	2.93	4.89	2.28	6.52
P034	1.98	0.80	8.26	2.21	6.40

4. PREGNANE, CARDIAC GLYCOSIDES, AND OTHER COMPOUNDS FROM *ASLCEPIAS SPP.*

4.1. Introduction

The genus *Asclepias* is widely distributed across the United States, especially in the Midwest geographical region. According to the United States Department of Agriculture Plant Database, over 130 plant species and subspecies within this genus have been described in the US territory and many of them are endemic to the Great Plains in the central area of the country.[175] Milkweed, the common name of *Asclepias*, refers to the milky latex that most of the plants within this genus exude upon mechanical damage as a mechanism of defense. The production of latex is a relatively common mechanism of defense as more than 20,000 species from over 40 families of angiosperms present this characteristic. The latex is typically composed of rubber, various enzymes and proteins as well as secondary metabolites with presumably defensive roles.[176] In the *Asclepias* genus, those secondary metabolites are cardenolides and the concentration varies greatly among its plant species. Cardenolides and cardiac glycosides are known to be highly toxic compounds to animals, including insects, thus providing defense to the producing plant against herbivory. Interestingly, the monarch butterfly (*Danaus plexippus*) has evolved to feed from cardenolide-containing plants and sequesters this type of compounds as a defensive mechanism defense against higher predators.[177] Furthermore, the monarch's Na^+,K^+-ATPase, the molecular target of cardenolides, has evolved to become insensitive to cardenolides through a mutation in the binding site: asparagine-122 has been replaced by a histidine.[178]

4.1.1. Ethnopharmacology of *Asclepias*

The name of the genus *Asclepias* was given by Lineus inspired by the ancient Greek god of medicine, Asclepius, due to the numerous medicinal uses of plants in this genus.[179] Considering the diversity and abundance of *Asclepias* species in the US territory, it is not surprising that Native Americans have used them as medicine and food for a wide range of health conditions. Table 4-1 summarizes the plant species known for these medicinal properties by different Native American groups as well as its health-related uses.

Table 4-1 Medicinal uses of *Asclepias* species by Native Americans[180-183]

Species	Native American group	Medicinal uses
A. asperula	Navajo, Kayenta, Ramah	Respiratory aid, emetic, veterinary aid
A. auriculata	Navajo, Kayenta	Respiratory aid
A. californica	Kawaiisu	Dermatological aid
A. cordiflolia	Miwok	Non specific medicine
A. cryptoceras	Paiute, Northern, Shoshoni	Analgesic, dermatological aid, veterinary aid
A. eriocarpa	Costanoan, Mendocino Indian	Cold remedy, dermatological aid, respiratory aid.
A. exaltata	Omaha, Ponca	Gastrointestinal aid
A. fascicularis	California Indian, Mendocino Indian	Snakebite remedy, poison
A. hallii	Navajo, Kayenta	Gynecological aid, veterinary aid
A. incarnata	Chippewa, Iroquois, Meskawaki	Pediatric aid, strengthener, dermatological aid, diuretic, kidney aid, orthopedic aid, toothache remedy, urinary aid, witchcraft medicine, anthelmintic, carminative, cathartic, emetic
A. involucrata	Keres, Western, Navajo, Kayenta, Zuni	Gastrointestinal aid, toothache remedy
A. latifolia	Isleta	Respiratory aid
A. nyctaginifolia	Navajo, Kayenta	Antidiarrheal, pediatric aid
A. perennis	Cherokee	Analgesic, dermatological aid, kidney aid, laxative, urinary aid, venereal aid, veterinary aid

A. pumila	Lakota	Antidiarrheal, pediatric aid
A. quadrifolia	Cherokee	Analgesic, dermatological aid, kidney aid, laxative, urinary aid, venereal aid, veterinary aid
A. speciosa	Cheyenne, Flathead, Lakota, Miwok, Navajo, Kayenta, Okanagan-Colville, Okanagon, Paiute, Thompson	Eye medicine, gastrointestinal aid, dermatological aid, emetic, antirheumatic, cough medicine, snakebite remedy, tuberculosis medicine, antidiarrheal, venereal aid, analgesic, dietary aid
A. stenophylla	Lakota	Dietary aid
A. subulata	Pima	Cathartic, emetic, eye medicine, gastrointestinal aid, panacea, poison
A. subverticillata	Hopi, Keres, Western	Gynecological aid
A. syriaca	Cherokee, Chippewa, Ojibwa, Potawatomi, Rappahannock, Menominee	Analgesic, dermatological aid, kidney aid, laxative, urinary aid, venereal aid, veterinary aid, antirheumatic (external), contraceptive, pulmonary aid, and as food
A. tuberosa	Cherokee, Delaware, Oklahoma, Iroquois, Menominee, Mohegan, Ramah, Omaha, Ponca, Rappahannock	Analgesic, antidiarrheal, gynecological aid, heart medicine, pulmonary aid, antirheumatic, orthopedic aid, dermatological aid, pulmonary aid, snakebite remedy
A. verticillata	Choctaw, Hopi, Lackota	Diaphoretic, snakebite remedy, stimulat, gynecological aid, throat aid
A. viridiflora	Blackfoot, Lakota	Antirheumatic (external), dermatolgical aid, eye medicine, oral aid, pediatric aid, throat aid, antidiarrheal, gynecological aid

4.1.2. Phytochemistry of *Asclepias*

Asclepias is known to contain cardiac and pregnane glycosides, however triterpenes, flavonoids, and lignans have also been reported for this genus. Interestingly, only a small fraction of the *Asclepias* species described in the US have been investigated for their chemistry or biological properties. A comprehensive revision of phytochemical investigations of *Asclepias* species published to date is presented in Table 4-2 and representative structures are shown in Figures 4-2, 4-3, and 4-4.

Table 4-2 Asclepias species with reported phytochemical studies*

Species	Compound type**	References
A. albicans	CG	Koike *et al*.[184]
A. amplexicaulis	PG	Piatak *et al*.,[185] Ahsan *et al*.[186]
A. asperula	CG	Martin *et al*.,[187] Bartlett *et al*.[188]
A. curassavica	PG, CG	Li *et al*.,[189, 190] Abe, *et al*.[191, 192]
A. eriocarpa	CG	Cheung *et al*.,[193] Seiber *et al*.[194]
A. furticosa	PG, CG, M, L	Warashina and Noro,[195, 196] Abe *et al*.,[197] Abe and Yamauchi[198]
A. glaucensces	CG	Fonseca *et al*.[199]
A. humistrata	CG	Nishio *et al*.[200]
A. incarnata	PG, CG	Warashina and Noro,[201, 202]
A. labriformis	CG	Seiber *et al*.[194]
A. linaria	CG	Rodriguezhahn *et al*.[203]
A. syriaca	PG, CG, F	Warashina and Noro,[204, 205] Sikorska,[206] Brown *et al*.,[207] *Gonnet et al*.,[208] Mitsuhas[209]
A. subulata	CG	Jolad *et a*l.[210]
A. tuberosa	PG, CG	Warashina and Noro,[211, 212] Abe and Yamauchi[213, 214]
A. vestita	CG	Cheung *et al*.[215, 216]

* Revision was done in SciFinder using "Asclepias" in title as search criteria.

** CG: cardiac glycosides, PG: pregnane glycosides, M: megastigmane, F: flavonoid, L: lignan

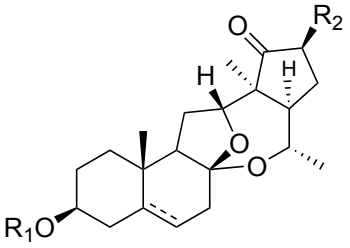

a: Ole (1➔4) Dig (1➔4) Ole
b: Ole (1➔4) Dig (1➔4) Ole (1➔4) Ole
c: Ole (1➔4) Cym (1➔4) Ole (1➔4) Ole
d: Cym (1➔4) Ole (1➔4) Ole (1➔4) Ole
e: Cym (1➔4) Ole (1➔4) Ole (1➔4) Cym
f: Cym (1➔4) Dig (1➔4) Ole (1➔4) Ole
g: Can (1➔4) Dig (1➔4) Ole (1➔4) Ole
h: Cym (1➔4) Ole (1➔4) Ole (1➔4) Dig (1➔4) Ole
i: Cym (1➔4) Cym (1➔4) Ole (1➔4) Dig (1➔4) Ole
j: Cym (1➔4) Ole (1➔4) Ole (1➔4) Cym (1➔4) Ole
k: Dig (1➔4) Ole (1➔4) Ole (1➔4) Cym (1➔4) Ole
l: Cym (1➔4) Ole (1➔4) Ole (1➔4) Dig (1➔4) Ole
m: Ole (1➔4) Cym (1➔4) Ole (1➔4) Dig (1➔4) Ole
n: Ole (1➔4) Cym (1➔4) Ole (1➔4) Cym (1➔4) Ole
o: Ole (1➔4) Cym (1➔4) Ole (1➔4) Ole (1➔4) Ole

Dig: D-digitoxopyranose
Can: D-canaropyranose
Cym: D-cymaropyranose
Ole: D-oleandropyranose

	R_1	R_2	5,6
i	a	H	α-H,H
i*	H	H	α-H,H
ii	b	OAc	α-H,H
iii	b	H	α-H,H
iv	c	OAc	α-H,H
v	c	H	α-H,H
vi	c	H	α-H,H
vi*	h	H	α-H,H
vii	c	H	Δ
viii	d	OH	α-H,H
ix	d	H	Δ
ix*	h	H	Δ
x	e	OH	α-H,H
x*	h	OH	α-H,H
xi	f	H	α-H,H
xii	f	H	Δ
xiii	g	H	α-H,H
xiv	h	H	α-H,H
xv	h	H	Δ
xvi	i	H	α-H,H
xvii	i	OAc	α-H,H
xviii	i	H	Δ
xix	j	H	α-H,H
xx	k	H	α-H,H
xi	l	H	α-H,H
xii	m	OH	α-H,H
xiii	n	H	α-H,H
xiv	o	H	α-H,H
xv	c	H	α-H,H

Figure 4-1 Secopregnane glycosides from *A. tuberosa*[211]

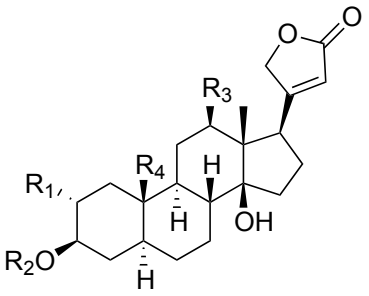

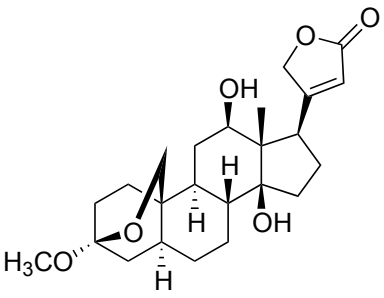

vi

	R_1	R_2	R_3	R_4
i	H	H	H	CH_2OH
ii	H	H	OH	CH_2OH
iii	OH	H	H	CHO
iv	H	β-D-Glc	H	CH_3
v	H	β-D-Glc$\xrightarrow{6}$Fer	H	CH_3

Fer:

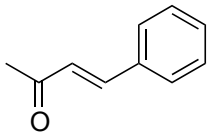

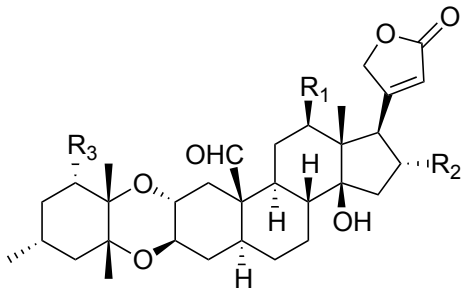

	R_1	R_2	R_3
vii	H	H	OH
viii	H	H	O=
ix	H	H	OAc
x	H	OH	OAc
xi	H	OAc	OH
xii	H	OAc	OAc
xiii	OH	H	OH

Figure 4-2 Cardiac glycosides and cardenolides from *A. curassavica*[190]

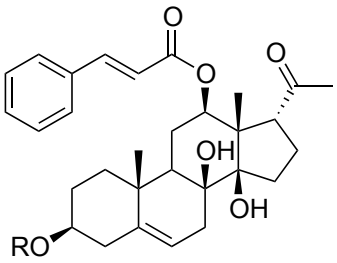

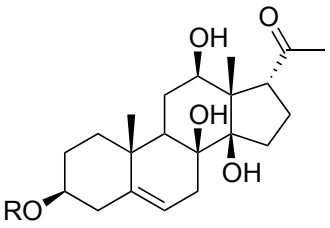

xiii R = Cym-Cym-Ole-Ole

	R
i	Cym-Cym-Ole
ii	Cym-Ole-Ole
iii	Cym-Cym-Ole-Thv
iv	Cym-Cym-Ole-Ole
v	Cym-Cym-Ole-Cym
vi	Cym-Cym-OleOle-Cym
vii	Cym-Cym-Ole-Ole-Cym-Glc
viii	Dig-Cym-Can-Dgt-Cym-Glc
ix	Cym-Cym-Can-Dgt-Cym-Glc
x	Cym-Cym-Ole-Cellobiose
xi	Cym-Cym-Ole-Ole-Cellobiose
xii	Cym-Cym-Ole-Ole-Cym-Cellobiose

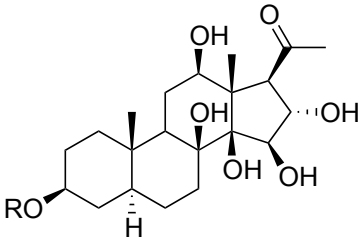

	R
xiv	Cym-Can-Can-Cym
xv	Cym-Can-Can-Cym-Glc
xvi	Cym-Can-Can-Cym-Cym-Cellobiose

Figure 4-3 Pregnane glycosides from *A. tuberosa*[213]

4.2. Project design

As described in the previous section, *Asclepias* represents a potentially rich source of bioactive natural products that have been under-explored. With the main goal to investigate the antiproliferative potential of secondary metabolites present in various species in this genus, we conducted this project in four stages as summarized in Figure 4-5 and described in detail in the subsequent sections.

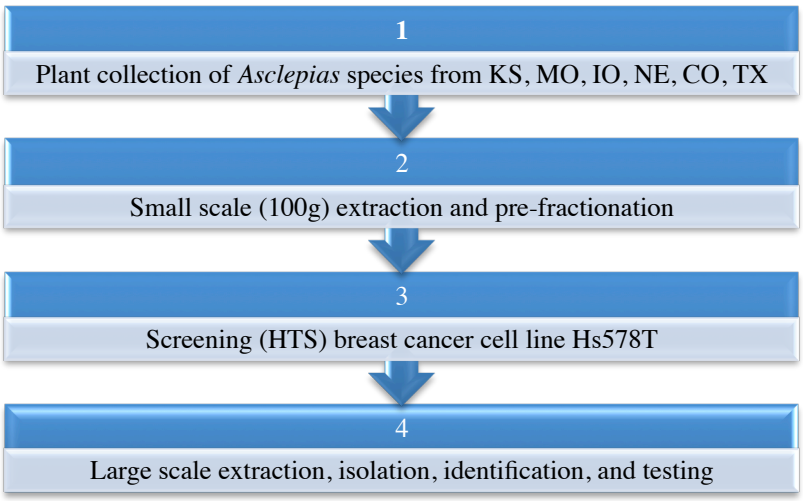

Figure 4-4 *Asclepias* project workflow

A total of ten plant species namely *Asclepias verticillata*, *A. syriaca*, *A. sullivantii*, *A. incarnata*, *A. speciosa*, *A. tuberosa*, *Apocynum cannabinum* (Apocynacaeae), *Cynanchum mucronatum*, *C. boerhaviifolium*, and *Diplolepis mensiesii* were fractionated in small-scale and screened for cytotoxicity. Three species, *A. verticillata*, *A. syriaca*, and *A. sullivantii* (Figure 4-6), were selected for detailed phytochemical investigation and the results are presented in sections 4.3, 4.4, and 4.5 respectively.

Figure 4-5 Images of (a) *Asclepias verticillata*, (b) *Asclepias sullivantii*, and (c) *Asclepias syriaca* * Image Copyright Thomas G. Barnes, University of Kentucky

4.2.1. Pre-fractionation and screening

As previously mentioned, biological testing of plant-derived mixtures is often challenging due to the low concentration of the active compounds as well as interference by other components in the complex mixture.[19] Therefore, in order to minimize those problems during the screening process, a small-scale (c.a. 100 g dried plant material) extraction and fractionation was conducted with each of the ten plant samples investigated (Figure 4-7). The plant material was not only partitioned using classic liquid/liquid extraction, but also the CH_2Cl_2 and BuOH fractions were subjected to small normal-phase and reverse-phase column chromatography, respectively. Accordingly, 14 samples were generated per plant and a total of 152 fractions were subjected to biological evaluation.

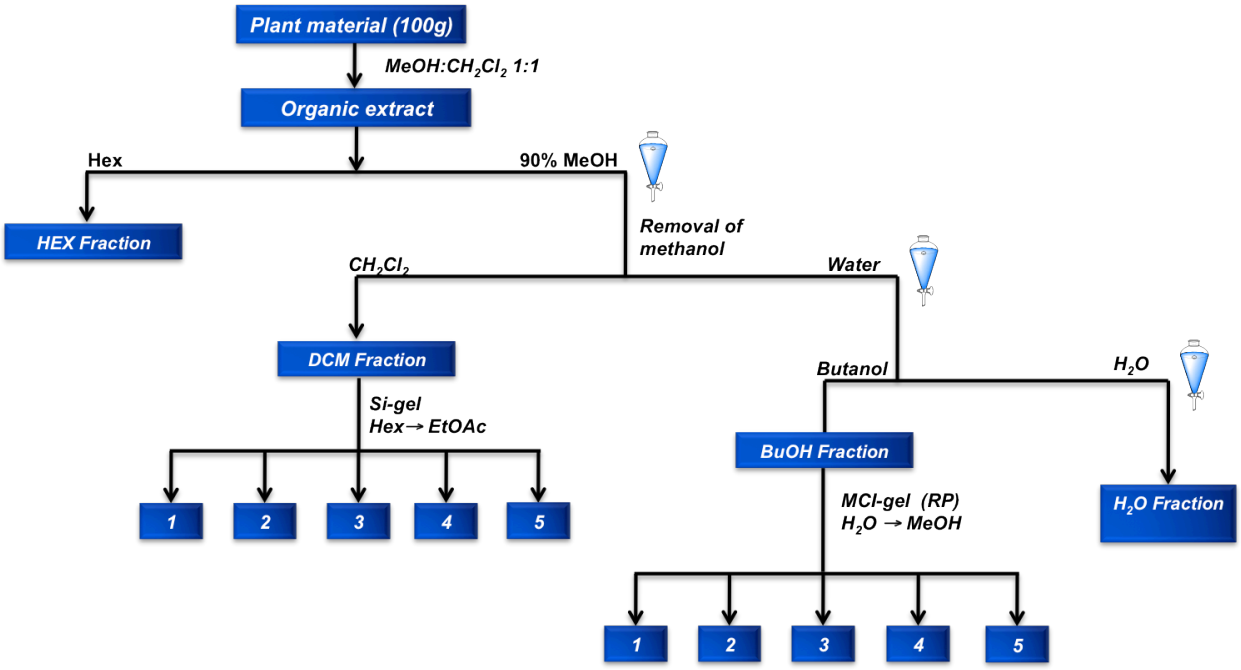

Figure 4-6 Small-scale extraction and pre-fractionation scheme

4.2.2. HTS cytotoxicity bioassay

The biological assays for this project were conducted by Dr. Peter McDonald in the High-Throughput Screening (HTS) laboratory at KU. The cytotoxic studies of plant extracts and fractions were carried out in 384-well plates using the paired breast cell lines Hs578T (cancer) and Hs578Bst (normal). These cell lines represent a great model for selectivity studies of cytotoxic compounds as they originated from the same patient.[217] The mother plates were prepared in 96-deep-well plates and the extracts and fractions were dissolved in 100% DMSO with a final concentration of 10.0 μg/L. Some of the fractions were viscous and difficult to handle using the traditional pipetting methods. Therefore, an ECHO system was used to transfer the samples from the mother plate to the daughter plates in order to reduce potential errors. The ECHO transfer system utilizes sound technology to transfer liquids by the use of radiofrequency pulse. The cancer and normal cells were exposed to a series of dilutions in the 0.1-50 μg/L range for each sample and incubated for 48h or 72h. The cell viability was then assessed using CellTiter-Glo assay.

The addition of extracts or compounds to cells introduced a small but significant percentage of DMSO in the media. Due to the varying cytotoxic effects of DMSO in different cell lines, a DMSO tolerance assessment was performed to determine the highest level of DMSO that could be tolerated by both cell lines used in this study. Cells were incubated in the presence of various DMSO amounts diluted in complete growth medium for 48 hours, and then cell viability was assessed using the CellTiter-Glo assay. From these results, 0.5% DMSO was selected as the maximum tolerable concentration of DMSO in cell culture medium. In addition, the cells were monitored using a microscope (Figures 4-9 and 4-10)

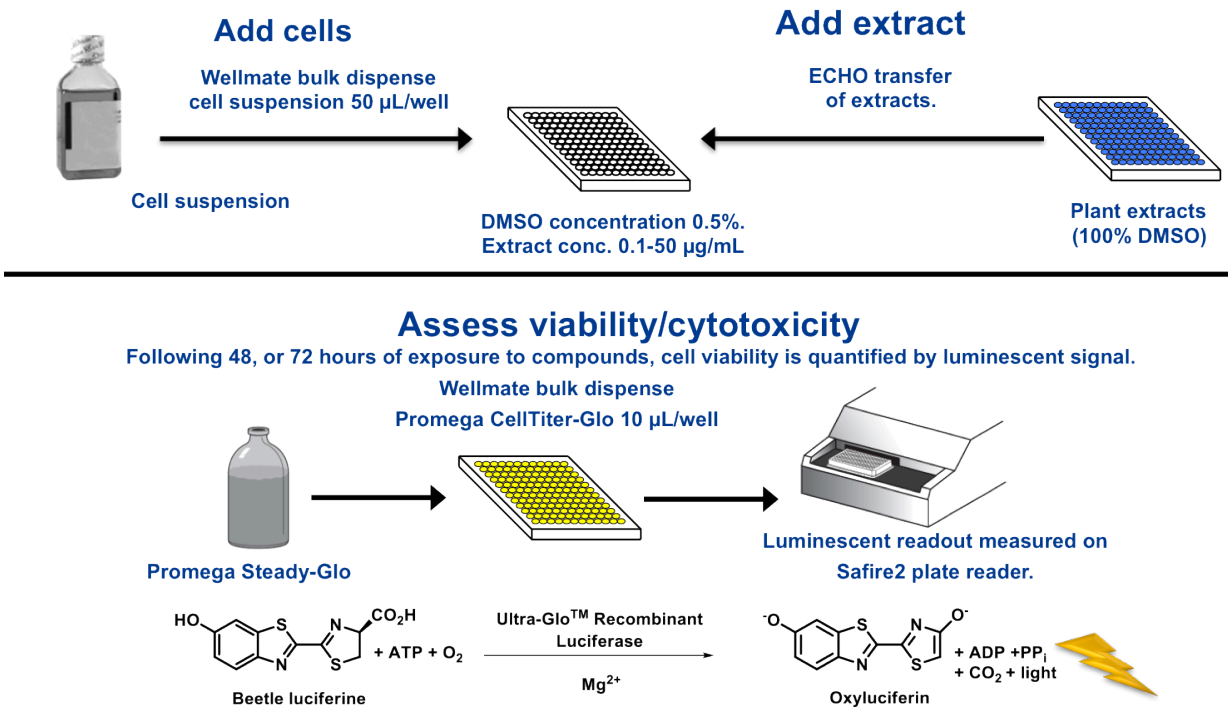

Figure 4-7 Bioassay schematic

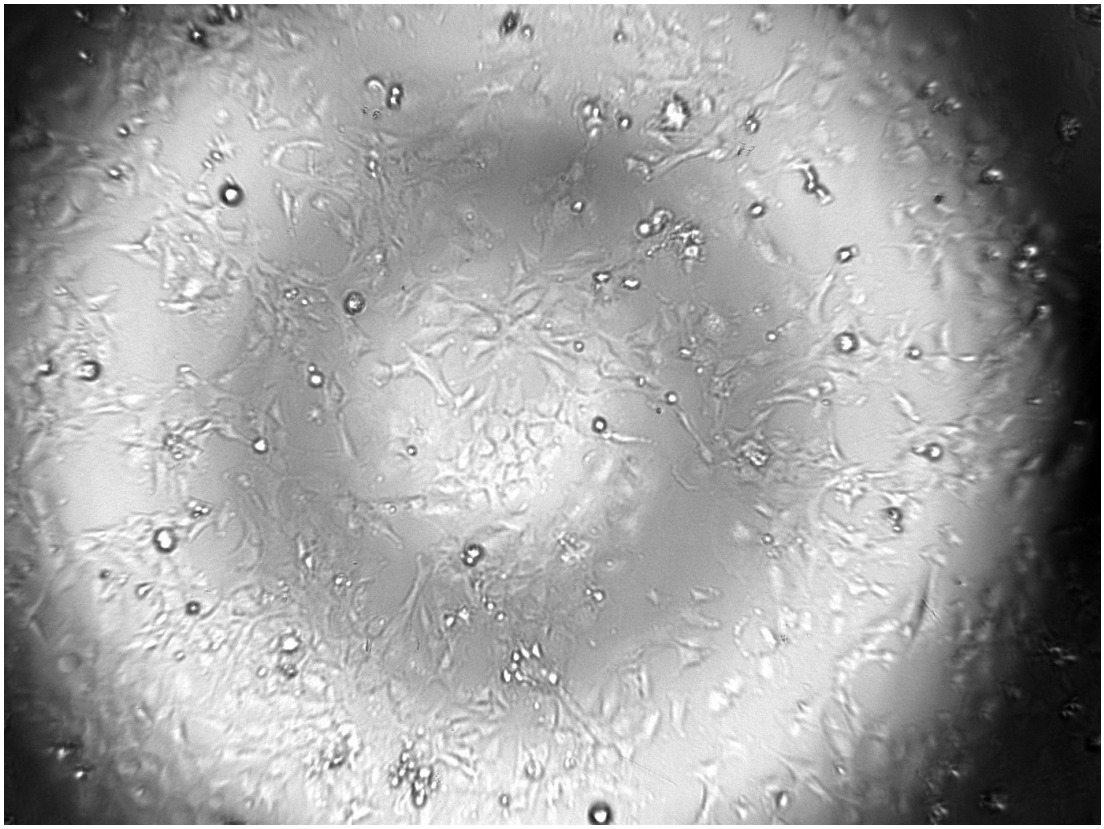

Figure 4-8 Micrograph of breast cancer (Hs578T) cell line (0.5% DMSO, control)

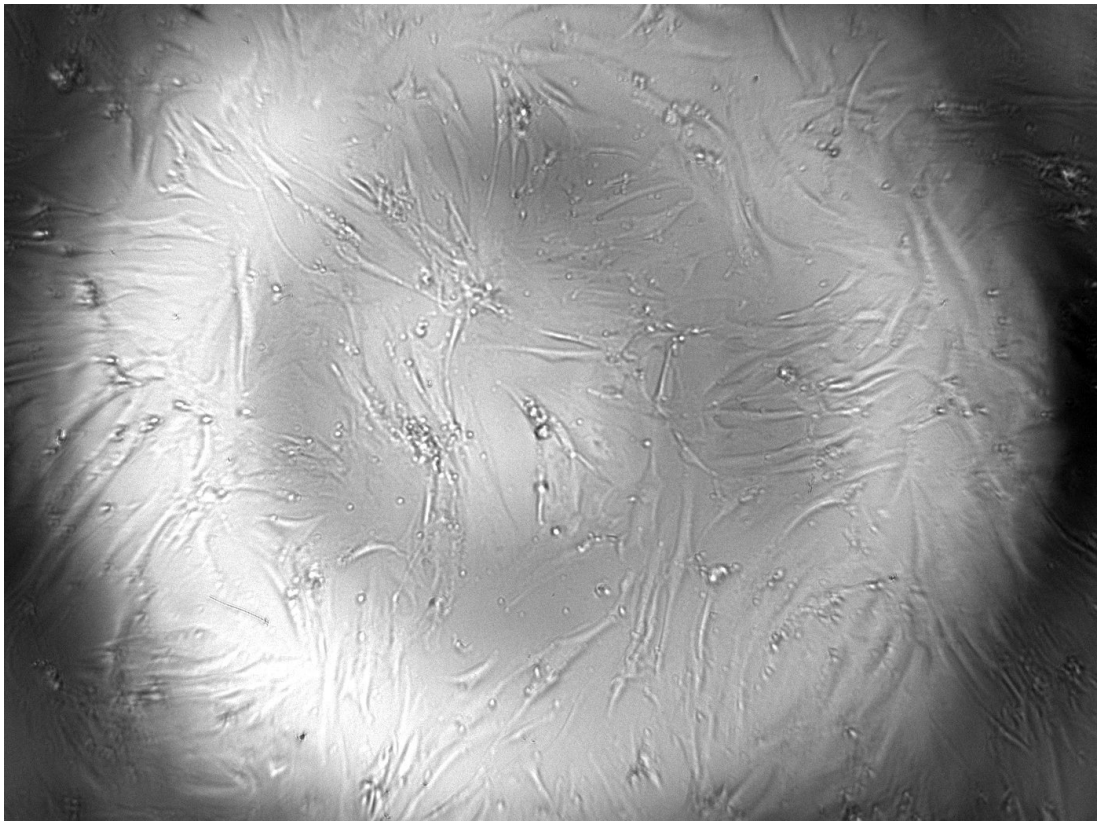

Figure 4-9 Micrograph of breast normal (Hs578Bst) cell line (0.5% DMSO, control)

Figure 4-10 presents an example of a complete data set from HTS for one plate containing 88 samples. The screening results for the 10 plants (a total of 152 extracts and fractions) can be found in Table 4-6 (Experimental data). As expected, a wide range of cytotoxicity values (expressed as percentage at maximum concentration of 50 μg/L) were observed within the data set (Figures 4-11 and 4-12). The average cytotoxicity for cancer and normal cell lines was 43.4% and 27.7%, respectively. A total of 44 samples showed more than 70% cytotoxicity against malignant cells, however a number of these highly toxic samples were also toxic to normal cells. In order to identify possible 'hits' form the data set, selectivity was calculated using the

difference in the area under the dose-response curve (AUC) for cancer cells and the AUC for normal cells. Hence, positive numbers represent selective toxic samples against malignant cells (Figure 4-13). The AUC values were used to calculate selectivity because several samples did not show a good dose-response curve preventing the IC_{50} calculation.

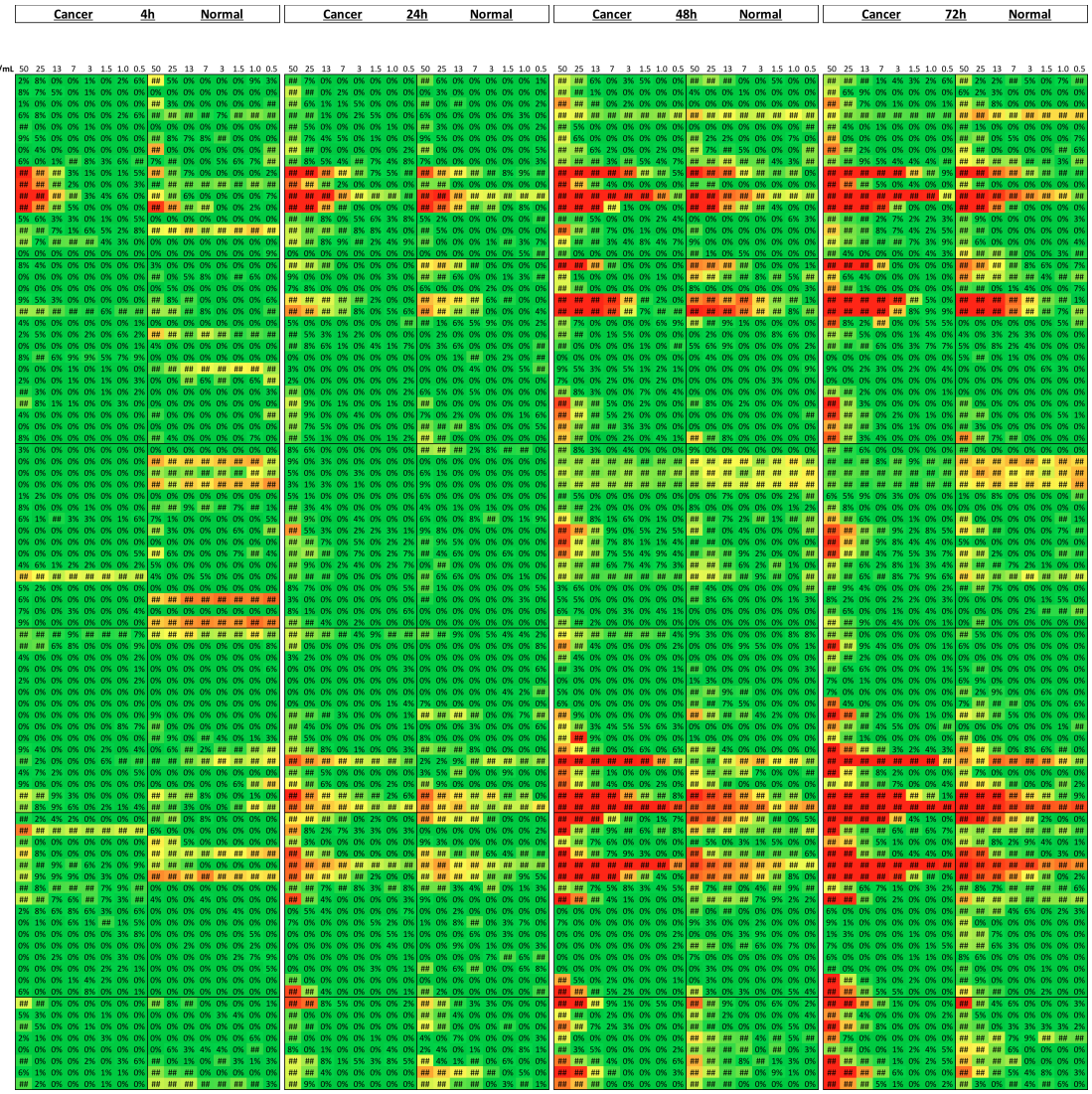

Figure 4-10 HTS cytotoxicity data set output for 88 samples

(Red color indicates grow inhibition and green color indicates normal grow with respect to control)

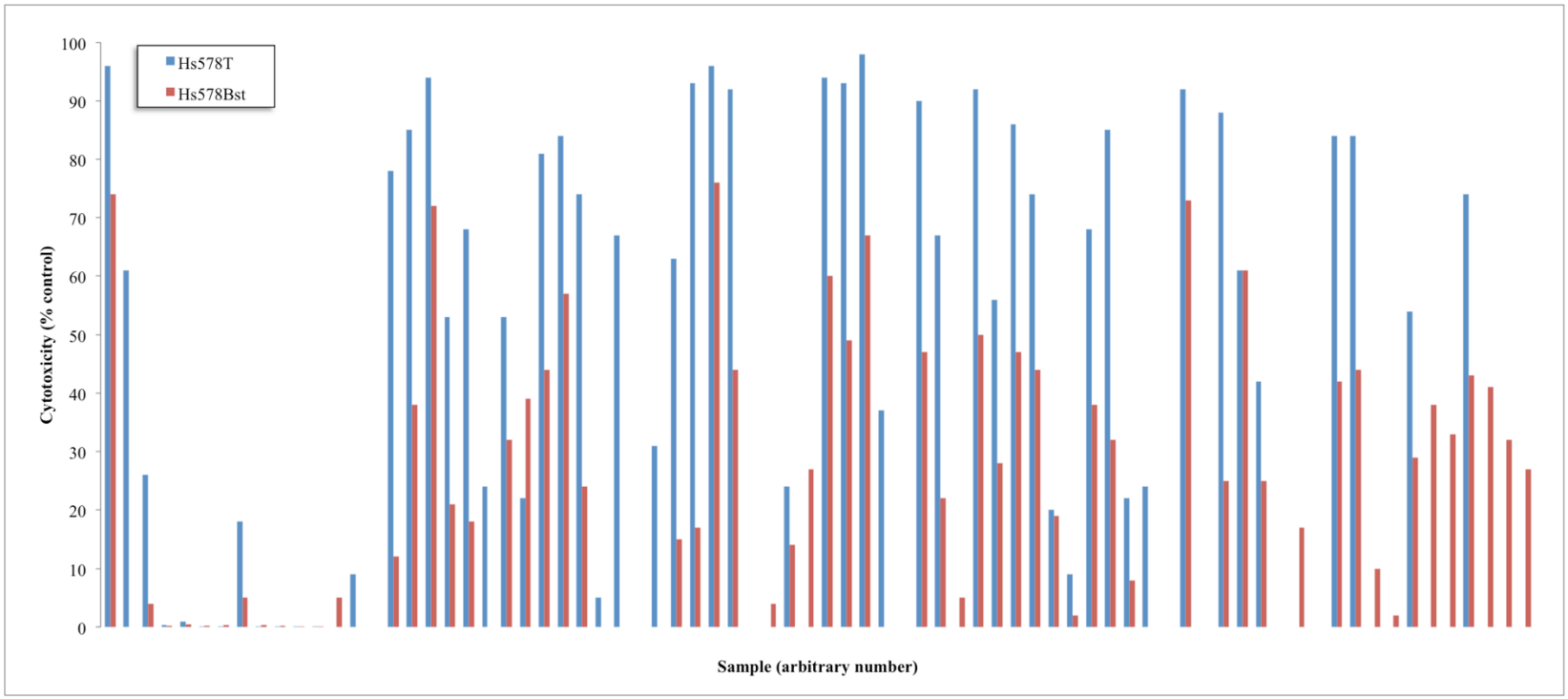

Figure 4-11 Cytotoxicity expressed as percentage of inhibition at maximum concentration (50 μg/mL) for cancer (Hs578T) and normal (Hs578Bst) cells after 72h incubation period - Part 1

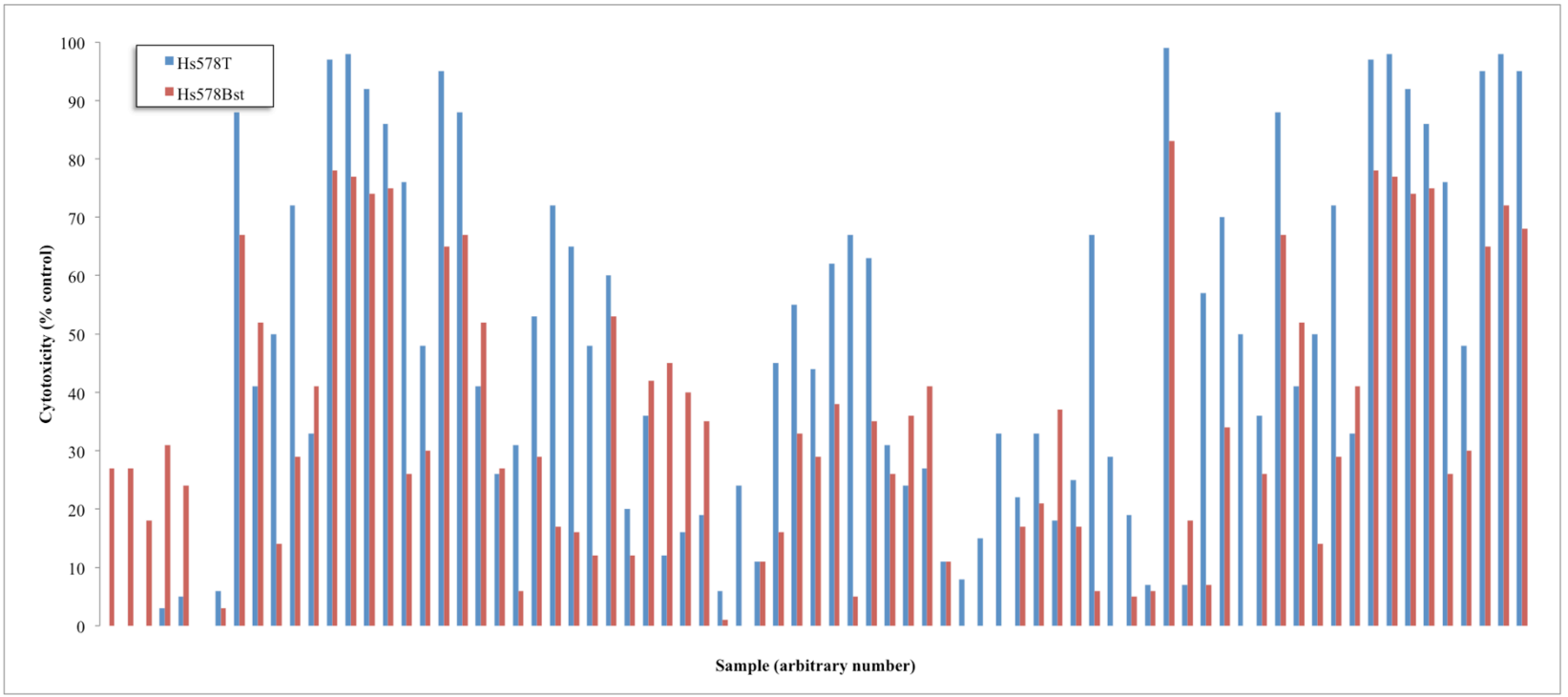

Figure 4-12 Cytotoxicity expressed as percentage of inhibition at maximum concentration (50 μg/mL) for cancer (Hs578T) and normal (Hs578Bst) cells after 72h incubation period - Part 2

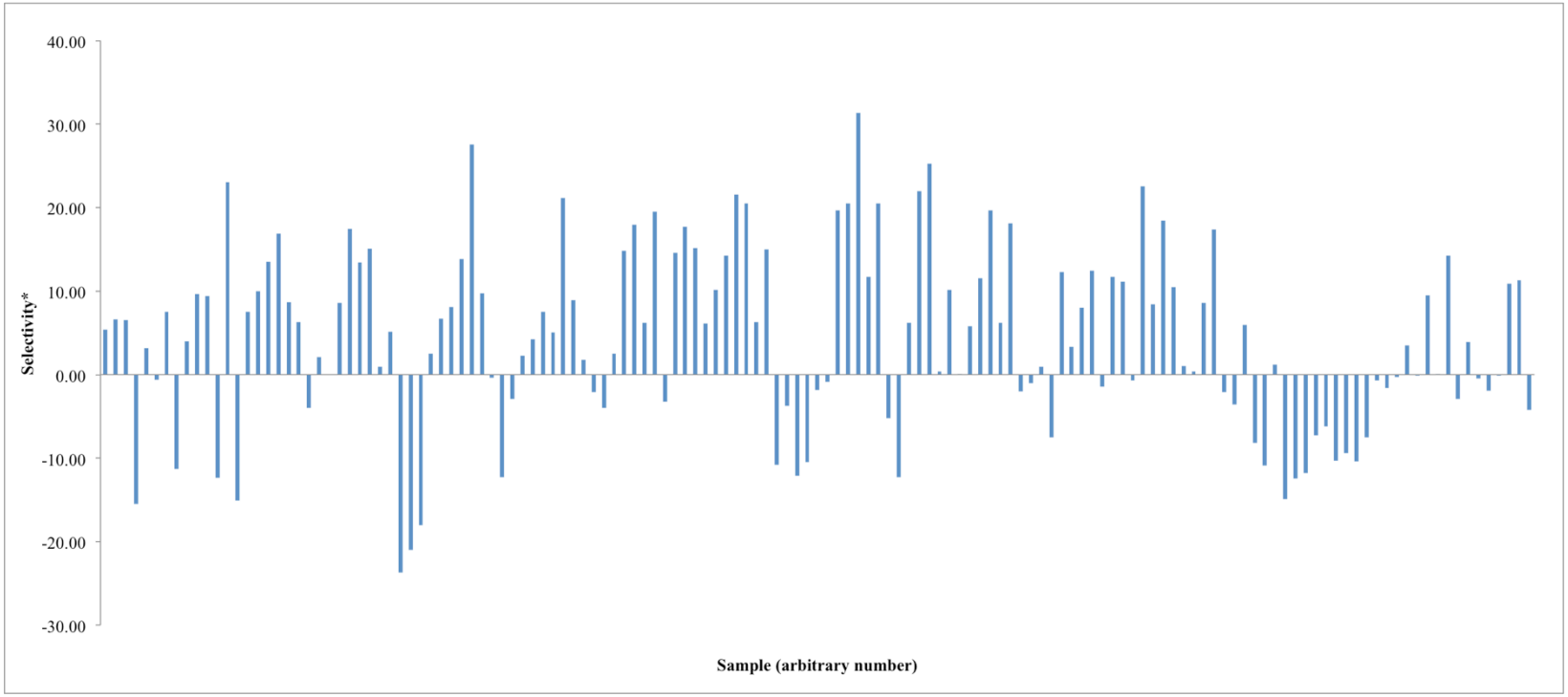

Figure 4-13 Selectivity growth inhibition after 72 h exposure of extracts and fractions during screening

* Calculated as difference in $AUC_{cancer} - AUC_{normal}$

In general, good dose-response curves were observed, so estimated IC_{50} values were calculated for those samples. For instance, in Figure 4-14 the dose-response curves for *A. syriaca* fraction BuOH-4 is plotted showing a selective inhibition of cancer over normal cells with IC_{50} values of 11 and 22 µg/L respectively (selectivity value 22.0). However, the IC_{50} values were not possible to calculate for some samples due to the lack of toxicity or the non-sigmoidal distribution of the experimental points.

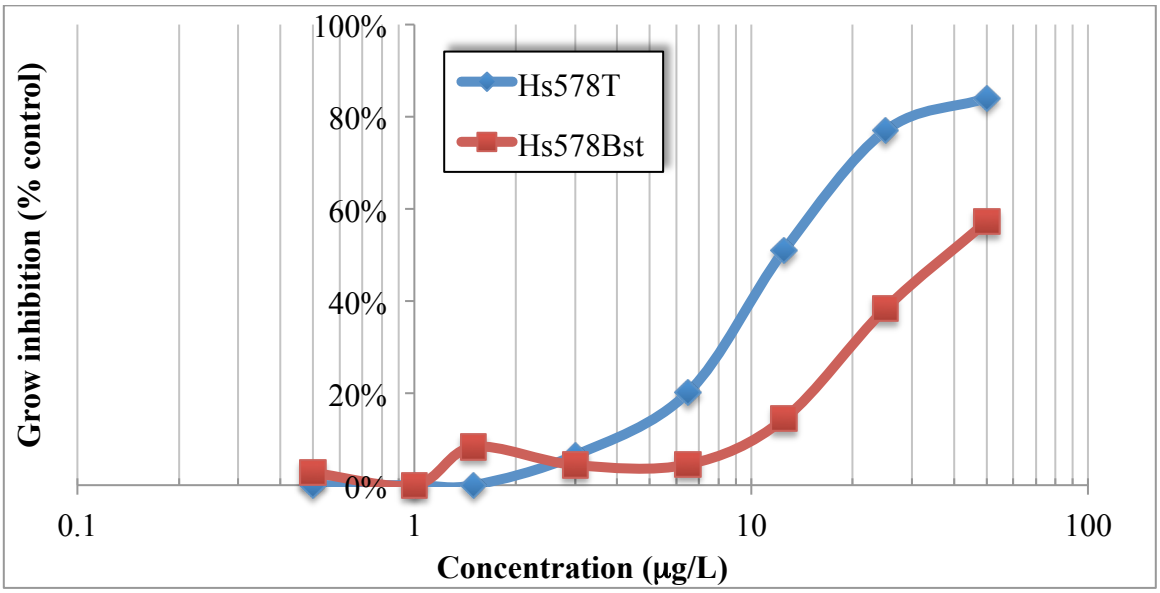

Figure 4-14 Dose-response curve of sample BuOH-4 from *A. syriaca* for cancer (Hs578T) and normal (Hs578Bst) cell lines (72 h exposure)

The exposure time of the cells to the plant extracts or fractions was also investigated using 4h, 24h, 48h, and 72h time points, in order to evaluate the optimal value. As presented in Figure 4-15, the active fraction BuOH-4 from *A. syriaca* displayed complete dose-response curves at the exposure times of 48h and 72h. However, 4h and 24h exposure times were insufficient to reach the plateau at high concentration, hence preventing a reliable IC_{50} calculation. Therefore,

subsequent screenings were only conducted at 48h and 72h. In addition to the negative control (0.5% DMSO), four positive controls were used in order to assess the quality of the cytotoxicity assay results including doxorubicin, digoxin, digitoxigenin, and ouabain (Figure 4-16).

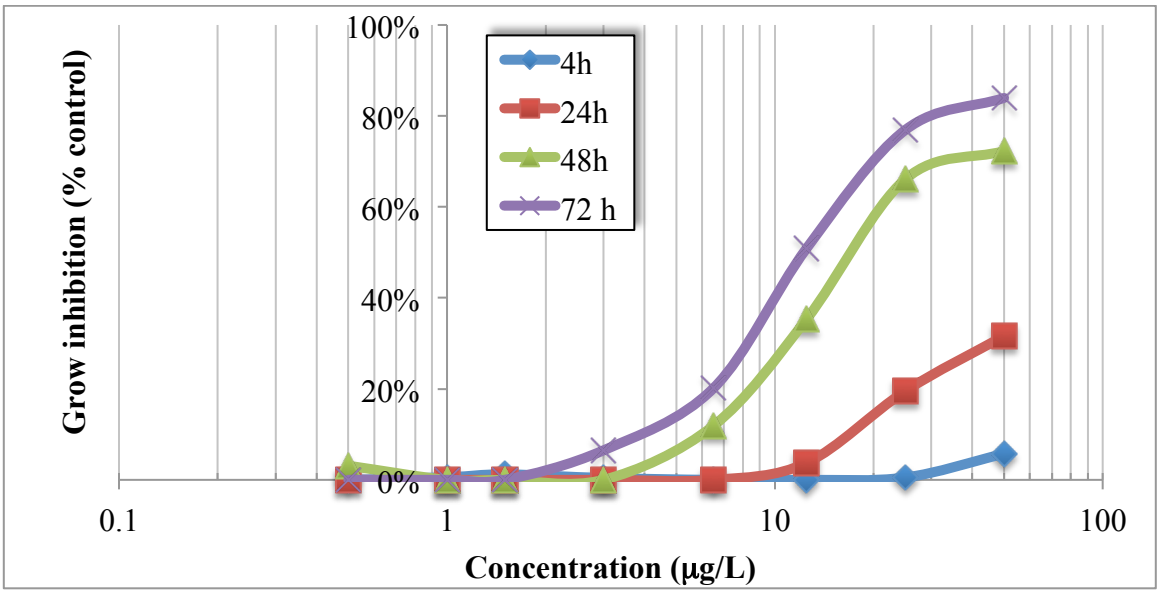

Figure 4-15 Effect of the exposure time on dose-response curves for sample BuOH-4 from *A. syriaca* (Hs578T cell line)

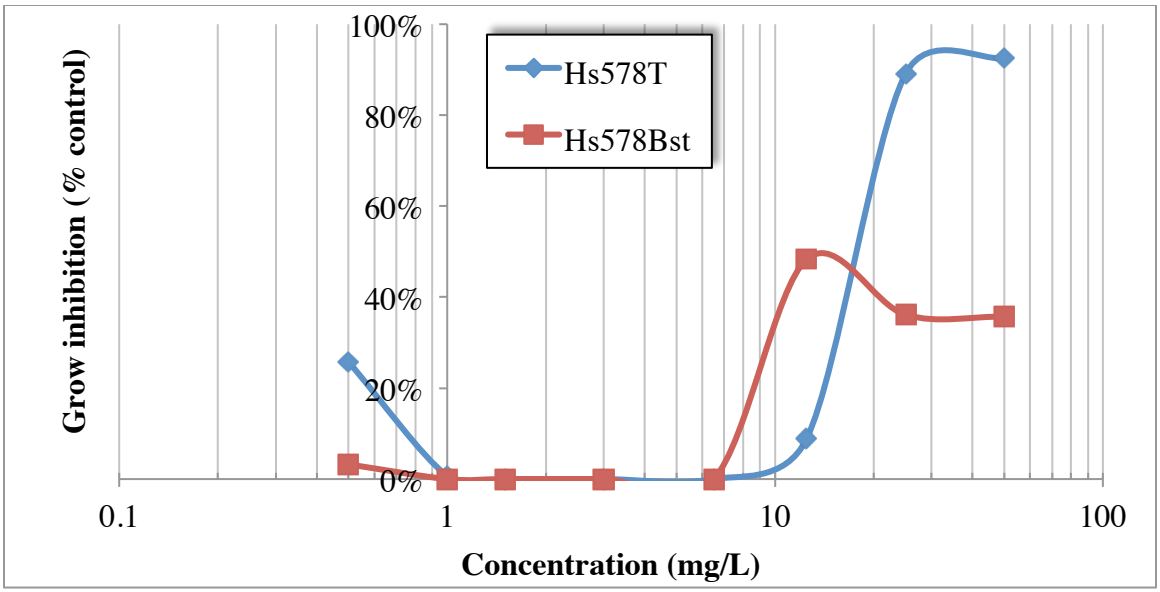

Figure 4-16 Dose-response curves for the positive control (ouabain)

With reliable bioassay results in hand, the plant selection for further investigation was done using both the cytotoxicity against cancer cell lines, and the selectivity against malignant cells over normal cells. In addition, ethnopharmacologic and phytochemical reports were also considered to move forward with the large-scale extraction and isolation. Based on the results obtained three *Asclepias spp.* were selected including *A. verticillata*, *A. syriaca*, and *A. sullivantii*. Each species will be discussed in detail in the following sections. These plants were extracted in large scale (~1 kg of dry plant material) and the separation scheme had to be accordingly scaled-up. TLC or HPLC comparison with authentic samples of the active fractions was used to guide the separation steps during the large-scale isolation.

4.3. Verticillosides A-M: pregnane glycosides from *Asclepias verticillata* L.

Although *A. verticillata* did not show strong activity in the initial bioassay results, this species was chosen for detailed investigation due to the lack of prior phytochemical reports. Interestingly, the initial activity (IC_{50} = 3.4 μg/L) observed in the crude extract was lost upon fractionation and no sub-fraction showed higher toxicity values. A possible explanation could be due to synergistic effects among the components in the initial mixture, however no confirmatory experiments were done to evaluate this hypothesis. The most active fraction corresponded to CH_2Cl_2-2 (IC_{50} = 20 μg/L, 93% inhibition), however no compounds were isolated thereafter due to the mixture complexity and the relatively small quantity of sample material. Nevertheless, from the butanolic layer a total of 13 new pregnane glycosides named verticillosides A-M were isolated and identified (Figure 4-17). As mentioned before, this represents the first phytochemical investigation for this species.[218] The isolates were named verticilloside A (**4.1**; 38 mg), B (**4.2**; 42 mg), C (**4.3**; 10 mg), D (**4.4**; 36 mg), E (**4.5**; 27 mg), F (**4.6**; 37 mg), G (**4.7**; 11 mg), H (**4.8**; 19 mg), I (**4.9**; 10 mg), J (**4.10**; 3 mg), K (**4.11**; 12 mg), L (**4.12**; 9 mg), and M (**4.13**; 14 mg).

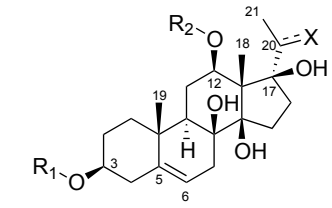

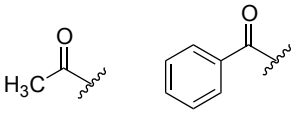

Ac: Acetyl

Bz: Benzoyl

	X	R_1	R_2
Verticilloside A (**4.1**)	O	R_A	Ac
Metaplexigenin (**4.1a**)	O	H	Ac
Verticilloside B (**4.2**)	O	R_B	Ac
Verticilloside C (**4.3**)	O	R_C	Ac
Verticilloside D (**4.4**)	O	R_D	Ac
Verticilloside E (**4.5**)	α-H,β-OH	R_A	H
Sarcostin (**4.5a**)	α-H,β-OH	H	H
Verticilloside F (**4.6**)	α-H,β-OH	R_B	H
Verticilloside G (**4.7**)	O	R_A	H
Verticilloside H (**4.8**)	O	R_B	H
Verticilloside I (**4.9**)	O	R_C	H
Verticilloside J (**4.10**)	α-H,β-OH	R_C	H
Verticilloside K (**4.11**)	α-H,β-OH	R_A	Bz
Verticilloside L (**4.12**)	α-H,β-OH	R_B	Bz
Verticilloside M (**4.13**)	α-H,β-OH	R_D	Bz

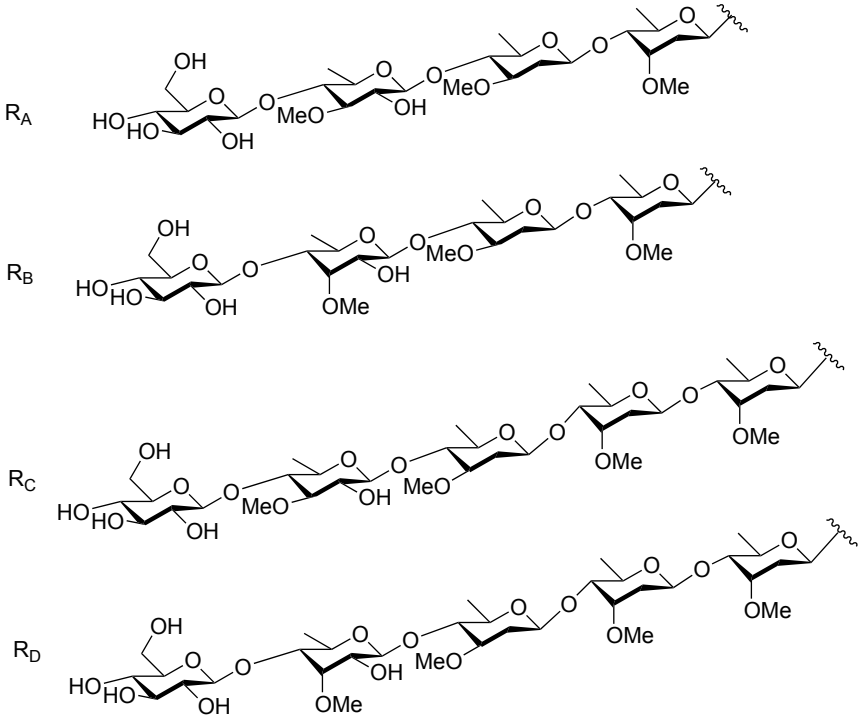

Figure 4-17 Structure of verticillosides A-M (**4.1-4.13**)

4.3.1. Structure Elucidation

Verticilloside A (**4.1**) was obtained as a white, amorphous powder. The HRMS displayed a $[M+Na]^+$ ion at *m/z* 1055.5276 consistent with a molecular formula of $C_{50}H_{80}NaO_{22}$ (calc. 1055.5039). The ^1H NMR spectrum showed four singlet signals (δ 2.49, 2.08, 1.94, 1.35) and an olefinic proton (δ 4.99) that indicated the presence of an acylated pregn-5-en-20-one skeleton (Table 4-10, Experimental data). The proposed carbon skeleton was supported by the HMBC correlations (Figure 4-18) between the proton signal δ 1.94 (Me-18) and the carbon resonances δ 58.3 (C-13), 73.9 (C-12), 89.8 (C-14), and 92.8 (C-17); and proton signal δ 1.35 (Me-19) and carbon resonances of δ 39.2 (C-1), 139.6 (C-5), 44.8 (C-9), and 38.0 (C-10). Also, the HMBC correlations between the methyl signal of the acetyl group (δ 2.49) and C-12 (δ 73.9) clarified the attachment position of the methyl ester functionality. Finally, ^1H,^1H DQFCOSY, HSQC and HMBC spectra allowed for the full assignment of the ^1H and ^{13}C signals (Tables 4-8 and 4-10, Experimental Data), and the aglycone moiety was deduced to be metaplexigenin (**4.1a**). Remarkably, the higher-resolution 800 MHz NMR spectra permitted the identification of the signals even in highly overlapped regions as shown in Figures 4-19 and 4-20 when compared with 500MHz experiments. The NMR data was in good agreement with previously reported values for metaplexigenin.[202, 219] The initially proposed stereochemistry was based on dipolar interactions observed in the ROESY spectrum (Figure 4-21) and further confirmed by X-ray crystallography of the aglycone obtained by acid hydrolysis of the glycoside (Figure 4-22). In addition, four anomeric protons were observed in the ^1H NMR spectrum (δ 5.29, 5.16, 4.90 and 4.70) suggesting that the same number of sugars were attached at the 3-position. Furthermore, the presence of three methyl doublets in the aliphatic region of the ^1H NMR spectrum (δ 1.78,

1.68 and 1.44) and three methoxy groups (δ 3.96, 3.56 and 3.49), indicated the presence of 6-deoxy-3-methoxy sugars, commonly found in the *Asclepias* glycosides. Using ^{1}H,^{1}H DQFCOSY, ^{1}H,^{1}H-TOCSY, and HSQC-TOCSY spectra (Figure 4-23), the proton spin systems and the carbon resonances of each sugar were fully assigned (Tables 4-9 and 4-11, Experimental Data). The sugar units were then identified as cymarose, oleandrose, thevetose, and glucose by NMR data analysis and comparison with previously reported values. The connectivity of the sugars was established by the following key HMBC correlations: cymarose anomeric proton H-1' (δ 5.29) and C-3 (δ 77.9); oleandrose anomeric proton H-1'' (δ 4.70) and C-4' (δ 83.6); thevetose anomeric proton H-1''' (δ 4.90) and C-4'' (δ 83.6), and glucose anomeric proton H-1'''' (δ 5.16) and C-4''' (δ 83.8) (Figure 4-17). The β-linkages of the four sugars were established by the large coupling constants (J = 7.8-9.7) observed for the anomeric protons. Finally, the optical rotation of the purified monomeric sugars after acid hydrolysis allowed us to establish the absolute configuration D for all the sugars present in this compound. Therefore, the structure of **4.1** was determined to be metaplexigenin 3-*O*-β-D-glucopyranosyl-(1→4)-β-D-thevetopyranosyl-(1→4)-β-D-oleandropyranosyl-(1→4)-β-D-cymaropyranose. Compound **4.1** represents a previously unreported metaplexigenin glycoside that we named verticilloside A.

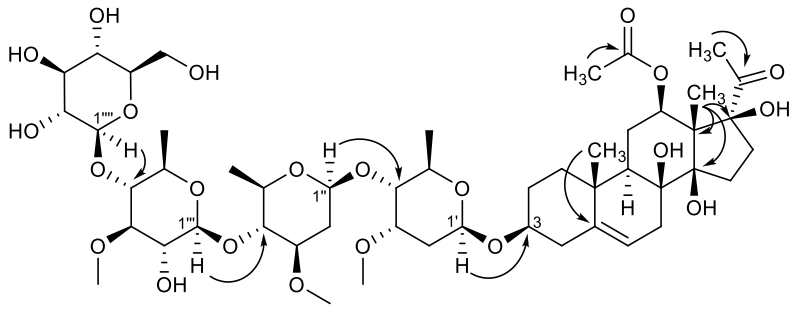

Figure 4-18 Selected HMBC correlations observed for verticilloside A (**4.1**)

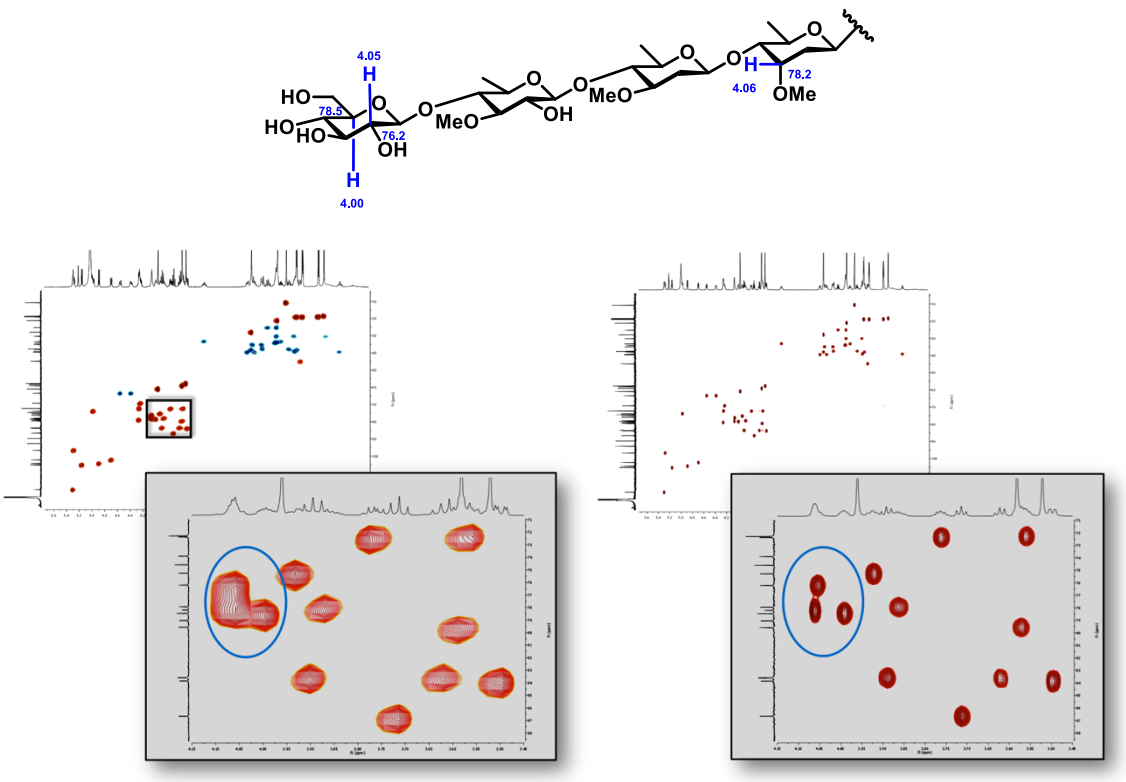

Figure 4-19 HSQC spectra of verticilloside A (**4.1**) at 500 MHz (left) and 800 MHz (right)

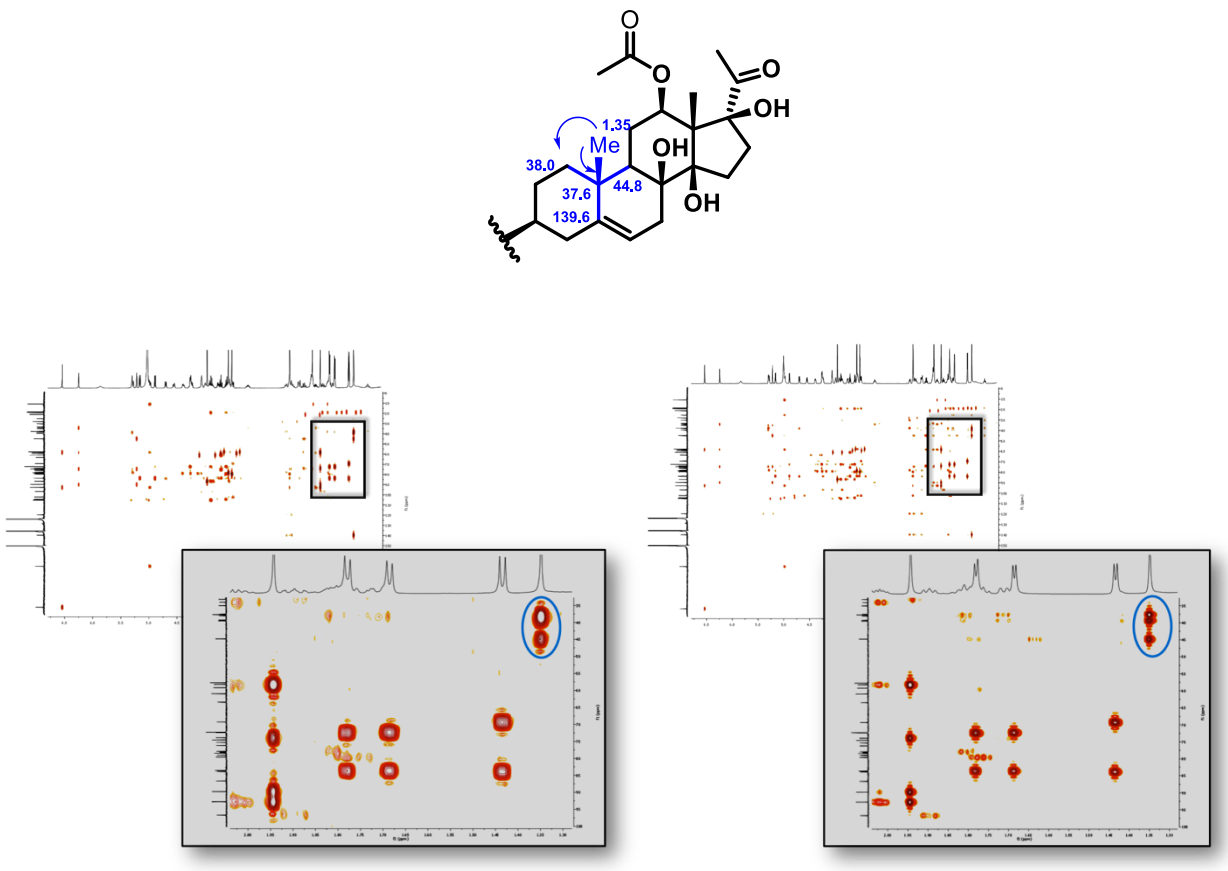

Figure 4-20 HMBC spectra of verticilloside A (**4.1**) at 500 MHz (left) and 800 MHz (right)

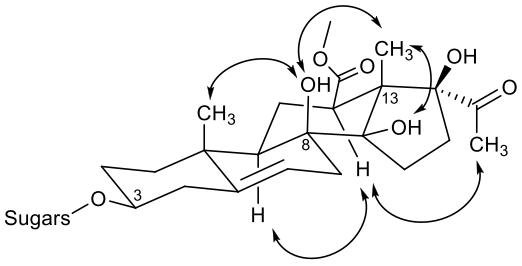

Figure 4-21 Selected ROE dipolar couplings of aglycone portion of verticilloside A (**4.1**)

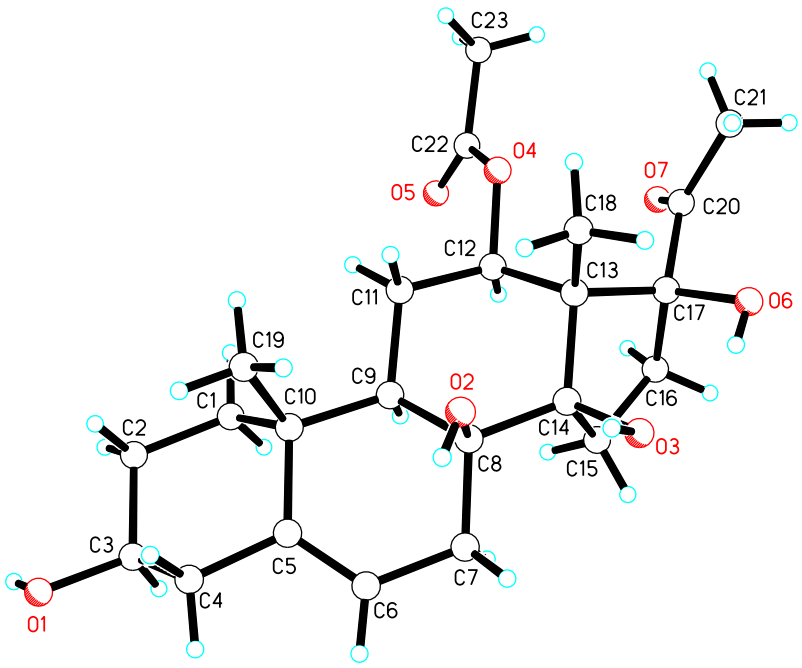

Figure 4-22 ORTEP representation of metaplexigenin (**4.1a**) obtained by hydrolysis of verticilloside A (**4.1**)

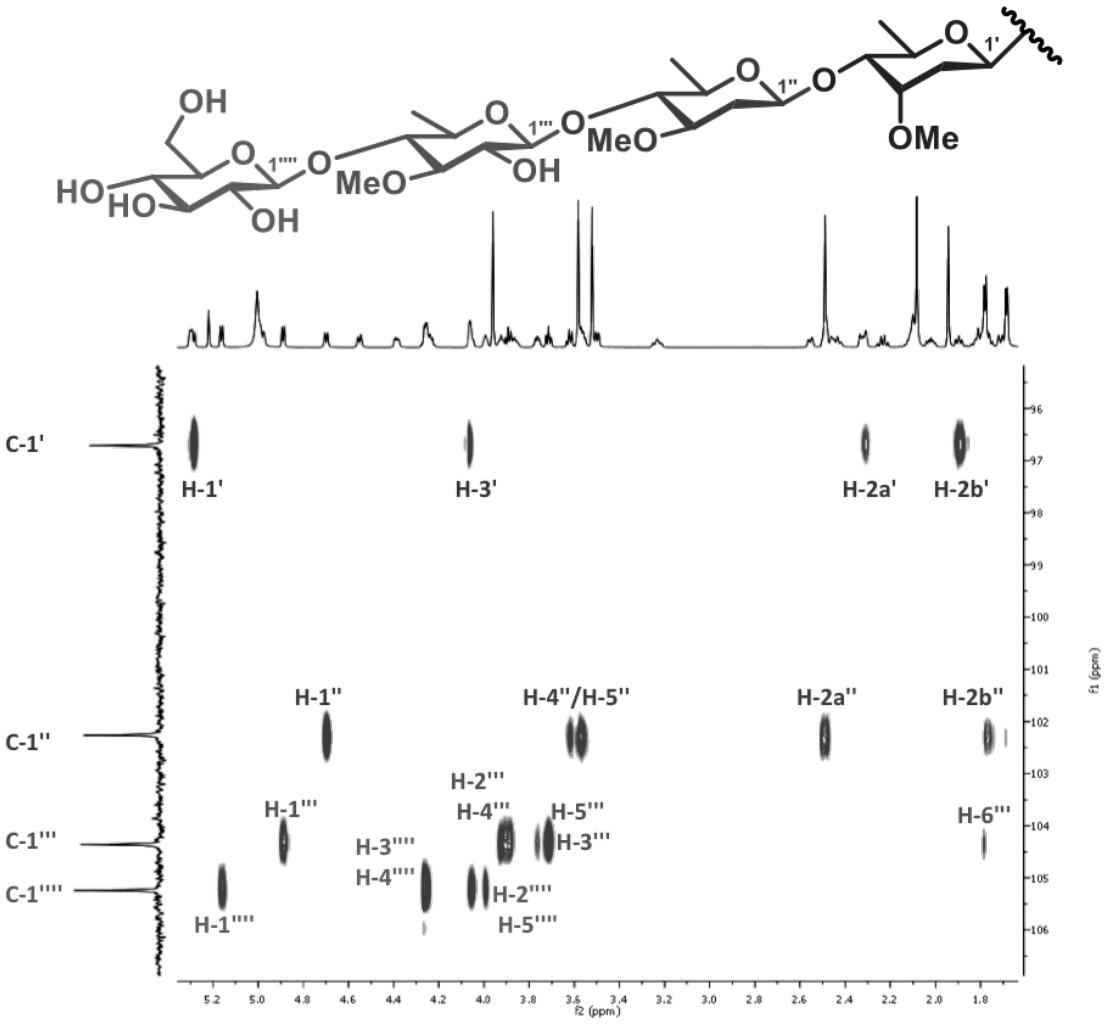

Figure 4-23 HSQC-TOCSY spectrum of verticilloside A (**4.1**)

Verticilloside B (**4.2**), an amorphous white powder, showed a HRMS $[M+Na]^+$ ion at *m/z* 1052.5271, suggesting the same molecular formula of $C_{50}H_{80}NaO_{22}$ (calc. 1055.5039) as for compound **1**. First, the aglycone present in **4.2** was determined to be metaplexigenin and it was identified as described before. Second, the ^1H NMR also showed the presence of four anomeric protons (δ 5.27, 5.26, 5.00 and 4.67); however, only the chemical shift of H-1''' changed significantly when compared with the anomeric protons of **4.1** (Tables 4-8 and 4-10,

Experimental data). After analysis of the spin systems of each sugar aided by ^{1}H,^{1}H-DQFCOSY, and ^{1}H,^{1}H-TOCSY and HSQC-TOCSY spectra, the ^{1}H and ^{13}C signals were completely assigned and the four sugars were elucidated as cymarose, oleandrose, 6-deoxy-3-*O*-methyl allopyranose, and glucose (Tables 4-9 and 4-11, Experimental data). The HMBC correlations unambiguously revealed the connectivity of the sugars: anomeric proton of cymarose H-1' (δ 5.26) with C-3 (δ 78.1); anomeric proton of oleandrose H-1'' (δ 4.67) and C-4' (δ 84.0); anomeric proton of 6-deoxy-3-*O*-methyl allopyranose H-1''' (δ 5.27) and C-4'' (δ 83.7); and anomeric proton of glucose H-1''' (δ 5.00) and C-4'' (δ 83.8). As a result, the structure of **4.2** was assigned to be metaplexigenin 3-*O*-β-D-glucopyranosyl-(1→4)-β-(6-deoxy-3-*O*-methyl)-D-allopyranosyl-(1→4)-β-D-oleandropyranosyl-(1→4)-β-D-cymaropyranose.

Verticillosides C (**4.3**) and D (**4.4**) were both isolated as white, amorphous powders. The HRMS of **4.3** and **4.4** showed very similar $[M+Na]^{+}$ ions at *m/z* 1199.5877 and 1199.5841 respectively, suggesting they both shared the same molecular formula $C_{57}H_{92}NaO_{25}$ (calc. 1199.5825). The aglycone structure in both compounds was established to be metaplexigenin (*vide supra*). However, five anomeric protons were identified in the ^{1}H NMR (**4.3**: δ 5.29, 5.16, 5.13, 4.89 and 4.68; **4.4**: δ 5.29, 5.28, 5.12, 5.01 and 4.67) indicating that each compound contained five sugar units. Only one proton signal corresponding to H-1'''' (δ 4.89 in **4.3**, and δ 5.28 in **3.4**) was significantly different when comparing the ^{1}H-NMR spectrum of **4.3** and **4.4**. The ^{1}H,^{1}H DQFCOSY and ^{1}H,^{1}H-TOCSY and HSQC-TOCSY spectra assisted significantly with the identification of the spin systems of each sugar as well as with the assignment of all the ^{1}H and ^{13}C signals (Tables 4-9 and 4-11, Experimental data). Two units of cymarose and single units of oleandrose, thevetose, and glucose were identified in **4.3**. On the other hand, the sugars

present in **4.4** were found to consist of two units of cymarose and single units of oleandrose, 6-deoxy-3-*O*-methyl allopyranose, and glucose. As previously described, HMBC correlations allowed for the establishment of the sugar sequence in **4.3**: cymarose I anomeric proton H-1' (δ 5.29) and C-3 (δ 78.0); cymarose II anomeric proton H-1'' (δ 5.13) and C-4' (δ 83.7); oleandrose anomeric proton H-1''' (δ 4.68) and C-4'' (δ 83.5); thevetose anomeric proton H-1'''' (δ 4.89) and C-4''' (δ 83.6); and glucose anomeric proton H-1''''' (δ 5.16) and C-4''''' (δ 83.6). In the same way, the HMBC of **4.4** showed correlations between cymarose I anomeric proton H-1' (δ 5.29) and C-3 (δ 78.0); cymarose II anomeric proton H-1'' (δ 5.12) and C-4' (δ 83.7); oleandrose anomeric proton H-1''' (δ 4.67) and C-4'' (δ 83.5); 6-deoxy-3-*O*-mehtyl allopyranose anomeric proton H-1'''' (δ 5.28) and C-4''' (δ 83.3); and glucose anomeric proton H-1''''' (δ 5.01) and C-4''''' (δ 83.6). Hence, **4.3** was determined to be metaplexigenin 3-*O*-β-D-glucopyranosyl-(1→4)-β-D-thevetopyranosyl-(1→4)-β-D-oleandropyranosyl-(1→4)-β-D-cymaropyranosyl-(1→4)-β-D-cymaropyranose. Also, **4.4** was established to be metaplexigenin 3-*O*-β-D-glucopyranosyl-(1→4)-β-(6-deoxy-3-*O*-methyl)-D-allopyranosyl-(1→4)-β-D-oleandropyranosyl-(1→4)-β-D-cymaropyranosyl-(1→4)-β-cymaropyranose.

Verticilloside E (**4.5**), isolated as a white amorphous powder, showed a calculated molecular formula of $C_{48}H_{80}NaO_{21}$ based on the observed HRMS ion $[M+Na]^+$ at *m/z* 1015.5098 (calc. 1015.5090). The observation in the ^1H NMR spectrum of two singlet methyl groups (δ 1.98, 1.43), a methyl doublet (δ 1.54), an olefinic proton (δ 5.40), and two olefinic carbons (δ 139.5 *s* and 120.2 *d*) in the ^{13}C NMR suggested the presence of the 20-hydroxy-pregn-5-ene skeleton. Using ^1H,^1H-COSY, HSQC and HMBC spectra, ^1H and ^{13}C signals in the pregnane skeleton were

unambiguously assigned (Tables 4-8 and 4-12, Experimental data) and allowed for the identification of the aglycone as sarcostin. Relative orientation of the hydroxyl group at position C-17 was determined as beta based on the X-ray structure of aglycone obtained by acid hydrolysis of **4.5** (Figure 4-24). The ^{1}H and ^{13}C NMR data were in good agreement with previously reported data for this sarcostin.[189] In addition, **4.5** showed four anomeric protons in the ^{1}H NMR spectra (δ 5.29, 5.16, 4.90, and 4.70) indicating the presence of four sugars attached to the aglycone. The sugars were found to be the same as those present in **4.1** based on their ^{1}H and ^{13}C NMR data. Consequently, **4.5** was elucidated as sarcostin 3-*O*-β-D-glucopyranosyl-(1→4)-β-D-thevetopyranosyl-(1→4)-β-D-oleandropyranosyl-(1→4)-β-D-cymaropyranose.

Moreover, verticilloside F (**4.6**) presented the same calculated molecular formula than **4.5** ($C_{48}H_{80}NaO_{21}$) based on the experimental HRMS ion $[M+Na]^{+}$ at m/z 1015.5153 (calc. 1015.5090). The ^{1}H and ^{13}C NMR signals of the aglycone portion of **4.5** and **4.6** were almost superimposable (Tables 4-8 and 4-12, Experimental data), indicating that **6** also had sarcostin as the pregnane core. On the other hand, after full assignment of the ^{1}H and ^{13}C NMR signals using 2D NMR spectra (Tables 4-10 and 4-13, Experimental data), the four sugars present in **4.6** were found to be the same as those present in compound **4.2** by means of comparison of their NMR data. Consequently, **4.6** was defined to be sarcostin 3-*O*-β-D-glucopyranosyl-(1→4)-β-(6-deoxy-3-*O*-methyl)-D-allopyranosyl-(1→4)-β-oleandropyranosyl-(1→4)-β-D-cymaropyranose.

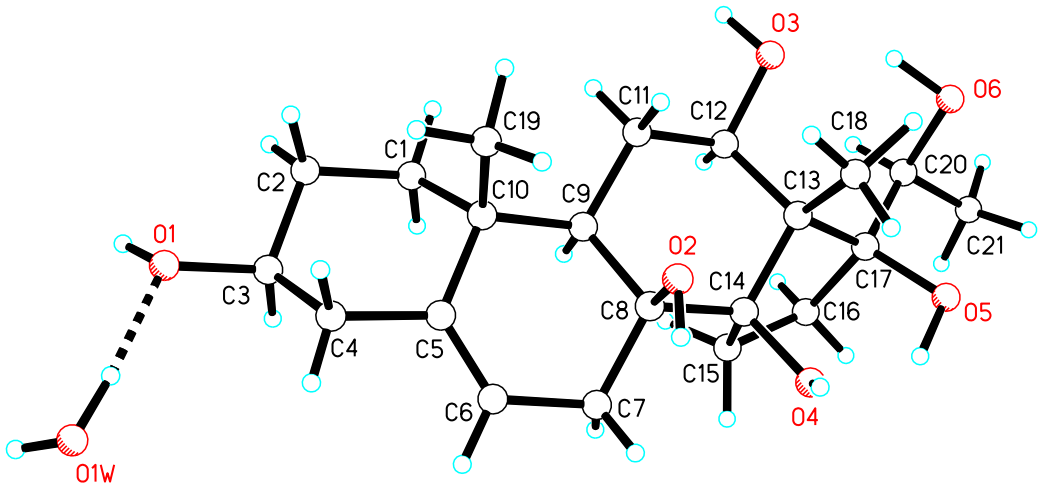

Figure 4-24 ORTEP representation of sarcostin (**4.5a**) obtained by hydrolysis of verticilloside E (**4.5**)

Verticillosides G (**4.7**) and H (**4.8**) displayed a HRMS ion $[M+Na]^+$ at *m/z* 1013.4913 and 1013.4921 respectively suggesting the same molecular formula of $C_{48}H_{78}NaO_{21}$ (calc. 1013.4933) for both compounds. Similar to compounds **4.1-4.4**, three methyl singlets were observed in the ^{1}H NMR (**4.7**: δ 2.60, 2.02, 1.42; **4.8**: δ 2.65, 2.02, 1.41); however, the acetyl ^{1}H and ^{13}C signals were missing in **4.7** and **4.8**. Following a similar analysis of the ^{1}H, ^{13}C and 2D NMR data as described before, the aglycone present in the two compounds was identified to be 12-*O*-deacylmetaplexigenin and the signal assignment was in good agreement with previously reported values.[202] The ^{1}H and ^{13}C signals were totally assigned for the sugar portion using 2D NMR spectra (Tables 4-9 and 4-13, Experimental data). While the sugars in **4.7** were found to be the same as in **4.1**, the sugars in **4.8** were identical to those present in **4.2** based on their NMR data comparison. The structures of **4.7** and **4.8** were determined to be 12-*O*-deacylmetaplexigenin 3-

O-β-D-glucopyranosyl-(1→4)-β-D-thevetopyranosyl-(1→4)-β-D-oleandropyranosyl-(1→4)-β-D-cymaropyranose and 12-*O*-deacylmetaplexigenin 3-*O*-β-D-glucopiranosyl-(1→4)-β-D-thevetopyranosyl-(1→4)-β-D-oleandropyranosyl-(1→4)-β-D-cymaropyranose, respectively.

Verticilloside I (**4.9**) had a HRMS ion $[M+Na]^+$ at *m/z* 1159.5904 indicating a molecular formula of $C_{55}H_{92}NaO_{24,}$ (calc. 1159.5876). Complete assignment of ^1H and ^{13}C NMR signals using 2D NMR (Tables 4-9 and 4-12, Experimental data) showed that the aglycone corresponded to 12-*O*-deacylmetaplexigenin. The five sugars present in **4.9** were identical to those found in **4.4** and their ^1H and ^{13}C sugar signals were almost identical (Tables 4-10 and 4-13, Experimental data). Hence, structure of **4.9** was confirmed to be 12-*O*-deacylmetaplexigenin 3-*O*-β-D-glucopyranosyl-(1→4)-β-(6-deoxy-3-*O*-methyl)-D-allopyranosyl-(1→4)-β-D-oleandropyranosyl-(1→4)-β-D-cymaropyranosyl-(1→4)-β-D-cymaropyranose. Likewise, verticilloside J (**4.10)** had a molecular formula of $C_{55}H_{90}NaO_{24}$ on the basis of the observed HRMS ion $[M+Na]^+$ at m/z 1057.5734 (calc. 1157.5720). Following the complete assignment of ^1H and ^{13}C NMR signals aided by 2D NMR data (Tables 4-9, 4-10, 4-14, and 4-15; Experimental data), the aglycone was found to be sarcostin and the sugars the same as those in **4.4**. Hence, **4.10** was determined as sarcostin 3-*O*-β-D-glucopyranosyl-(1→4)-β-(6-deoxy-3-*O*-methyl)-D-allopyranosyl-(1→4)-β-D-oleandropyranosyl-(1→4)-β-D-cymaropyranosyl-(1→4)-β-D-cymaropyranose.

Verticillosides K (**4.11**) and L (**4.12**) displayed very similar $[M+Na]^+$ ions at *m/z* 1119.5337 and 1119.5364 respectively, thus sharing the same calculated molecular formula of $C_{55}H_{84}NaO_{22}$ (calcld 1119.5352). Unlike previously described compounds, ^1H NMR spectrum of **4.11** showed aromatic signals corresponding to a benzoyl group (δ 8.59, 7.50, and 7.41) and further confirmed

by ^{13}C NMR resonances (δ 167.0, 133.6, 132.1, 130.8, and 129.2). The benzoyl group was found to be attached to position 12 by means of the observed HMBC correlation between H-12 (δ 5.40) and benzoyl carbonyl signal (δ 167.0). The aglycone was established as 12-*O*-benzoylsarcostin based on the HMBC correlations between the proton signal δ 2.24 (H-18) with carbon resonances of δ 57.8 (C-13), 75.7 (C-12), 89.0 (C-14), and 89.2 (C-17); and between proton signal δ 1.37 (Me-19) and carbon resonances of δ 39.2 (C-1), 139.5 (C-5), 44.5 (C-9), and 37.7 (C-10). The experimental NMR data (Tables 4-8 and 4-14, Experimental data) of the algycone were in good agreement with previously reported values.[220] The ^{1}H-NMR and ^{13}C-NMR values of the aglycone in compound **4.12** and **4.13** were almost identical to those just described for **4.11**, indicating that the three compounds share the same aglycone. Furthermore, following full assignment of ^{1}H and ^{13}C NMR data using 2D NMR spectra, close comparison of their spectra revealed that the sugars present in **4.11** and **4.12** were identical to those present in **4.1** and **4.2**, respectively. Consequently, the structure of **4.11** was established as 12-*O*-benzoylsarcostin 3-*O*-β-D-glucopyranosyl-(1→4)-β-D-thevetopyranosyl-(1→4)-β-D-oleandropyranosyl-(1→4)-β-D-cymaropyranose, and structure of **4.12** as sarcostin 3-*O*-β-D-glucopiranosyl-(1→4)-β-(6-deoxy-3-*O*-methyl)-D-allopyranosyl-(1→4)-β-D-oleandropyranosyl-(1→4)-β-D-cymaropyranose.

Finally, verticilloside M (**4.13**) had a HRMS $[M+Na]^{+}$ ion at *m/z* 1263.6037 (calc. 1263.6138) suggesting a molecular formula of $C_{62}H_{96}NaO_{25}$. As described before, by closed comparison of the 1D and 2D NMR spectra, the aglycone was identified to be 12-*O*-benzoylsarcostin, like in compound **4.11**. The sugar moiety contained the same sequence of five units as those in compound **4.4**. Hence, compound **4.13** was identified as 12-*O*-benzoylsarcostin 3-*O*-β-D-

glucopyranosyl-(1→4)-β-(6-deoxy-3-*O*-methyl)-D-allopyranosyl-(1→4)-β-D-oleandropyranosyl-(1→4)-β-D-cymaropyranosyl-(1→4)-β-D-cymaropyranose.

4.3.2. Biological evaluation

The cytotoxicity of the isolates (**4.1-4.13**) was evaluated against the paired breast cell lines Hs578T (cancer) and Hs578Bst (normal), however no toxicity was observed in the experimental concentration range of 0.2-50 μM.

4.4. Cytotoxic Cardiac Glycosides and Other Components from *Asclepias syriaca* L.

Asclepias syriaca is also known as "common milkweed" and, besides its various medicinal uses, it was studied several years ago as an alternative crop for different products such as natural rubber from latex, alternative fuels, as well as fibers for paper fabrication; however several factors at that time prevented its further commercialization.[181, 221] Nevertheless, in recent years *A. syriaca* has received industrial crop status in the United States due to the use of its silky seed floss in hypoallergenic pillows, comforters, and insulating fiber manufacture.[222] After the removal of the floss, the remaining plant biomass is typically disposed without regard of its potentially valuable products.[223] Furthermore, the boiled young sprouts, floral buds, and immature fruits have found historical and contemporary use as food, in the form of soup by the Omaha, Dakota, Pawnee, Ponca, and Winnebago tribes.[183] The bitter-tasting compounds have been shown to be removed by four minutes of boiling and changing the water.[181]

Encouraged by the cytotoxicity results observed during the screening of *A. syriaca*, its traditional uses, and by its current industrial interest, in this plant's chemistry was studied in further detail. A total of five new compounds were isolated and identified including the cardiac glycoside **4.15** (4.5 mg), the quercetin triglycoside **4.19** (24.7 mg), the neolignan **4.20** (16.1 mg), the phenylethanoid **4.21** (7.8 mg), and the megastigmane glycoside **4.22** (6.5 mg); along with 19 known compounds (Figures 4-25 and 4-26). The known compounds included the pentacyclic triterpenes α-amyrin (**4.23**), β-amyrin (**4.25**), α-amyrin acetate (**4.24**), β-amyrin acetate (**4.26**), lupeol acetate (**4.27**), and oleanolic acid (**4.28**); the cardiac glycosides 3-*O*-β-D-glucopyranosyl-(1→4)-6-desoxy-β-D-allopyranosyl uzarigenin (**4.14**), 3-*O*-β-D-glucopyranosyl-(1→4)-β-D-glucpyranosyl uzarigenin (**4.16**), and desglucouzarin (**4.17**); the free fatty acids linolenic acid

(**4.29**) and linoleic acid (**4.30**); the glycosylated flavonoids quercetin 3-*O*-β-galactopyranosyl-(1→2)-β-xylopyranoside (**4.31**), kaempferol 3-*O*-β-galactopyranosyl-(1→2)-β-xylopyranoside (**4.18**), 3'-*O*-methyl-quercetin 3-*O*-β-galactopyranosyl-(1→2)-β-xylopyranoside (**4.32**), and quercetin-3-*O*-β-galactopyranoside (**4.33**); the lignans *epi*-syringaresinol (**4.34**) and prupaside (**4.35**); the phenolics *cis*-cinnamic acid (**4.36**), *trans*-cinnamic acid (**4.37**), isovanillinic acid (**4.38**), and 4-(β-glucopyranosyloxy)benzoic acid (**4.39**). The structures of the new compounds were elucidated using a range of spectroscopic techniques, including 1D and 2D NMR and HRMS. In the case of the known compounds, their structures were identified by comparison of their measured spectroscopic data with literature values.

As mentioned before, many *Asclepias* species are an important food source for the Monarch butterfly caterpillar and *A. syriaca* is not an exception. Several authors have suggested that flavonoids play an important role in the attraction and oviposition preference for the Monarch butterfly.[224, 225] Therefore, it is interesting to note that our investigation revealed the presence of several glycosylated flavonoids in the aerial parts of this species, however, their ecological role remains to be solved.

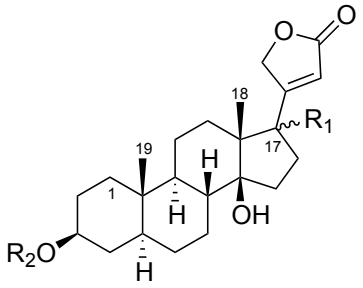

	R_1	R_2
4.14	α-H	S_1
4.15	β-OH	S_1
Uzarin (**4.16**)	α-H	S_2
Desglucouzarin (**4.17**)	α-H	Glu

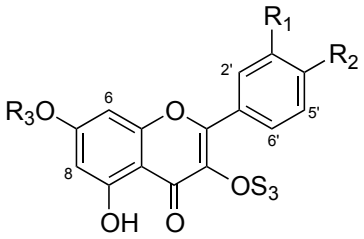

	R_1	R_2	R_3
4.18	OH	H	H
Syriacatin (**4.19**)	OH	OH	Glu

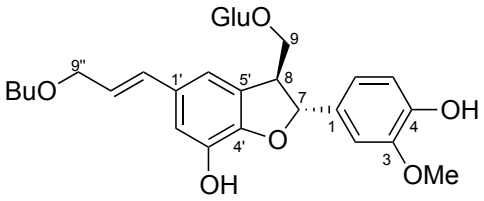

4.20

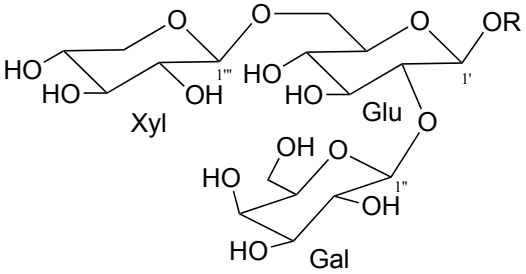

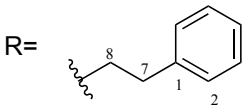

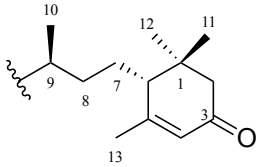

Kansanoside A(**4.21**) Oreadoside A (**4.22**)

S_1: β-glucopyranosyl-(1→4)-β-(6-deoxy)allopyranoside
S_2: β-glucopyranosyl-(1→4)-β-glucopyranoside
S_3: β-galactopyranosyl-(1→2)-β-xylopyranoside
Glu: β-glucopyranosyl
Gal: β-galactopyranosyl
Xyl: β-xylopyranosyl
Bu: *n*-butyl

Figure 4-25 Structures of active and new compounds (**4.14-4.22**) from *A. syriaca*

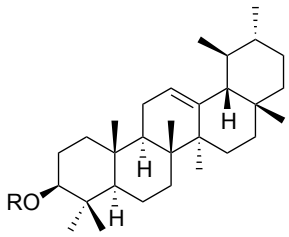

R=H, α-Amyrin (**4.23**)
R=Ac, α-Amyrin acetate (**4.24**)

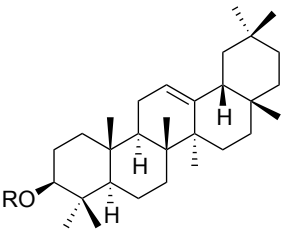

R=H, β-Amyrin (**4.25**)
R=H, β-Amyrin acetate (**4.26**)

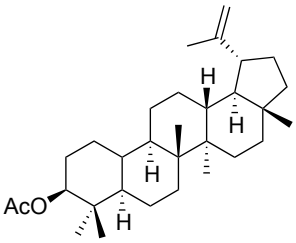

Lupeol acetate (**4.27**)

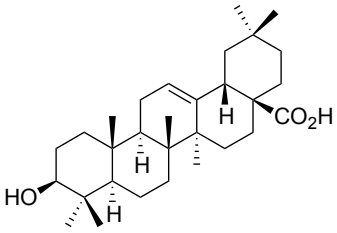

Oleanolic acid (**4.28**)

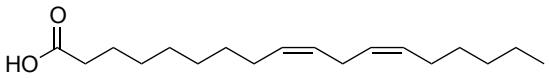

Linoleic acid (**4.29**)

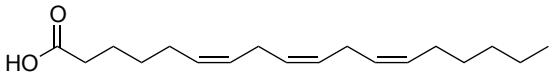

γ-Linolenic acid (**4.30**)

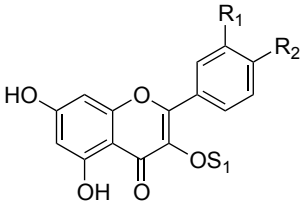

	R_1	R_2	R_3
4.31	OH	H	S_1
4.32	OMe	OH	S_1
4.33	OH	OH	Gal

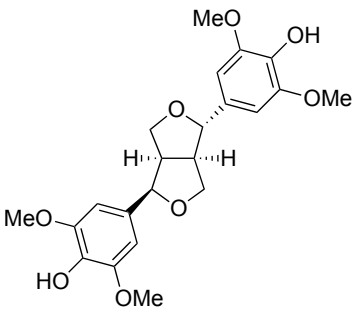

epi-Syringaresinol (**4.34**)

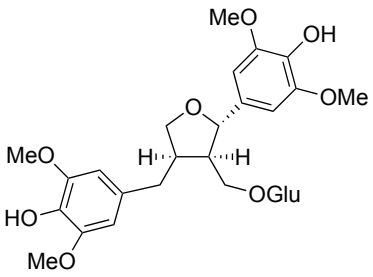

Prupaside (**4.35**)

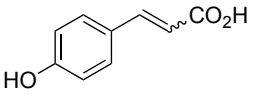

trans-Cinnamic acid (**4.36**)
cis-Cinnamic acid (**4.37**)

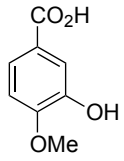

Isovainillinic acid (**4.38**)

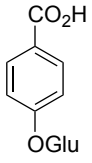

4.39

S_1: β-galactopyranosyl-(1→2)-β-xylopyranoside
Glu: β-glucopyranosyl
Gal: β-galactopyranosyl
Xyl: β-xylopyranosyl

Figure 4-26 Structures of known compounds (**4.23-4.18**) from *A. syriaca*

4.4.1. Structure Elucidation

Compound **4.15** was isolated as a white amorphous powder. The HRMS showed an $[M+Na]^+$ ion at *m/z* 721.3401 suggesting a molecular formula of $C_{35}H_{54}NaO_{14}$ (calc. 721.3411). The ^1H NMR spectrum of **4.15** showed the characteristic proton signals of the butenolide ring at δ_H 6.26 (dd, J = 1.8, 1.7 Hz, H-22), δ_H 5.23 (dd, J = 18.3, 1.7 Hz, H-21a), and δ_H 5.09 (dd, J = 18.3, 1.8 Hz, H-21b). The cardenolide steroidal tetracyclic ring system was confirmed using the key HMBC correlations between CH_3-18 (δ_H 1.22, s, H-18) and C-1, C-2, C-5, and C-10 and CH_3-19 (δ_H 0.67, s, H-19) and C-12, C-14, C-15, and C-17 (Table 4-16, Experimental Data). Moreover, the ^1H,^1H-COSY, HSQC, and HMBC experiments permitted full assignment of the signals in the aglycone which was further identified as 17β-hydroxyuzarigenin. The spectroscopic data of the aglycone was in agreement with previously reported values for similar compounds.[195, 205] Two anomeric proton signals at δ_H 5.42 (d, J = 7.9 Hz, H-1') and δ_H 5.10 (d, J = 7.6 Hz, H-1'') and the corresponding carbon resonances at δ_C 99.7 (CH, C-1') and δ_C 106.8 (CH, C-1''), suggested the presence of an equal number of sugar units and, after assignment of the NMR data using 1D and 2D NMR experiments, these were identified as 6-deoxyallose and glucose, both with a β-linkage based on the coupling constants of the anomeric protons. In addition, HMBC correlations between H-1' and C-3, and H-1'' and C-4' clearly established the connectivity of the sugars. When taken in conjunction with the acid-hydrolysis results (Experimental data), the structure of compound **4.15** was determined to be 3-*O*-β-D-glucopyranosyl-(1→4)-6-deoxy-β-D-allopyranosyl-17β-hydroxyuzarigenin. Although the 17β-hydroxyuzarigenin has been reported with other C-3 sugar moieties,[205] compound **4.15** represents a new structure.

Compound **4.19** was isolated as a yellow amorphous powder and the molecular formula of $C_{32}H_{38}NaO_{21}$ was suggested based on the HRMS $[M+Na]^+$ ion at *m/z* 781.1816 (calc. 781.1803). Two aromatic rings were assigned by inspection of its ^1H NMR data, the first showing two signals at δ_H 6.73 (d, *J* = 2.2 Hz, H-6) and δ_H 6.78 (d, *J* = 2.2 Hz, H-8), the second with three signals at δ_H 8.32 (d, *J* = 2.3 Hz, H-2'), δ_H 7.31 (d, *J* = 8.6 Hz, H-5'), and δ_H 8.36 (dd, *J* = 8.6, 2.3 Hz, H-6'). The presence of 12 aromatic carbon resonances was confirmed by ^{13}C NMR (Table 4-17, Experimental data). The observed oxygenation pattern in the aromatic rings, the presence of an additional carbonyl at δ_C 179.3 (C-4), and two olefinic carbons at δ_C 157.5 (C-2) and δ_C 135.5 (C-3) suggested the presence of a flavonol carbon skeleton which was further confirmed by HMBC correlations and corroborated by comparison with literature data of related structures.[226, 227] In addition, three sugar units were identified based on the presence of the same number of anomeric proton signals at δ_H 6.62 (d, *J* = 7.7 Hz, H-1''), δ_H 5.48 (d, *J* = 7.2, H-1'''), and δ_H 5.76 (d, *J* = 7.8, H-1''''). Using 1D and 2D NMR data, the signals of the sugar units were fully assigned (Table 4-18, Experimental data) and their identities were established as β-glucose, β-galactose, and β-xylose. The correlations observed in the HMBC experiment between the glucosyl anomeric proton (H-1'''') and C-7, between the galactosyl anomeric proton (H-1'') and C-3, and the xylosyl anomeric proton (H-1''') and C-2'', established the connectivities of the sugar units. Consequently, the structure of **4.19** was defined as quercetin-7-*O*-β-glucopyranosyl-3-*O*-β-D-galactopyranosyl-(1→2)-β-D-xylopyranoside. This compound has not been previously reported and we named it syriacatin.

Compound **4.20** was isolated as a white amorphous powder. The HRMS $[M+Na]^+$ ion at *m/z* 585.2298 suggested a molecular formula of $C_{29}H_{38}NaO_{11}$ (calc. 585.2312). Two independent

aromatic spin systems were identified in the ^{1}H NMR spectrum: the first with only two signals at δ_H 7.36 (d, *J* = 1.4 Hz, H-2') and δ_H 7.41 (d, *J* = 1.4 Hz, H-6') suggesting a 1,2,3,5-tetrasubstitution pattern, and the second displaying three signals at δ_H 7.34 (d, *J* = 1.6 Hz, H-2), δ_H 7.16 (d, *J* = 8.6 Hz, H-5) and δ_H 7.19 (dd, *J* = 8.6 Hz, 1.6, H-6) indicating a 1,2,4-trisubstituted ring. The previous observation was further confirmed by assignment of the corresponding 12 aromatic carbon resonances aided by HSQC and HMBC spectra (Table 4-18, Experimental data). Furthermore, two C_3 (propyl) equivalents linked to the aromatic rings were identified by means of ^{1}H,^{1}H-COSY and HMBC spectra, suggesting the presence of a lignan structure. The first propyl fragment showed two vinylic protons at δ_H 6.78 (d, *J* = 16.0 Hz, H-7') and δ_H 6.47 (ddd, *J* = 16.0, 6.0, 6.0 Hz, H-8') and an oxygenated methylene at δ_H 4.12 (2H, m, H-9'). The olefin signals for H-7' and H-8' clearly showed HMBC correlations with C-1' thus indicating a linkage to the first aromatic ring. The second propyl equivalent showed two methine protons at δ_H 5.99 (d, *J* = 6.5 Hz, H-7) and δ_H 4.08 (m, H-8) and an oxygenated methylene at δ_H 4.66, 4.44 (each 1H, m, H-9). The HMBC correlations observed between H-2, H-5, H-6 with C-7 and H-6' with C-8, as well as the chemical shift of C-7 (δ_C 88.8, CH), typical of a benzylic ether linkage, suggested the presence of a 4',7-epoxy-8,3'-neolignan unit, which was further confirmed by NMR data comparison with reported structures containing the same benzofuran neolignan skeleton.[228, 229] The 7,8-*trans* relative configuration of the dihydropyran ring was proposed based on the coupling constant of H-7 and the NOE signal observed between H-7 and H-9. Also, an anomeric proton at δ_H 5.03 (d, *J* = 7.6 Hz, H-1") indicated the presence of a sugar moiety further identified as glucose using 2D NMR experiments. Furthermore, the spin system of an *n*-butoxy group was readily identified from a ^{1}H ^{1}H-COSY experiment. Finally, the HMBC correlations

observed between the glucose anomeric proton (H-1") and C-9, and between the butoxymethylene (H-1'") and C-9' established the linkage of the sugar and butyl units to the neolignan skeleton. Consequently, the structure of **4.20** was determined to be 9'-*O*-butyl-3-*O*-demethyl-9-*O*-β-D-glucopyranosyl dehydrodiconiferylalcohol, differing from previously described neolignans by the presence of an unusual *O*-butyl substituent.[229] Although other plant-derived metabolites containing *n*-butyl substituents are known,[230, 231] an artificial origin for compound **4.20** can not be ruled out as *n*-butanol was the solvent used during the initial liquid-liquid partition of the crude extract.

Compound **4.21** was obtained as an amorphous white powder and displayed an $[M+Na]^+$ ion in HRMS at *m/z* 601.2087 suggesting a molecular formula of $C_{25}H_{38}NaO_{15}$ (calc. 601.2108). The ^{1}H NMR showed three aromatic signals for a monosubstituted benzene ring, and two methylene signals corresponding to a phenylethanoid group further confirmed by ^{1}H ^{1}H-COSY and HMBC correlations. In addition, the ^{1}H NMR spectrum also revealed three anomeric protons at δ_H 4.83 (d, J = 7.8 Hz, H-1'), δ_H 5.33 (d, J = 7.9 Hz, H-1"), and δ_H 4.88 (d, J = 7.0 Hz, H-1'") that were used as starting points to fully characterize each structure using ^{1}H ^{1}H-COSY, HSQC-TOCSY, HSQC, and HMBC experiments (Table 4-19, Experimental data). Hence, the sugar moieties were identified as β-galactose, β-glucose, and β-xylose. The connectivities of the phenylethanoid and sugar moieties were elucidated using the HMBC correlations between the galactosyl anomeric proton (H-1') and C-8, the glucosyl anomeric proton H-1" and C-2', and the xylosyl anomeric proton H-1'" and C-6'. Thus, compound **4.21** was determined to be phenylethyl-β-D-glucopyranosyl-(1→2)-[β-D-xylopyranosyl-(1→6)]-β-D-galactopyranoside and we named it

kansanoside A. The occurrence of phenylethanoids is not common in the Asclepiadaceae family and this is the first report of this compound class in the *Asclepias* genus.[232, 233]

Finally, compound **4.22**, an amorphous white powder, showed a HRMS $[M+Na]^+$ ion at *m/z* 689.2974, suggesting a molecular formula of $C_{30}H_{50}NaO_{16}$ (calc. 689.2974). Three anomeric protons at δ_H 4.87 (d, J = 7.7 Hz, H-1'), δ_H 5.23 (d, J = 7.8 Hz, H-1''), and δ_H 4.89 (d, J = 7.0 Hz, H-1''') indicated the presence of three sugar units that, after comparison of their NMR data (Table 4-19, Experimental data) were determined to be the same as those present in compound **4.21**. In addition, a total of 13 carbons were left to be assigned: four methyls, three methylenes, a trisubstituted olefin, two methines, a quaternary carbon, and a conjugated carbonyl. Several HMBC correlations suggested a megastigmane carbon skeleton, namely of H-12 with C-1, C-2, C-6, and C-13; H-13 with C-1, C-2, C-6, and C-12; H-2 with C-1, C-3, and C-4; H-4 with C-3, C-13, and C-6; H-6 with C-1, C-4, C-7, and C-8; and H-10 with C-9, and C-8. The proposed skeleton was confirmed by the ^{1}H ^{1}H-COSY crosspeaks showing the spin coupling sequence H-6, H-7, H-8, H-9, and H-10; as well as allylic coupling (J = 1.2 Hz) between H-13 and H-4. In addition, the NMR data were in agreement with reported data for structurally related compounds, including the proposed relative configuration.[234, 235] Hence, compound **4.22** was established as 9-hydroxymegastigma-4-en-3-one β-D-glucopyranosyl-(1→2)-[β-D-xylopyranosyl-(1→6)]-β-D-galactopyranoside and named oreadoside A. Although a couple of reports have identified megastigmane glycosides in *Asclepias* species, this is the first account of this type of compound in *A. syriaca*.[214, 236]

4.4.2. Biological evaluation

The isolates were screened against the human cancer breast cell line Hs578T; however, only compounds showing $IC_{50} < 50$ μM were chosen for further testing. Although most of the isolated compounds did not show cytotoxicity in our preliminary screening, many of them have been reported as biologically active in various tests and could have potential value against other disease targets. Particularly, the highly abundant pentacyclic triterpenes have been previously reported as chemopreventive,[237] anti-inflammatory,[238] and as analgesic agents.[239, 240]

The isolates that showed activity in the preliminary screening (**4.14-4.18**) were submitted for testing in a panel of three additional breast cancer cell lines (MCF-7, T47D, and Sk-Br-3) and a normal breast cell line (Hs578Bst), and the results are shown in Figure 4-27 (Table 4-5, Experimental data). In addition, the classic cardiac glycosides digoxin, digitoxigenin, and ouabain were included for comparison purposes. The tested compounds displayed cytoxicity in a range of 0.59 to 40 μM, compound **4.14** being the most active across the panel of cell lines tested. Actually, the cytotoxicity observed for compound **4.14** was comparable to the positive controls doxorubicin and digoxin. Cardenolides **4.15-4.17** showed reduced cytotoxicity when compared to compound **4.14**, revealing the important role of the C-17 configuration as well as the nature and number of sugars attached to C-3. In addition, the relative potency of the classic cardiac glycosides tested here (ouabain > digoxin > digitoxigenin) is in agreement with previously reported data.[241, 242] Even though the kaempferol glycoside **4.18** showed cytotoxicity during the initial screening ($IC_{50} < 50$ μM), further testing reveled low activity ($IC_{50} > 40$ μM) in all cancer cell lines and a low percentage of inhibition (32.7 ± 2.2%) at maximum concentration for the cancer cell line Hs578T.

Furthermore, cytotoxicity data from the paired breast human cell lines Hs578T and Hs578Bst revealed information about selectivity of tested compounds against malignant cells.[217] In our assay the tested compounds showed lower IC_{50} values against the normal cells than cancer cells (Figure 4-26), however the toxicity (expressed as percentage of control at maximum concentration) was significantly higher in the cancer cells when compared with normal cells (Figures 4-27 and 4-28; Table 4-6, Experimental data). Further investigation is needed to explain the reason behind this behavior but it can possibly be due to the significant growing rate differences between the two cell lines.

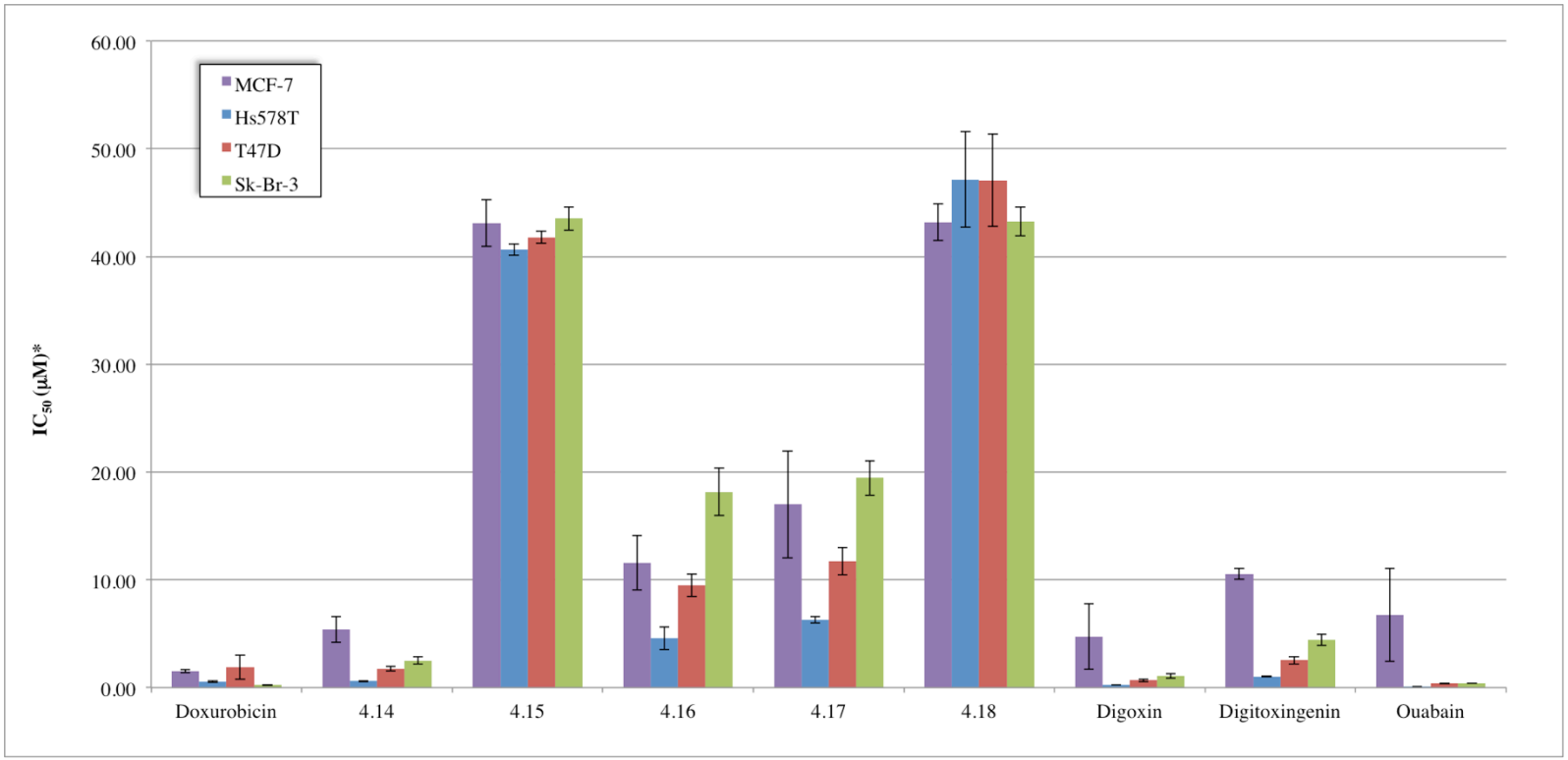

Figure 4-27 IC_{50} values (μM) of isolates **4.14-4.18** in four breast cancer cell lines MCF-7, Hs578T, T47D, and Sk-Br-3

* Values are average of three replicas and error bars indicated ±SD

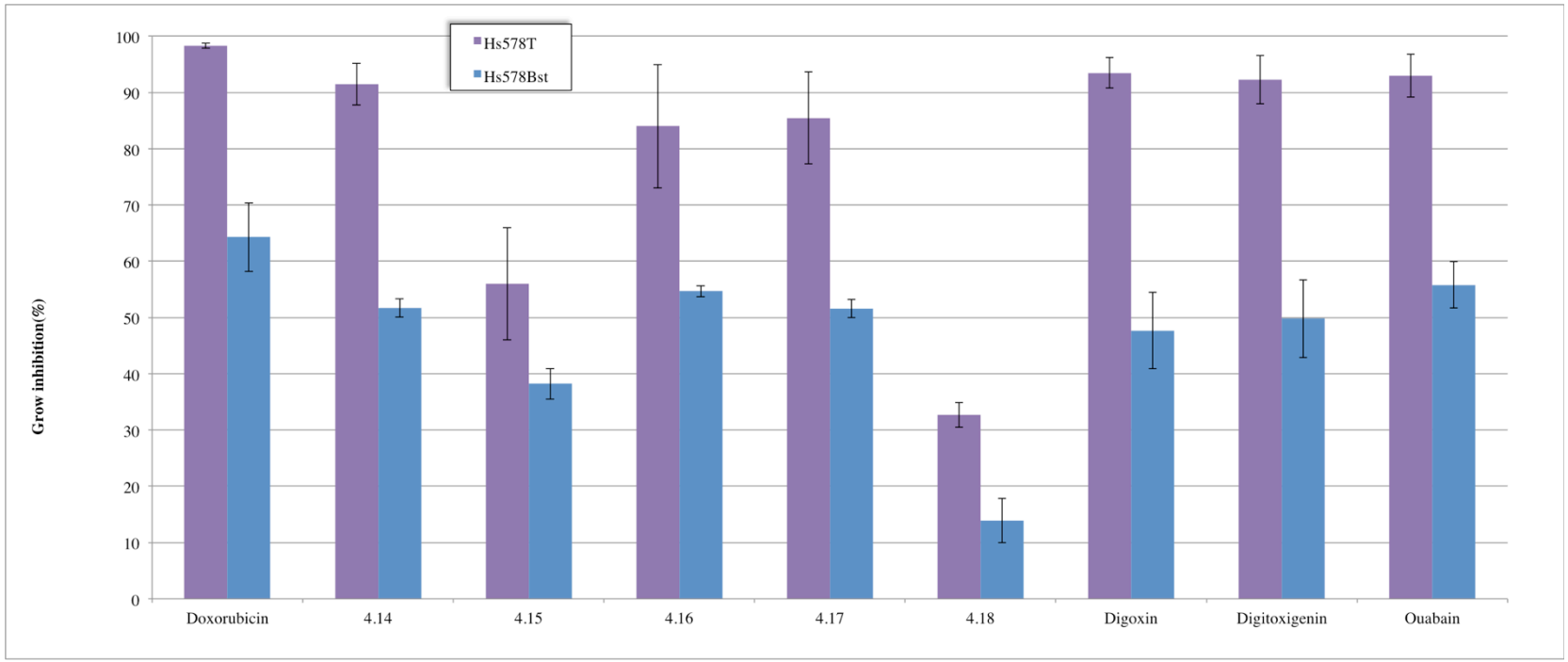

Figure 4-28 Percentage of cytotoxicity at maximum concentration of isolates **4.14-4.18** in the paired breast cell lines Hs578T (cancer) and Hs578Bst (normal)

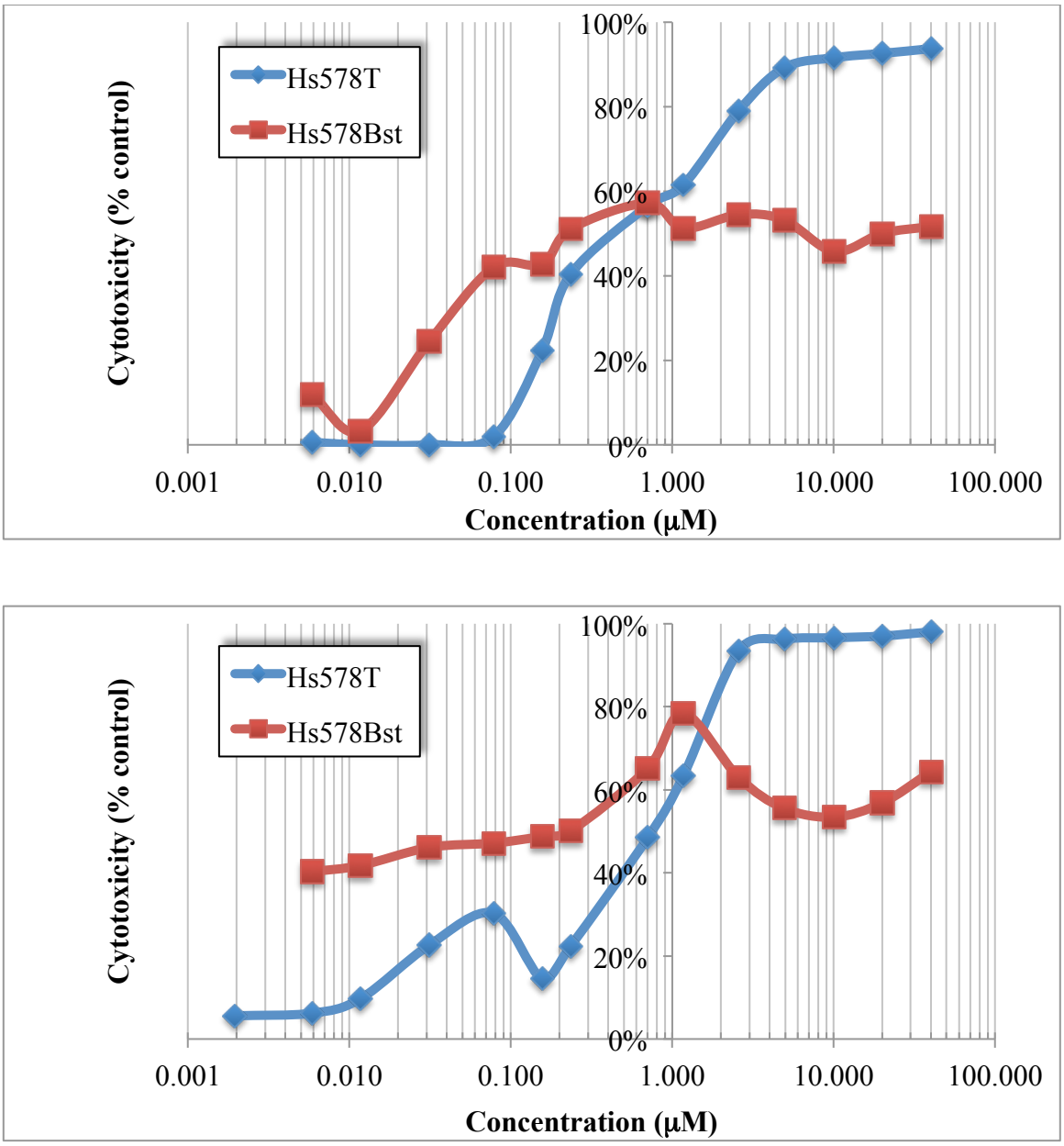

Figure 4-29 Dose-response curves of compound **4.14** (above) and doxorubicin (below) for the paired breast cell lines Hs578T (squares) and Hs578Bst (triangles)

4.5. Pregnane and cardiac glycosides from *Asclepias sullivantii*

A. sullivantii is commonly known as "prairie milkweed" and is native to the United States and Canada. *A. sullivantii* is listed as a threatened species in the states of Minnesota, Wisconsin, and Michigan.[175] There are no prior phytochemical reports for this species and information is lacking for traditional or medicinal uses. However, very encouraging results during the screening of the DCM and BuOH fractions (Table 4-6, Experimental data), lead us to choose this plant for detailed investigation. From the BuOH fraction, the known cardiac glycosides glycosides 3-*O*-β-D-glucopyranosyl-(1→4)-6-desoxy-β-D-allopyranosyl uzarigenin (**4.14**; 80 mg) and 3-*O*-β-D-glucpyranosyl-(1→4)-β-D-glucpyranosyl uzarigenin (**4.16**; 5 mg) were identified as well as the lignan 9'-*O*-butyl-3-*O*-demethyl-9-*O*-β-D-glucopyranosyl dehydrodiconiferylalcohol (**4.20**; 6 mg). These compounds were also found during investigation of *A. syriaca*. In addition, six new pregnane glycosides named sullivantosides A-F (Figure 4-30) were isolated and identified from the CH_2Cl_2 fraction: sullivantoside A (**4.50**; 9 mg), B (**5.51**; 7.6 mg), C (**5.52**; 10 mg), D (**5.53**; 6 mg), E (**5.54**; 4 mg), and F (**5.55**; 2.5 mg).

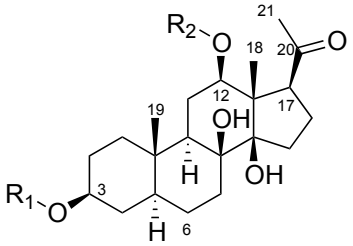

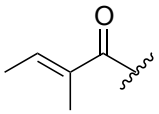

Tg: Tiglate

	R_1	R_2
Sullivantoside A (**4.40**)	R_A	Tg
Sullivantoside B (**4.41**)	R_B	Tg
Sullivantoside C (**4.42**)	R_C	Tg
Sullivantoside D (**4.43**)	R_A	H
Sullivantoside E (**4.44**)	R_B	H
Sullivantoside F (**4.45**)	R_C	H

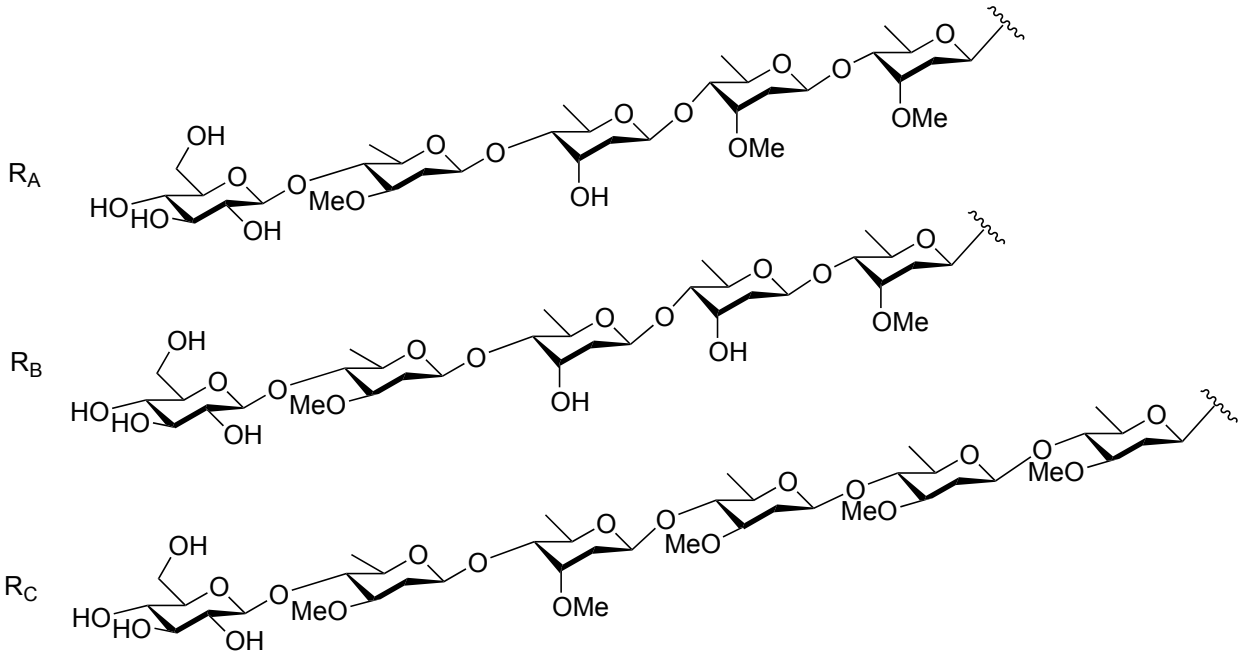

Figure 4-30 Structures of sullivantosides A-F (**4.40-4.45**)

4.5.1. Structure elucidation

Sullivantoside A (**4.40**) was obtained as a white, amorphous powder. The HRMS displayed a $[M+Na]^+$ ion at *m/z* 1195.6150 consistent with a molecular formula of $C_{59}H_{96}NaO_{23}$ (calc. 1195.6240). The ^1H NMR spectrum showed three methyl-singlet signals at δ 2.24 (s, H-21), 1.54 (s, H-18), and 1.18 (s, H-19). Based on the observed HMBC correlations between CH_3-21 and carbon resonances at δ 214.9 (C-20) and 59.3 (C-17), CH_3-18 and carbon resonances at δ 55.5 (C-12), 78.6 (C-13), 59.3 (C-17), and 86.4 (C-14), and CH_3-19 and carbon resonances at δ 38.5 (C-1), 37.0 (C-10), 45.6 (C-5), and 48.5 (C-9) (Figure 4-31); the presence of a pregn-20-one skeleton was proposed. Furthermore, the $^1H,^1H$-COSY spectrum allowed identification of the spin coupling sequences within the steroidal core (Figure 4-31) which, in combination with the HMBC and HSQC spectra, revealed the structure of the aglycone portion (Tables 4-20 and 4-22, Experimental data). In addition, an isolated spin system corresponding to a tiglate group was identified based on $^1H,^1H$-COSY and this was found to be attached to C-8 by means of the observed HMBC correlation between H-12 (δ 5.02, m) and carbonyl resonance of the tigloyl group at δ 168.1. Hence, the carbon skeleton was deduced to be 12β-tigloyl-8β,14β-dihydroy-pregn-20-one, and the NMR data were in good agreement with literature data observed for similar compounds.[243, 244] The proposed relative configuration was based on dipolar interactions observed in the ROESY spectrum (Figure 4-32). In addition, five anomeric protons were observed in the ^1H NMR spectrum at δ 5.35 (dd, *J* = 8.2, 1.5, H-1'''), 5.32 (dd, *J* = 8.1, 1.7 H-1'''), 5.14 (d, *J* = 8, H-1'''), 5.14 (br d, *J* = 9.4, H-1''') and 4.76 (dd, *J* = 9.8, 1.5, H-1''') suggesting the presence of equal number of sugars attached at C-3. Furthermore, the identification of four methyl doublet signals in the in the ^1H NMR spectrum at δ 1.68 (d, *J* = 5.3, H-6''''), 1.44 (d, *J* =

6.1, H-6'''), 1.44 (d, *J* = 6.1, H-6'), and 1.34 (d, *J* = 6.3, H-6'') as well as three methoxy groups at δ 3.65 (s, C-3'-OCH_3), 3.65 (s, C-3'''-OCH_3) and 3.54(s, C-3''''-OCH_3), suggested the presence of three 6-deoxy-3-methoxy and one 6-deoxy sugars which commonly occur in *Asclepias* as described previously. Using ^{1}H,^{1}H DQFCOSY, ^{1}H,^{1}H-TOCSY, and HSQC-TOCSY spectra, the proton spin systems and the carbon resonances allowed for the full assignment of each sugar (Tables 4-21 and 4-23, Experimental data). Comparison of the NMR data with those reported in the literature revealed the identity of the sugars as two cymaroses, oleandrose, digitoxose, and glucose. The carbon resonances of atom 4 of the 6-deoxysugars were extremely close to each other at δ 83.8 (C-4'), 83.6 (C-4''), 83.5 (C-4'''), and 83.5 (C-4'''') limiting the use of HMBC correlations between the anomeric proton and these carbons in order to assign the sugars' connectivity. Instead, the H-4 signals of each sugar were utilized as they were not so closely overlapped and the following correlations observed in the HMBC spectrum allowed for the elucidation of the sugar moieties as follows: cymarosyl anomeric proton H-1' (δ 5.32, dd, *J* = 8.1, 1.7) and C-3 (δ 76.9), oleandrosyl proton H-4'''' (δ 3.69) and glucosyl anomeric carbon C-1''''' (δ 104.8); and digitoxyl proton H-4''' (δ 3.45, dd, *J* = 9.5, 2.5) and oleandrosyl anomeric carbon C-1'''' (δ 101.8). As the NMR data suggested, the glucose unit was the fifth and terminal sugar, hence the sugar moiety was determined to be Glu-Ole-Dig-Cym-Cym. Furthermore, the β-linkages of the five sugars were established by the large coupling constants (*J* = 8.0-9.8) observed for the anomeric protons. Finally, the optical rotation of the purified monomeric sugars after their acid hydrolysis allowed us to establish the absolute configuration D for all the sugars present in this compound (see Experimental Section). Therefore, the structure of **4.40** was determined to be 12-*O*-tygloyl-3β,8β,12β,14β-tetrahydroxypregn-20-one-3-*O*-β-D-

glucopyranosyl-(1→4)-β-D-oleandropyranosyl-(1→4)-β-D-digitoxypyranosyl-(1→4)-β-D-cymaropyranosyl-(1→4)-β-D-cymaropyranose. Compound **4.40** was named sullivantoside A.

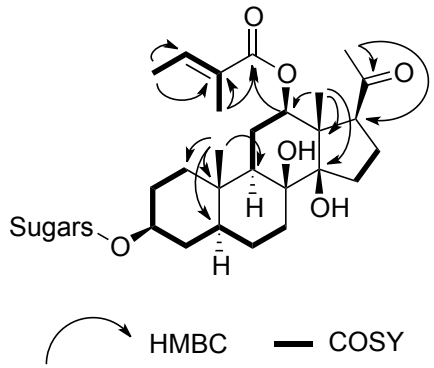

Figure 4-31 Selected HMBC and ^{1}H,^{1}H-COSY correlations observed for sullivantoside A (**4.40**)

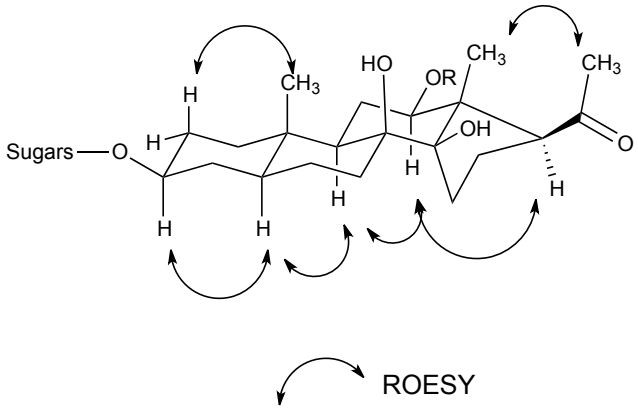

Figure 4-32 Selected ROESY dipolar interactions observed for sullivantoside A (**4.40**)

Sullivantoside B (**4.41**) was obtained as a white, amorphous powder. The HRMS displayed a $[M+Na]^{+}$ ion at *m/z* 1181.6076 consistent with the molecular formula $C_{58}H_{94}NaO_{23}$ (calc.

1181.6084) for). Analysis of the ^{1}H and ^{13}C NMR data permitted the identification of the aglycone as the same as in **4.40** (*vide supra*). In addition, five sugars were identified to be present in the structure on the basis of the same number of anomeric protons at δ 5.41 (br d, *J* = 9.4, H-1'''), 5.35 (br d, *J* = 9.7, H-1''), 5.33 (br d, *J* = 9.8, H-1'), 5.14 (d, *J* = 7.6, H-1'''') and 4.74 (br d, *J* = 9.7, H-1''''). Sugar signals in the ^{1}H and ^{13}C spectra were assigned using 2D NMR spectra and the identity of the sugars determined to be two digitoxoses, and single units of cymarose, oleandrose, and glucose. As previously described for **4.40**, the connectivity of the sugars was achieved through the HMBC correlations between cymarosyl anomeric proton H-1' (δ 5.33, dd, *J* = 9.5, 1.6) and C-3 (δ 76.9), oleandrosyl proton H-4'''' (δ 3.67, m) and glucosyl anomeric carbon C-1'''' (δ 104.8), digitoxyl-2 proton H-4''' (δ 3.43, dd, *J* = 9.6, 2.5) and oleandrosyl anomeric carbon C-1'''' (δ 101.8), and digitoxyl-1 proton H-4'' (3.50, dd, *J* = 9.6, 2.5) and digitoxyl-2 anomeric carbon C-1''' (δ 100.3). Consequently, the structure of **4.41** was determined to be 12-*O*-tygloyl-3β,8β,12β,14β-tetrahydroxypregn-20-one-3-*O*-β-D-glucopyranosyl-(1→4)-β-D-oleandropyranosyl-(1→4)-β-D-digitoxypyranosyl-(1→4)-β-D-digitoxypyranosyl-(1→4)-β-D-cymaropyranoside.

Sullivantoside C (**4.42**) was obtained as a white, amorphous powder. The HRMS displayed a $[M+Na]^{+}$ ion at *m/z* 1330.7278 consistent with the molecular formula $C_{60}H_{98}NaO_{23}$ (calc. 1330.7285). After assignment of the ^{1}H and ^{13}C NMR data of the aglycone portion using 2D NMR spectra (Tables 4-20 and 4-22), the signals were almost superimposable to those of **4.40**, thus it was concluded that both structures shared the same 12-*O*-tygloyl-3β,8β,12β,14β-tetrahydroxypregn-20-one steroidal skeleton. Unlike compounds **4.40** and **4.41,** this compound presented six sugars unit, as six anomeric protons were identified in the ^{1}H NMR spectrum at δ

5.30 (dd, *J* = 9.7, 1.6, H-1'''), 5.16 (d, *J* = 7.8, H-1'''), 4.93 (dd, *J* = 9.8, 1.6, H-1'''), 4.91 (dd, *J* = 9.8, 1.6, H-1'''), 4.88 (dd, *J* = 9.7, 1.5, H-1''') and 4.70 (dd, *J* = 9.7, 1.6, H-1'''). The identity of the sugars was determined as a single cymarose, four oleandroses, and one glucose by means of ^{1}H and ^{13}C NMR data analysis after all signals were assigned (Tables 4-21 and 4-23) using ^{1}H,^{1}H-DQFCOSY, ^{1}H,^{1}H-TOCSY, and HSQC-TOCSY spectra. The carbon-4 resonances of the sugar units in the ^{13}C NMR spectrum collapsed very close to each other at δ 83.6 (C-4'), 83.6 (C-4''), 83.6 (C-4'''), 83.4 (C-4''''), and 83.3 (C-4''''') making any HMBC correlation for these carbons inconclusive. Nonetheless, it was still possible to determine the sequence of the sugars by key HMBC correlations: olandrosyl anomeric proton H-1' (δ 4.88) and carbon C-3 (δ 76.8) of the aglycone, the olandrosyl-4 proton H-4''''' (δ 3.75, m) and the terminal glucosyl anomeric carbon C-1''''' (δ 104.4), cymarosyl proton H-4'''' (δ 3.45, m) and the oleandrosyl-4 anomeric carbon C-1'''' (δ 102.2), leaving two units of oleandrose left to assign at positions 2 and 3. In fact, the NMR data of oleandrose-2 and oleandrose-3 units are virtually undistinguishable between one another (Tables 4-21 and 4-23). Therefore, the structure of **4.42** was determined to be 12-*O*-tygloyl-3β,8β,12β,14β-tetrahydroxypregn-20-one-3-*O*-β-D-glucopyranosyl-(1→4)-β-D-oleandropyranosyl-(1→4)-β-D-cymaropyranosyl-(1→4)-β-D-oleandropyranosyl-(1→4)-β-D-oleandropyranosyl-(1→4)-β-D-oleandropyranose.

Sullivantoside D (**4.43**), an amorphous white powder, displayed an HRMS $[M+Na]^{+}$ ion at *m/z* 1113.5798 consistent with the molecular formula $C_{54}H_{90}NaO_{22}$ (calc. 1113.5821). Although the ^{1}H and ^{13}C NMR signals were similar to those present in **4.40**, the most noticeable change was the absence of signals for the tiglate group. In fact, the ^{13}C NMR signals at δ 75.2 (C-12), 57.6 (C-13), and 27.9 (C-11) as well as the ^{1}H NMR signal at 3.71 (m, H-12) were significantly

shifted when compared with the counterparts in **4.40**. Aided by 2D NMR spectra, the ^{1}H and ^{13}C NMR signals were completely assigned and the structure of the aglycone was elucidated as 3β,8β,12β,14β-tetrahydroxypregn-20-one. In addition, five anomeric protons were identified in the ^{1}H NMR spectrum at δ 5.35 (dd, *J* = 9.5, 1.6, H-1'''), 5.34 (dd, *J* = 9.5, 1.7 H-1'''), 5.16 (d, *J* = 8.0, H-1'''), 5.14 (br d, *J* = 9.4, H-1''') and 4.76 (dd, *J* = 9.8, 1.7, H-1'''). After assignment of the ^{1}H and ^{13}C NMR of each sugar unit using 2D NMR spectra, the sugar moiety present in this compound was determined to be the same as in **4.40** as the values were superimposable. Therefore, the structure of **4.43** was determined to be 3β,8β,12β,14β-tetrahydroxypregn-20-one-3-*O*-β-D-glucopyranosyl-(1→4)-β-D-oleandropyranosyl-(1→4)-β-D-digitoxypyranosyl-(1→4)-β-D-cymaropyranosyl-(1→4)-β-D-cymaropyranose

Sullivantoside E (**4.44**), an amorphous white powder with a HRMS $[M+Na]^{+}$ ion at *m/z* 1199.5668 consistent with the molecular formula $C_{53}H_{88}NaO_{22}$ (calc. 1099.5665) was also found to have the same aglycone as compound **4.43**. The sugar moiety was determined to be equal to the one present in compound **4.41** by NMR data comparison. Consequently, compound **4.44** was determined to be 3β,8β,12β,14β-tetrahydroxypregn-20-one-3-*O*-β-D-glucopyranosyl-(1→4)-β-D-oleandropyranosyl-(1→4)-β-D-digitoxypyranosyl-(1→4)-β-D-digitoxypyranosyl-(1→4)-β-D-cymaropyranoside.

Finally, sullivantoside F (**4.45**) was obtained as a white, amorphous powder. The HRMS displayed a $[M+Na]^{+}$ ion at *m/z* 1271.6756 consistent with the molecular formula $C_{55}H_{92}NaO_{22}$ (calc. 1271.6764). The aglycone was identified as the same as in **4.43** by comparison of the assigned ^{1}H and ^{13}C NMR data. Furthermore, the six sugars present in this compound were

identical to those described for compound **4.42**. Hence, the identity of **4.45** was determined as 3β,8β,12β,14β-tetrahydroxypregn-20-one-3-*O*-β-D-glucopyranosyl-(1→4)-β-D-oleandropyranosyl-(1→4)-β-D-cymaropyranosyl-(1→4)-β-D-oleandropyranosyl-(1→4)-β-D-oleandropyranosyl -(1→4)-β-D-oleandropyranose.

4.6. Conclusions

A total of nine plant species from the Asclepiadaceae family, including six species in the genus *Asclepias* genus were collected, extracted, fractionated, and screened against the breast cancer cell line Hs578T. A number of 'hits' were identified among the evaluated plants and three species were selected for detailed investigation. The phytochemical investigation of *Asclepias verticillata*, *A. syriaca*, and *A. sullivantii* lead us to isolate and identify a total of 46 compounds, half of which represented novel structures. The isolates showed a wide variety of structures including pregnane and cardiac glycosides, pentacyclic triterpenes, glycosylated flavonoids and lignans, among others. Furthermore, a group of cardiac glycosides were found to have strong cytotoxicity against breast cancer cell lines. The present work shows the chemical diversity and the medicinal potential of the secondary metabolites present in *Asclepias*, a widely distributed genus in the US Midwest, is poorly investigated. In addition, the elucidation of some of the highly complex structures isolated in this study was made possible by selective spectroscopic data, including 800 MHz 2D NMR experiments, and X-ray crystallography.

As a result of this work, two articles were published as follows:

- Araya, J.J.; Binns, F.; Kindscher, K.; Timmermann, B.N. **Verticillosides A-M: Polyoxygenated Pregnane Glycosides from *Asclepias verticillata* L**. *Phytochemistry*. 2012. *In press.* 10.1016/j.phytochem.2012.02.019
- Araya, J.J.; Kindscher, K.; Timmermann, B.N. **Cardiac Glycosides and other Compounds from *Asclepias syriaca*** *J. Nat. Prod.* 2012. *75*, 400-407

4.7. Experimental Data

4.7.1. Plant Material

Above ground biomass of *A. verticillata* was collected on July 10th of 2009 by H. Loring and Q. Long in Dog Leg Prairie of the Nelson Environmental Study Area, Lawrence, Kansas (N. 39.0550 W. 95.1967). Botanical identification was performed by Kelly Kindscher and a voucher specimen was deposited in the R.L. McGregor Herbarium (Collection number H. Loring 3559). Above ground biomass of *A. syriaca* was collected on June 17th of 2009 by Q. Long and R. Loring. The plant material was collected 100 m. east of NE Ohio and 1400, on 1400 Rd, Anderson, Kansas. GPS location of the collection site was latitude: 38.22676°, longitude 95.20080°. Botanical identification was performed by Kelly Kindscher and a voucher specimen was deposited in the McGregor Herbarium of the University of Kansas (H. Loring 3547). Above-ground biomass (stems, leaves, and flowers) of *A. sullivantii* was collected on April 24, 2010, by Kelly Kindscher. The plant material was collected 2 km northeast of Welda, Kansas. The GPS location of the collection site was LAT 38.18052°, LONG 95.27485°. Botanical identification was performed by Kelly Kindscher, and a botanical specimen was deposited in the McGregor Herbarium of the University of Kansas (Kindscher 4039).

4.7.2. Bioassay results

Table 4-3 Screening IC_{50} (μg/L), grow inhibition, and selectivity data for extracts and fractions using the paired human breast (Hs578T) and cancer (Hs578Bst) cell lines.

Plant name	Ext./Frac.	Hs587T IC_{50}	Hs578Bst IC_{50}	Hs578T In. %	Hs578Bst In. %	Select.*
A. verticillata	Crude	3.4	4.4	96	74	13.56
	HEX	>50	NC	61	0	16.91
	DCM	23	NC	26	4	8.69
	DCM-1	22	0.9	34	16	6.29
	DCM-2	20	>50	93	47	14.96
	DCM-3	NC	NC	6	18	-10.77
	DCM-4	27	NC	9	30	-3.72
	BUOH	26	NC	18	5	6.25
	BUOH-1	NC	NC	1	27	-12.10
	BUOH-2	NC	NC	7	24	-10.50
	BUOH-3	NC	NC	6	8	-1.87
	BUOH-4	NC	NC	10	14	-0.90
A. syriaca	Crude	NC	NC	0	5	-3.99
	HEX	NC	NC	9	0	2.12
	DCM	NC	NC	0	0	0.00
	DCM-1	>50	NC	78	12	19.69
	DCM-2	23	>50	85	38	20.52
	DCM-3	12	68	94	72	31.32
	DCM-4	28	26	53	21	11.74
	DCM-5	24	23	68	18	20.52
	BUOH	24	NC	24	0	8.57
	BUOH-1	27	>50	53	32	-5.23
	BUOH-2	24	12	22	39	-12.28
	BUOH-3	>50	>50	81	44	6.18
	BUOH-4	11	22	84	57	22.01
	BUOH-5	20	NC	74	24	25.24

A. sullivantii	Crude	NC	NC	5	0	-2.29
	HEX	29	NC	67	0	14.88
	DCM	NC	NC	0	0	-0.16
	DCM-1	27	NC	31	0	9.79
	DCM-2	47	>50	63	15	24.70
	DCM-3	28	>50	93	17	36.32
	DCM-4	30	>50	96	76	15.53
	DCM-5	5	0.9	92	44	34.41
	BUOH	NC	NC	0	0	-4.81
	BUOH-1	NC	NC	0	4	-1.57
	BUOH-2	77.9	1.5	24	14	1.27
	BUOH-3	1.6	NC	0	27	-12.12
	BUOH-4	3.8	<0.5	94	60	24.10
	BUOH-5	39	>50	93	49	6.59
A. incarnata	Crude	30	76	98	67	25.89
	HEX	21	NC	37	0	29.88
	DCM	NC	NC	0	0	-2.72
	DCM-1	27	26	90	47	25.14
	DCM-2	24	25	67	22	21.92
	DCM-3	NC	NC	0	5	-4.34
	DCM-4	3.3	NC	92	50	37.59
	DCM-5	23	4898	56	28	5.08
	BUOH	11	3.6	86	47	26.42
	BUOH-1	15	>50	74	44	12.30
	BUOH-2	>50	>50	20	19	1.16
	BUOH-3	26	0.9	9	2	-3.49
	BUOH-4	17	5.9	68	38	6.15
	BUOH-5	4.0	1.5	85	32	45.13

A. speciosa	Crude	80.36	NC	22	8	4.09
	HEX	>50	<0.5	24	0	8.81
	DCM	>50	<0.5	0	0	-0.07
	DCM-1	25.72	89.6	92	73	18.28
	DCM-2	<0.5	<0.5	0	0	-0.09
	DCM-3	37.1	NC	88	25	25.03
	DCM-4	27.7	NC	61	61	-8.65
	DCM-5	28.5	>50	42	25	-2.17
	BUOH	0.98	<0.5	0	0	-0.45
	BUOH-1	0.30	>50	0	17	-3.20
	BUOH-2	<0.5	11.0	0	0	-0.90
	BUOH-3	8.7	1.8	84	42	15.55
	BUOH-4	9.4	3.0	84	44	19.43
	BUOH-5	1.1	<0.5	0	10	-9.33
A. tuberosa (aerial)	Crude	1.2	>50	0	2	-8.11
	HEX	37.5	NC	54	29	10.35
	DCM	<0.5	19.9	0	38	-8.28
	DCM-1	>50	18.3	0	33	-10.91
	DCM-2	20.6	7.2	74	43	13.59
	DCM-3	>50	21	0	41	-14.91
	DCM-4	>50	19.4	0	32	-12.42
	DCM-5	>50	NC	0	27	-11.80
	BUOH	>50	17.2	0	27	-10.45
	BUOH-1	>50	16.3	0	18	-9.59
	BUOH-2	1.0	17.4	3	31	-11.45
	BUOH-3	26.1	22.6	5	24	-7.74
	BUOH-4	0.95	3.0	0	0	-1.17
	BUOH-5	3.0	NC	6	3	-1.89

	Crude	6.6	10.7	88	67	23.03
	HEX	>50	>50	41	52	-15.10
	DCM	33	NC	50	14	7.50
	DCM-1	62	26	72	29	19.55
	DCM-2	9.7	9.9	33	41	-3.28
	DCM-3	1.5	2.7	97	78	14.57
Apocynum	DCM-4	< 0.5	43.1	98	77	17.68
cannabinum	DCM-5	3.2	4.2	92	74	15.17
	BUOH	1.9	2.5	86	75	10.03
	BUOH-1	>50	NC	76	26	6.16
	BUOH-2	15	21	48	30	10.19
	BUOH-3	15	15	95	65	14.30
	BUOH-4	6.6	10.7	88	67	21.55
	BUOH-5	>50	>50	41	52	20.53
	Crude	>50	>50	26	27	5.37
	HEX	31	25	31	6	6.62
	DCM	>50	NC	53	29	6.55
	DCM-1	>50	17	72	17	17.47
	DCM-2	>50	26	65	16	13.43
	DCM-3	29	>50	48	12	15.05
Cynanchum	DCM-4	>50	NC	60	53	0.99
mucronatum	DCM-5	NC	NC	20	12	5.11
	BUOH	29	27	36	42	-15.48
	BUOH-1	NC	NC	12	45	-12.30
	BUOH-2	27	NC	16	40	-2.91
	BUOH-3	NC	NC	19	35	2.27
	BUOH-4	26	NC	6	1	4.23
	BUOH-5	>50	NC	24	0	7.49

	Crude	NC	NC	11	11	3.14
	HEX	28	28	45	16	-0.62
	DCM	45	10	55	33	7.52
	DCM-1	18	20	44	29	8.11
	DCM-2	25	NC	62	38	13.86
	DCM-3	35	24	67	5	27.55
Cynanchum	DCM-4	>50	>50	63	35	9.77
boerhaviifolium	DCM-5	27	26	31	26	-0.37
	BUOH	1.7	5.9	24	36	-11.27
	BUOH-1	16	12	27	41	-12.30
	BUOH-2	NC	NC	11	11	-2.91
	BUOH-3	26	NC	8	0	2.27
	BUOH-4	>50	NC	15	0	4.23
	BUOH-5	24	NC	33	0	7.49
	Crude	>50	NC	22	17	4.02
	HEX	< 0.5	< 0.5	33	21	9.69
	DCM	29	17	18	37	9.44
	DCM-1	49	NC	25	17	5.08
	DCM-2	31	NC	67	6	21.19
	DCM-3	>50	NC	29	0	8.92
Diplolepis	DCM-4	>50	NC	19	5	1.78
mensiesii	DCM-5	NC	NC	7	6	-2.10
	BUOH	5.7	24.9	99	83	-12.34
	BUOH-1	28	5.8	7	18	-3.97
	BUOH-2	17	15	57	7	2.47
	BUOH-3	43	1.0	70	34	14.82
	BUOH-4	27	>50	50	0	17.94
	BUOH-5	19	21	36	26	6.18
	Doxorubicin	< 0.5	< 0.5			
	Digitoxigenin	< 0.5	NC	94	27	51.72
Controls	Digoxin	< 0.5	NC	91	28	49.11
	Ouabain	< 0.5	NC	93	36	26.02
	Withaferin A	2.3	2.8	92	93	4.97

Table 4-4. Cytotoxicity (IC_{50}, μM) values of compounds **4.1-4.13** against breast cancer cell lines Hs578T and normal cell line Hs578Bst.

compound	cell line	
	Hs578T	**Hs578Bst**
4.1	>50	>50
4.1a	>50	>50
4.2	>50	>50
4.3	>50	>50
4.4	>50	>50
4.5	>50	>50
4.5a	>50	>50
4.6	>50	>50
4.7	>50	>50
4.8	>50	>50
4.9	>50	>50
4.10	>50	>50
4.11	>50	>50
4.11a	>50	>50
4.12	>50	>50
4.13	>50	>50
Digoxin[1]	0.1100 ± 0.0059	0.006 ± 0.005
Doxorubicin[1]	0.546 ± 0.055	0.18 ± 0.17

[1] Cytotoxicity is the average (N=3, ± SD) of calculated IC_{50}

Table 4-5. Cytotoxicity[1] (IC_{50}, μM, ± SD) values of compounds **4.14-4.18** against breast cancer cell lines MCF-7, T47D, SK-BR-3, and Hs578T and normal breast cell line Hs578Bst.

Compound	Cell line				
	MCF-7	**T47D**	**SK-BR-3**	**Hs578T**	**Hs578Bst**
4.14	5.3 ± 1.2	1.76 ± 0.21	2.52 ± 0.35	0.593 ± 0.051	0.043 ± 0.010
4.15	>40	>40	>40	>40	14.2 ± 3.3
4.16	11.6 ± 2.5	9.5 ± 1.0	19.4 ± 1.6	4.58 ± 0.64	0.76 ± 0.51
4.17	17.0 ± 4.9	11.7 ± 1.3	18.1 ± 2.2	6.28 ± 0.27	1.05 ± 0.11
4.18	>40	>40	>40	>40	>40
Digoxin	4.7 ± 3.0	0.66 ± 0.12	1.08 ± 0.21	0.251 ± 0.026	0.040 ± 0.017
Digitoxigenin	9.1 ± 2.6	2.53 ± 0.34	4.42 ± 0.51	1.022 ± 0.058	0.15 ± 0.12
Ouabain	10.6 ± 0.5	0.385 ± 0.026	0.403 ± 0.023	0.1100 ± 0.0059	0.006 ± 0.005
Doxorubicin	1.54 ± 0.15	1.9 ± 1.1	0.210 ± 0.033	0.546 ± 0.055	0.18 ± 0.17

[1] Cytotoxicity is the average (n=3) of calculated IC_{50}

Table 4-6. Percentage of toxicity (%, ± SD) for compounds **4.14-4.18** for the paired breast cell lines Hs578T (cancer) and Hs578Bst (normal).

Compound	Cell line	
	Hs578T	**Hs578Bst**
4.14	91.5 ± 3.7	51.7 ± 1.6
4.15	56 ± 10	38.2 ± 2.7
4.16	84 ± 11	54.7 ± 1.0
4.17	85.5 ± 8.2	51.6 ± 1.6
4.18	32.7 ± 2.2	13.9 ± 3.9
Digoxin	93.5 ± 2.7	47.7 ± 6.8
Digitoxigenin	92.3 ± 4.3	49.8 ± 6.9
Ouabain	93.0 ± 3.8	55.8 ± 4.1
Doxorubicin	98.32 ± 0.43	64.3 ± 6.1

[1] At maximum concentration (40 μM) expressed as percentage of control (n=3, ± SD)

4.7.3. Plant extraction and isolation

Asclepias verticillata. *A. verticillata* fresh biomass (5.5 kg) was left to dry at room temperature. The dry material (1.2 kg) was then ground to a fine powder and extracted four times with a mixture of MeOH and CH_2Cl_2 (1:1, v/v) at room temperature. The organic solvents (c.a. 20 L) were removed under reduced pressure to afford 138 g of the crude extract (11.5% w/w of dry weight). The organic extract was suspended in MeOH:H_2O 9:1 (1 L) and extracted with hexanes (500 mL, three times) to give a hexanes fraction. Then, methanol was removed from the aqueous layer under reduced pressure, the volume adjusted to 500 mL with distilled water, and successively extracted with CH_2Cl_2 (500 mL, three times) and butanol (500 mL, three times) to give dichlorometane and butanolic fractions respectively. The butanolic extract (41 g) was suspended in water (500 mL) and adsorbed on a MCI gel (500 g) column, washed with 2 L of water, and then eluted with mixtures of water and methanol starting with 10% methanol (v/v in H_2O) to 100% methanol in 10% step increments (2 L each fraction) to afford a total of 10 fractions (1-10). Fractions 6-9 were purified as follows: first a sephadex LH-20 (500 g) column chromatography using MeOH as eluent, then a silica gel column chromatography using $CHCl_3$:MeOH 95:5 (v/v) or $CHCl_3$:MeOH 90:10 (v/v) as mobile phase, and finally semi-preparative or preparative HPLC chromatography using mixtures of acetonitrile and water for elution. A total of 13 pregnane glycosides were isolated and chemically elucidated using ^{1}H-NMR, ^{13}C-NMR, 2D NMR, IR, UV, and HRMS.

A. syriaca. The plant's fresh biomass (12 kg) was left to dry at room temperature, then the dry material (2.5 kg) was ground to a fine powder and extracted four times with a mixture of MeOH and CH_2Cl_2 (1:1, v/v) at room temperature. The organic solvents (c.a. 20 L) were removed under

vacuum to afford 196.1 g (7.8% w/w based on dry biomass) of the crude organic extract. The extract was suspended in MeOH and H_2O 9:1 (v/v, 1 L) and extracted with hexanes (3x 500 mL). After removal of the MeOH, the volume of aqueous residue was adjusted to 500 mL with distilled H_2O and extracted successively with CH_2Cl_2 (3x 500 mL) and *n*-butanol (3x 500 mL) to give CH_2Cl_2 and *n*-BuOH fractions, respectively. After organic solvent removal, the CH_2Cl_2 fraction (32.7 g) was partitioned using silica gel (350 g, 24-40 μm) flash chromatography using mixtures of hexanes and EtOAc as mobile phase. The resulting fractions were purified using an automated flash chromatography apparatus with pre-packed silica gel columns (CombiFlash Teledyne Isco, San Diego, CA) using different solvent systems. A mixture of α- and β-amyrin was obtained (1.1 g, 0.04% w/w based on dry biomass) and it was resolved by means of semipreparative HPLC for identification (isocratic 90% MeCN and 10% acetone mixture as mobile phase during 60 min). Also, a mixture of α- and β-amyrin acetates and lupeol acetate (2.1 g, 0.08% w/w based on dry biomass) was separated for identification using semipreparative HPLC (MeCN and acetone mixture as mobile phase). Finally, oleanolic acid (3.5 g, 0.12% w/w based on dry biomass) was obtained by recrystallization (CH_2Cl_2:MeOH 1:1, v/v). The structures of these pentacyclic triterpenes were elucidated using spectroscopic methods and NMR data was in agreement with those already reported. The *n*-BuOH (24.5 g) and H_2O (78.0 g) fractions were combined, suspended in H_2O, adsorbed on MCI gel column (500 g), and eluted using mixtures of H_2O and MeOH starting with 10% MeOH (v/v) to 100% MeOH in 10% increments (2 L each fraction) to afford a total of 10 fractions (BuOH 1-10). Subsequently, fractions BuOH 4-10 were purified following the next separation steps: first Sephadex LH-20 (500 g) column chromatography (MeOH as eluent), then automated flash chromatography with pre-packed silica gel column columns using $CHCl_3$:MeOH:H_2O 10:1:0.1 (v/v/v) as mobile phase, and finally

semipreparative or preparative HPLC chromatography using mixtures of MeCN (solvent A), H_2O (solvent B) or 0.1% HCO_2H acidified H_2O (solvent C) as follows: fractions obtained from BuOH-7 were separated using a linear gradient of solvents A:B from 20:80 to 60:40 (v/v) in 40 min and fractions obtained from BuOH-4 and BuOH-5 were separated using a linear gradient of solvents A:C from 5:95 to 25:75 (v/v) in 50 min. Furthermore, fractions BuOH 1-3 were subjected to an automated flash chromatography using a reverse phase C_{18} column (80 g, linear gradient 5% MeOH to 50% MeOH in 60 min), then to an automated normal phase flash chromatography (EtOAc:MeOH:H_2O 88:11:8, v/v/v, with 0.5% of HCO_2H as mobile phase), and finally purified using semi-preparative or preparative HPLC with a linear gradient of solvents A:C from 1:99 to 15:85 in 60 min. From fraction BuOH-7 the known cardiac glycosides 3-*O*-β-D-glucopyranosyl-(1→4)-6-deoxy-β-D-allopyranosyluzarigenin (**4.14**), 3-*O*-β-D-glucopyranosyl-(1→4)-β-D-glucopyranosyl uzarigenin (**4.17**), and deglucouzarin (**4.18**) were isolated, their structures were elucidated using spectroscopic methods and shown to be in agreement with literature data. The glycosylated flavonoids quercetin 3-*O*-β-galactopyranosyl-(1→2)-β-xylopyranoside (**4.31**), kaempferol 3-*O*-β-galactopyranosyl-(1→2)-β-xylopyranoside (**4.18**), quercetin-7-*O*-β-glucopyranosyl-3-*O*-β-D-galactopyranosyl-(1→2)-β-D-xylopyranoside (**4.19**), 3'-*O*-methylquercetin 3-*O*-β-galactopyranosyl-(1→2)-β-xylopyranoside (**4.32**), and quercetin 3-*O*-β-galactopyranoside (**4.33**) were isolated from fractions BuOH-4 and BuOH-5. In addition, from fraction BuOH-7 the known lignans episyringaresinol (**4.34**) and prupaside (**4.35**) were obtained. The phenylethanoid **4.21** and the megastigmane **4.22** were isolated from fractions BuOH-4 and BuOH-5, respectively. Finally, from the highly polar fractions BuOH 1-3 the following compounds were purified: *trans*- and *cis*- cinnamic acids (**4.36** and **4.37** respectively),

isovanillinic acid (**4.38**), and 4-(β-glucopyranosyloxy)benzoic acid (**4.39**). The structures of the new compounds **4.15** and **4.19-4.22**, were elucidated using UV, IR, HRMS and NMR experiments.

A. sullivantii. The plant's fresh biomass (5.5 kg) was left to dry at room temperature. The dry material (1.12 kg) was then ground to a fine powder and extracted four times with a mixture of MeOH and CH_2Cl_2 (1:1, v/v) at room temperature. The organic solvents (c.a. 10 L) were removed under reduced pressure to afford 102 g of the crude extract (9.1% w/w of dry weight). The organic extract was suspended in MeOH:H_2O 9:1 (1 L) and extracted with hexanes (500 mL, three times) to give a hexanes fraction. Then, methanol was removed from the aqueous layer under reduced pressure, the volume adjusted to 500 mL with distilled water, and successively extracted with CH_2Cl_2 (500 mL, three times) and butanol (500 mL, three times) to give dichloromethane and butanolic fractions respectively. The CH_2Cl_2 fraction (20g) was subjected to a large silica gel CC (200 g) to afford 14 fractions. Subfraction 13 (26.6g) was separated using automatic flash chromatography (RP-C_{18} prepacked column, 200g) using a linear gradient from 20% MeOH to 100% MeOH in 45 min to give 7 fractions. The subfraction 5 from the previous column was subjected to sephadex LH-20 column (MeOH as mobile phase) in order to remove pigments and then submitted to preparative HPLC resulting in the isolation of the six new compounds sullivantoside A-F (**4.40-4.45**). The butanolic extract (22.9 g) was suspended in water (500 mL) and adsorbed in a MCI gel (500 g) column, washed with 2 L of water, and then eluted with mixtures of water and methanol starting with 10% methanol (v/v in H_2O) to 100% methanol in 10% step increments (2 L each fraction) to afford a total of 10 fractions (1-10). Fractions 6-10 were purified as follows: first Sephadex LH-20 (500 g) column chromatography

using MeOH as eluent, then silica gel column chromatography using $CHCl_3$:MeOH 95:5 (v/v) or $CHCl_3$:MeOH 90:10 (v/v) as mobile phase, and finally semi-preparative or preparative HPLC chromatography using mixtures of acetonitrile and water for elution. Using these separation steps, the common flavonoid rutin (**4.46**) was isolated from fraction BuOH 6 and the neolignan **4.19** and the cardiac glycosides **4.14** and **4.16** were obtained from the fraction BuOH 8.

4.7.4. Acid hydrolysis of glycosides

Acid hydrolysis of 4.1-4.13. Hydrolysis of glycosides was conducted as described elsewhere.[211] Acid hydrolysis of a mixture of **4.1-4.4** (50 mg) afforded the aglycone metaplexigenin (**4.1a**); mixtures of **4.5**, **4.6** and **4.10** (50 mg) produced sarcostin (**4.5a**); a mixture of **4.7-4.9** (50 mg) gave 12-*O*-deacylmetaplexigenin; and a mixture of **4.11-4.13** (50 mg) afforded 12-*O*-benzoylsarcostin (**4.11a**). The structures of the aglycones were established by spectroscopic methods and compared with previously reported data. From the combined aqueous layers the following purified sugars were recovered and identified, then identified by comparison of spectroscopic data reported in the literature. Optical rotations were measured 24 h after dissolution in water providing the following values: D-cymarose $[\alpha]_D^{25}$ = +50.1 (c. 0.1 H_2O); lit. +51.6;[245] D-thevetoside $[\alpha]_D^{25}$ = +38.0 (c. 0.1 H_2O); lit. +42.3; D-oleandrose $[\alpha]_D^{25}$ = -9.8 (c. 0.1 H_2O); lit. -10.3;[246] (6-deoxy-3-*O*-methyl)-D-allose $[\alpha]_D^{25}$ = +3.9 (c. 0.1 H_2O) (lit. +5);[247] and D-glucose $[\alpha]_D^{25}$ = +50 (c. 0.1 H_2O) (lit. +56).[248]

Acid Hydrolysis of 4.15, 4.19, 4.20, 4.21-4.22. Aliquots of pure compounds (approx. 1-2 mg) were hydrolyzed using 3 mL of 1M HCl (dioxane:H_2O 1:1, v/v) for 4 hours at 70°C. The resulting mixtures were neutralized with 3M NaOH and extracted three times with EtOAc. The

aqueous layer was concentrated and the residue was fractionated in a small silica gel column using mixtures of $CHCl_3$, MeOH, and H_2O. The purified sugars were compared by TLC with authentic samples and the optical rotation values were recorded in H_2O after equilibration during 24 h. Compound **4.15** afforded D-glucose $[\alpha]_D^{25}$ = +50.1 (*c* 0.1, H_2O); 6-deoxy-D-allose $[\alpha]_D^{25}$ = +2.1 (*c* 0.1, H_2O), lit. +2.[249] Compound **4.19** afforded D-glucose $[\alpha]_D^{25}$ = 48.7 (*c* 0.1, H_2O); D-galactose $[\alpha]_D^{25}$ = +62.6 (*c* 0.1, H_2O), lit. +84.2;[250] and D-xylose $[\alpha]_D^{25}$ = +18.2 (*c* 0.1, H_2O), lit. +19.4.[251] Compound **4.20** afforded D-glucose $[\alpha]_D^{25}$ = +51.3 (*c* 0.1, H_2O), lit. +56.[248] Compounds **4.21-4.22** afforded D-glucose $[\alpha]_D^{25}$ = +50.4 (*c* 0.1, H_2O); D-galactose $[\alpha]_D^{25}$ = +68.6 (*c* 0.1, H_2O); and D-xylose $[\alpha]_D^{25}$ = +17.3 (*c* 0.1, H_2O).

4.7.5. X-ray structure determination.

Crystallization of the aglycones metaplexigenin (**4.1a**) and sarcostin (**4.5a**) was carried out using mixtures of CH_2Cl_2, MeOH, and acetonitrile using a slow evaporation technique. Next, the obtained crystals were submitted for X-ray diffraction determination. The crystal structures have been deposited at the Cambridge Crystallographic Data Center and allocated the deposition number CCDC 840311 and CCDC 840314, respectively

4.7.6. Cytotoxicity assay.

Four cancer breast (Hs578T, T47D, Sk-Br-3, and Mcf-7) and one normal breast (Hs578Bst) cell lines were seeded in separate 384-well plates (seeding density of 3,000 cells per well, in a volume of 30 μL per well) and allowed to attach and grow overnight in a cell incubator. Then, compounds were added using a Lybcyte ECHO acoustic liquid handling instrument (14

concentrations in the range 0.002-40 μM) and plates were incubated for 72 hours. Next, cell viability was determined by adding 10 μL of CellTiter-Glo (CTG) reagent, shaking plates for 2 minutes followed by reading of luminescence after a 15 minutes stabilizing period. Each dose-response curve was determined in triplicate. The data were normalized by dividing by the median value and IC_{50} calculations were done using GraphPad Prism software.

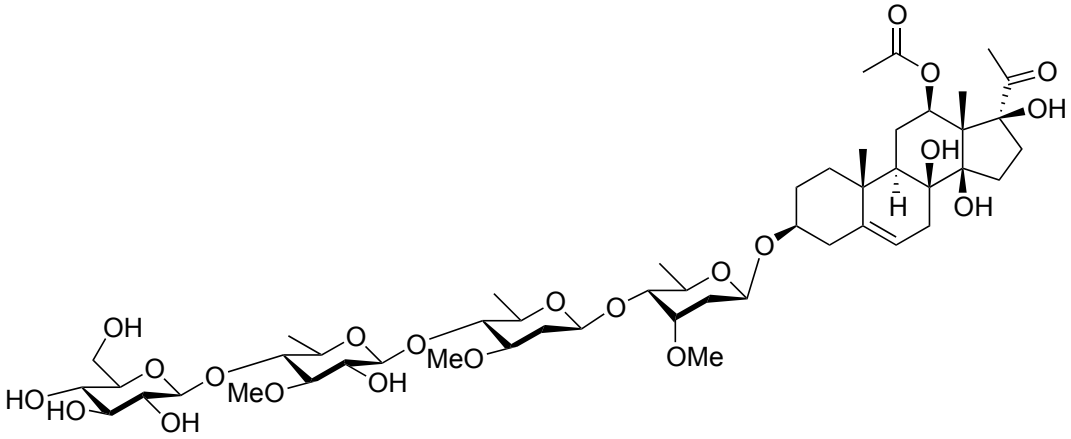

4.1

Verticilloside A (4.1). Amorphous white powder; mp 164.9-166.9°C; $[\alpha]_D^{25}$ = -14.3 (c. 0.412, MeOH); IR ν_{max} (film) cm^{-1}: 3366.6 (OH), 1706.0 (C=O), 1635.8 (C=O), 1158.4 (C-O), 1059.8 (C-O); UV_{max} 206.9, 277.5; HRMS *m/z*: 1055.5276 $[M+H]^+$ (1055.5039 calc. for $C_{50}H_{80}NaO_{22}$) ^1H and ^{13}C NMR: see Tables 4-7, 4-8, 4-9, and 4-10.

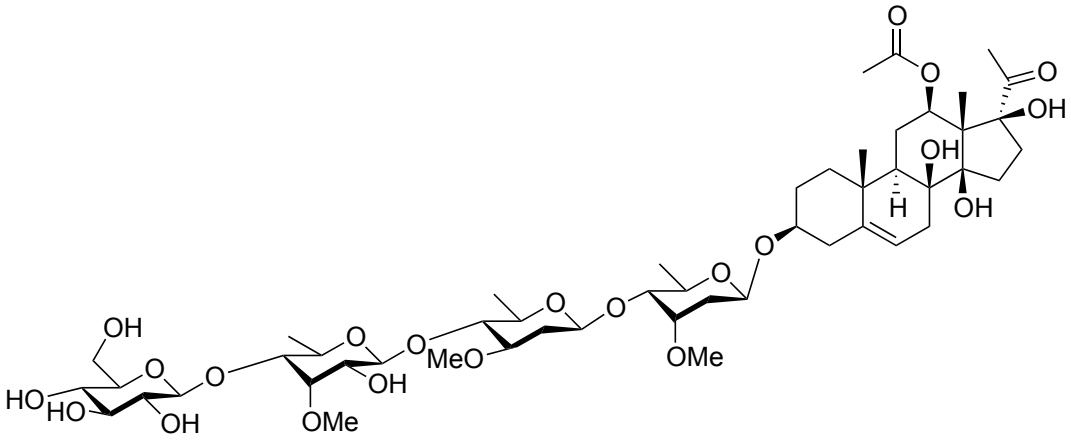

4.2

Verticilloside B (4.2). Amorphous white powder; mp. 169.8-172.7°C; $[\alpha]_D^{25}$ = -5.0 (c. 0.735, MeOH); IR ν_{max} (film) cm^{-1}: 3394.8 (OH), 1708.6 (C=O), 1635.0 (C=O), 1058.7 (C-O), 1035.2 (C-O); UV_{max} (nm, MeOH): 208.3, 267.9; HRMS m/z: 1052.5271 $[M+H]^+$ (1055.5039 calc. for $C_{50}H_{80}NaO_{22}$) ^1H and ^{13}C NMR: see Tables 4-7, 4-8, 4-9, and 4-10.

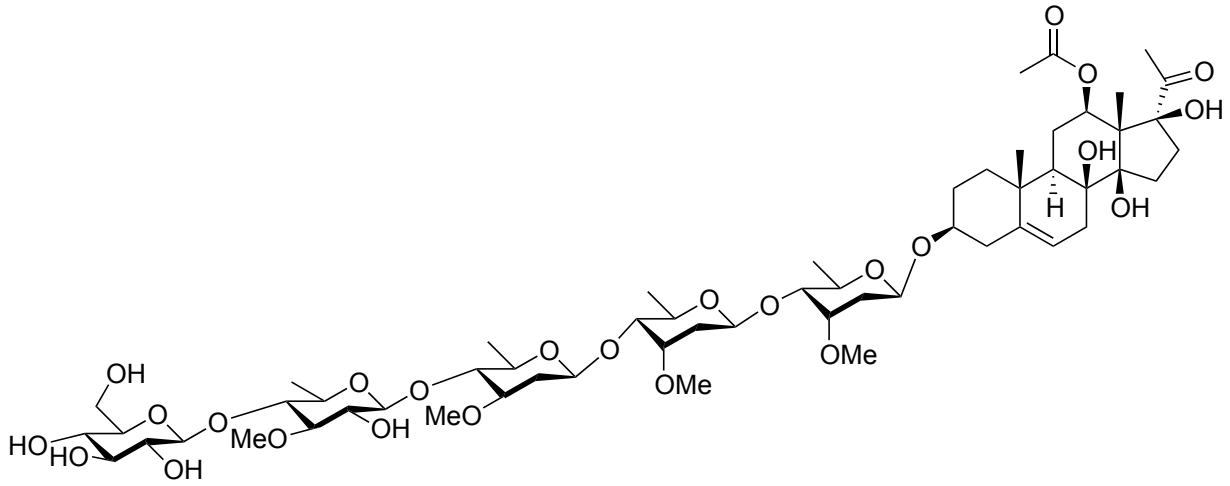

4.3

Verticilloside C (4.3). Amorphous white powder; mp 169.0-170.5°C; $[\alpha]_D^{25}$ = 6.6 (c. 0.378, MeOH); IR ν_{max} (film) cm^{-1}: 3389.7 (OH), 1708.7 (C=O), 1644.8 (C=O), 1156.2 (C-O), 1059.8

(C-O); UV_{max} (nm, MeOH): 206.9, 274.1; HRMS m/z: 1199.5877 $[M+H]^+$ (1199.5825 calc. for $C_{57}H_{92}NaO_{25}$) ^1H and ^{13}C NMR: see Tables 4-7, 4-8, 4-9, and 4-10.

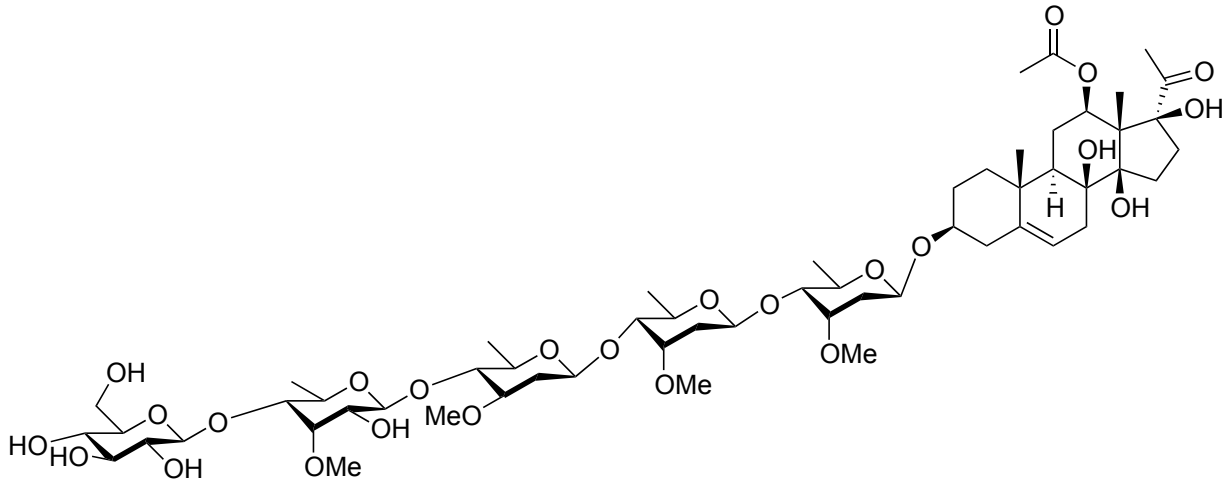

4.4

Verticilloside D (4.4). Amorphous white powder; mp 171.1-175.2°C; $[\alpha]_D^{25}$ = 31.8 (c. 1.63, MeOH); IR ν_{max} (film) cm^{-1}: 3388.7 (OH), 1703.8.0 (C=O), 1642.2 (C=O), 1148.3, 1054.7; UV_{max} (nm, MeOH): 207.0, 282.0; HRMS *m/z*: 1199.5845 $[M+H]^+$ (1199.5825 calc. for $C_{57}H_{92}NaO_{25}$) ^1H and ^{13}C NMR: see Tables 4-7, 4-8, 4-9, and 4-10.

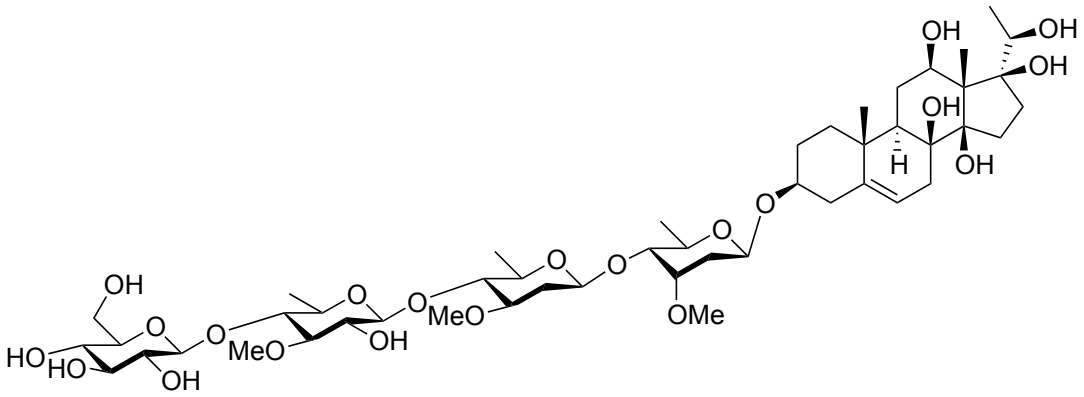

4.5

Verticilloside E (4.5). Amorphous white powder; mp 160.1-162.6°C; $[\alpha]_D^{25}$ = 17.5 (c. 0.48, MeOH); IR ν_{max} (film) cm^{-1}: 3378.3 (OH), 1150.1 (C-O), 992.8 (C-O); UV_{max} (nm, MeOH):

207.0, 267.0; HRMS *m/z*: 1015.5098 $[M+H]^+$ (1015.5090 calc. for $C_{48}H_{80}NaO_{21}$) ^1H and ^{13}C NMR: see tables Tables 4-7, 4-8, 4-9, and 4-10.

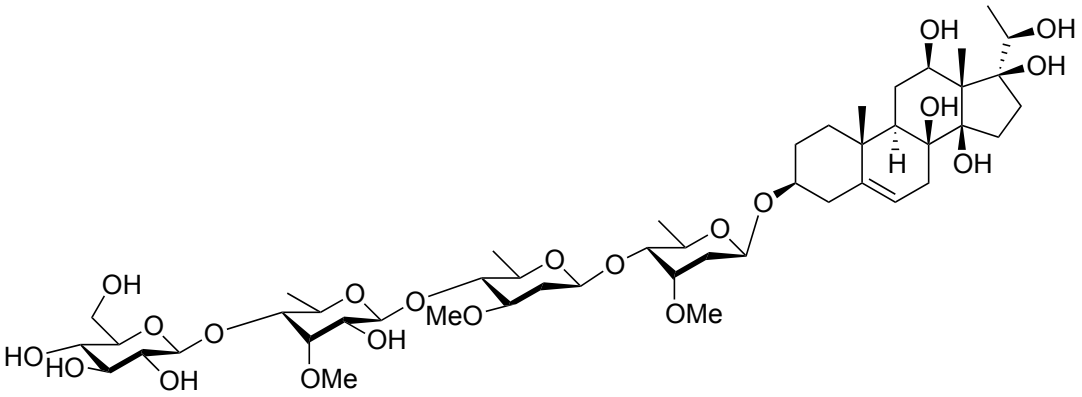

4.6

Verticilloside F (4.6). Amorphous white powder; mp 165.8-167.6°C; $[\alpha]_D^{25} = 21.7$ (c. 0.974, MeOH); IR ν_{max} (film) cm^{-1}: 3385.3 (OH), 1152.8 (C-O), 996.3 (C-O); UV_{max} (nm, MeOH): 207.2, 272.5; HRMS *m/z*: 1015.5153 $[M+H]^+$ (1015.5090 calc. for $C_{48}H_{80}NaO_{21}$) ^1H and ^{13}C NMR: see Tables 4-7, 4-7, 4-11, and 4-12.

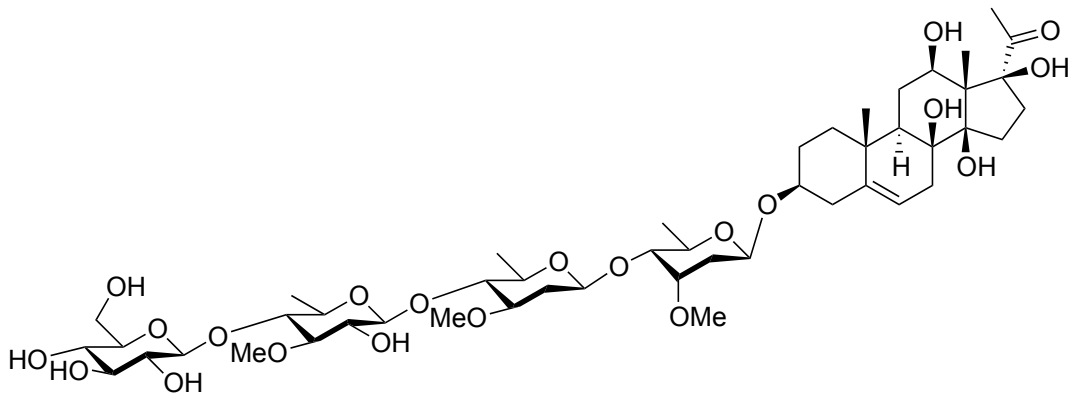

4.7

Verticilloside G (4.7). Amorphous white powder; mp 157.6-159.8°C; $[\alpha]_D^{25} = 13.6$ (c. 0.366, MeOH); IR ν_{max} (film) cm^{-1}: 3385.3 (OH), 1685.8 (C=O), 1152.8 (C-O), 996.3 (C-O); UV_{max}

(nm, MeOH): 207.1, 282.0; HRMS *m/z*: 1013.4913 $[M+H]^+$ (1013.4933 calc. for $C_{48}H_{78}NaO_{21}$) ^1H and ^{13}C NMR: see Tables 4-7, 4-7, 4-11, and 4-12.

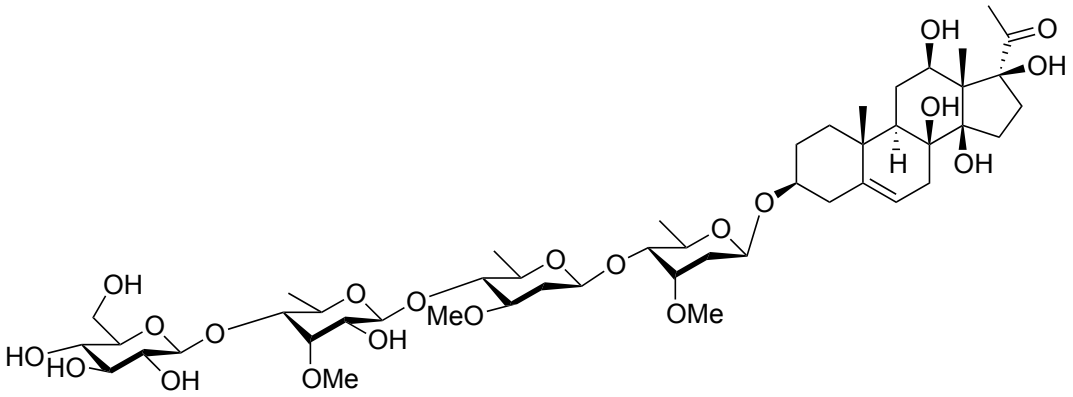

4.8

Verticilloside H (4.8). Amorphous white powder; mp 163.1-164.3°C; $[\alpha]_D^{25}$ = 12.3 (c. 0.674, MeOH); IR ν_{max} (film) cm^{-1}: 3425.2 (OH), 1696.5 (C=O), 1152.1 (C-O), 997.4 (C-O); UV_{max} (nm, MeOH): 206.1, 280.7; HRMS *m/z*: 1013.4921 $[M+H]^+$ (1013.4933 calc. for $C_{48}H_{78}NaO_{21}$) ^1H and ^{13}C NMR: see Tables 4-7, 4-7, 4-11, and 4-12.

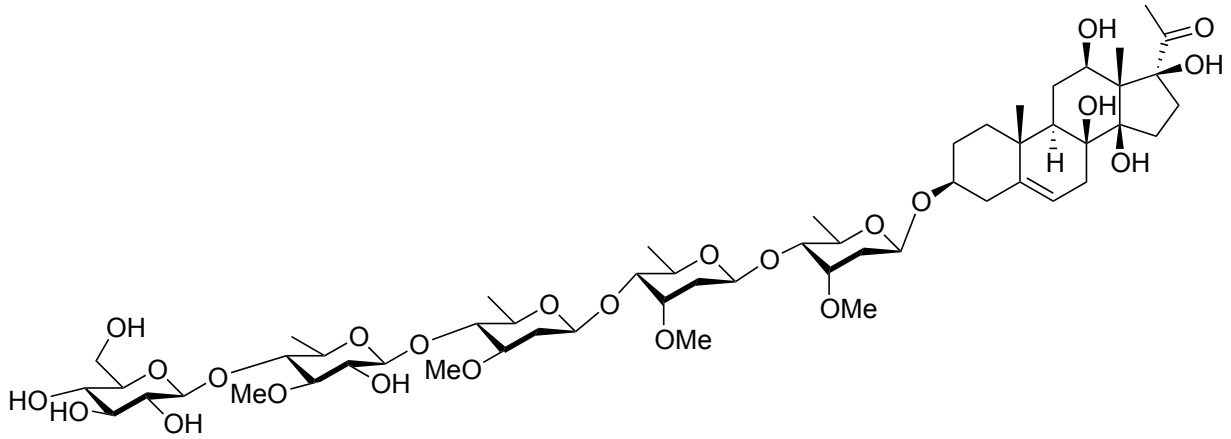

4.9

Verticilloside I (4.9). Amorphous white powder; mp 172.2-174.0°C; $[\alpha]_D^{25}$ = 25.2 (c. 0.447, MeOH); IR ν_{max} (film) cm^{-1}: 3391.3 (OH), 1149.6 (C-O), 999.4 (C-O); UV_{max} (nm, MeOH):

206.1, 269.2; HRMS *m/z*: 1159.5904 $[M+H]^+$ (1159.5876 calc. for $C_{55}H_{92}NaO_{24}$) ^1H and ^{13}C NMR: see Tables 4-7, 4-7, 4-11, and 4-12.

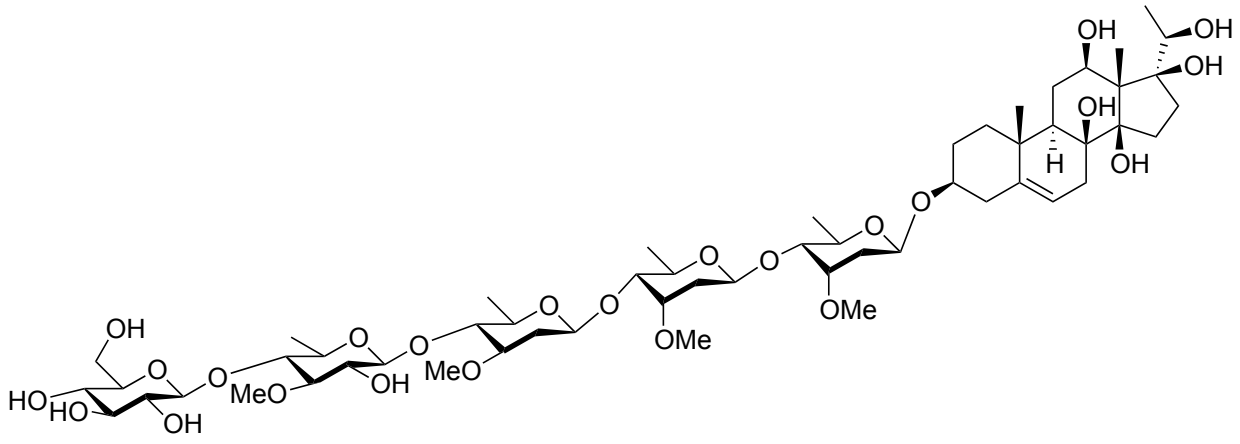

4.10

Verticilloside J (4.10). Amorphous white powder; mp 170.9-172.1°C; $[\alpha]_D^{25} = 13.1$ (c. 0.288, MeOH); IR ν_{max} (film) cm^{-1}: 3455.0 (OH), 1154.8 (C-O), 1051.3 (C-O); UV_{max} (nm, MeOH): 206.0, 268.9; HRMS *m/z*: 1057.5734 $[M+H]^+$ (1157.5720 calc. for $C_{55}H_{90}NaO_{24}$) ^1H and ^{13}C NMR: see Tables 4-7, 4-7, 4-11, and 4-12.

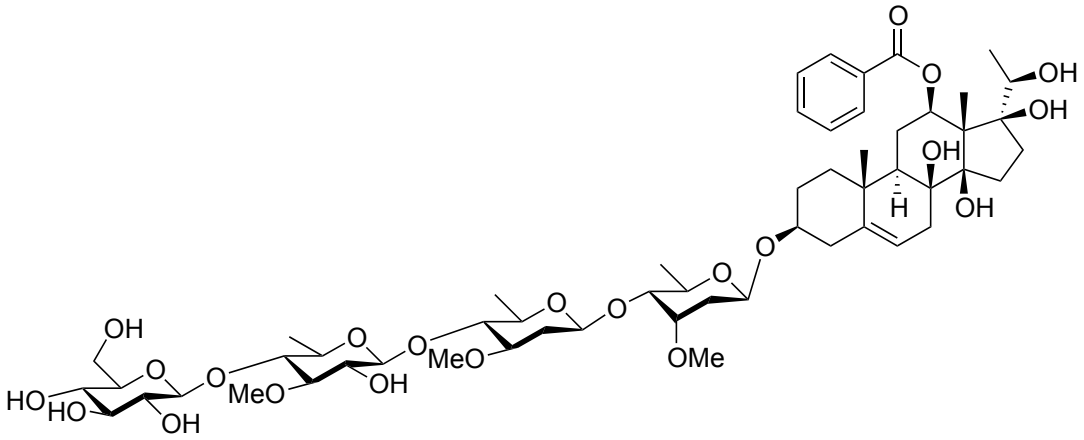

4.11

Verticilloside K (4.11). Amorphous white powder; mp 173.1-174.8°C; $[\alpha]_D^{25} = 53.6$ (c. 0.467, MeOH); IR ν_{max} (film) cm^{-1}: 3389.0 (OH), 3032.3 (Ar-H), 1732.5 (C=O), 1635.8 (C=O), 1155.5

(C-O), 977.7 (C-O); UV_{max} (nm, MeOH): 204.1, 226.1, 274.1; HRMS *m/z*: 1119.5337 $[M+H]^+$ (1119.5352 calc. for $C_{55}H_{84}NaO_{22}$) ^1H and ^{13}C NMR: see tables Tables 4-7, 4-7, 4-13, and 4-14.

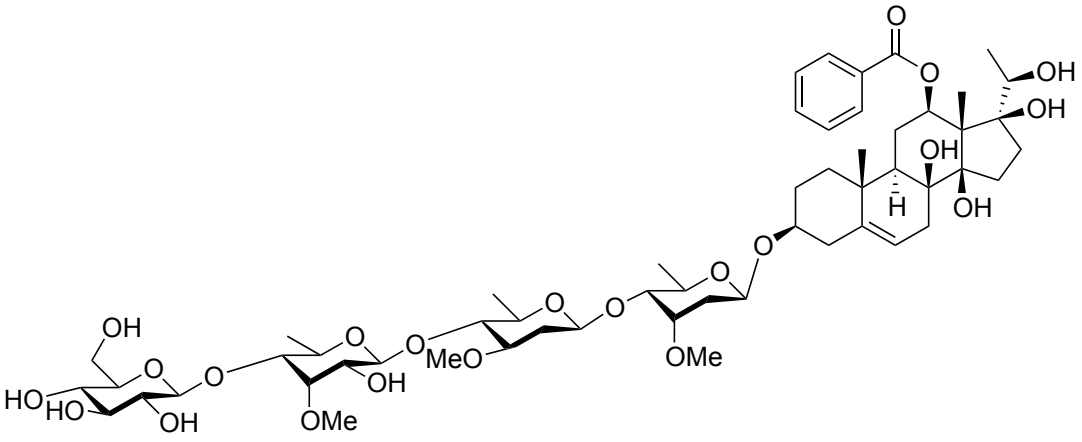

4.12

Verticilloside L (4.12). Amorphous white powder; mp 176.8-178.2°C; $[\alpha]_D^{25} = 25.2$ (c. 0.254, MeOH); IR ν_{max} (film) cm^{-1}: 3340.5 (OH), 3031.8 (Ar-H), 1698.8 (C=O), 1635.8 (C=O), 1153.4 (C-O), 978.5 (C-O); UV_{max} (nm, MeOH): 204.0, 226.0, 274.1; HRMS *m/z*: 1119.5364 $[M+H]^+$ (1119.5352 calc. for $C_{55}H_{84}NaO_{22}$) ^1H and ^{13}C NMR: see tables Tables 4-7, 4-7, 4-13, and 4-14.

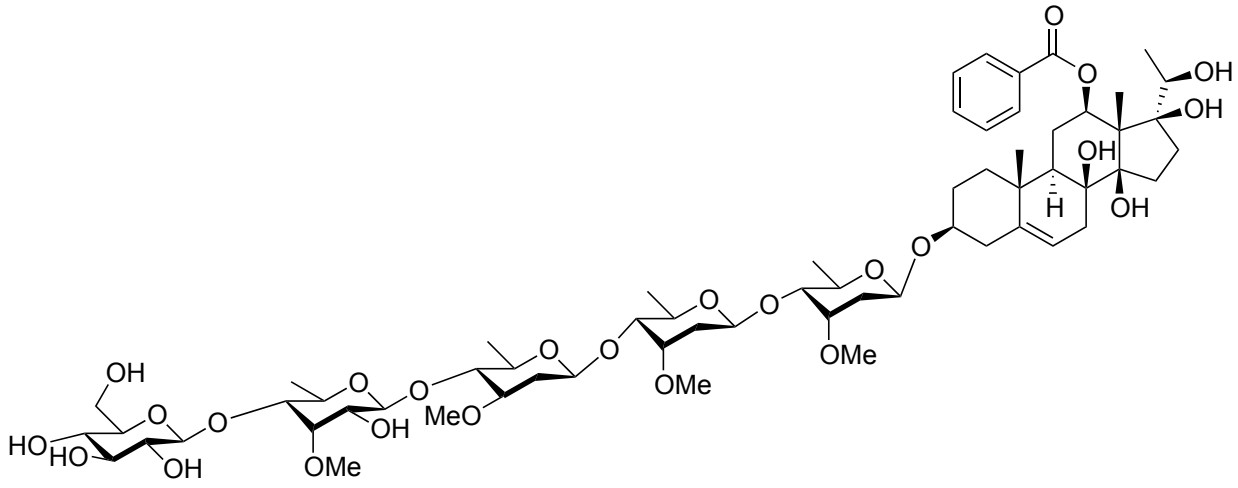

4.13

Verticilloside M (4.13). Amorphous white powder; mp 176.8-178.2°C; $[\alpha]_D^{25} = 25.2$ (c. 0.254, MeOH); IR ν_{max} (film) cm^{-1}: 3340.5 (OH), 3031.8 (Ar-H), 1698.8 (C=O), 1635.8 (C=O), 1153.4 (C-O), 978.5 (C-O); UV_{max} (nm, MeOH): 204.0, 226.0, 274.1; HRMS *m/z*: 1263.6037 $[M+H]^+$ (1263.6138 calc. for $C_{62}H_{96}NaO_{25}$) ^1H and ^{13}C NMR: see Tables 4-7, 4-7, 4-13, and 4-14.

Table 4-7 ^{13}C-NMR (125 MHz, C_5D_5N) data for the aglycone part of verticillosides A-M (**4.1-4.13**)

Atom	4.1	4.2	4.3	4.4	4.5	4.6	4.7	4.8	4.9	4.10	4.11	4.12	4.13
1	39.2, CH_2	39.4, CH_2	39.3, CH_2	39.3, CH_2	39.4, CH_2	39.4, CH_2	39.3, CH_2	39.3, CH_2	39.3, CH_2	39.4, CH_2	39.2, CH_2	39.2, CH_2	39.2, CH_2
2	30.2, CH_2	30.4, CH_2	30.2, CH_2	30.2, CH_2	30.3, CH_2	30.3, CH_2	30.3, CH_2	30.3, CH_2	30.3, CH_2	30.3, CH_2	30.3, CH_2	30.3, CH_2	30.3, CH_2
3	77.9, CH	78.1, CH	78.0, CH	78.0, CH	78.1, CH	78.1, CH	78.1, CH	78.1, CH	78.1, CH	78.1, CH	78.0, CH	78.0, CH	78.1, CH
4	39.5, CH_2	39.7, CH_2	39.6, CH_2	39.6, CH_2	39.7, CH_2	39.7, CH_2	39.7, CH_2	39.7, CH_2	39.7, CH_2	39.7, CH_2	39.6, CH_2	39.6, CH_2	39.6, CH_2
5	139.6, C	139.8, C	139.6, C	139.6, C	139.5, C	139.5, C	139.5, C	139.5, C	139.7, C	139.5, C	139.5, C	139.5, C	139.5, C
6	119.6, CH	119.7, CH	119.5, CH	119.5, CH	120.2, CH	120.2, CH	119.9, CH	120.2, CH	119.9, CH	120.1, CH	120.0, CH	120.0, CH	120.0, CH
7	35.0, CH_2	35.2, CH_2	35.0, CH_2	35.0, CH_2	35.7, CH_2	35.7, CH_2	35.4, CH_2	35.4, CH_2	35.4, CH_2	35.6, CH_2	35.4, CH_2	35.4, CH_2	35.4, CH_2
8	74.6, C	74.1, C	74.6, C	74.6, C	74.4, C	74.4, C	74.6, C	74.6, C	74.1, C	74.1, C	74.6, C	74.6, C	74.6, C
9	44.8, CH	45.0, CH	44.8, CH	44.8, CH	44.9, CH	44.9, CH	45.3, CH	45.3, CH	44.9, CH	44.9, CH	44.5, CH	44.4, CH	44.5, CH
10	38.0, C	38.2, C	37.7, C	37.7, C	37.7, C	37.7, C	37.7, C	37.7, C	37.7, C	37.7, C	37.7, C	37.6, C	37.6, C
11	25.2, CH_2	25.4, CH_2	25.2, CH_2	25.2, CH_2	29.5, CH_2	29.5, CH_2	29.8, CH_2	29.8, CH_2	29.8, CH_2	29.5, CH_2	26.0, CH_2	26.0, CH_2	26.0, CH_2
12	73.9, CH	74.8, CH	73.9, CH	73.9, CH	71.1, CH	71.1, CH	69.2, CH	69.3, CH	69.2, CH	71.1, CH	75.7, CH	75.7, CH	75.7, CH
13	58.3, C	58.4, C	58.3, C	58.2, C	59.2, C	59.2, C	60.7, C	60.7, C	60.7, C	58.4, C	57.8, C	57.8, C	57.8, C
14	89.8, C	90.0, C	89.8, C	89.8, C	89.2, C	89.2, C	89.7, C	89.7, C	89.7, C	89.2, C	89.0, C	89.0, C	89.0, C
15	34.1, CH_2	34.3, CH_2	34.1, CH_2	34.1, CH_2	34.9, CH_2	34.9, CH_2	34.6, CH_2	34.6, CH_2	34.6, CH_2	34.9, CH_2	34.6, CH_2	34.6, CH_2	34.6, CH_2
16	33.2, CH_2	33.4, CH_2	33.2, CH_2	33.2, CH_2	34.6, CH_2	34.6, CH_2	33.1, CH_2	33.1, CH_2	33.2, CH_2	34.6, CH_2	33.2, CH_2	33.2, CH_2	33.2, CH_2
17	92.8, C	92.0, C	92.8, C	92.8, C	89.4, C	89.3, C	92.9, C	92.9, C	92.9, C	89.4, C	89.2, C	89.2, C	89.2, C
18	10.8, CH_3	11.0, CH_3	10.8, CH_3	10.8, CH_3	11.8, CH_3	11.8, CH_3	9.8, CH_3	9.8, CH_3	9.8, CH_3	11.8, CH_3	12.2, CH_3	12.1, CH_3	12.1, CH_3
19	18.5, CH_3	18.7, CH_3	18.5, CH_3	18.5, CH_3	18.6, CH_3	18.7, CH_3	18.7, CH_3	18.7, CH_3	18.8, CH_3	18.7, CH_3	18.5, CH_3	18.5, CH_3	18.5, CH_3
20	210.6, C	210.8, C	210.6, C	210.6, C	73.5, CH	73.5 *d*	209.9, C	209.9, C	209.9, C	73.5, CH	71.3, CH	71.3, CH	71.3, CH
21	28.0, CH_3	28.2, CH_3	28.0, CH_3	28.0, CH_3	18.2, CH_3	18.2, CH_3	28.2, CH_3	28.2, CH_3	28.2, CH_3	18.2, CH_3	19.8, CH_3	19.8, CH_3	19.8, CH_3
	12-Ac	**12-Ac**	**12-Ac**	**12-Ac**	-	-	-	-	-	-	**12-Bz**	**12-Bz**	**12-Bz**
1	170.3, C	170.5, C	170.3 *s*	170.3 *s*							167.0, C	167.0, C	167.0, C
2	21.1, CH_3	21.3, CH_3	21.1, CH_3	21.1, CH_3							132.1, C	132.1, C	132.1, C
3											130.8, CH	130.8, CH	130.8, CH
4											129.2, CH	129.2, CH	129.2, CH
5											133.6, CH	133.6, CH	133.6, CH

Table 4-8 ^{13}C-NMR (125 MHz, C_5D_5N) data for the sugar moiety of verticillosides A-M (**4.1-4.13**)

Atom	4.1	4.2	4.3	4.4	4.5	4.6	4.7	4.8	4.9	4.10	4.11	4.12	4.13
	D-Cym	**D-Cym**	**D-Cym**	**D-Cym**	**D-Cym**	**D-Cym**	**D-Cym**	**D-Cym**	**D-Cym**	**D-Cym**	**D-Cym**	**D-Cym**	**D-Cym**
1'	96.7, CH	96.9, CH	96.7, CH	96.7, CH	96.7, CH	96.7, CH	96.7, CH	96.7, CH	96.7, CH	96.7, CH	96.7, CH	96.7, CH	96.7, CH
2'	37.6, CH_2	37.7, CH_2	37.3, CH_2	37.6, CH_2	37.6, CH_2	37.6, CH_2	37.6, CH_2	37.5, CH_2	37.6, CH_2	37.5, CH_2	37.6, CH_2	37.6, CH_2	37.6, CH_2
3'	78.2, CH	78.4, CH	78.4, CH	78.4, CH	78.2, CH	78.7, CH	78.2, CH	78.2, CH	78.4, CH	78.4, CH	78.2, CH	78.2, CH	78.4, CH
4'	83.6, CH	84.0, CH	83.7, CH	83.7, CH	83.6, CH	83.8, CH	83.9, CH	83.8, CH	83.7, CH	83.7, CH	83.5, CH	83.8, CH	83.8, CH
5'	69.3, CH	69.2, CH	69.4, CH	69.4, CH	69.3, CH	69.3, CH	69.3, CH	69.2, CH	69.4, CH	69.4, CH	69.3, CH	69.3, CH	69.4, CH
6'	19.0, CH_3	19.0, CH_3	18.8, CH_3	18.8, CH_3	19.0, CH_3	19.0, CH_3	19.0, CH_3	19.0, CH_3	18.7, CH_3	18.8, CH_3	19.0, CH_3	19.0, CH_3	18.9, CH_3
3'-OMe	59.2, CH_3	59.4, CH_3	59.3, CH_3	59.3, CH_3	59.2, CH_3	59.0, CH_3	59.2, CH_3	59.0, CH_3	59.2, CH_3	59.2, CH_3	59.2, CH_3	59.2, CH_3	59.2, CH_3
	D-Ole	**D-Ole**	**D-Cym**	**D-Cym**	**D-Ole**	**D-Ole**	**D-Ole**	**D-Ole**	**D-Cym**	**D-Cym**	**D-Ole**	**D-Ole**	**D-Cym**
1"	102.3, CH	102.5, CH	100.8, CH	100.8, CH	102.3, CH	102.3, CH	102.3, CH	102.3, CH	100.8, CH	100.8, CH	102.3, CH	102.3, CH	100.8, CH
2"	37.7, CH_2	37.9, CH_2	37.3, CH_2	37.3, CH_2	37.7, CH_2	38.0, CH_2	38.0, CH_2	38.0, CH_2	37.3, CH_2	37.3, CH_2	38.0, CH_2	38.0, CH_2	37.3, CH_2
3"	79.6, CH	79.8, CH	78.1, CH	78.0, CH	79.6, CH	79.6, CH	79.6, CH	79.6, CH	78.7, CH	78.7, CH	79.6, CH	79.6, CH	78.0, CH
4"	83.6, CH	83.7, CH	83.5, CH	83.5, CH	83.6, CH	83.3, CH	83.6, CH	83.3, CH	83.5, CH	83.4, CH	83.6, CH	83.3, CH	83.5, CH
5"	72.4, CH	72.4, CH	69.2, CH	69.2, CH	72.4, CH	72.2, CH	72.3, CH	72.3, CH	69.2, CH	69.2, CH	72.3, CH	72.3, CH	69.2, CH
6"	19.1, CH_3	19.4, CH_3	18.9, CH_3	18.9, CH_3	19.1, CH_3	19.2, CH_3	19.1, CH_3	19.2, CH_3	18.8, CH_3	18.9, CH_3	19.1, CH_3	19.2, CH_3	18.8, CH_3
3"-OMe	57.8, CH_3	58.0, CH_3	59.2, CH_3	59.2, CH_3	57.8, CH_3	57.8, CH_3	57.8, CH_3	57.8, CH_3	59.3, CH_3	59.2, CH_3	57.5, CH_3	57.5, CH_3	59.3, CH_3
	D-Thv	**D-Allme**	**D-Ole**	**D-Ole**	**D-Thv**	**D-Allme**	**D-Thv**	**D-Allme**	**D-Ole**	**D-Ole**	**D-Thv**	**D-Allme**	**D-Ole**
1"'	104.4, CH	102.4, CH	102.3, CH	102.2, CH	104.4, CH	102.2, CH	104.4, CH	102.2, CH	102.2, CH	102.2, CH	104.4, CH	102.2, CH	102.2, CH
2"'	75.3, CH	73.2, CH	37.6, CH_2	38.0, CH_2	75.3, CH	73.0, CH	75.3, CH	73.0, CH	38.0, CH_2	38.0, CH_2	75.3, CH_2	73.0, CH	38.0, CH_2
3"'	86.7, CH	83.7, CH	79.6, CH	79.6, CH	86.7, CH	83.5, CH	86.7, CH	83.5, CH	79.6, CH	79.6, CH	86.7, CH	83.5, CH	79.6, CH
4"'	83.8, CH	83.8, CH	83.6, CH	83.3, CH	83.8, CH	83.6, CH	83.6, CH	83.6, CH	83.3, CH	83.3, CH	83.6, CH	83.6, CH	83.3, CH
5"'	72.3, CH	70.1, CH	72.3, CH	72.3, CH	72.3, CH	70.0, CH	72.3, CH	69.9, CH	72.3, CH	72.3, CH	72.4, CH	70.0, CH	72.3, CH
6"'	19.1, CH_3	18.8, CH_3	19.0, CH_3	19.2, CH_3	19.1, CH_3	18.6, CH_3	19.1, CH_3	18.6, CH_3	19.2, CH_3	19.2, CH_3	19.1, CH_3	18.7, CH_3	19.2, CH_3
3"'-OMe	61.0, CH_3	62.3, CH_3	57.8, CH_3	57.8, CH_3	61.0, CH_3	62.1, CH_3	61.0, CH_3	62.1, CH_3	57.8, CH_3	57.8, CH_3	60.9, CH_3	62.1, CH_3	57.5, CH_3
	D-Glc	**D-Glc**	**D-Thv**	**D-Allme**	**D-Glc**	**D-Glc**	**D-Glc**	**D-Glc**	**D-Allme**	**D-Allme**	**D-Glc**	**D-Glc**	**D-Allme**
1""	105.2, CH	107.2, CH	104.4, CH	102.3, CH	105.2, CH	107.0, CH	105.2, CH	107.0, CH	102.3, CH	102.3, CH	105.3, CH	107.0, CH	102.3, CH
2""	76.2, CH	76.2, CH	75.3, CH	73.0, CH	76.2, CH	75.8, CH	76.2, CH	75.8, CH	73.0, CH	73.0, CH	76.2, CH	76.0, CH	73.0, CH
3""	79.0, CH	78.9, CH	86.7, CH	83.5, CH	79.0, CH	78.7, CH	79.0, CH	78.8, CH	83.4, CH	83.5, CH	79.1, CH	78.8, CH	83.5, CH
4""	72.3, CH	72.5, CH	83.6, CH	83.6, CH	72.3, CH	72.2, CH	72.4, CH	72.2, CH	83.6, CH	83.6, CH	72.3, CH	72.2, CH	83.6, CH
5""	78.5, CH	78.5, CH	72.3, CH	69.9, CH	78.5, CH	78.2, CH	78.5, CH	78.7, CH	69.8, CH	69.8, CH	78.5, CH	78.8, CH	69.9, CH
6""	63.3, CH_2	63.5, CH_2	19.1, CH_3	18.2, CH_3	63.3, CH_2	63.3, CH_2	63.4, CH_2	63.3, CH_2	18.6, CH_3	18.2, CH_3	63.5, CH_2	63.3, CH_2	18.7, CH_3
3""-OMe			61.0, CH_3	62.1, CH_3					62.0, CH_3	62.0, CH_3			62.1, CH_3
	-	-	**D-Glc**	**D-Glc**	-	-	-	-	**D-Glc**	**D-Glc**	-	-	**D-Glc**
1"'"			105.0, CH	107.0, CH					107.0, CH	107.0, CH			107.0, CH
2"'"			76.2, CH	75.8, CH					75.8, CH	75.8, CH			75.9, CH
3"'"			79.1, CH	78.8, CH					78.8, CH	78.8, CH			78.8, CH
4"'"			72.4, CH	72.2, CH					69.8, CH	72.2, CH			72.2, CH
5"'"			78.5, CH	78.7, CH					78.8, CH	78.8, CH			78.7, CH
6"'"			63.5, CH_2	63.3, CH_2					63.5, CH_2	63.3, CH_2			63.3, CH_2

Table 4-9 ^{1}H-NMR (500 MHz, C_5D_5N) data for aglycone part of verticillosides A-E (**4.1-4.5**).

Atom	4.1	*J* (Hz)	4.2	*J* (Hz)	4.3	*J* (Hz)	4.4	*J* (Hz)	4.5	*J* (Hz)
1	1.82, m		1.78, m		1.79, m		1.80, m		1.94, m	
	1.12, ddd	14.3, 13.4, 3.9	1.08, ddd	14.2, 13.5, 3.8	1.09, ddd	13.9, 13.2, 3.9	1.09, ddd	13.8, 13.3, 3.9	1.19, ddd	13.3, 13.2, 3.7
2	2.10, m		2.08, m		2.08, m		2.08, m		2.13, m	
	1.82, m		1.80, m		1.81, m		1.80, m		1.86, m	
3	3.86, m		3.85, m		3.85, m		3.85, m		3.91, m	
4	2.56, br dd	12.8, 4.6	2.54, br dd	12.9, 4.6	2.56, br dd	12.5, 4.5	2.54, br dd	13.0, 4.6	2.60, br dd	12.7, 4.8
	2.45, m		2.41, m		2.44, m		2.43, m		2.50, m	
6	5.31, m		5.29, m		5.28, m		5.29, m		5.40, m	
7	2.47, m		2.45, m		2.47, m		2.47, m		2.50, m	
	2.33, m		2.32, m		2.32, m		2.32, m		2.38, m	
9	1.72, m		1.69, m		1.70, m		1.71, m		1.66, m	
11	2.24, ddd	12.7, 12.3, 12.0	2.22, ddd	12.9, 12.6, 12.4	2.24, m		2.23, ddd	12.5, 12.3, 12.2	2.54, m	
	2.10, m		2.08, m		2.09, m		2.09, m		2.01, m	
12	4.99, dd	12.1, 4.1	4.97, dd	11.6, 3.9	4.98, m		4.98, dd	12.2, 4.2	3.92, m	
15	2.12, m		2.10, m		2.10, m		2.11, m		2.06, m	
16	3.25, m		3.23, m		3.23, m		3.23, m		2.01, m	
	2.02, m		2.01, m		2.03, m		2.02, m			
18	1.94, s		1.94, s		1.94, s		1.94, s		1.98, s	
19	1.35, s		1.34, s		1.34, s		1.34, s		1.43, s	
20										
21	2.08, s		2.08, s		2.48, s		2.48, s		1.54, d	6.4
	12-Ac		**12-Ac**		**12-Ac**		**12-Ac**		**-**	
	2.49, s		2.48, s		2.08, s		2.08, s			

Table 4-10 ^{1}H-NMR (500 MHz, C_5D_5N) data for sugar moiety of verticillosides A-E (**4.1-4.5**)

Atom	4.1	*J* (Hz)	4.2	*J* (Hz)	4.3	*J* (Hz)	4.4	*J* (Hz)	4.5	*J* (Hz)
	D-Cym		**D-Cym**		**D-Cym**		**D-Cym**		**D-Cym**	
1'	5.29, br d	9.1	5.26, br d	9.4	5.29, m		5.29, m		5.29, dd	9.5, 1.7
2'	2.32, m		2.28, m		2.32, m		2.31, m		2.32, m	
	1.90, ddd	13.2, 9.8, 2.6	1.88, ddd	13.5, 9.6, 2.4	1.92, m		1.92, m		1.90, m	
3'	4.05, m		4.02, m		4.10, m		4.10, m		4.05, m	
4'	3.49, dd	9.6, 2.7	3.47, dd	9.5, 2.7	3.52, m		3.52, m		3.49, dd	9.5, 2.7
5'	4.23, m		4.22, m		4.24, m		4.23, m		4.25, m	
6'	1.44, d	6.1	1.43, d	6.2	1.40, d	6.0	1.38, d	6.2	1.44, d	6.0
3'-OMe	3.56, s		3.55, s		3.58, s		3.62, s		3.56, s	
	D-Ole		**D-Ole**		**D-Cym**		**D-Cym**		**D-Ole**	
1''	4.70, dd	9.7, 1.6	4.67, dd	9.6, 1.7	5.13, dd	9.7, 1.6	5.12, dd	9.6, 1.5	4.70, dd	9.7, 1.7
2''	2.50, m		2.46, m		2.32, m		2.31, m		2.50, m	
	1.78, m		1.73, m		1.82, m		1.81, m		1.78, m	
3''	3.59, m		3.56, m		4.02, m		4.00, m		3.59, m	
4''	3.62, dd	9.0, 8.8	3.56, m		3.44, dd	9.6, 2.6	3.42, dd	9.6, 2.6	3.62, m	
5''	3.56, m		3.54, m		4.20, m		4.17, m		3.56, m	
6''	1.68, d	6.1	1.61, d	5.4	1.39, d	6.0	1.37, d	6.2	1.68, d	6.0
3''-OMe	3.49, s		3.53, s		3.63, s		3.55, s		3.49, s	
	D-Thv		**D-Allme**		**D-Ole**		**D-Ole**		**D-Thv**	
1'''	4.90, d	7.9	5.27, d	8.1	4.68, dd	9.7, 1.5	4.67, dd	9.7, 1.4	4.90, d	7.9
2'''	3.93, dd	9.0, 7.9	3.83, m		2.49, m		2.48, m		3.93, m	
					1.77, m		1.73, m			
3'''	3.71, dd	9.2, 9.0	4.50, dd	2.6, 2.5	3.56, m		3.57, m		3.71, dd	8.9, 8.9
4'''	3.89, dd	9.3, 9.2	3.76, dd	9.5, 2.2	3.62, m		3.57, m		3.89, m	
5'''	3.77, dq	9.3, 6.1	4.29, m		3.57, m		3.55, m		3.77, m	9.4, 6.2
6'''	1.78, d	6.1	1.66, d	6.2	1.68, d	6.0	1.61, d	5.5	1.78, d	6.1
3'''-OMe	3.96, s		3.84, s		3.52, s		3.53, s		3.96, s	
	D-Glc		**D-Glc**		**D-Thv**		**D-Allme**		**D-Glc**	
1''''	5.16, d	7.8	5.00, d	8.2	4.89, d	7.8	5.28, m		5.16, d	7.8
2''''	4.07, m		4.05, dd	8.6, 8.5	3.93, m		3.85, m		4.07, m	
3''''	4.26, m		4.28, m		3.71, dd	9.0, 8.8	4.50, dd	2.7, 2.6	4.26, m	
4''''	4.26, m		4.24, m		3.89, m		3.77, dd	9.5, 2.4	4.26, m	
5''''	4.00, ddd	8.6, 5.4, 2.9	4.02, m		3.76, m		4.30, m		4.00, ddd	8.6, 5.4, 3.0
6''''	4.56, dd	11.5, 2.1	4.57, dd	11.5, 2.0	1.79, d	6.1	1.67, d	6.2	4.56, dd	11.5, 2.7
	4.38, dd	11.5, 5.3	4.41, dd	11.5, 5.3					4.38, dd	11.5, 5.6
3''''-OMe					3.96, s		3.84, s			
					D-Glc		**D-Glc**			
1'''''					5.16, d	7.8	5.01, d	7.9		
2'''''					4.06, m		4.06, m			
3'''''					4.26, m		4.28, m			
4'''''					4.25, m		4.25, m			
5'''''					4.01, m		4.02, m			
6'''''					4.56, br d	11.7	4.58, br d	11.5		
					4.40, br d	11.7	4.40, br d	11.5		

Table 4-11 ^{1}H-NMR (500 MHz, C_5D_5N) data for aglycone part of verticillosides F-J (**4.6-4.10**)

Atom	4.6	*J* (Hz)	4.7	*J* (Hz)	4.8	*J* (Hz)	4.9	*J* (Hz)	4.10	*J* (Hz)
1	1.93, m		1.89, m		1.89, m		1.90, m		1.92, m	
	1.18, ddd	13.4, 13.2, 3.5	1.14, ddd	13.4, 13.2, 3.6	1.13, ddd	13.8, 13.7, 3.5	1.13, dd	13.8, 13.7, 3.5	1.20, ddd	13.5, 13.1, 3.8
2	2.13, m		2.12, m		2.11, m		2.12, m		2.13, m	
	1.86, m		1.87, m		1.86, m		1.85, m		1.86, m	
3	3.90, m		3.89, m		3.89, m		3.89, m		3.90, m	
4	2.60, br dd	12.6, 4.5	2.59, br d	12.6, 4.6	2.58, br dd	12.8, 4.7	2.59, br dd	12.8, 4.6	2.61, br dd	12.6, 3.6
	2.49, m		2.48, m		2.47, m		2.49, m		2.50, m	
6	5.41, m		5.38, m		5.36, m		5.36, m		5.39, m	
7	2.48, m		2.49, m		2.49, m		2.50, m		2.49, m	
	2.37, m		2.37, m		2.37, m		2.38, m		2.38, m	
9	1.65, m		1.64, m		1.64, m		1.65, m		1.67, m	
11	2.53, m		2.54, m		2.46, m		2.47, m		2.54, m	
	2.00, m		1.90, m		1.90, m		1.92, m		2.01, m	
12	3.92, m		3.95, m		3.96, m		3.96, m		3.91, m	
15	2.06, m		2.13, m		2.14, m		2.15, m		2.07, m	
16	2.00, m		3.39, m		3.40, m		3.41, dd	9.8, 2.7	2.01, m	
			2.13, m		2.12, m		2.03, m			
18	1.97, s		2.02, s		2.02, s		2.02, s		1.98, s	
19	1.43, s		1.42, s		1.41, s		1.41, s		1.43, s	
20	-		-		-		-		4.49, q	6.4
21	1.54, d	6.4	2.60, s		2.65, s		2.66, s		1.54, d	6.4

Table 4-12 ^{1}H-NMR (500 MHz, C_5D_5N) data for sugar moiety of verticillosides F-J (**4.6-4.10**)

Atom	4.6	*J* (Hz)	4.7	*J* (Hz)	4.8	*J* (Hz)	4.9	*J* (Hz)	4.10	*J* (Hz)
	D-Cym		**D-Cym**		**D-Cym**		**D-Cym**		**D-Cym**	
1'	5.30, dd	9.6, 1.7	5.30, dd	9.5, 1.6	5.30, dd	9.4, 1.6	5.30, dd	9.6, 1.6	5.32,dd	9.5, 1.60
2'	2.30, m		2.32, m		2.30, m		2.33, m		2.33, m	
	1.90, m		1.89, m		1.89, m		1.92, m		1.92, m	
3'	4.03, m		4.05, m		4.03, m		4.10, m		4.11, m	
4'	3.48, dd	9.6, 2.7	3.48, dd	9.6, 2.7	3.48, dd	9.5, 2.6	3.52, m		3.52, m	
5'	4.23, m		4.23, m		4.23, m		4.24, m		4.25, m	
6'	1.43, d	6.2	1.42, d	6.2	1.41, d	6.2	1.38, d	6.2	1.38, d	6.2
3'-OMe	3.56, s		3.58, s		3.55, s		3.63, s		3.63, s	
	D-Ole		**D-Ole**		**D-Ole**		**D-Cym**		**D-Cym**	
1"	4.67, dd	9.7, 1.6	4.69, dd	9.7, 1.6	4.68, dd	9.6, 1.6	5.12, dd	9.6, 1.5	5.11, dd	9.7, 1.5
2"	2.47, m		2.48, m		2.40, m		2.33, m		2.32, m	
	1.74, m		1.75, m		1.74, m		1.88, m		1.81, m	
3"	3.56, m		3.57, m		3.56, m		4.02, m		4.00, m	
4"	3.56, m		3.60, m		3.56, m		3.43, dd	9.8, 2.7	3.43, dd	9.6, 2.6
5"	3.53, m		3.76, dq	9.4, 6.1	3.54, m		4.18, dq	9.8, 6.2	4.17, dq	9.6, 6.2
6"	1.60, d	5.8	1.68, d	6.0	1.61, d	5.8	1.38, d	6.2	1.38, d	6.2
3"-OMe	3.53, s		3.51, s		3.52, s		3.55, s		3.56, s	
	D-Allme		**D-Thv**		**D-Allme**		**D-Ole**		**D-Ole**	
1'''	5.28, d	8.0	4.89, d	7.9	5.27, d	8.0	4.68, dd	9.8, 1.5	4.67, dd	9.6, 1.4
2'''	3.84, m		3.92, m		3.83, m		2.48, m		2.48, m	
							1.74, m		1.74, m	
3'''	4.50, dd	2.7, 2.7	3.71, dd	9.0, 9.0	4.50, dd	2.7, 2.7	3.58, m		3.57, m	
4'''	3.76, dd	9.6, 2.4	3.89, dd	9.0, 8.8	3.77, dd	9.6, 2.4	3.57, m		3.58, m	
5'''	4.29, m		3.55, m		4.29, m		3.55, m		3.54, m	
6'''	1.67, d	6.2	1.78, d	6.1	1.66, d	6.2	1.62, d	5.5	1.60, d	5.4
3'''-OMe	3.85, s		3.95, s		3.84, s		3.53, s		3.53, s	
	D-Glc		**D-Glc**		**D-Glc**		**D-Allme**		**D-Allme**	
1''''	5.01, d	7.7	5.16, d	7.8	5.01, d	7.8	5.27, d	8.1	5.28, d	8.1
2''''	4.06, dd	8.8, 8.4	4.05, m		4.06, m		3.85, m		3.86, m	
3''''	4.28, m		4.26, m		4.27, m		4.51, dd	2.7, 2.7	4.51, dd	2.7, 2.7
4''''	4.25, m		4.25, m		4.25, m		3.77, dd	9.5, 2.5	3.77, dd	9.6, 2.4
5''''	4.00, m		3.99, m		4.04, ddd	8.9, 5.4, 2.4	4.26, m		4.30, m	
6''''	4.58, dd	11.6, 2.4	4.55, dd	11.4, 2.4	4.58, br d	11.8	1.67, d	6.2	1.68, d	6.2
	4.41, dd	11.6, 5.4	4.39, dd	11.4, 5.5	4.41, dd	11.8, 5.9				
3''''-OMe					-		3.85, s		3.86, s	
	-		-		-		**D-Glc**		**D-Glc**	
1'''''							5.02, d	8.0	5.02, d	8.2
2'''''							4.07, m		4.06, dd	8.6, 8.2
3'''''							4.29, m		4.29, m	
4'''''							4.30, m		4.26, m	
5'''''							4.05, m		4.03, ddd	9.0, 5.6, 2.5
6'''''							4.58, dd	11.5, 5.4	4.58, dd	11.6, 2.5
							4.41, dd	11.5, 2.5	4.42, dd	11.6, 5.6

Table 4-13 ^{1}H-NMR (500 MHz, C_5D_5N) data for aglycone part of verticillosides K-M (**4.11-4.13**)

Atom	4.11	J (Hz)	4.12	J (Hz)	4.13	J (Hz)
1	1.80, m 1.13, ddd	14.1, 13.8, 3.6	1.81, m 1.12, ddd	14.1, 13.8, 3.4	1.80, m 1.12, ddd	14.1, 13.5, 3.6
2	2.10, m 1.82, m		2.10, m 1.82, m		2.09, m 1.84, m	
3	3.89, m		3.89, m		3.89, m	
4	2.60, br dd 2.47, m	13.1, 4.4	2.59, br dd 2.47, m	13.0, 4.5	2.59, br dd 2.47, m	13.0, 4.3
6	5.40, m		5.39, m		5.38, m	
7	2.52, m 2.40, m		2.51, m 2.40, m		2.51, m 2.39, m	
9	1.82, m		1.82, m		1.81, m	
11	2.53, m 2.19, m		2.53, m 2.19, m		2.52, m 2.19, m	
12	5.40, m		5.40, m		5.40, m	
15	2.14, m		2.14, m		2.13, m	
16	1.99, m		1.99, m		1.98, m	
18	2.24, s		2.24, s		2.24, s	
19	1.37, s		1.37, s		1.36, s	
20	4.12, dq	6.1, 6.1, 6.1, 5.3	4.12, dq	6.2, 6.2, 6.2, 5.6	4.12, m	
21	1.29, d	6.1	1.29, d	6.2	1.29, d	6.1
	12-Bz		**12-Bz**		**12-Bz**	
	8.59, br d	8.2	8.59, br d	8.2	8.59, br d	8.2
	7.41, br dd	8.2, 7.6	7.41, br dd	8.2, 7.6	7.41, br dd	8.2, 7.6
	7.50, m		7.50, m		7.50, m	

Table 4-14 ^{1}H-NMR (500 MHz, C_5D_5N) data for sugar moiety of verticillosides K-M (**4.11-4.13**)

Atom	4.11	*J* (Hz)	4.12	*J* (Hz)	4.13	*J* (Hz)
	D-Cym		**D-Cym**		**D-Cym**	
1'	5.31, dd	9.7, 1.5	5.30, dd	9.7, 1.5	5.30, dd	9.6, 1.6
2'	2.33, ddd	13.5, 2.9, 1.5	2.31, m		2.32, m	
	1.90, m		1.89, m		1.90, m	
3'	4.06, m		4.04, m		4.10, m	
4'	3.50, m		3.49, dd	9.6, 2.4	3.53, m	
5'	4.25, m		4.24, m		4.24, m	
6'	1.45, d	6.2	1.44, d	6.2	1.38, d	6.2
3'-OMe	3.59, s		3.56, s		3.63, s	
	D-Ole		**D-Ole**		**D-Cym**	
1"	4.70, dd	9.6, 1.6	4.68, dd	9.6, 1.6	5.12, dd	9.4, 1.3
2"	2.49, m		2.49, m		2.31, m	
	1.78, m		1.75, m		1.81, m	
3"	3.56, m		3.57, m		4.00, m	
4"	3.63, m		3.56, m		3.41, dd	9.6, 2.5
5"	3.56, m		3.54, m		4.17, m	
6"	1.69, d	6.0	1.62, d	5.9	1.38, d	6.2
3"-OMe	3.52, s		3.54, s		3.55, s	
	D-Thv		**D-Allme**		**D-Cym**	
1"'	4.89, d	7.9	5.28, d	7.9	4.67, dd	9.6, 1.2
2"'	3.92, m		3.85, m		2.48, m	
					1.73, m	
3"'	3.72, dd	9.0, 8.9	4.50, dd	2.7, 2.7	3.56, m	
4"'	3.89, dd	9.4, 9.0	3.76, m		3.57, m	
5"'	3.76, dq	9.4, 6.1, 6.1, 6.1	4.31, m		3.55, m	
6"'	1.67, d	6.1	1.68, d	6.4	1.61, d	5.3
3"'-OMe	3.84, s		3.85, s		3.53, s	
	D-Glc		**D-Glc**		**D-Allme**	
1""	5.16, d	7.7	5.01, d	7.7	5.28, d	8.0
2""	4.06, m		4.07, m		3.85, m	
3""	4.26, m		4.28, m		4.50, dd	2.6, 2.4
4""	4.26, m		4.26, m		3.76, dd	9.6, 2.4
5""	4.00, m		4.04, m		4.29, m	
6""	4.55, br d	11.5	4.58, br d	11.5	1.68, d	6.2
	4.40, br d	11.5	4.41, br d	11.5		
3""-OMe					3.85, s	
					D-Glc	
1"""					5.01, d	7.8
2"""					4.05, m	
3"""					4.28, m	
4"""					4.25, m	
5"""					4.00, m	
6"""					4.59, br d	11.5
					4.42, m	

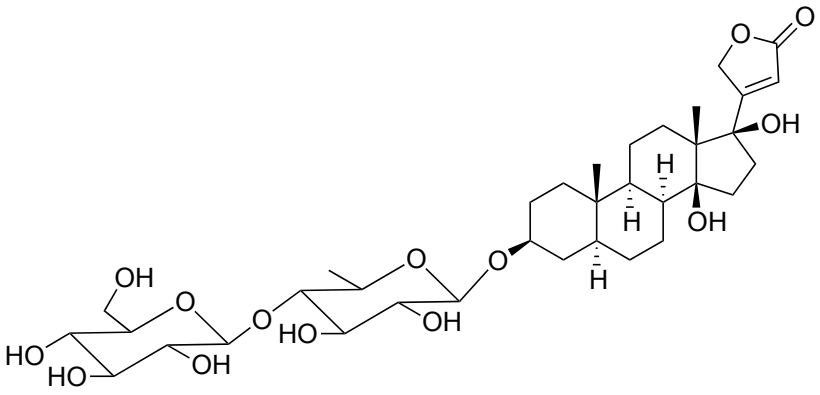

4.15

3-*O*-β-D-Glucopyranosyl-(1→4)-6-desoxy-β-D-allopyranosyl-17β-hydroxyuzarigenin (4.15). Amorphous white powder; mp 263.2-264.8°C; $[\alpha]_D^{25}$ = -6.7 (c. 0.09, MeOH); IR ν_{max} (film) cm^{-1}: 3343.6 (OH), 1706.0 (C=O), 1735.8 (C=O), 1158.4, 1059.8; UV_{max} 217.1 nm; HRMS *m/z*: 721.3401 $[M+Na]^+$ (721.3411 calc. for $C_{35}H_{54}NaO_{14}$) ^1H and ^{13}C NMR: see Table 4-15.

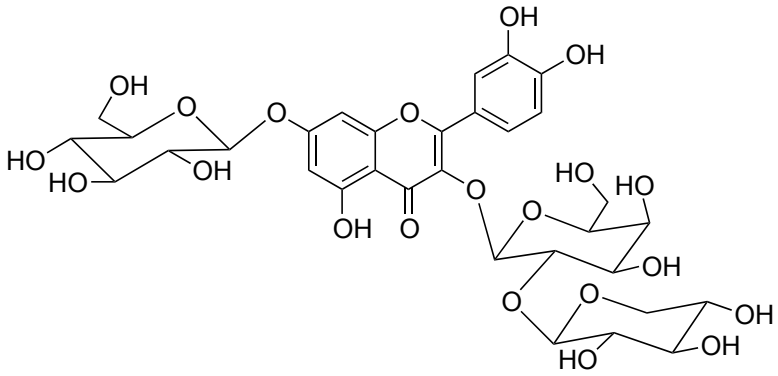

4.19

Syriacatin (4.19). Amorphous yellow powder; mp 195.6-197.0°C; $[\alpha]_D^{25}$ = -39.3 (c. 0.38, MeOH); IR ν_{max} (film) cm^{-1}: 3282.4 (OH), 1651.6 (C=O), 1044.8, 989.1; UV_{max} 358.0, 256.9 nm; HRMS *m/z*: 781.1816 $[M+Na]^+$ (781.1803 calc. for $C_{32}H_{38}NaO_{21}$) ^1H and ^{13}C NMR: see Table 4-16.

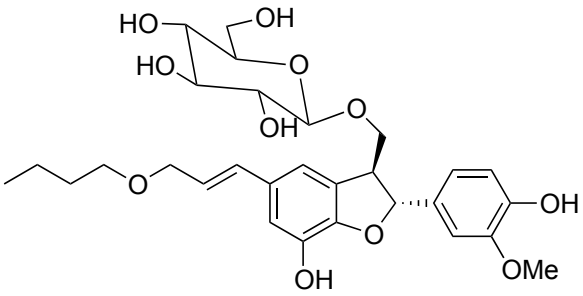

4.20

9'-*O*-butyl-3-*O*-demethyl-9-*O*-β-D-glucopyranosyl dehydrodiconiferyl alcohol (4.20). Amorphous white powder; mp 234.2-235.9°C; $[\alpha]_D^{25}$ = +25.1 (c. 0.72, MeOH); IR ν_{max} (film) cm^{-1}: 3326.9 (OH), 3025.1 (Ar-H), 1336.3, 1073.6, 1058.5; UV_{max} 278.9, 220.5 nm; HRMS *m/z*: 585.2298 $[M+Na]^+$ (585.2312 calc. for $C_{29}H_{38}NaO_{11}$) ^1H and ^{13}C NMR: see Table 4-17.

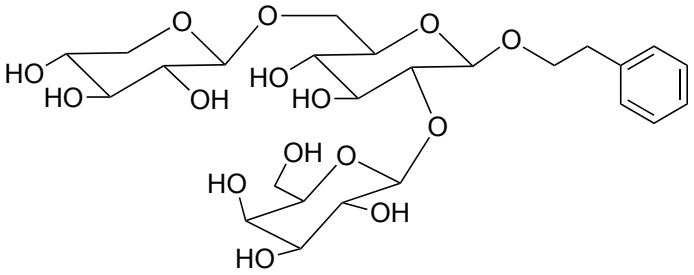

4.21

Kansanoside A (4.21). Amorphous white powder; mp. 267.2-269.0°C; $[\alpha]_D^{25}$ = +12.1 (c. 0.28, MeOH); IR ν_{max} (film) cm^{-1}: 3310.28 (OH), 1161.4, 1055.5; UV_{max} 237.9 nm; HRMS *m/z*: 601.2087 $[M+Na]^+$ (601.2108 calc. for $C_{25}H_{38}NaO_{15}$) ^1H and ^{13}C NMR: see Table 4-18.

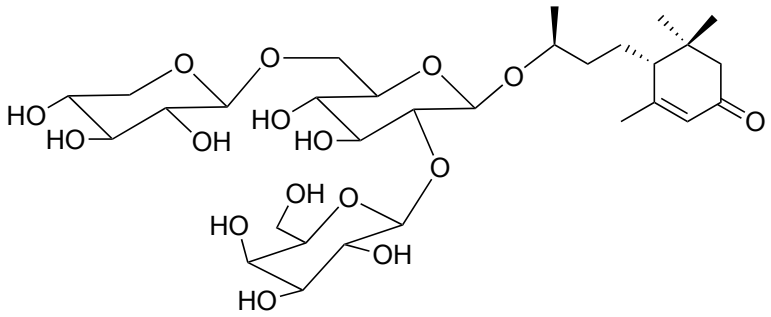

4.22

Oreadoside A (4.22). Amorphous white powder; mp 254.3-255.9°C; $[\alpha]_D^{25}$ = -28.9 (c. 0.69, MeOH); IR ν_{max} (film) cm^{-1}: 3350.2 (OH), 1642.6 (C=O), 1377.6, 1058.9; UV_{max} 278.9, 262.0, 256.0 nm; HRMS *m/z*: 689.2974 $[M+Na]^+$ (689.2997 calc. for $C_{30}H_{50}NaO_{16}$) ^1H and ^{13}C NMR: see Table 4-18.

Table 4-15 NMR Spectroscopic Data (500 MHz, C_5D_5N) for 3-*O*-β-D-glucopyranosyl-(1→4)-6-desoxy-β-D-allopyranosyl-17β-hydroxyuzarigenin (**4.15**)

	4.15	
position	δ_C, type	δ_H (*J* in Hz)
1	37.6, CH_2	1.65 *m* 0.96 *m*
2	30.4, CH_2	2.10 *m* 1.66 *m*
3	77.5, CH	3.92 *m*
4	35.1, CH_2	1.78 *m* 1.36 *ddd* (12.6, 12.5, 11.5)
5	44.6, CH	0.90 *m*
6	29.2, CH_2	1.15 *m* 1.10 *m*
7	27.3, CH_2	1.12 *m* 2.27 *m*
8	41.8, CH	1.75 *m*
9	50.1, CH	0.79 *ddd* (12.1, 11.9, 3.2)
10	36.3, C	
11	21.6, CH_2	1.41 *m* 1.11 *m*
12	33.6, CH_2	1.06 *m* 0.95 *m*
13	52.2, C	
14	88.0, C	
15	31.7, CH_2	2.02 *m* 2.12 *m*
16	37.6, CH_2	2.36 *m*
17	87.0, C	
18	13.4, CH_3	1.22 *s*
19	12.5, CH_3	0.67 *s*
20	173.6, C	
21	73.7, CH_2	5.23 *dd* (18.3, 1.7) 5.09 *dd* (18.3, 1.8)
22	117.0, CH	6.26 *dd* (1.8, 1.7)
23	174.4, C	
1'	99.7, CH	5.42 *d* (7.9)
2'	72.5, CH	3.96 *m*
3'	72.9, CH	5.10 *brd* (7.8)
4'	84.0, CH	3.87 *dd* (9.6, 2.5)
5'	69.2, CH	4.56 *dq* (9.4, 6.2, 6.2, 6.2)
6'	18.9, CH_3	1.76 *d* (6.2)
1"	106.8, CH	5.10 *d* (7.6)
2"	75.6, CH	4.02 *m*
3"	78.7, CH	4.28 *m*
4"	72.0, CH	4.29 *m*
5"	78.6, CH	3.98 *m*
6"	62.9, CH_2	4.48 *ddd* (11.8, 5.1, 2.6) 4.38 *ddd* (11.8, 5.9, 5.1)

Table 4-16 NMR Spectroscopic Data (500 MHz, C_5D_5N) for syriacatin (**4.19**)

	4.19	
position	δ_C, type	δ_H (*J* in Hz)
2	157.5, C	
3	135.5, C	
4	179.3, C	
4a	107.3, C	
5	162.7, C	
6	100.6, CH	6.73, *d* (2.2)
7	164.1, C	
8	94.6, CH	6.78, *d* (2.2)
8a	157.1, C	
1'	123.6, C	
2'	118.0, CH	8.32, *d* (2.3)
3'	151.1, C	
4'	147.4, C	
5'	116.5, CH	7.31, *d* (8.6)
6'	122.9, CH	8.36, *dd* (8.6, 2.3)
1''	100.9	6.62, *d* (7.7)
2''	82.2	4.94, *dd* (9.3, 7.7)
3''	76.0	4.30, *m*
4''	70.2	4.57, *m*
5''	79.6	4.15, *m*
6''	62.3	4.33, *m*
1'''	106.9	5.48,*d* (7.2)
2'''	76.1	4.24, *m*
3'''	78.2	4.14, *m*
4'''	71.4	4.17, *m*
5'''	67.6	4.41, *m* 3.68, *dd* (11.2, 9.2)
1''''	102.1	5.76, *d* (7.8)
2''''	75.2	4.33, *m*
3''''	78.9	4.42, *m*
4''''	71.5	4.36, *m*
5''''	78.3	4.14, *m*
6''''	62.8	4.56, *m* 4.42, *m*

Table 4-17 NMR spectroscopic data (500 MHz, C_5D_5N) for 9'-*O*-butyl-3-*O*-demethyl-9-*O*-β-D-glucopyranosyl dehydrodiconiferyl alcohol (**4.20**)

	4.20	
position	δ_C, type	δ_H (*J* in Hz)
1	133.3, C	
2	111.2, CH	7.34, d (1.6)
3	149.1, C	
4	148.5, C	
5	116.8, CH	7.16, d (8.6)
6	120.1, CH	7.19, dd (8.6, 1.6)
7	88.8, CH	5.99, d (6.5)
8	52.5, CH	4.08, m
9	71.9, CH_2	4.66, m 4.44, m
1'	132.1, C	
2'	114.9, CH	7.36, d (1.4)
3'	143.3, C	
4'	148.5, C	
5'	133.0, C	
6'	116.4, CH	7.41, d (1.4)
7'	130.2, CH	6.78, d (16.0)
8'	124.9, CH	6.47, ddd (16.0, 6.0, 6.0)
9'	72.1, CH_2	4.12, m
1"	105.2, CH	5.03, d (7.6)
2"	75.5, CH	4.12, m
3"	79.0, CH	4.30, m
4"	72.0, CH	4.29, m
5"	79.1, CH	4.02, m
6"	63.0, CH_2	4.65, m 4.45, m
OBu		
1""	70.3, CH_2	3.43, dd (6.5, 6.5)
2""	32.6, CH_2	1.57, dddd (7.5, 7.5, 6.5, 6.5)
3""	20.0, CH_2	1.37, ddq (7.5, 7.5, 7.3, 7.3, 7.3)
4""	14.4, CH_3	0.85, dd (7.3, 7.3)

Table 4-18 NMR spectroscopic data (500 MHz, C_5D_5N) for compounds kansanoside A (**4.21**) and oreadoside A (**4.22**)

	4.21		**4.22**	
Position	δ_C, type	δ_H (*J* in Hz)	δ_C, type	δ_H (*J* in Hz)
1	139.8, C		36.7, C	
2	130.3, CH	7.32, *d* (7.2)	48.0, CH_2	2.56, *d* (17.1) 2.10, *d* (17.1)
3	128.0, CH	7.27, *dd* (7.4, 7.2)	198.9, C	
4	126.8, CH	7.17, *dd* (7.4, 7.4)	125.5, CH	5.95, *br s*
5	130.3, CH	7.32, *d* (7.2)	166.0, C	
6	128.0, CH	7.27, *dd* (7.4, 7.2)	51.4, CH	1.82, m
7	36.9, CH_2	3.09, *m*	26.1, CH_2	2.02, m 1.59, m
8	71.2, CH_2	4.26, *m* 3.75, *m*	37.6, CH_2	1.70, m 1.80, m
9			75.4, CH	4.01, m
10			20.2, CH_3	1.34 d (6.2)
11			26.6, CH_3	1.01, *s*
12			29.0, CH_3	0.93, *s*
13			24.8, CH	1.95, *d* (1.2)
1'	103.2, CH	4.83, *d* (7.8)	101.3, CH	4.87, *d* (7.7)
2'	84.2, CH	4.08, *dd* (8.8, 7.8)	84.2, CH	4.08, *m*
3'	78.2, CH	4.29, *m*	78.1, CH	4.26, *m*
4'	69.7, CH	4.38, *m*	69.5, CH	4.34, *m*
5'	77.2, CH	4.01, *m*	77.0, CH	4.02, *m*
6'	69.8, CH_2	4.83, *dd* (11.5, 2.3) 4.24, *m*	69.9, CH_2	4.82, *m* 4.21, *m*
1"	106.9, CH	5.33, *d* (7.9)	106.9, CH	5.23, *d* (7.8)
2"	77.2, CH	4.13, *m*	77.2, CH	4.12, *dd* (8.9, 7.8)
3"	78.5, CH	4.28, *m*	78.4, CH	4.26, *m*
4"	71.9, CH	4.30, *m*	71.9, CH	4.30, *m*
5"	79.2, CH	3.98, *m*	79.2, CH	3.97, *ddd* (9.4, 4.6, 2.6)
6"	63.1, CH	4.56, *dd* (11.8, 2.5) 4.43, *dd* (11.8, 4.9)	63.1, CH_2	4.54, *dd* (11.5, 2.4) 4.43, *dd* (11.5, 4.8)
1"'	105.8, CH	4.88, *d* (7.0)	105.8, CH	4.89, *d* (7.0)
2"'	72.7, CH	4.48, *dd* (8.5, 7.0)	72.7, CH	4.46, *dd* (8.4, 7.0)
3"'	77.2, CH	4.13, *m*	77.4, CH	4.12, *dd* (8.4, 3.3)
4"'	74.8, CH	4.14, *m*	69.5, CH	4.34, *m*
5"'	67.12, CH_2	4.30, *m* 3.73, *m*	66.9, CH_2	4.33, *m* 3.77, *dd* (11.8, 1.4)

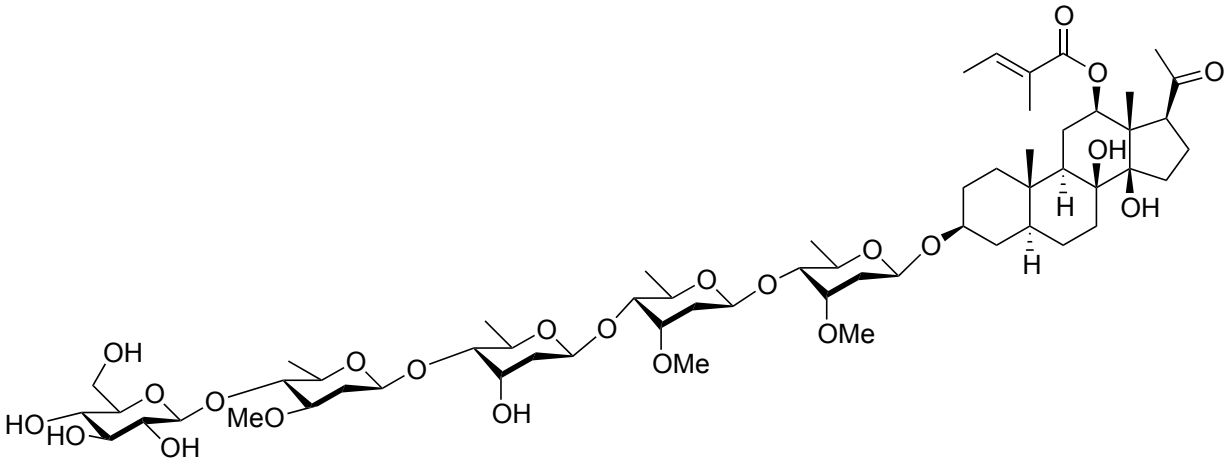

4.40

Sullivantoside A (4.40). Amorphous white powder; mp 141.7-143.0°C; $[\alpha]_D^{25}$ = -2.8 (*c* 0.38, MeOH); IR ν_{max} (film) cm^{-1}: 3389.3 (OH), 1708.7 (C=O), 1644.8 (C=O), 1156.6 (C-O); HRMS *m/z*: 1195.6150 $[M+H]^+$ (1195.6240 calc. for $C_{59}H_{96}NaO_{23}$) ^1H and ^{13}C NMR: see Tables 4-19, 4-20, 4-21, and 4-22.

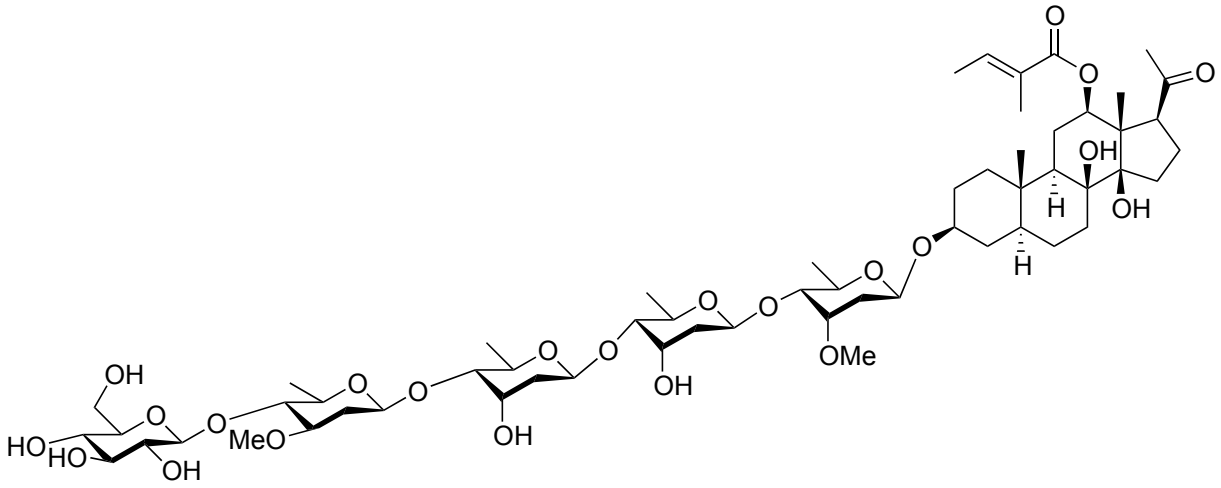

4.41

Sullivantoside B (4.41). Amorphous white powder; mp 153.7-154.9°C; $[\alpha]_D^{25}$ = +18 (*c* 0.5, MeOH); IR ν_{max} (film) cm^{-1}: 3389.7 (OH), 1708.5 (C=O), 1644.6 (C=O), 1156.9 (C-O); HRMS

m/z: 1181.6076 $[M+H]^+$ (1181.6084 calc. for $C_{58}H_{94}NaO_{23}$) ^1H and ^{13}C NMR: Tables 4-19, 4-20, 4-21, and 4-22.

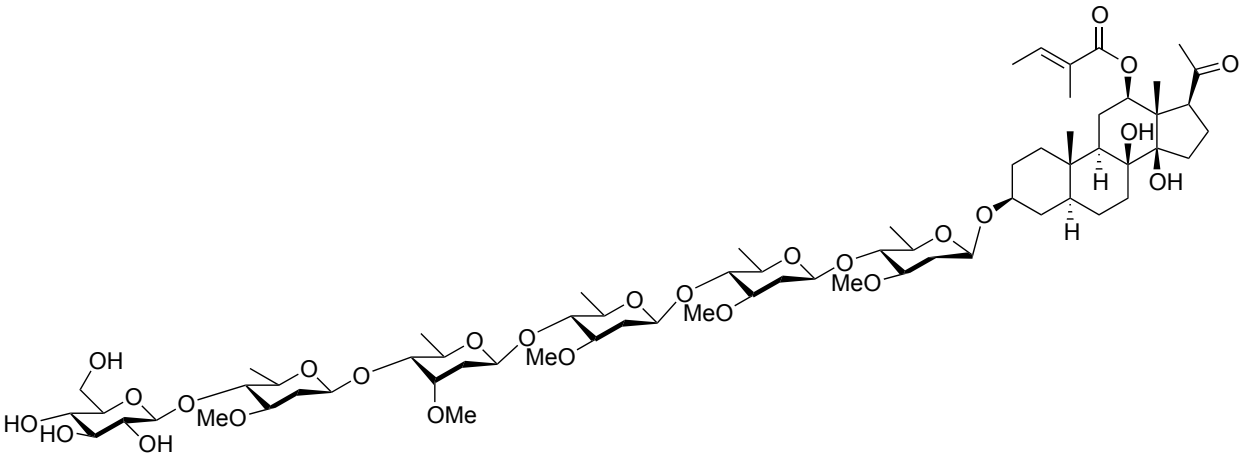

4.42

Sullivantoside C (4.42). Amorphous white powder; mp 158.9-160.0°C; $[\alpha]_D^{25}$ = +15.3 (*c* 0.45, MeOH); IR ν_{max} (film) cm^{-1}: 3389.3 (OH), 1708.7 (C=O), 1644.8 (C=O), 1156.6 (C-O); HRMS *m/z*: 1330.7278 $[M+H]^+$ (1330.7285 calc. for $C_{67}H_{110}NaO_{26}$) ^1H and ^{13}C NMR: see Tables 4-19, 4-20, 4-21, and 4-22.

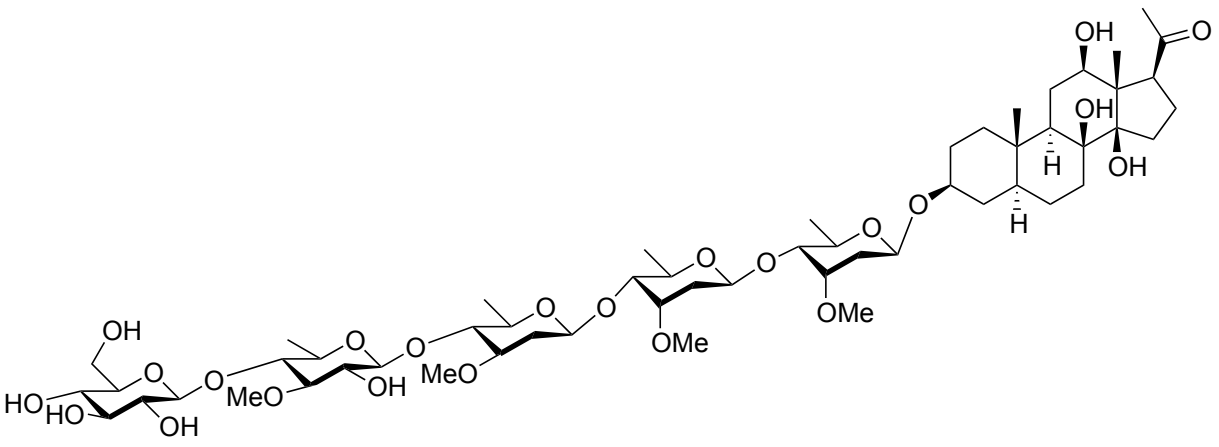

4.43

Sullivantoside D (4.43). Amorphous white powder; mp 155.1-157.0°C; $[\alpha]_D^{25}$ = -1.6 (*c* 0.1, MeOH); IR ν_{max} (film) cm^{-1}: 3389.3 (OH), 1708.5 (C=O), 1644.5 (C=O), 1156.3 (C-O); HRMS *m/z*: 1113.5798 $[M+H]^+$ (1113.5821 calc. for $C_{55}H_{92}NaO_{23}$) ^1H and ^{13}C NMR: see Tables 4-19, 4-20, 4-21, and 4-22.

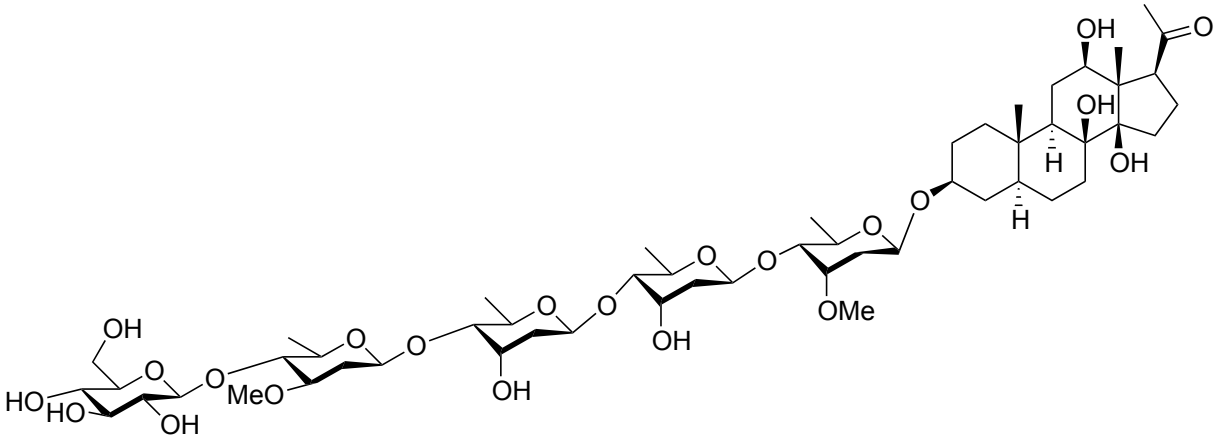

4.44

Sullivantoside E (4.44). Amorphous white powder; mp 164.7-165.4°C; $[\alpha]_D^{25}$ = +15.5 (*c* 0.2, MeOH); IR ν_{max} (film) cm^{-1}: 3389.4 (OH), 1708.3 (C=O), 1644.7 (C=O), 1156.8 (C-O); HRMS *m/z*: 1199.5668 $[M+H]^+$ (1099.5665 calc. for $C_{53}H_{88}NaO_{22}$) ^1H and ^{13}C NMR: Tables 4-19, 4-20, 4-21, and 4-22.

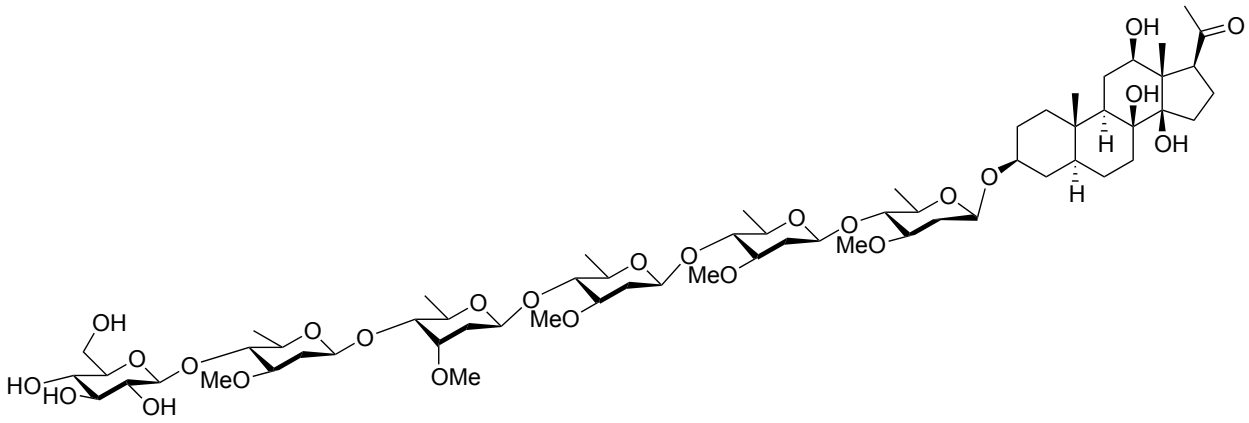

4.45

Sullivantoside F (4.45). Amorphous white powder; mp 138.9-140.1°C; $[\alpha]_D^{25}$ = +20.3 (c. 0.3, MeOH); IR ν_{max} (film) cm^{-1}: 3389.2 (OH), 1708.4 (C=O), 1644.9 (C=O), 1156.5 (C-O); HRMS *m/z*: 1271.6756 $[M+H]^+$ (1271.6764 calc. for $C_{62}H_{104}NaO_{25}$) ^1H and ^{13}C NMR: see Tables 4-19, 4-20, 4-21, and 4-22.

Table 4-19 ^{13}C-NMR (125 MHz, C_5D_5N) data for the aglycone part of sullivantosides A-E (**4.40-4.45**)

Atom	4.40	4.41	4.42	4.43	4.44	4.45
1	38.5, CH_2	38.5, CH_2	38.4, CH_2	38.6, CH_2	38.5, CH_2	38.6, CH_2
2	29.9, CH_2	29.9, CH_2	29.9, CH_2	30.0, CH_2	30.0, CH_2	29.9, CH
3	76.9, CH	76.9, CH	77.3, CH	77.0, CH	76.9, CH	77.2, CH_2
4	34.8, CH_2	34.8, CH_2	34.8, CH_2	34.9, CH_2	34.9, CH_2	34.9, CH_2
5	45.6, CH	45.6, CH	45.7, CH	45.8, CH	45.7, CH	45.8, CH
6	25.6, CH_2	25.6, CH_2	25.7, CH_2	25.8, CH_2	25.8, CH_2	25.9, CH_2
7	35.8, CH_2	35.8, CH_2	35.9, CH_2	36.1, CH_2	36.0, CH_2	36.8, CH_2
8	76.4, C	76.4, C	76.4, C	76.5, C	76.9, C	76.6, C
9	48.5, CH	48.1, CH	48.2, CH	48.8, CH	48.5, CH	48.8, CH
10	37.0, C	37.0, C	37.0, C	37.0, C	37.0, C	37.0, C
11	24.1, CH_2	24.1, CH_2	24.1, CH_2	27.9, CH_2	24.1, CH_2	28.0, CH_2
12	78.6, CH	78.6, CH	78.6, CH	75.2, CH	78.6, CH	75.2, CH
13	55.5, C	55.6, C	55.6, C	57.3, C	57.3, C	57.3, C
14	86.4, C	86.7, C	86.7, C	86.8, C	86.8, C	86.8, C
15	36.2, CH_2	36.2, CH_2	36.3, CH_2	36.8, CH_2	36.8, CH_2	36.8, CH_2
16	25.4, CH_2	25.3, CH_2	25.4, CH_2	25.5, CH_2	25.5, CH_2	25.5, CH_2
17	59.3, CH	59.5, CH	59.5, CH	59.1, CH	59.2, CH	59.0, CH
18	13.4, CH_3	13.4, CH_3	13.4, CH_3	12.4, CH_3	12.4, CH_3	12.4, CH_3
19	13.5, CH_3	13.5, CH_3	13.6, CH_3	13.7, CH_3	13.7, CH_3	13.7, CH_3
20	214.9, C	214.9, C	215.0, C	217.4, C	217.3, C	217.4, C
21	32.3, CH_3	32.3, CH_3	32.3, CH_3	32.8, CH_3	32.8, CH_3	32.8, CH_3
	12-An	**12-An**	**12-An**			
1	168.1, C	168.1, C	168.2, C			
2	129.7, C	129.7, C	129.7, C			
3	138.1, CH	138.1, CH	138.1, CH			
4	14.7, CH_3	14.7, CH_3	14.7, CH_3			
5	12.7, CH_3	12.7, CH_3	12.7, CH_3			

Table 4-20 ^{13}C-NMR (125 MHz, C_5D_5N) data for the sugar moiety of compounds **4.40-4.44**

Atom	4.40	4.41	4.42	4.43	4.44	4.45
	D-Cym	**D-Cym**	**D-Ole**	**D-Cym**	**D-Cym**	**D-Ole**
1'	96.3, CH	96.3, CH	98.0, CH	96.2, CH	96.2, CH	97.9, CH
2'	37.7,CH_2	37.7,CH_2	38.3,CH_2	37.7,CH_2	37.7,CH_2	38.3,CH_2
3'	78.4, CH	78.4, CH	79.6, CH	78.4, CH	78.4, CH	79.7, CH
4'	83.8, CH	83.8, CH	83.6, CH	83.8, CH	83.8, CH	83.6, CH
5'	69.3, CH	69.3, CH	72.2, CH	69.4, CH	69.3, CH	72.2, CH
6'	19.0 CH_3	19.0 CH_3	19.1 CH_3	19.0 CH_3	19.0 CH_3	19.1 CH_3
3'-OMe	59.3 CH_3	59.2 CH_3	57.6 CH_3	59.3 CH_3	59.2 CH_3	57.6 CH_3
	D-Cym	**D-Dig**	**D-Ole**	**D-Cym**	**D-Dig**	**D-Ole**
1''	100.9, CH	100.9, CH	100.6, CH	100.9, CH	100.9, CH	100.6, CH
2''	37.4, CH_2	39.1, CH_2	38.2, CH_2	37.4, CH_2	39.1, CH_2	38.2, CH_2
3''	78.3, CH	67.8, CH	79.5, CH	78.3, CH	67.8, CH	79.5, CH
4''	83.5, CH	83.5, CH	83.6, CH	83.5, CH	83.5, CH	83.6, CH
5''	69.2, CH	68.9, CH	71.9, CH	69.4, CH	68.9, CH	72.0, CH
6''	18.9, CH_3	18.8, CH_3	19.1, CH_3	18.9, CH_3	18.8, CH_3	19.1, CH_3
3''-OMe	59.3, CH_3		57.8, CH_3	59.3, CH_3		57.8, CH_3
	D-Dig	**D-Dig**	**D-Ole**	**D-Dig**	**D-Dig**	**D-Ole**
1'''	100.9, CH	100.3, CH	100.6, CH	100.8, CH	100.3, CH	100.6, CH
2'''	39.4, CH_2	39.3, CH_2	38.2, CH_2	39.4, CH_2	39.3, CH_2	38.2, CH_2
3'''	67.9, CH	67.9, CH	79.7, CH	67.9, CH	67.9, CH	79.7, CH
4'''	83.6, CH	83.6, CH	83.6, CH	83.6, CH	83.6, CH	83.6, CH
5'''	68.8, CH	68.8, CH	72.3, CH	68.8, CH	68.9, CH	72.3, CH
6'''	18.7, CH_3	18.7, CH_3	19.2, CH_3	18.8, CH_3	18.9, CH_3	19.2, CH_3
3'''-OMe			57.8, CH_3			57.8, CH_3
	D-Ole	**D-Ole**	**D-Cym**	**D-Ole**	**D-Ole**	**D-Cym**
1''''	101.8, CH	101.8, CH	98.9, CH	101.8, CH	101.8, CH	98.9, CH
2''''	37.4, CH_2	37.6, CH_2	37.4, CH_2	37.6, CH_2	37.6, CH_2	37.6, CH_2
3''''	79.6, CH	79.6, CH	78.5, CH	79.6, CH	79.6, CH	78.3, CH
4''''	83.5, CH	83.4, CH	83.4, CH	83.5, CH	83.4, CH	83.4, CH
5''''	72.3, CH	72.6, CH	69.5, CH	72.3, CH	72.3, CH	69.5, CH
6''''	19.2, CH_3	19.2, CH_3	19.9, CH_3	19.2, CH_3	19.2, CH_3	19.9, CH_3
3''''-OMe	57.6, CH_3	57.2, CH_3	59.2, CH_3	57.6, CH_3	57.3, CH_3	59.2, CH_3
	D-Glc	**D-Glc**	**D-Ole**	**D-Glc**	**D-Glc**	**D-Ole**
1'''''	104.8, CH	104.8, CH	102.2, CH	104.8, CH	104.9, CH	102.3, CH
2'''''	76.1, CH	76.1, CH	37.8, CH_2	76.1, CH	76.1, CH	37.8, CH_2
3'''''	79.1, CH	79.1, CH	79.7, CH	79.1, CH	79.1, CH	79.3, CH
4'''''	72.4, CH	72.4, CH	83.3, CH	72.4, CH	72.4, CH	83.3, CH
5'''''	78.6, CH	78.6, CH	72.0, CH	78.6, CH	78.6, CH	72.2, CH
6'''''	63.4, CH_2	63.4, CH_2	19.2, CH_3	63.4, CH_2	63.4, CH_2	19.2, CH_3
3'''''-OMe			57.6, CH_3			57.6, CH_3
			D-Glc			**D-Glc**
1''''''			104.4, CH			104.9, CH
2''''''			76.1, CH			76.1, CH
3''''''			79.1, CH			79.1, CH
4''''''			72.4, CH			72.4, CH
5''''''			78.5, CH			78.5, CH
6''''''			63.4, CH_2			63.4, CH_2

Table 4-21 ^{1}H-NMR (500 MHz, C_5D_5N) data for aglycone part of compounds sullivantosides A-F (**4.40-4.45**)

Atom	**4.40** (*J* in Hz)	**4.41** (*J* in Hz)	**4.42** (*J* in Hz)	**4.43** (*J* in Hz)	**4.44** (*J* in Hz)	**4.45** (*J* in Hz)
1	1.62, m 0.91, m	1.62, m 0.91, m	1.65, m 0.92, m	1.76, m 0.98, m	1.75, m 0.96, m	1.75, m 0.96, m
2	2.02, m 1.72, m	2.02, m 1.72, m	2.04, m 1.75, m	2.04, m 1.77, m	2.03, m 1.75, m	2.03, m 1.75, m
3	3.90, m	3.90, m	3.92 m	3.96, m	3.92, m	3.93, m
4	1.76, m 1.44, m	1.75, m 1.42, m	1.82, m 1.49, m	1.83, m 1.50, m	1.77, m 1.44, m	1.77, m 1.45, m
5	1.00, m	1.00, m	1.05, m	1.05 m	1.01, m	1.01, m
6	1.81, m 1.10, m	1.80, m 1.10, m	1.88, m 1.18, m	1.88, m 1.20, m	1.84, m 1.12, m	1.82, m 1.11, m
7	2.18, m 1.41, br dd (10.5, 4.3)	2.17, m 1.40, br dd (10.5, 4.3)	2.22, m 1.42, br dd	2.22, m 1.43, m	2.20, m 1.42, br dd (10.5, 4.3)	2.20, m 1.41, br dd (10.5, 4.3)
9	1.34, m	1.35, br d (12.8)	1.37, m	1.31, br d (13.0)	1.29, m	1.29, br d (12.7)
11	2.18, m 1.92, m	2.17, m 1.92, m	2.20, m 1.94, m	2.33, m 1.94, m	2.31, m 1.93, m	2.32, m 1.92, m
12	5.02, m	5.01, m	5.03, m	3.74, m	3.72, m	3.74, m
15	2.10, m 1.98, m	2.11, m 1.98, m	2.12, m 1.99, m	2.12, m 2.00, m	2.11, m 1.98, m	2.10, m 1.98, m
16	2.22, m 1.99, m	2.23, m 1.92, m	2.24, m 1.94, m	2.19, m 1.97, m	2.19, m 1.96, m	2.18, m 1.96, m
17	3.21, dd (9.2, 5.9)	3.19, dd (9.3, 5.8)	3.21, dd (9.2, 5.8)	3.87, dd (9.3, 5.4)	3.85, dd (9.5, 5.4)	3.85, dd (9.5, 5.4)
18	1.54, s	1.54, s	1.56, s	1.57, s	1.56, s	1.56, s
19	1.18, s	1.18, s	1.21, s	1.24, s	1.21, s	1.21, s
21	2.24, s	2.24, s	2.25, s	2.30, s	2.30, s	2.29, s
	12-An	**12-An**	**12-An**			
2						
3	7.14, m	7.14, m	7.14, m			
4	1.72, br d (7.2)	1.72, br d (7.2)	1.73, br d (7.2)			
5	1.98, br s	1.98, br s	1.99, br s			

Table 4-22 ^{1}H-NMR (500 MHz, C_5D_5N) data for sugar moiety compounds sullivantosides A-F (**4.40-4.45**)

Atom	4.40 (*J* in Hz)	4.41 (*J* in Hz)	4.42 (*J* in Hz)	4.43 (*J* in Hz)	4.45 (*J* in Hz)	4.44 (*J* in Hz)
	D-Cym	**D-Cym**	**D-Ole**	**D-Cym**	**D-Cym**	**D-Ole**
1'	5.32, dd (9.5, 1.7)	5.33, dd (9.5, 1.6)	4.88, dd (9.7, 1.5)	5.34, dd (9.5, 1.7)	5.34, dd (9.5, 1.6)	4.90, dd (9.7, 1.7)
2'	2.34, m	2.34, m	2.50, m	2.36, m	2.35, m	2.51, m
	1.92, m	1.92, m	1.84, m	1.92, m	1.94, m	1.80, m
3'	4.11, m	4.13, m	3.63, m	4.10, m	4.13, m	3.63, m
4'	3.54, dd (9.5, 2.8)	3.56, dd (9.6, 2.7)	3.54, m	3.47, dd (9.5, 2.8)	3.56, dd (9.6, 2.7)	3.54, m
5'	4.28, m	4.28, dq (9.6, 6.3)	3.63, m	4.28, dq (9.5, 6.1)	4.30, dq (9.6, 6.3)	3.62, m
6'	1.44, d (6.1)	1.42, d (6.3)	1.53, d (5.4)	1.44, d (6.1)	1.42, d (6.3)	1.48, d (5.4)
3'-OMe	3.65, s	3.65, s	3.54, s	3.65, s	3.66, s	3.54, s
	D-Cym	**D-Dig**	**D-Ole**	**D-Cym**	**D-Dig**	**D-Ole**
1''	5.14, br d (8.0)	5.35, dd (9.5, 1.6)	4.93, dd (9.8, 1.6)	5.15, br d (9.5)	5.36, dd (9.5, 1.6)	4.93, dd (9.8, 1.7)
2''	2.35, m	2.43, m	2.52, m	2.36, m	2.43, m	2.52, m
	1.87, m	1.98, m	1.80, m	1.87, m	2.01, m	1.81, m
3''	4.10, m	4.65, m	3.64, m	4.10, m	4.67, m	3.60, m
4''	3.50, m	3.50, dd (9.6, 2.5)	3.54, m	3.52, dd (9.8, 2.8)	3.52, dd (9.6, 2.5)	3.55, m
5''	4.19, dq (9.2, 6.1)	4.28, dq (9.6, 6.3)	3.64, m	4.19, dq (9.8, 6.3)	4.30, dq (9.6, 6.3)	3.62, m
6''	1.44, d (6.1)	1.38, d (6.3)	1.46, d (5.4)	1.44, d (6.1)	1.39, d (6.3)	1.46, d (5.4)
3''-OMe	3.65, s		3.58, s	3.68, s		3.58, s
	D-Dig	**D-Dig**	**D-Ole**	**D-Dig**	**D-Dig**	**D-Ole**
1'''	5.35, dd (8.2, 1.5)	5.41, dd (9.6, 1.6)	4.91, dd (9.8, 1.6)	5.35, dd (9.5, 1.5)	5.40, dd (9.6, 1.6)	4.93, dd (9.8, 1.7)
2'''	2.42, m	2.46, m	2.52, m	2.43, m	2.43, m	2.52, m
	1.99, m	1.98, m	1.80, m	1.97, m	2.01, m	1.81, m
3'''	4.62, m	4.66, m	3.63, m	4.63, *m*	4.62, m	3.60, m
4'''	3.45, dd (9.5, 2.5)	3.43, dd (9.6, 2.5)	3.54, m	3.50, dd (9.8, 2.5)	3.44, dd (9.6, 2.5)	3.55, m
5'''	4.30, dq (9.5, 6.3)	4.32, dq (9.6, 6.3)	3.64, m	4.30, dq (9.8, 6.3)	4.30, dq (9.6, 6.3)	3.62, m
6'''	1.34, d (6.3)	1.39, d (6.3)	1.47, d (5.4)	1.34, d (6.3)	1.40, d (6.3)	1.46, d (5.4)
3'''-OMe			3.58, s			3.58, s
	D-Ole	**D-Ole**	**D-Cym**	**D-Ole**	**D-Ole**	**D-Cym**
1''''	4.76, dd (9.8, 1.5)	4.74, dd (9.7, 1.6)	5.30, dd (9.7, 1.6)	4.76, dd (9.8, 1.5)	4.75, dd (9.7, 1.6)	5.31, dd (9.5, 1.6)
2''''	2.48, m	2.45, m	2.32, m	2.48, ddd (12.5, 5.1, 1.6)	2.47, m	2.34, m
	1.66, m	1.63, m	1.82, m	1.66, m	1.65, m	1.83, m
3''''	3.64, m	3.54, m	4.05, *m*	3.64, m	3.64, m	4.06, *m*
4''''	3.69, m	3.67, m	3.45, m	3.70, m	3.68, m	3.50, m
5''''	3.67, m	3.65, m	4.22, m	3.68, m	3.67, m	4.22, m
6''''	1.68, d (5.3)	1.66, d (5.8)	1.41, d (6.3)	1.69, d (5.4)	1.67, d (5.8)	1.41, d (6.3)
3''''-OMe	-	3.54, s	3.58, s		3.55, s	3.59, s
	D-Glc	**D-Glc**	**D-Ole**	**D-Glc**	**D-Glc**	**D-Ole**
1'''''	5.14, d (8.0)	5.14, d (7.8)	4.71, dd (9.7, 1.6)	5.16, d (8.0)	5.14, d (7.8)	4.71, dd (9.7, 1.5)
2'''''	4.04, m	4.03, m	2.50, m	4.06, dd (8.3, 7.9)	4.01, m	2.51, m
			1.75, m			1.75, m
3'''''	4.25, m	4.25, m	3.66, m	4.24, m	4.25, m	3.67, m
4'''''	4.24, m	4.24, m	3.75, m	4.25, m	4.24, m	3.75, m
5'''''	3.99, ddd (9.7, 5.3, 2.1)	3.98, ddd (9.8, 5.2, 2.7)	3.68, m	3.99, ddd (9.8, 5.4, 2.1)	3.98, ddd (9.8, 5.2, 2.7)	3.63, m
6'''''	4.56, dd (11.4, 2.1)	4.57, dd (11.2, 2.7)	1.75, d (5.3)	4.57, dd (11.4, 2.1)	4.57, dd (11.2, 2.7)	1.53, d (5.3)
	4.38, dd (11.4, 5.3)	4.38, dd (11.2, 5.2)		4.40, dd (11.4, 5.4)	4.38, dd (11.2, 5.2)	
3'''''-OMe			3.54, s			3.54, s
			D-Glc			**D-Glc**
1''''''			5.16, d (7.8)			5.16, d (7.8)
2''''''			4.04, m			4.04, m
3''''''			4.25, m			4.25, m
4''''''			4.24, m			4.24, m
5''''''			3.99, ddd (9.8, 5.4, 2.1)			3.99, ddd (9.8, 5.4, 2.1)
6''''''			4.56, dd (11.4, 2.1)			4.57, dd (11.4, 2.1)
			4.39, dd (11.4, 5.4)			4.39, dd (11.4, 5.4)

5. SYNTHETIC METHODS FOR STRUCTURE DIVERSIFICATION OF CARDIAC GLYCOSIDES

5.1.Introduction

Nature has provided and continues to provide compounds with extraordinary structural complexity and highly selective biological activity that inspire medicinal and organic chemists in the drug discovery process.[12] In fact, the new combinatorial synthetic approaches include more focused libraries (100 to ~3000 plus compounds) that incorporate more "natural-product-likeness" into compound design. Such approaches, also referred as "diversity-oriented synthesis" and "natural-product mimic synthesis", demonstrate that including natural products scaffolds and privileged structures into organic synthesis is crucial for small-molecule drug lead development.[252-256] Furthermore, synthetic modifications of natural products allow investigation of SAR and to improve pharmacodynamic and pharmacokinetic properties.

As described in the previous chapter, in the last few decades, cardiac glycosides have emerged as potential anti-cancer agents with a novel mechanism of action. These compounds are currently investigated as alternative treatments for cancers that are unresponsive to standard therapies.[45] This growing interest has attracted the attention of various synthetic research groups, targeting cardiac glycosides for total synthesis. In fact, the wide variety of natural products with a steroid framework including sex hormones, were among the first complex molecules synthesized in modern history.[257] Total synthesis of *Digitalis*-type cardiac glycosides typically involves a large number of steps making SAR studies difficult.[258-260] For instance, the Deslongchamps' research group has been using a key polyanionic cyclization between a highly functionalized Nazarov substrate and a cyclohexenone followed by intramolecular aldol cyclization to afford the required *cis*-*cis* configuration (Figure 5-1).[261] On the other hand, semi-synthesis is the preferred approach to prepare steroids, even in the pharmaceutical industry, taking advantage of readily available

steroids with the tetracyclic core already assembled.[257] Templeton *et al*.[262] have described the oxidative degradation of digitoxin and digitoxigenin using ozonolysis to prepare analogs at C-17, however degradation approaches are limited by the availability of the starting materials. In contrast, commercially available simple steroids can be used to prepare cardiac glycosides. This process requires, however, a C-14 oxidation with inversion of configuration. This transformation has been reported by the use of several strategies including remote functionalization,[263] SeO_2 allylic oxidation,[264] dioxirane-mediated oxyfunctionalization,[265] benzyl nitrosoformate [4+2] cycloaddition,[266] and singlet oxygen addition followed by oxidative fragmentation.[267] In addition, epimerization at C-5 is a requirement for the formation of *Digitalis*-type compounds.

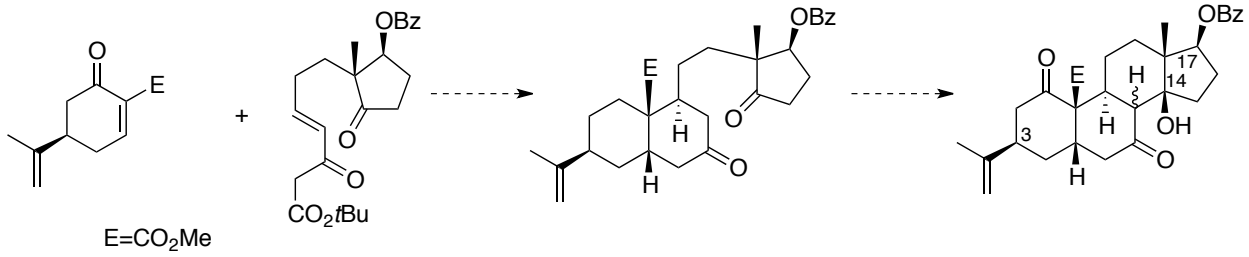

Figure 5-1 Representative approach for the total synthesis of *Digitalis*-type cardenolides

Although the *Asclepias* cardenolides are structurally similar to those found in *Digitalis*, the first group has not been targeted for semi- or total-synthetic efforts to the same extent as the *Digitalis*-type counterparts and much less is known about their SAR. In the present work, we isolated several cardenolides form *Asclepias* species that showed cytotoxic effects toward malignant breast cancer cell lines (Chapter 4). In addition, most of the isolated compounds were found in very small quantities preventing their semi-synthetic modifications to further investigate

SAR. In order to investigate the biological effects of structural diversification at the 17-position of the cardenolides scaffold, we developed synthetic methods toward functionalization of the commercially available steroid *trans*-androsterone as well as an evaluation of palladium-mediated coupling to install an aryl groups at C-17.

5.2. Rationale and synthetic strategy

Structurally, cardiac glycosides contain three distinct elements: the sugar moiety, the steroidal core, and the unsaturated lactone (Figure 5-2). The sugar moiety has been extensively investigated using the well-established methodologies of neoglycorandomization and glycorandomization. Using this approach, the cardiotoxicity was reduced and selective toxicity against cancer cells was enhanced for classic cardenolides scaffolds.[87-89, 268] The steroidal core is considered the pharmacophore, hence only minor structural modifications have been reported. In addition, several modifications to the butenolide ring have been carried out; however, most of the analogs were only investigated for their ionotropic activity.[269] Therefore, in order to investigate the structure diversification of *Asclepias*-type cardenolides, we started with the development of methods to modify the commercially available steroid *trans*-androsterone as well as an evaluation of a palladium-mediated coupling of boronic acids to obtain analogs at C-17 position.

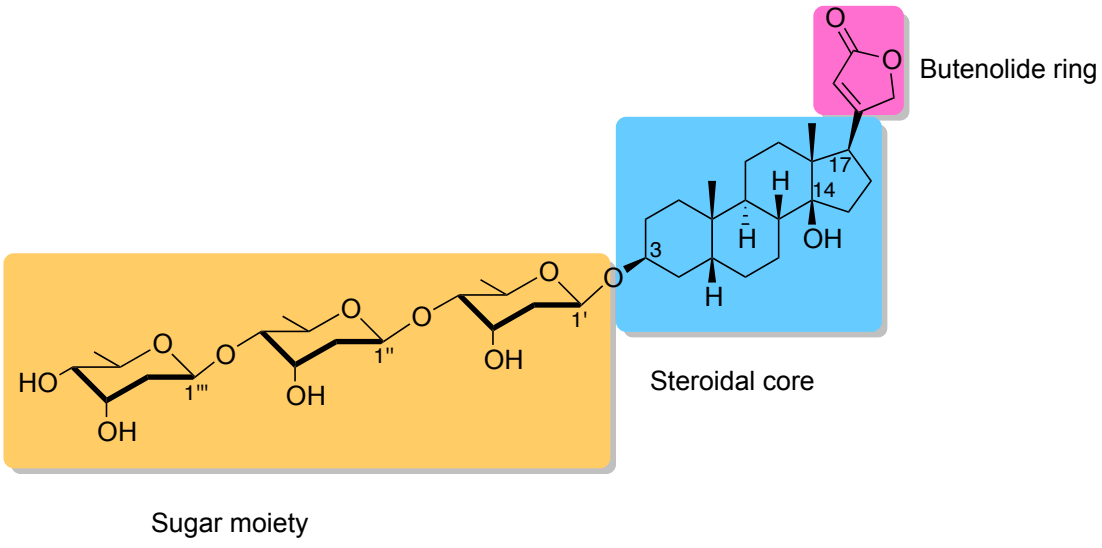

Figure 5-2 Structural regions of cardiac glycosides

The structure of cardiac glycosides offer several difficulties from the synthetic point of view, but probably assembling the steroidal core bearing eight stereocenters is by far the most challenging. Fortunately, a wide variety of steroids are commercially available and can be used as starting materials to build up more complex structures such as the cardenolide type molecules. As proposed in Figure 5-3, in order to synthesize structurally diverse analogs at position C-17, an appropriately functionalized enol-triflate could be subjected to a Suzuki-Miyaura cross-coupling with boronic acids.[270] Given the large number of commercially available boronic acids and boronate ethers, this coupling at a later step gives flexibility for analog preparation. The enol-triflate can be obtained from the appropriate ketone by KHMDS treatment followed by $PhNTf_2$. An allylic oxidation using SeO_2 (Riley oxidation) was proposed for the diasteroselective installation of the 14β-hydroxyl group from the respective enone. This key oxidation step has been employed early by Groszek *et al*.[264] using a similar substrate. This reaction is, however, not commonly used probably due to the extended refluxing periods needed for this reaction to take place. We proposed in this study the alternative use of microwave irradiation. In addition, the synthesis of the protected enone from commercially available *trans*-androsterone using a palladium-mediated oxidative elimination has been previously reported.

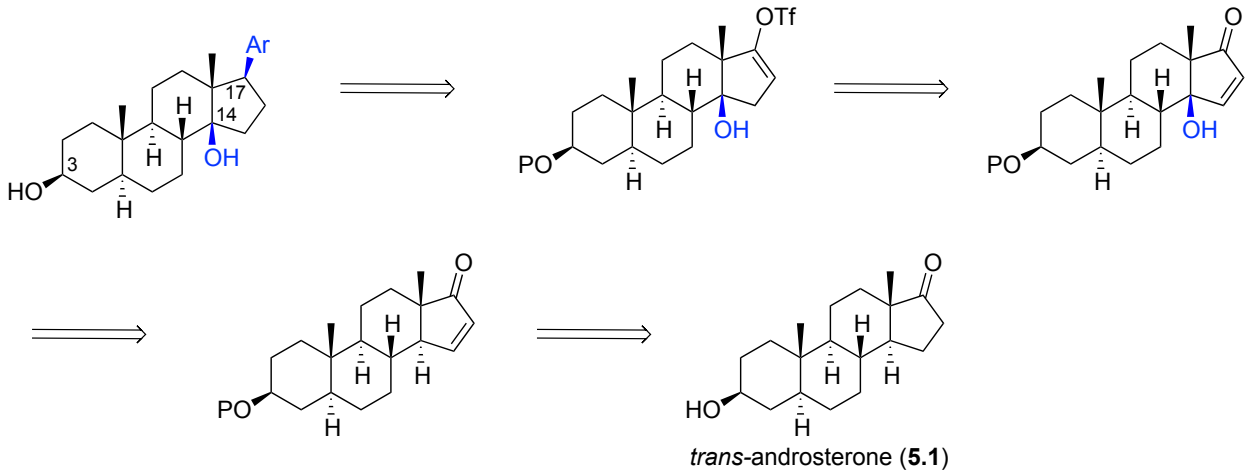

Figure 5-3 Retrosynthetic analysis for the proposed analogs (P: protecting group)

5.3. Synthetic efforts towards 17β-aryl analogs

The proposed synthetic route to obtain the 17β-aryl analogs of cardiac glycosides is shown Figure 5-4. The 3-*O*-acetyl enone **5.2** was prepared in a three-step sequence using a Tsuji-type oxidation recently applied by Hilton *et al.*[271] to a similar substrate during the preparation of bufadienolide analogs. Treatment of *trans*-aldosterone (**5.1**) with acetic anhydride afforded the 3-*O*-acetyl-trans-aldosterone quantitatively, which was transformed into the TMS-enol ether using KHMDS followed by TMSCl. A palladium-mediated oxidative elimination gave the desired α,β-unsaturated ketone **5.2** in 54% yield (three steps). Next, the installation of the 14-β-hydroxyl group (**5.3**) was conducted by oxidation with SeO_2.[264, 272] The relative configuration was confirmed by X-ray crystallography (Figure 5-5). In order to explain the observed stereoselectivity, the proposed mechanism for this oxidation step involves an initial keto-enol tautomerization followed by an ene reaction with SeO_2 (Figure 5-6). The resulting allyl selenic acid undergoes [2,3] sigmatropic rearrangement to form an allyl selenite ester that can be readily hydrolyzed to the corresponding alcohol.[273, 274] Although Groszek *et al.* reported a 60% yield

using a similar substrate, in our experiments, the 14-β-hydroxy enone **5.3** was obtained in 40% yield from **5.2** under reflux conditions for 6h (20% water in dioxane). Using the same solvent system, this reaction was investigated using microwave irradiation (Figure 5-7), which resulted in an improvement in the yield to 56% and reducing the reaction time to only 30 minutes. In general, microwave irradiation can often replace extended periods of reflux due to the more efficient heating.[275, 276] Microwave-based acceleration for SeO_2 oxidations have not been frequently reported.[277] The preparation of **5.3** under microwave irradiation allowed for an important reduction of reaction time and an increase in the yield when compared with the same transformations under reflux conditions and represents an important contribution to the selenium chemistry field.

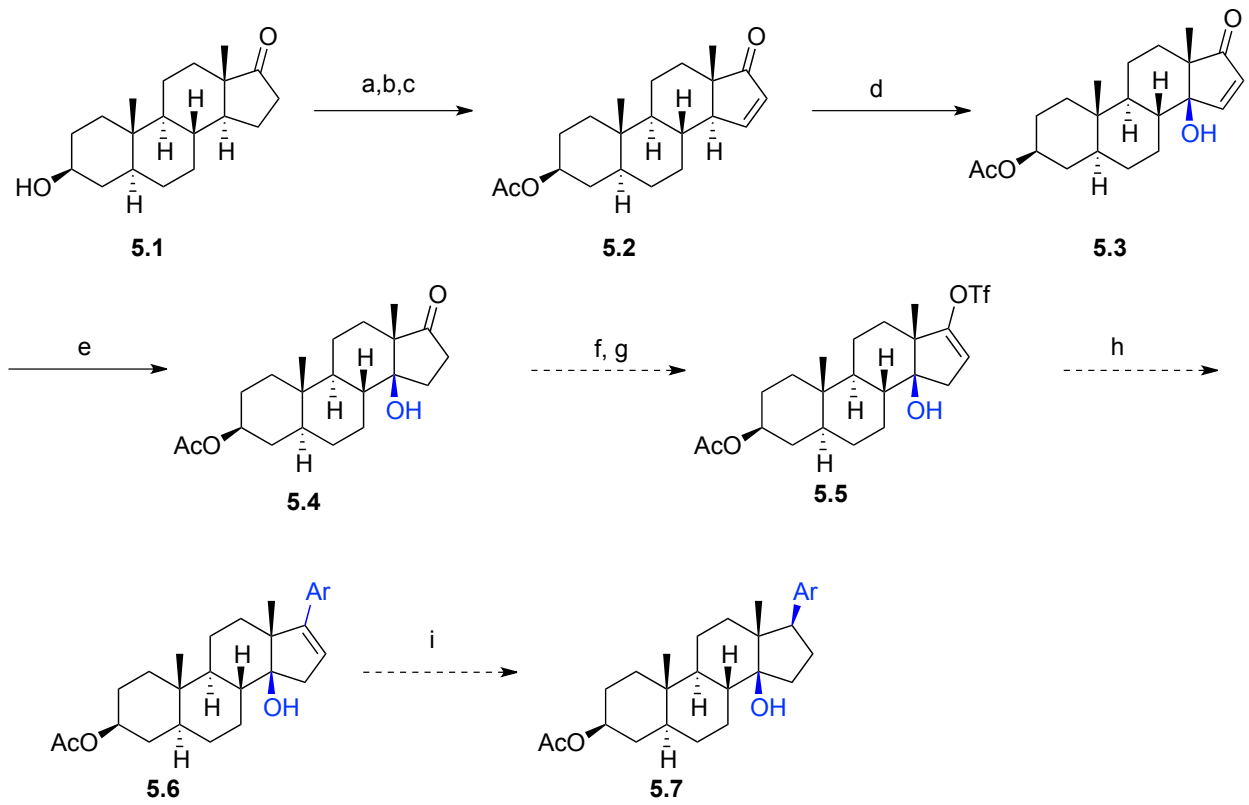

Figure 5-4 Synthetic route for proposed analogs (dotted arrows indicated proposed conversions) a) Ac_2O 2 eq., DMAP cat., CH_2Cl_2, 18h; b) KHMDS 0.5 M in toluene 1.1 eq., -78°C, THF, 60 min then Et_3N 1.5 eq, TMSCl 1.1 eq, -78°C to RT, 30 min then workup; c) $Pd(OAc)_2$ 1.0 eq, CH_2Cl_2:MeCN 4:1, 30°C, 6h; d) SeO_2, 1.2 eq, dioxane:H_2O 4:1, MW, 110°C, 30 min; e) H_2 (balloon), EtOH, 10% Pd/C; f) KHMDS 2.1 eq, -78°C, THF, 1h; g) $PhNTf_2$ 1.1 eq, -78°C to RT, 2h; h) $ArB(OH)_2$ 2 eq, Na_2CO_3 2N 3 eq, $Pd(PPh_3)_4$ 10 mol%, dioxane, MW 170°C, 30 min; i) H_2 (balloon), EtOH, 10% Pd/C

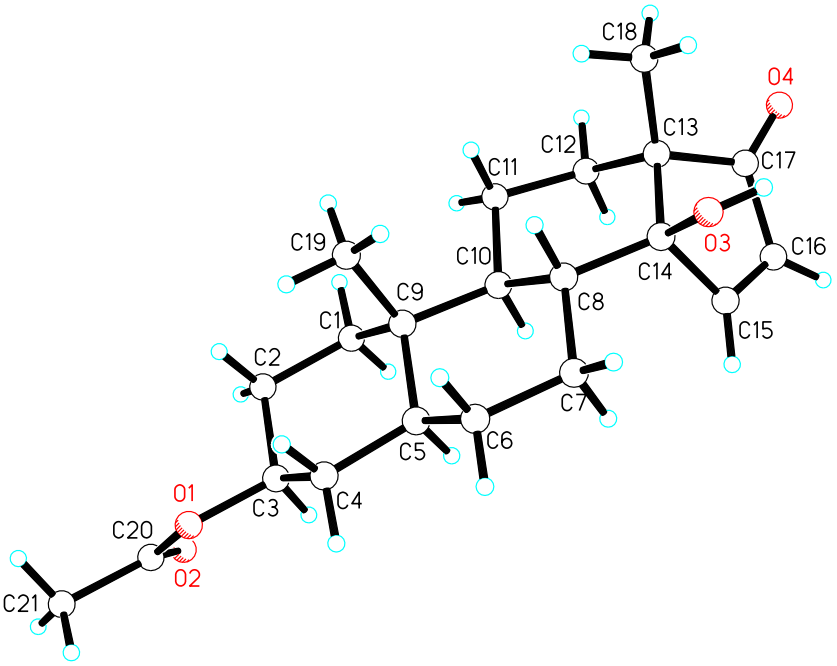

Figure 5-5 ORTEP representation of compound **5.3**

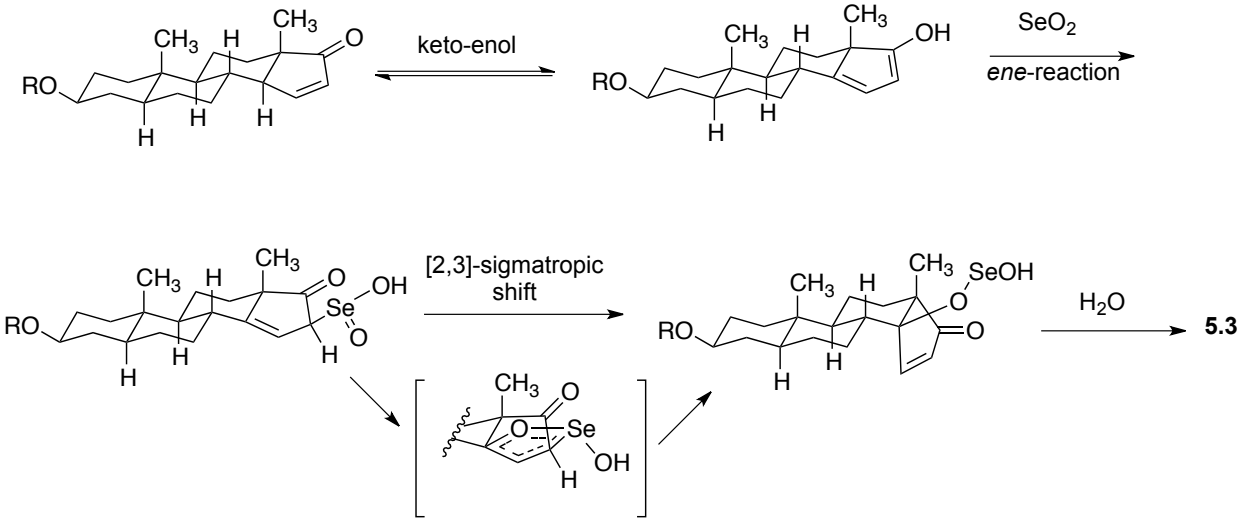

Figure 5-6 Proposed mechanism for the formation of **5.3**

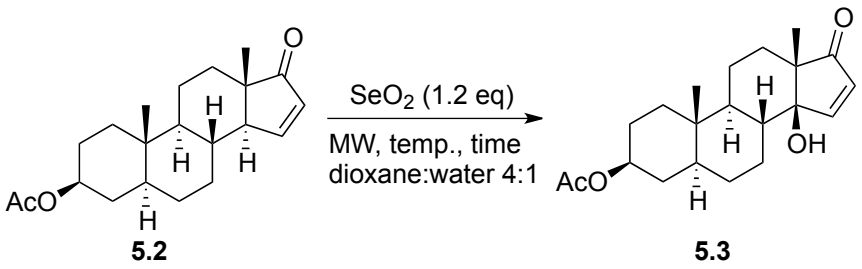

5.2 **5.3**

Entry	Temp.	Time	Yield
1	150 °C	5 min	5 %
2	130 °C	10 min	30 %
3	110 °C	30 min	56 %

Figure 5-7 Temperature optimization of SeO_2-mediated oxidation under microwave conditions

Preparation of enol-triflate was attempted by treatment of the ketone **5.15a** with KHMDS at a low temperature followed by the addition of $PhNTf_2$ as described by Liu and Meinwald.[266] In our experiment, the reaction conditions afforded an undesired elimination product **5.15a'** in 30% yield (Figure 5-8). An optimization of the reaction conditions is currently underway to resolve this problem. At the same time, a model compound was utilized to investigate the Suzuki-Miyaura cross-coupling reaction. As shown in Figure 5-9, TBDMS-protected *trans*-aldosterone **5.9** was efficiently converted (82%) to the enol-triflate **5.10**. With the enol triflate in hand, the coupling reaction catalyzed by $Pd(PPh_3)_4$ was carried out under microwave irradiation at 170°C with moderate yields (30-46%). We observed that temperatures lower than 170°C only afforded modest yields (Figure 5-10). We also observed that the use of $PdCl_2(PPh_3)_2$ as a catalyst did not improve the final product yields. Although this reaction conditions can likely be further optimized, the MW-based coupling allowed for a quick access to analogs for biological evaluation.

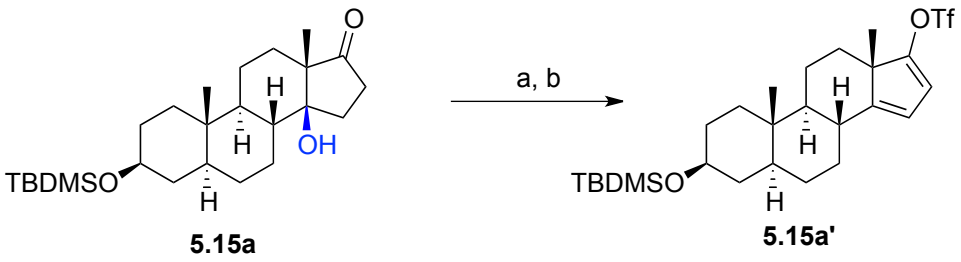

Figure 5-8 Undesired elimination product during enol-triflate preparation. a) KHMDS 2.1 eq, THF, -78°C, 2h, b) $PhNTf_2$ 1.1 eq, -78°C, 2h

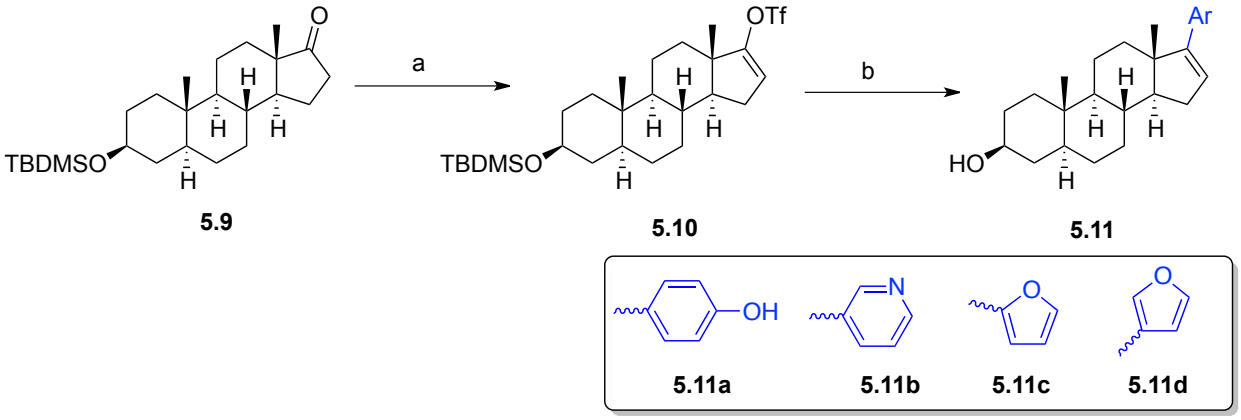

Figure 5-9 Model Suzuki-Miyaura cross-coupling reaction. a) $PhNTf_2$ 1.1 eq, THF, -78°C, then KHMDS 1.1 eq, 2h; b) $ArB(OH)_2$ 2 eq, Na_2CO_3 2N 3 eq, $Pd(PPh_3)_4$ 10 mol%, dioxane, MW 170°C, 30 min

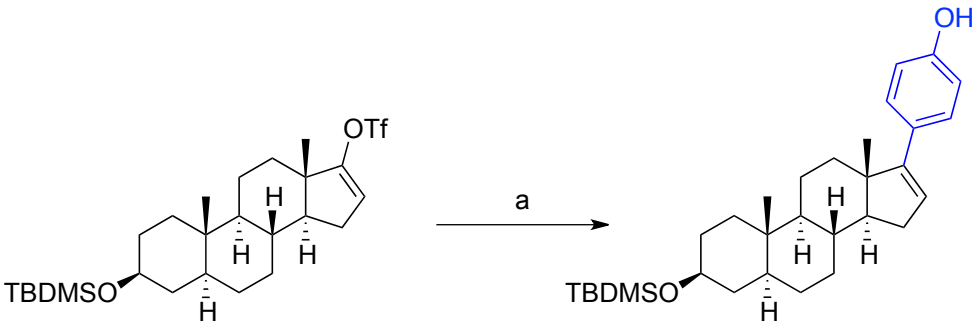

5.11 **5.12a**

Entry	Cat.	Temp.	Yield
1	$Pd(PPh_3)_4$	130 °C	traces
2	$Pd(PPh_3)_4$	150 °C	5 %
3	$Pd(PPh_3)_4$	170 °C	30 %
4	$PdCl_2(PPh_3)_2$	170 °C	32 %

Figure 5-10 Suzuki-Miyaura cross-coupling temperature optimization. a) $ArB(OH)_2$ 2 eq, Na_2CO_3 2N 3 eq, catalyst (cat.) 10 mol%, dioxane, MW, temperature (temp.), 30 min

In addition to the 3-*O*-acetyl group, we also investigated TMS and TBDMS protecting groups at C-3 for the reaction sequences shown in Figures 5-11 and 5-12. Both protecting groups, however, were cleaved during the allylic oxidation step when SeO_2 was used, presumably due to the generation of the acidic byproduct H_2SeO_2. As anticipated, TBDMS was more resistant to this acidic condition when compared with the TMS-protected counterpart; but a more complex reaction mixture was obtained due to incomplete oxidation or by TBDMS group cleavage or both thus leading to a more complex chromatographic separation.

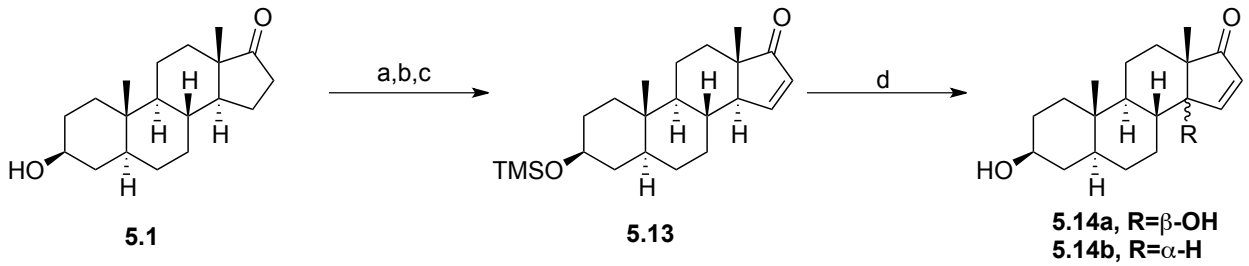

Figure 5-11 Evaluation of 3-*O*-TMS protected substrate for the proposed reaction sequence. a) LDA 3.0 eq., -78°C, THF, 30 min; b) Et_3N 4 eq., TMSCl 2.7 eq., -78°C to RT, 30 min then workup; c) $Pd(OAc)_2$ 1.0 eq, CH_2Cl_2:MeCN 4:1, 30°C, 6h; d) SeO_2, 1.2 eq, dioxane:H_2O 4:1, MW, 110°C, 30 min

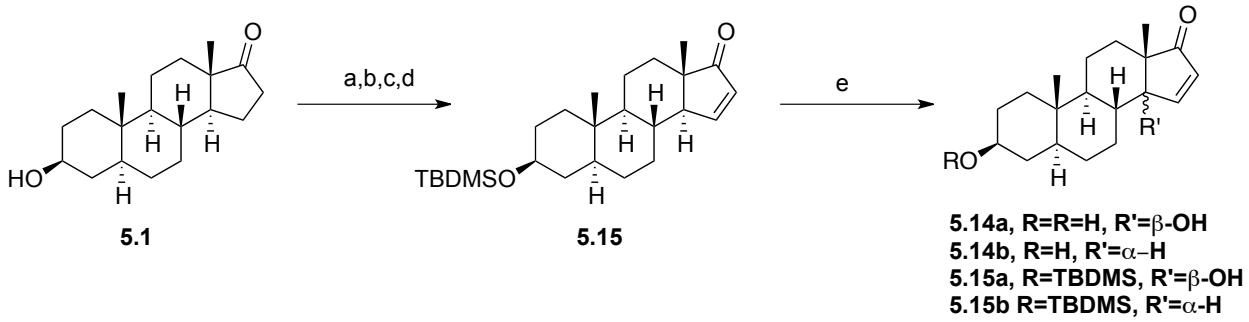

Figure 5-12 Evaluation of 3-*O*-TBDMS protected substrate for the proposed reaction sequence. a) TBDMSCl 1.2 eq, imidazole 3 eq, DMF, RT, 3h; b) LDA 3.0 eq., -78°C, THF, 30 min; b) Et_3N 2 eq., TMSCl 1.5 eq., -78°C to RT, 30 min then workup; c) $Pd(OAc)_2$ 1.0 eq, CH_2Cl_2:MeCN 4:1, 30°C, 6h; d) SeO_2, 1.2 eq, dioxane:H_2O 4:1, MW, 110°C, 30 min

Finally, during the process of microwave-assisted oxidation with SeO_2 the enone **5.15a** was unexpectedly converted to the α,β-unsaturated diketone **5.16** under anhydrous conditions (Figure 5-13). A plausible mechanism for the formation of this product is shown in Figure 5-14. After keto-enol tautomerization, the allylselenic acid intermediate could be formed upon ene reaction with SeO_2. Rather than hydrolysis to form the alcohol, in anhydrous conditions, a Pummerer-type rearrangement may have taken place to form the diketone product.

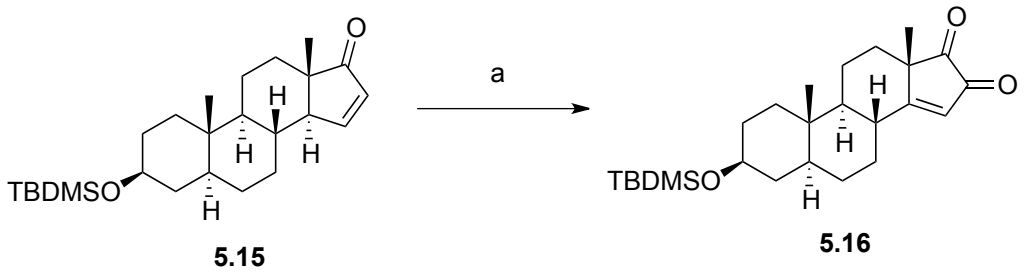

Figure 5-13 Preparation of **5.16** a) SeO_2, 1.2 eq, dry dioxane, MW, 110°C, 30 min

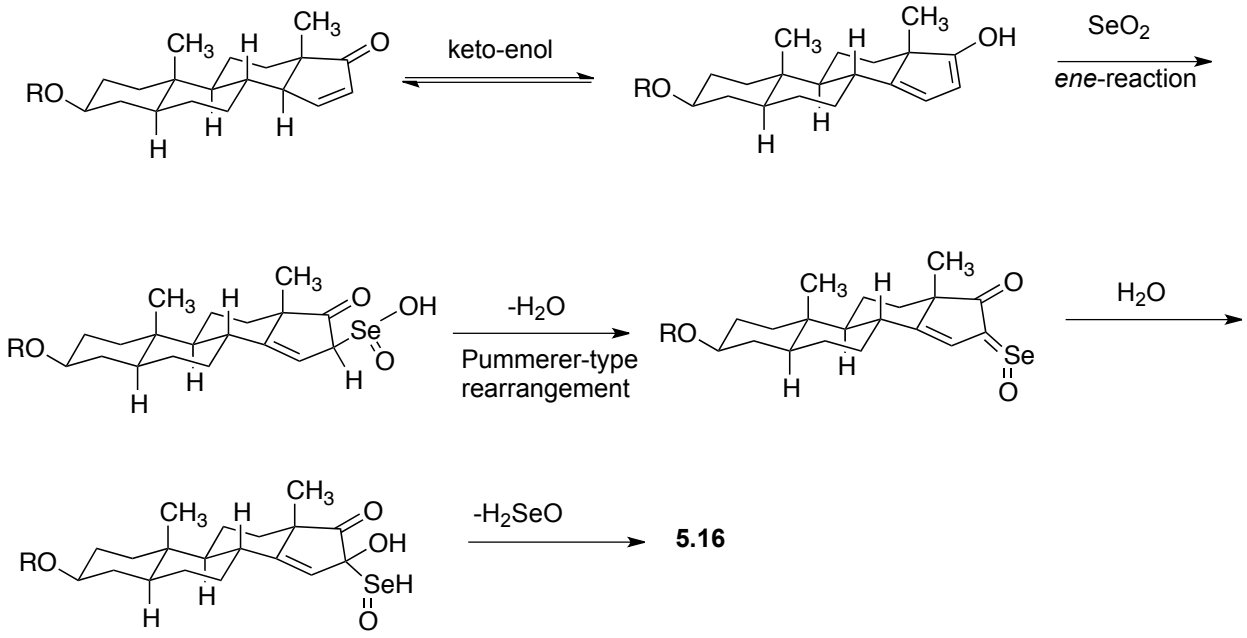

Figure 5-14 Proposed mechanism of reaction for the formation of **5.16**

5.4. Conclusions and future work

This work has shown that preparation of structurally diversified cardiac glycoside analogs is potentially viable using a semi-synthetic approach from readily commercially available steroids. Some of the key transformations investigated include a microwave-promoted allylic oxidation using SeO_2 (Riley oxidation) and microwave-promoted Miyaura-Suzuki cross-coupling. Although the synthesis of the desired analogs has not been completed to date, the findings from this work will help future attempts to achieve our initial goals. In the near future, the synthetic scheme depicted in Figure 5-4 will be further pursued in order to prepare the desired analogs with the goal to evaluate them against breast cancer cell lines Hs578T.

5.5. Experimental data

5.5.1. Materials and methods

All starting materials, reagents and solvents are commercially available and were used without further purification. Flash column chromatography was carried out on Teledyne Isco Automatic CombiFlash system (San Diego, CA) using Gold silica gel pre-packed columns, TLC was conducted on silica gel 250 micron, F_{254} plates. ^{1}H NMR spectra were recorded with a 500 MHz NMR instrument. Chemical shifts are reported in ppm $CHCl_3$ as an internal standard ($CHCl_3$: 7.26 ppm). Data are reported as follows: chemical shift, multiplicity (s = singlet, d = doublet, t = triplet, q = quartet, b = broad, m = multiplet), integration and coupling constants (Hz). ^{13}C NMR spectra were recorded with a 126 MHz NMR spectrometer with complete proton decoupling. Chemical shifts are reported in ppm with the solvent as internal standard ($CHCl_3$: 77.2 ppm).

5.5.2. Experimental procedures

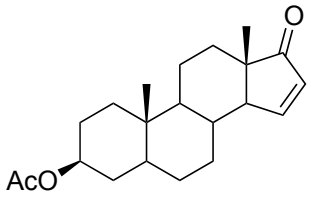

5.2

3-*O*-acetyl-3β-dihydroxy-5α-androst-15-en-17-one (5.2). To a solution of *trans*-androsterone (200 mg, 0.69 mmol) DMAP (8 mg, 10 mol%) acetic anhydride (0.16 mL, 1.38 mmol, 2 eq.) were added and the reaction mixture was left under stirring conditions for 16h at RT. After the starting material was consumed (shown by TLC), the reaction was quenched with $NaHCO_3$ (sat), extracted twice with CH_2Cl_2, and dried over Na_2SO_4. The acetyl-*trans*-androsterone was obtained

quantitatively (230 mg) as a white powder after organic solvent removal and it was used without further purification in the next step: mp 105.0-105.6°C; HRMS *m/z* 687.4591 [2M+Na] (687.4601 calc. for $C_{42}H_{64}NaO_6$); ^{1}H NMR (500 MHz, $CDCl_3$) δ 7.49 (dd, *J* = 1.1, 6.0, 1H), 6.00 (dd, *J* = 3.2, 6.0, 1H), 4.72 – 4.62 (m, 1H), 2.30 – 2.20 (m, 1H), 2.00 (s, 3H), 1.95 (ddd, *J* = 3.6, 6.6, 12.7, 1H), 1.88 – 1.65 (m, 3H), 1.65 – 1.55 (m, 2H), 1.55 – 1.42 (m, 1H), 1.42 – 1.26 (m, 1H), 1.21 (m, 1H), 1.13 – 1.04 (m, 1H), 1.03 (s, 3H), 0.87 (s, 3H), 0.84 – 0.74 (m, 1H); ^{13}C NMR (126 MHz, $CDCl_3$) δ 213.30, 170.71, 158.62, 131.72, 73.40, 56.87, 55.57, 51.13, 44.88, 36.44, 35.89, 33.90, 32.36, 30.70, 29.12, 28.11, 27.37, 21.47, 20.75, 20.19, 12.27.

A solution of the previously obtained acetyl-*trans*-androsterone (230 mg, 0.69 mmol) in dry THF (3 mL) was cooled down to -78°C, then KHMDS 0.5 M in toluene (1.5 mL, 0.75 mmol, 1.1 eq) was added dropwise and the resulting mixture stirred for 1h. Next, Et_3N (0.2 mL, 1.38 mmol, 2.0 eq) and TMSCl (0.15 mL, 0.83 mmol, 1.2 eq) were added to the flask dropwise and stirred for 30 min. The reaction mixture was then warmed to RT and stirred for an additional 25 min and quenched with $NaHCO_3$ (sat). The aqueous layer was extracted twice with EtOAc. The organic layer was washed with water, brine, dried over Na_2SO_4 and concentrated under vacuum. The crude TMS-enol ether was then dissolved in CH_2Cl_2 (3 mL) and CH_3CN (1 mL). Next, $Pd(OAc)_2$ (150 mg, 0.69 mmol, 1.0 eq) was added in one portion and the reaction mixture was stirred for 6h at 30°C (water bath). Finally, the reaction mixture was filtered through celite and concentrated under vacuum. The resulting dark semi-solid was purified by flash column chromatography (5-15% EtOAc/Hexanes) to give 123 mg (54%, three steps) of **5.2** as a white solid: mp 96.1-98.2 °C; HRMS *m/z* 683.4276 [2M+Na] (683.4288 calc. for $C_{42}H_{60}NaO_6$); ^{1}H NMR (500 MHz, $CDCl_3$) δ 7.49 (dd, *J* = 1.1, 6.0, 1H), 6.00 (dd, *J* = 3.2, 6.0, 1H), 4.72 – 4.62 (m, 1H), 2.30 – 2.20 (m, 1H), 2.00 (s, 3H), 1.95 (ddd, *J* = 3.6, 6.6, 12.7, 1H), 1.88 – 1.65 (m,

5H), 1.65 – 1.55 (m, 2H), 1.55 – 1.42 (m, 3H), 1.42 – 1.26 (m, 3H), 1.21 (ddd, *J* = 8.7, 12.0, 12.8, 1H), 1.13 – 1.04 (m, 1H), 1.03 (s, 3H), 0.87 (s, 3H), 0.84 – 0.74 (m, 1H); ^{13}C NMR (126 MHz, $CDCl_3$) δ 213.30, 170.71, 158.62, 131.72, 73.40, 56.87, 55.57, 51.13, 44.88, 36.44, 35.89, 33.90, 32.36, 30.70, 29.12, 28.11, 27.37, 21.47, 20.75, 20.19, 12.27.

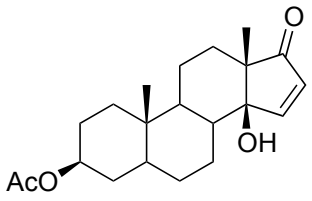

5.3

3-*O*-acety-3β,14β-dihydroxy-5α-androst-15-en-17-one (5.3). Compound **5.2** (500 mg, 1.5 mmol) was dissolved in dioxane:water 1:1 v/v (10 mL) in a 10-20 mL microwave tube. Selenium oxide (200 mg, 1.8 mmol, 1.2 eq.) was added and the microwave tube sealed. The reaction mixture was then heated for 30 minutes in a microwave reactor to 110 °C. Then, the mixture was filtered over celite and concentrated under vacuum. The resulting orange oil was re-dissolved in acetone and treated with activated charcoal (50 mg) during 5 min, then filtered and concentrated under vacuum to give a pale-yellow oil which was purified by column chromatography (20-30% EtOAc/Hexanes) to give 235 mg (56%) of **5.3** as a white powder: mp 143.3-144.9 °C; HRMS *m/z* 715.4180 [2M+Na] (715.4186 calc. for $C_{42}H_{60}NaO_8$); ^{1}H NMR (500 MHz, $CDCl_3$) δ 7.48 (d, *J* = 5.9, 1H), 6.13 (d, *J* = 5.9, 1H), 4.65 – 4.53 (m, 1H), 2.10-2.16 (m, 1H), 1.94 (s, 3H), 1.83 – 1.75 (m, 1H), 1.75 – 1.67 (m, 1H), 1.55-1.65 (m, 3H), 1.54 – 1.13 (m, 8H), 1.12 – 1.04 (m, 1H), 1.02 (s, 3H), 0.89 – 0.80 (m, 2H), 0.74 (s, 3H), 0.68 (ddd, *J* = 7.7, 12.2, 12.6, 1H); ^{13}C NMR (126 MHz, $CDCl_3$) δ 213.23, 170.91, 161.24, 133.15, 83.34, 73.54, 52.20, 46.49, 44.37, 40.79, 36.75, 36.46, 33.94, 33.24, 28.24, 27.28, 27.11, 21.66, 20.16, 17.68, 11.72.

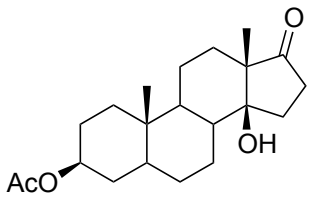

5.4

3-*O*-acety-3β,14β-dihydroxy-5α-androst-17-one (5.4). Compound **5.3** (100 mg, 0.29 mmol) was dissolved in ethanol (10 mL) and 10% Pd/C (10 mg) was added. The mixture was purged with H_2 balloon and left to stir for 3h, then it was filtered over celite and concentrated under vacuum to give 100 mg (99%) of **5.4** as a white powder: mp 145.1-146.2°C; HRMS *m*/*z*: 719.4486 [2M+Na] (719.4499 calc. for $C_{42}H_{64}NaO_8$); ^{1}H NMR (500 MHz, $CDCl_3$) δ 4.74 – 4.65 (m, 1H), 2.43 – 2.37 (m, 2H), 2.14 (m, 1H), 2.02 (s, 3H), 2.01 – 1.94 (m, 1H), 1.88 – 1.73 (m, 3H), 1.69 – 1.45 (m, 4H), 1.45 – 1.33 (m, 3H), 1.33 – 1.13 (m, 6H), 1.05 (s, 3H), 1.03 – 0.93 (m, 2H), 0.83 (s, 3H); ^{13}C NMR (126 MHz, $CDCl_3$) δ 221.34, 170.86, 82.63, 73.48, 53.66, 50.01, 44.33, 41.42, 36.95, 35.87, 33.89, 33.12, 31.95, 28.22, 27.48, 27.43, 25.64, 21.60, 19.95, 12.94, 12.23.

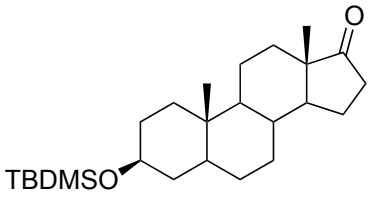

5.9

3-*O*-terbutyldimethylsylil-3β-dihydroxy-5α-androst-17-one (5.9). A solution of *trans*-androstane (200 mg, 0.69 mmol), TBDMSCl (125 mg, 0.83 mmol, 1.2 eq), and imidazol (140 mg, 2.07 mmol, 3 eq) in dry DMF (4 mL) was stirred for 3h under Ar. When the starting material

was consumed (TLC analysis, 9:1 Hex/EtOAc), the reaction was quenched adding 2 mL of water and extracted 3 times with CH_2Cl_2. The organic layer was washed with water, $Na_2S_2O_3$ (sat.), brine, and dried over Na_2SO_4. The resulting white solid was purified by column chromatography (2% EtOAc/Hexanes) to give 260 mg (93%) of **5.9** as a white powder: mp 161.7-162.2°C; HRMS *m/z* 831.6156 [2M+Na] (831.6119 calc. for $C_{50}H_{88}NaO_4Si_2$); ^{1}H NMR (500 MHz, $CDCl_3$) δ 3.55 (ddd, J = 15.6, 10.8, 4.7 Hz, 1H), 2.43 (dd, J = 19.3, 8.8 Hz, 1H), 2.11 – 2.01 (m, 1H), 1.96 – 1.89 (m, 1H), 1.82 – 1.75 (m, 2H), 1.72 – 1.61 (m, 4H), 1.55 – 1.36 (m, 4H), 1.29 (m, 6H), 1.13 – 1.04 (m, 1H), 0.94 (m, 2H), 0.88 (s, 9H), 0.85 (s, 3H), 0.82 (s, 3H), 0.05 (s, 6H). ^{13}C NMR (126 MHz, $CDCl_3$) δ 224.23, 72.02, 54.55, 51.47, 47.85, 45.03, 38.61, 37.14, 35.89, 35.69, 35.07, 31.89, 31.59, 30.98, 28.47, 25.96, 21.80, 20.50, 18.29, 13.83, 12.37, -4.55, -4.56.

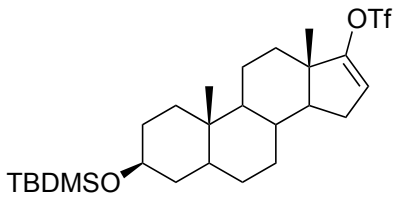

5.10

3-*O*-terbutyldimethylsylil-3β-hydroxy-5α-androst-15-en-17-yl trifluromethanesulfonate (5.10). A solution of **5.9** (500 mg, 1.24 mmol) and $PhNTf_2$ (530.2 mg, 1.48 mmol, 1.2 eq) in dried THF (20 mL) was cooled down to -78°C and KHMDS 0.5 M in toluene (3 mL, 1.48 mmol, 1.2 eq) was added dropwise via syringe under Ar. The resulting mixture was stirred at the same temperature for 2h. Then, the reaction was quenched by adding NH_4Cl (sat.) and extracted twice with CH_2Cl_2. The organic layer was washed with brine and dried over Na_2SO_4. The solvent was removed at reduced pressure and the residue was purified by column chromatography (2% EtOAc/Hexanes) to give 540 mg (82%) of **5.10** as a white powder: mp 106.5-107.1 °C; HRMS

m/z 1095.5095 [2M+Na] (1095.5105 calc. for $C_{52}H_{86}F_6O_8S_2Si_2$) ^{1}H NMR (500 MHz, $CDCl_3$ δ 5.55 (dd, *J* = 3.2, 1.7 Hz, 1H), 3.61 – 3.45 (m, 1H), 2.25 – 2.14 (m, 1H), 2.02 – 1.89 (m, 1H), 1.77 – 1.57 (m, 6H), 1.57 – 1.49 (m, 3H), 1.48 – 1.22 (m, 6H), 1.14 – 1.00 (m, 2H), 0.95 (s, 3H), 0.88 (s, 9H), 0.83 (s, 3H), 0.78 – 0.68 (m, 1H), 0.05 (s, 6H); ^{13}C NMR (126 MHz, $CDCl_3$) δ 159.52, 118.63 (q, CF_3, *J* = 320 Hz), 114.63, 72.12, 54.98, 54.41, 45.35, 45.01, 38.74, 37.04, 35.89, 33.62, 32.86, 32.00, 31.04, 28.69, 28.56, 26.09, 20.67, 18.42, 15.44, 12.44, -4.42, -4.43.

General procedure A: Suzuki-Miyaura coupling under microwave irradiation. A solution of **5.10** (50 mg, 0.18 mmol), the appropriate boronic acid (0.28 mmol, 1.5 eq), $Pd(PPh_3)_4$ (0.02 mmol, 10 mol%) and Na_2CO_3 2M (0.54 mmol , 3 eq) in dry dioxane (5 mL) were placed in a sealed microwave tube. The reaction mixture was heated at 170°C in a microwave reactor for 30 minutes. The resulting dark solution was filtered through celite and the solvent removed under reduced pressure and further purified using column chromatography.

General procedure B. Deprotection of TMS or TBDMS groups using TBAF. The substrate (1 eq) was dissolved in dry THF (2 mL) under Ar. TBAF 1 M in THF (3 eq) was added via syringe to the reaction mixture and left for 48h under stirring conditions. The reaction mixture was quenched by the addition of 1 mL of water and extracted twice with EtOAc. The organic layer was washed with water and brine, dried over Na_2SO_4, and concentrated under reduced pressure. The resulting residue was purified by column chromatography.

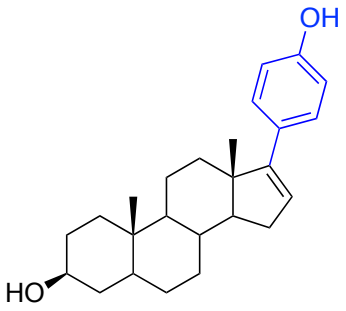

5.11a

3β-hydroxy-17-(4-hydroxyphenyl)-5α-androst-15-ene (5.11a). Compound **5.11a** was prepared following the general procedure A. The crude residue was purified by column chromatography (5% EtOAc/Hexanes) to give 26 mg (30%), which were submitted to general procedure B. The resulting product was purified using column chromatography (15-25% EtOAc/Hexanes) to afford **5.11a** as white powder; mp 148.1-150.0 °C; HRMS *m/z* 755.5015 [2M+Na] (755.5015 calc. for $C_{50}H_{68}NaO_4$); ^{1}H NMR (500 MHz, $CDCl_3$) δ 7.24 – 7.23 (m, 2H), 6.75 – 6.73 (m, 2H), 5.80 – 5.75 (m, 1H), 3.50 – 3.40 (m, 1H), 2.22 – 2.12 (m, 2H), 1.98 (m, 2H), 1.81 – 1.54 (m, 6H), 1.54 – 1.17 (m, 9H), 1.12-1.02 (m, 2H), 0.98 (s, 3H), 0.84 (s, 3H); ^{13}C NMR (126 MHz, $CDCl_3$) δ 154.61, 154.44, 128.11, 125.74, 115.10, 71.38, 57.75, 54.94, 47.49, 45.42, 38.83, 37.17, 35.86, 35.76, 34.23, 32.12, 32.07, 31.56, 28.88, 26.12, 26.10, 18.46, 16.83, 12.53.

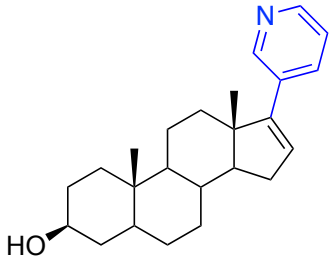

5.11b

3β-hydroxy-17-(3-pyridiyl)-5α-androst-15-ene (5.11b). Compound **5.11b** was prepared following the general procedure A. The crude residue was purified by column chromatography (5-10% EtOAc/Hexanes) to give 30 mg (36%), which were submitted to general procedure B. The resulting product was purified using column chromatography (15-25% EtOAc/Hexanes) to afford **5.11a** as white powder: mp 154.1-155.5 °C; HRMS *m/z* 352.2676 [M+H] (352.2640 calc. for $C_{24}H_{34}NO$); ^{1}H NMR (500 MHz, $CDCl_3$) δ 8.67 (d, *J* = 1.3 Hz, 1H), 8.53 (d, *J* = 4.9 Hz, 1H), 8.19 (d, *J* = 8.1 Hz, 1H), 7.70 (dd, *J* = 8.0, 5.5 Hz, 1H), 6.25 (dd, *J* = 3.3, 1.8 Hz, 1H), 3.66 – 3.54 (m, 1H), 2.37 – 2.28 (m, 1H), 2.14 – 2.03 (m, 1H), 2.02 – 1.96 (m, 1H), 1.88 – 1.78 (m, 1H), 1.78 – 1.54 (m, 6H), 1.49 – 1.38 (m, 3H), 1.38 – 1.22 (m, 4H), 1.19 – 1.10 (m, 1H), 1.03 (s, 3H), 1.01 – 0.95 (m, 1H), 0.87 (s, 3H), 0.83 – 0.72 (m, 2H); ^{13}C NMR (126 MHz, $CDCl_3$) δ 148.92, 140.56, 139.99, 139.83, 136.66, 134.85, 125.83, 71.32, 57.56, 54.52, 47.82, 45.14, 38.22, 36.90, 35.81, 35.26, 34.01, 32.25, 31.87, 31.57, 28.62, 21.19, 16.86, 12.44.

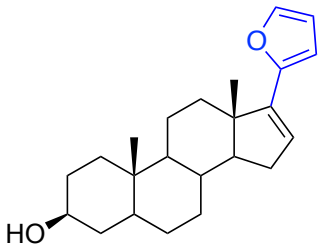

5.11c

3β-hydroxy-17-(2-furanyl)-5α-androst-15-ene (5.11c). Compound **5.11c** was prepared following the general procedure A. The crude residue was purified by column chromatography (5-10% EtOAc/Hexanes) to give 38 mg (47%), which were submitted to general procedure B. The resulting product was purified using column chromatography (15-25% EtOAc/Hexanes) to afford **5.11c** as a white powder: mp 137.9-138.6 °C; HRMS *m/z* 703.4712 [2M+Na] (703.4702

calc. for $C_{46}H_{64}NaO_4$); ^{1}H NMR (500 MHz, $CDCl_3$) δ 7.35 (dd, *J* = 2.7, 2.6 Hz, 1H), 6.38 – 6.33 (m, 1H), 6.28 – 6.24 (m, 1H), 6.08 – 6.02 (m, 1H), 3.67 – 3.54 (m, 1H), 2.28 – 2.19 (m, 1H), 2.18 – 2.11 (m, 1H), 2.01 – 1.92 (m, 1H), 1.86 – 1.77 (m, 1H), 1.72 (m, 2H), 1.68 – 1.37 (m, 9H), 1.35 – 1.23 (m, 2H), 1.21 – 1.10 (m, 2H), 1.08 – 0.97 (m, 1H), 0.95 (s, 3H), 0.86 (s, 3H), 0.82 – 0.72 (m, 1H); ^{13}C NMR (126 MHz, $CDCl_3$) δ 151.70, 144.59, 141.36, 125.04, 110.98, 105.23, 71.46, 56.97, 54.86, 46.71, 45.18, 38.34, 36.94, 35.83, 35.66, 34.01, 32.05, 31.64, 31.59, 28.78, 21.44, 16.69, 12.45.

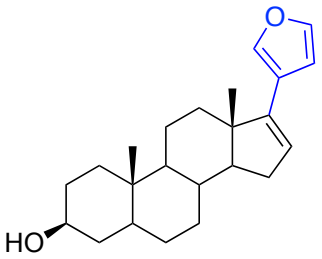

5.11d

3β-hydroxy-17-(3-furanyl)-5α-androst-15-ene (5.11d). Compound **5.11d** was prepared following the general procedure A. The crude residue was purified by column chromatography (5-10% EtOAc/Hexanes) to give 35 mg (45%), which were submitted to general procedure B. The resulting product was purified using column chromatography (15-25% EtOAc/Hexanes) to afford **5.11d** as a white powder: mp 119.0-120.1 °C; HRMS *m/z* 703.4716 [2M+Na] (703.4702 calc. for $C_{46}H_{64}NaO_4$); ^{1}H NMR (500 MHz, $CDCl_3$) δ 7.46 (s, 1H), 7.36 – 7.34 (m, 1H), 6.47 (dd, *J* = 1.8, 0.8 Hz, 1H), 5.81 (dd, *J* = 3.2, 1.9 Hz, 1H), 3.65 – 3.55 (m, 1H), 2.22 – 2.14 (m, 1H), 2.02 – 1.86 (m, 1H), 1.81 (dd, *J* = 12.5, 1.8 Hz, 1H), 1.73-1.56 (m, 2H), 1.69 – 1.57 (m, 4H), 1.53 – 1.38 (m, 4H), 1.37 – 1.20 (m, 4H), 1.19 – 1.08 (m, 1H), 1.07 – 0.96 (m, 1H), 0.92 (s, 3H), 0.86 (s, 3H), 0.85 – 0.83 (m, 1H); ^{13}C NMR (126 MHz, $CDCl_3$) δ 146.19, 142.73, 137.60,

125.28, 121.49, 109.48, 71.46, 57.17, 54.89, 46.70, 45.18, 38.35, 36.95, 35.73, 35.68, 34.10, 32.03, 31.65, 31.53, 28.79, 21.45, 16.44, 12.46.

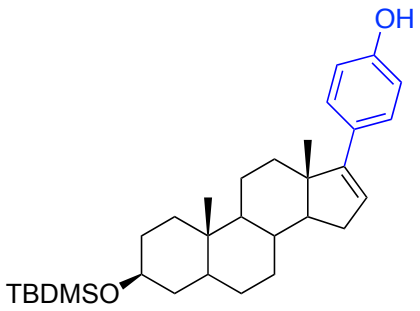

5.12a

3-*O*-terbutyldimethylsylil-3β-hydroxy-17-(4-hydroxyphenyl)-5α-androst-15-ene (5.12a). Compound **5.12a** was prepared following the general procedure A. The crude residue was purified by column chromatography (5% EtOAc/Hexanes) to give 26 mg (30%) as white powder; mp 163.1-164.8 °C; HRMS *m/z* 983.6733 [2M+Na] (983.6745 calc. for $C_{62}H_{96}O_4Si_2$) ^{1}H NMR (500 MHz, $CDCl_3$) δ 7.26 – 7.22 (m, 2H), 6.78 – 6.74 (m, 2H), 5.80 – 5.75 (m, 1H), 3.60 – 3.50 (m, 1H), 2.22 – 2.12 (m, 2H), 1.98 (m, 2H), 1.81 – 1.54 (m, 6H), 1.54 – 1.17 (m, 9H), 1.12-1.02 (m, 2H), 0.98 (s, 3H), 0.89 (s, 9H), 0.84 (s, 3H), 0.05 (s, 6H); ^{13}C NMR (126 MHz, $CDCl_3$) δ 154.61, 154.44, 128.11, 125.74, 115.10, 72.38, 57.75, 54.94, 47.49, 45.42, 38.83, 37.17, 35.86, 35.76, 34.23, 32.12, 32.07, 31.56, 28.88, 26.12, 26.10, 21.40, 18.46, 16.83, 12.53, -4.41.

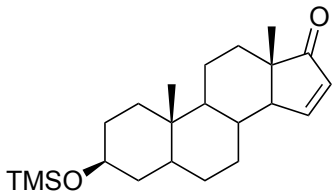

5.13

3-*O*-trimethylsylil-3β-dihydroxy-5α-androst-15-en-17-one (5.13). To a solution of DIPA (0.29 mL, 2.1 mmol, 3 eq) in THF (3 mL) at -78°C, was added a solution of BuLi 1.6 M in hexanes (1.32 mL, 2.1 mmol, 3 eq) dropwise via syringe under Ar and the resulting mixture was stirred for 15 min. A solution of *trans*-androstane (210 mg, 0.7 mmol) in THF (1.5 mL) was added dropwise over 30 min period, and the reaction mixture was stirred at -78°C for an additional 15 min. Then, Et_3N (0.39 mL, 2.8 mmol, 4 eq) and TMSCl (0.27 mL, 1.9 mmol, 2.7 eq) were added dropwise via syringe. The mixture was warmed to RT, stirred for additional 25 min, quenched with $NaHCO_3$ (sat.) and extracted twice with EtOAc. The organic layer was washed with water and brine, dried over Na_2SO_4, and concentrated under reduced pressure. The crude enol ether was then dissolved in CH_2Cl_2 (3 mL) and CH_3CN (1 mL) under Ar. Next $Pd(OAc)_2$ (160 mg, 0.7 mmol, 1 eq) was added in one portion and the mixture was stirred for 6 h at 30°C. The resulting dark solution was filtered through celite and concentrated under reduced pressure. The dark semi-solid was purified by column chromatography (5-15% EtOAc/Hexanes) to give 170 mg of **5.13** (68%, three steps) as a white powder; mp 153.2-154 °C; HRMS *m/z* 743.4836 [2M+Na] (743.4867 calc. for $C_{44}H_{72}NaO_4Si_2$). ^{1}H NMR (500 MHz, $CDCl_3$) δ 7.44 (dd, *J* = 1.1, 6.0, 1H), 6.02 (dd, *J* = 3.2, 6.0, 1H), 3.55 (ddd, *J* = 15.6, 10.8, 4.7 Hz, 1H), 2.43 (dd, *J* = 19.3, 8.8 Hz, 1H), 2.11 – 2.01 (m, 1H), 1.96 – 1.89 (m, 1H), 1.72 – 1.61 (m, 2H), 1.55 – 1.36 (m, 2H), 1.29 (m, 4H), 1.13 – 1.04 (m, 1H), 0.88 (s, 9H), 0.85 (s, 3H), 0.82 (s, 3H), 0.05 (s, 6H). ^{13}C NMR (126 MHz, $CDCl_3$) δ 213.30, 158.56, 131.33, 72.02, 54.55, 51.47, 47.85, 45.03, 38.61, 37.14, 35.89, 35.69, 35.07, 30.98, 28.47, 25.96, 20.50, 18.29, 12.37, 0.14.

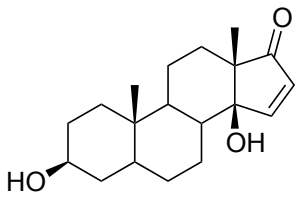

5.14a

3β,14β-dihydroxy-5α-androst-15-en-17-one (5.14a). Compound **5.13** (180 mg, 0.5 mmol) was dissolved in dioxane (4 mL) and water (1 mL). Then, SeO_2 (590 mg, 6.0 mmol, 1.2 eq) was added and the RM was refluxed for 6h under Ar. The reaction mixture was then left to cool to RT and filtered over celite and concentrated under reduced pressure to a third of the original volume and extracted twice with CH_2Cl_2. Organic layers were washed with water, brine, dried over Na_2SO_4, and concentrated under reduced pressure. The resulting orange oil was purified by column chromatography (40-60% EtOAc/Hexanes) to give 60.4 mg of **5.14a** (40%) as a white powder: mp 167.3-168.9 °C; HRMS *m/z* 631.3886 [2M+Na] (631.3975 calc. for $C_{38}H_{56}NaO_6$) ^{1}H NMR (500 MHz, CDCl3) δ 7.61 – 7.50 (m, 1H), 6.21 (dd, *J* = 15.5, 5.1 Hz, 1H), 3.66 – 3.51 (m, 1H), 2.26 – 2.14 (m, 1H), 1.92 – 1.83 (m, 1H), 1.83 – 1.71 (m, 2H), 1.70 – 1.64 (m, 1H), 1.64 – 1.50 (m, 7H), 1.45 – 1.22 (m, 10H), 1.09 (d, *J* = 6.1 Hz, 3H), 1.07 – 1.03 (m, 1H), 0.96 – 0.83 (m, 3H), 0.79 (s, 2H), 0.77 – 0.69 (m, 1H); ^{13}C NMR (126 MHz, CDCl3) δ 213.24, 161.25, 133.00, 83.31, 71.23, 52.16, 46.46, 44.49, 40.80, 37.99, 36.70, 36.63, 33.14, 31.24, 28.28, 27.11, 20.14, 17.68, 11.76. In addition, 315 mg of unprotected starting material **5.14b** (22%) were recovered from the reaction mixture.

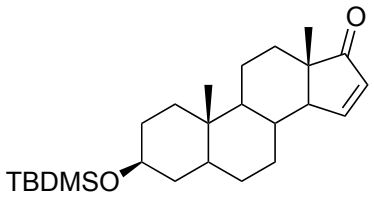

5.15

3-*O*-trimethylsylil-3β-dihydroxy-5α-androst-15-en-17-one (5.15). To a solution of DIPA (0.16mL, 1.5 mmol, 1.5 eq) in THF (3 mL) at -78°C, was added a solution of BuLi 1.6 M in hexanes (0.94 mL, 1.5 mmol, 3 eq) dropwise via syringe under Ar and the resulting mixture was stirred for 15 min. A solution of **5.9** (280 mg, 0.7 mmol) in THF (1.5 mL) was added dropwise over 30 min period, and the reaction mixture was stirred at -78°C an additional 15 min. Next, Et_3N (0.19 mL, 1.4 mmol, 2 eq) and TMSCl (0.14 mL, 1.0 mmol, 1.5 eq) were added dropwise via syringe. The mixture was warmed to RT, stirred for 25 min more, quenched with $NaHCO_3$ (sat.) and extracted twice with EtOAc. The organic layer was washed with water and brine, dried over Na_2SO_4, and concentrated under reduced pressure. The crude enol ether was then dissolved in CH_2Cl_2 (3 mL) and CH_3CN (1 mL) under Ar. Then, $Pd(OAc)_2$ (160 mg, 0.7 mmol, 1 eq) was added in one portion and the mixture stirred for 6 h at 30°C. The resulting dark solution was filtered through celite and concentrated under reduced pressure. The dark semi-solid was purified by column chromatography (5-15% EtOAc/Hexanes) to give 170 mg of **5.15** (60%, three steps) as a white powder; mp 125.0-126.3 °C; HRMS *m/z* 831.6156 [2M+Na] (831.6119 calc. for $C_{50}H_{88}NaO_4Si_2$. ^{1}H NMR (500 MHz, $CDCl_3$) δ 7.45 (dd, *J* = 1.1, 5.9, 1H), 6.01 (dd, *J* = 3.2, 5.9, 1H), 3.54 (ddd, *J* = 15.6, 10.8, 4.7 Hz, 1H) δ 3.55 (ddd, J = 15.6, 10.8, 4.7 Hz, 1H), 2.43 (dd, J = 19.3, 8.8 Hz, 1H), 2.11 – 2.01 (m, 1H), 1.96 – 1.89 (m, 1H), 1.82 – 1.75 (m, 2H), 1.72 – 1.61 (m, 3H), 1.55 – 1.36 (m, 4H), 1.29 (m, 4H), 1.13 – 1.04 (m, 1H), 0.94 (m, 3H), 0.88 (s, 9H), 0.85 (s,

3H), 0.82 (s, 3H), 0.05 (s, 6H). ^{13}C NMR (126 MHz, $CDCl_3$) δ 213.30, 158.56, 131.33, 72.02, 54.55, 51.47, 47.85, 45.03, 38.61, 37.14, 35.89, 35.69, 35.07, 31.59, 25.96, 21.80, 20.50, 18.29, 13.83, 12.37, -4.55, -4.56.

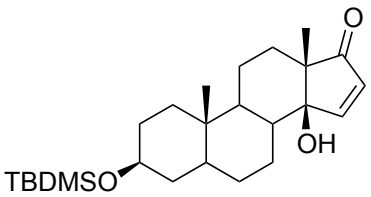

5.15a

3-*O*-terbutyldimethylsylil-3β,14β-dihydroxy-5α-androst-15-en-17-one (5.15a). Compound **5.15** (180 mg, 0.5 mmol) was dissolved in dioxane (4 mL) and water (1 mL). Next, SeO_2 (59 mg, 0.60 mmol, 1.2 eq) was added and the RM was refluxed for 6h under Ar. The reaction mixture was then left to cool to RT and filtered over celite and concentrated under reduced pressure to a third of the original volume and extracted twice with CH_2Cl_2. Organic layers were washed with water, brine, dried over Na_2SO_4, and concentrated under reduced pressure. The resulting orange oil was purified by column chromatography (40-60% EtOAc/Hexanes) to give 60.4 mg of **5.14a** (40%) as a white powder: mp 128.1-129.3 °C; HRMS *m/z* 831.6156 [2M+Na] (831.6119 calc. for $C_{50}H_{88}NaO_4Si_2$. ^{1}H NMR (500 MHz, $CDCl_3$) δ 3.55 (ddd, J = 15.6, 10.8, 4.7 Hz, 1H), 2.43 (dd, J = 19.3, 8.8 Hz, 1H), 2.11 – 2.01 (m, 1H), 1.96 – 1.89 (m, 1H), 1.82 – 1.75 (m, 2H), 1.72 – 1.61 (m, 3H), 1.56 (s, 4H), 1.55 – 1.36 (m, 4H), 1.29 (dddd, J = 26.6, 21.9, 13.3, 2.7 Hz, 9H), 1.13 – 1.04 (m, 1H), 0.94 (ddd, J = 23.5, 8.2, 1.9 Hz, 3H), 0.88 (s, 6H), 0.85 (s, 3H), 0.82 (s, 2H), 0.05 (s, 6H). ^{13}C NMR (126 MHz, $CDCl_3$) δ 72.02, 54.55, 51.47, 47.85, 45.03, 38.61, 37.14, 35.89, 35.69, 35.07, 31.89, 31.59, 30.98, 28.47, 25.96, 21.80, 20.50, 18.29, 13.83, 12.37, -4.55, -4.56.

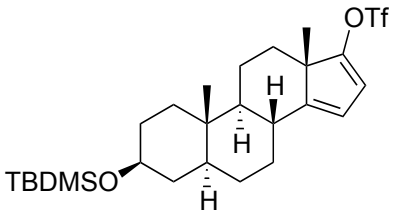

5.15a'

3-*O*-acetyl-3β-hydroxy-5α-androst-14,16-dien-17-yl trifluromethanesulfonate (5.15a'). A solution of **5.15** (50 mg, 0.12 mmol) in dried THF (2 mL) was cooled down to -78°C and KHMDS 0.5 M in toluene (0.5 mL, 25 mmol, 2.1 eq) was added dropwise via syringe under Ar and the mixture was left to stir for 1 h. Then, a solution $PhNTf_2$ (51.4 mg, 0.14 mmol, 1.2 eq) in THF (1 mL) was added dropwise and left to stir at the same temperature for 2 h. Next, the reaction was quenched by adding NH_4Cl (sat.) and extracted twice with CH_2Cl_2. The organic layer was washed with brine and dried over Na_2SO_4. The solvent was removed at reduced pressure and the residue was purified by column chromatography (2% EtOAc/Hexanes) to give 38.5 mg (60%) of **5.15a** as a white powder: mp 108.5-109.1 °C; HRMS *m/z* 1091.4783 [2M+Na] (1091.4792 calc. for $C_{52}H_{82}F_6NaO_8S_2Si_2$); ^{1}H NMR (500 MHz, $CDCl_3$ δ 6.08 (dd, *J* = 10.2, 2.9 Hz, 1H), 5.73 (dd, *J* = 5.2, 2.9 Hz, 1H), 3.63 (ddd, *J* = 16.0, 11.1, 4.8 Hz, 1H), 2.19 (ddd, *J* = 11.1, 5.8, 1.9 Hz, 2H), 2.05 – 1.96 (m, 1H), 1.96 – 1.88 (m, 1H), 1.87 – 1.78 (m, 2H), 1.74 (ddd, *J* = 13.8, 8.7, 3.2 Hz, 1H), 1.70 – 1.57 (m, 3H), 1.51 – 1.29 (m, 8H), 1.12 (s, 3H), 0.91 (s, 5H), 0.86 (s, 2H), 0.71 – 0.62 (m, 1H), 0.10 (s, 3H); ^{13}C NMR (126 MHz, $CDCl_3$) δ 160.29, 156.11, 118.70 (CF_3, q, *J* = 319.4)114.99, 114.00, 71.56, 57.49, 50.72, 44.67, 37.85, 37.39, 36.12, 35.63, 34.60, 31.28, 28.90, 28.20, 25.84, 25.76, 20.77, 17.42, 12.48, -2.80, -3.48.

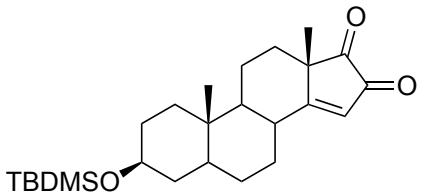

5.16

3-*O*-Trimethylsylil-14-*O*-trimethylsylil-3β,14β-dihydroxy-5α-androst-14-en-16,17-dione (5.16). In a microwave tube, compound **5.15** (20 mg, 0.05 mmol) and SeO_2 (16.6 mg, 0.15 mmol, 3 eq) were added followed by 1 mL of dry dioxane. The reaction mixture was heated in a microwave reaction at 110°C for 10 min. The product was filtered through celite and concentrated under reduced pressure. The resulting orange oil was purified by column chromatography (20-30% EtOAc/Hexanes) to give 12 mg of **5.16** (60%) as a white powder mp 165.9-166.6°C; HRMS *m/z* 855.5384 [2M+Na] (855.5391 calc. for $C_{50}H_{80}NaO_6Si_2$) ^{1}H NMR (500 MHz, CDCl3) δ 6.54 (d, *J* = 1.5 Hz, 1H), 3.61 – 3.50 (m, 1H), 2.58 (dd, *J* = 7.5, 5.4 Hz, 1H), 2.03 – 1.87 (m, 2H), 1.85 – 1.67 (m, 3H), 1.62 – 1.31 (m, 8H), 1.29 (s, 3H), 1.13 (ddd, *J* = 14.8, 6.1, 6.0 Hz, 1H), 1.13 (ddd, *J* = 14.8, 6.1, 6.0 Hz, 1H), 0.99 (ddd, *J* = 11.6, 5.7, 3.3 Hz, 1H), 0.92 (s, 3H), 0.88 (s, 9H), 0.05 (s, 6H); ^{13}C NMR (126 MHz, CDCl3) δ 203.41, 190.58, 188.20, 127.88, 71.73, 55.18, 46.44, 44.35, 38.42, 37.62, 36.98, 36.77, 33.33, 31.89, 28.54, 27.65, 26.05, 20.33, 19.74, 18.38, 12.29, -4.44, -4.45.

REFERENCES

1. Newman, D. J.; Cragg, G. M.; Kingston, D. G. I., Natural products as pharmaceuticals and sources for lead structures. In *The Practice of Medicinal Chemistry*, 3rd ed.; Wermuth, C. G., Ed. Elsevier: Burlignton, MA, 2008.

2. WHO Traditional Medicine. http://www.who.int/medicines/areas/traditional/en/ (accessed 09/21/2011).

3. Vargas-Murga, L.; Garcia-Alvarez, A.; Roman-Vinas, B.; Ngo, J.; Ribas-Barba, L.; van den Berg, S. J. P. L.; Williamson, G.; Serra-Majem, L. Plant food supplement (PFS) market structure in EC Member States, methods and techniques for the assessment of individual PFS intake. *Food Funct.* **2011,** *2*, 731-739.

4. Newman, D. J.; Cragg, G. M. Natural products as sources of new drugs over the last 25 years. *J. Nat. Prod.* **2007,** *70* (3), 461-477.

5. Cragg, G. M.; Grothaus, P. G.; Newman, D. J. Impact of natural products on developing new anti-cancer agents. *Chem. Rev.* **2009,** *109* (7), 3012-3043.

6. Lockermann, G. Friedrich Wilhelm Serturner, the discoverer of morphine. *J. Chem. Educ.* **1951,** *28* (5), 277.

7. Gulland, J. M.; Robinson, R. The morphine group. Part I. A discussion of the constitutional problem. *J. Chem. Soc.* **1923,** *123*, 980-998.

8. Gulland, J. M.; Robinson, R. The morphine group. Part II. Thebainone, thebainol, and dihydrothebainone. *J. Chem. Soc.* **1923,** *123*, 998-1011.

9. Gates, M.; Tschudi, G. The synthesis of morphine. *J. Am. Chem. Soc.* **1952,** *74* (4), 1109-1110.

10. Pert, C. B.; Pasterna.G; Snyder, S. H. Opiate agonists and antagonist discriminated by receptor binding in brain. *Science* **1973,** *182* (4119), 1359-1361.

11. Hughes, J.; Smith, T. W.; Kosterlitz, H. W.; Fothergill, L. A.; Morgan, B. A.; Morris, H. R. Identification of 2 related pentapeptides from brain with potent opiate agonisitic activity *Nature* **1975,** *258* (5536), 577-579.

12. Newman, D. J.; Cragg, G. M. Natural products as sources of new drugs over the 30 years from 1981 to 2010. *J. Nat. Prod.* **2012**.

13. Koehn, F. E.; Carter, G. T. The evolving role of natural products in drug discovery. *Nat. Rev. Drug. Discov.* **2005,** *4* (3), 206-220.

14. Carter, G. T. Natural products and pharma 2011: strategic changes spur new opportunities. *Nat. Prod. Rep.* **2011**.

15. Balandrin, M. F.; Kinghorn, A. D.; Farnsworth, N. R. plant-derived natural-products in drug discovery and development - an overview. *ACS Symp. Ser.* **1993,** *534*, 2-12.

16. Raskin, I.; Ribnicky, D. M.; Komarnytsky, S.; Ilic, N.; Poulev, A.; Borisjuk, N.; Brinker, A.; Moreno, D. A.; Ripoll, C.; Yakoby, N.; O'Neal, J. M.; Cornwell, T.; Pastor, I.; Fridlender, B. Plants and human health in the twenty-first century. *Trends Biotechnol.* **2002,** *20* (12), 522-531.

17. Sarker, S. D.; Latif, Z.; Gray, A. I., *Natural products isolation*. 2nd Ed. ed.; Humana Press Inc.: Totowa, NJ, 2006.

18. Kinghorn, A. D.; Pan, L.; Fletcher, J. N.; Chai, H. The relevance of higher plants in lead compound discovery programs. *J. Nat. Prod.* **2011,** *74* (6), 1539-1555.

19. Li, J. W. H.; Vederas, J. C. Drug discovery and natural products: end of an era or an endless frontier? *Science* **2009,** *325* (5937), 161-165.

20. Farnsworth, N. R., Ethnopharmacology and Drug Development. In *Ethnobotany and the Search for New Drugs*, Chadwick, D. J.; Marsh, J., Eds. 1994; Vol. 185, pp 42-51.

21. Kinghorn, A. D. Pharmacognosy in the 21st century. *J. Pharm. Pharmacol.* **2001,** *53* (2), 135-148.

22. Soejarto, D. D. Logistics and politics in plant drug discovery - the other end of the spectrum *ACS Symp. Ser.* **1993,** *534*, 96-111.

23. Barbault, R. 2010: A new beginning for biodiversity? *C. R. Biol.* **2011,** *334* (5-6), 483-488.

24. Spangenberg, J. H. Biodiversity pressure and the driving forces behind. *Ecol. Econ.* **2007,** *61* (1), 146-158.

25. Soejarto, D. D. Biodiversity prospecting and benefit-sharing: Perspectives from the Field. *J. Ethnopharmacol.* **1996,** *51* (1-3), 1-15.

26. Aalbersberg, W. G. L.; Mazan, R. D.; Soejarto, D. D.; Farnsworth, N. R.; Garcia, R.; McChesney, J. D.; Cragg, G. M.; Jato, J.; Sittenfeld, A. Legal issues in sharing the benefits of biodiversity prospecting - Discussion. *J. Ethnopharmacol.* **1996,** *51* (1-3), 102-105.

27. Wall, M. E.; Wani, M. C.; Brown, D. M.; Fullas, F.; Olwald, J. B.; Josephson, F. F.; Thornton, N. M.; Pezzuto, J. M.; Beecher, C. W. W.; Farnsworth, N. R.; Cordell, G. A.; Kinghorn, A. D. Effect of tannins on screening of plant extracts for enzyme inhibitory activity and techniques for their removal. *Phytomedicine* **1996,** *3* (3), 281-285.

28. Cordell, G. A.; Shin, Y. G. Finding the needle in the haystack. The dereplication of natural product extracts. *Pure Appl. Chem.* **1999,** *71* (6), 1089-1094.

29. Johansen, K. T.; Wubshet, S. G.; Nyberg, N. T.; Jaroszewski, J. W. From retrospective assessment to prospective decisions in natural product isolation: HPLC-SPE-NMR analysis of *Carthamus oxyacantha*. *J. Nat. Prod.* **2011,** *74* (11), 2454-2461.

30. Halabalaki, M.; Tchoumtchoua, J.; Skaltsounis, L. A. A structure-oriented approach for the accelerated and focused isolation of possible bioactive natural products based on UHPLC-HRMS/MS methods. *Planta Medica* **2011,** *77* (12), 1252-1252.

31. Berger, S.; Sicker, D., *Classics in spectroscopy: isolation and structure elucidation of natural products*. Wiley-VCH: Weinheim, 2009.

32. Dewick, P. M., *Medicinal natural products: a biosynthetic approach*. 3rd ed.; Wiley: West Sussex, 2009.

33. Samuelsson, G.; Bohlin, L., *Drugs of natural origin a treatise of pharmacognosy*. 6th ed.; Apotekarsocieteten: Stocholm, 2009.

34. Rahimtoola, S. H.; Tak, T. The use of digitalis in heart failure. *Curr. Probl. Cardiol.* **1996,** *21* (12), 787-853.

35. Newman, R. A.; Yang, P. Y.; Pawlus, A. D.; Block, K. I. Cardiac glycosides as novel cancer therapeutic agents. *Mol. Interventions* **2008,** *8* (1), 36-49.

36. Mijatovic, T.; Van Quaquebeke, E.; Delest, B.; Debeir, O.; Darro, F.; Kiss, R. Cardiotonic steroids on the road to anti-cancer therapy. *Biochim. Biophys. Acta* **2007,** *1776* (1), 32-57.

37. Pauli, G. F.; Friesen, J. B.; Godecke, T.; Farnsworth, N. R.; Glodny, B. Occurrence of progesterone and related animal steroids in two higher plant. *J. Nat. Prod.* **2010,** *73* (3), 338-345.

38. Schatzma, H. J. Role of Na+ and K+ in ouabain-inhibition of Na+ plus K+-activated membrane adenosine triphosphatase *Biochim. Biophys. Acta* **1965,** *94* (1), 89-96.

39. Suhail, M. Na+,K+-ATPase: ubiquitous multifunctional transmembrane protein and its relevance to various pathophysiological conditions. *J. Clin. Med. Res.* **2010,** *2* (1), 1-17.

40. Liu, L. J.; Abramowitz, J.; Askari, A.; Allen, J. C. Role of caveolae in ouabain-induced proliferation of cultured vascular smooth muscle cells of the synthetic phenotype. *Am. J. Physiol. Heart Circ.* **2004,** *287* (5), H2173-H2182.

41. Barwe, S. P.; Anilkumar, G.; Moon, S. Y.; Zheng, Y.; Whitelegge, J. P.; Rajasekaran, S. A.; Rajasekaran, A. K. Novel role for Na,K-ATPase in phosphatidylinositol 3-kinase signaling and suppression of cell motility. *Mol. Biol. Cell* **2005,** *16* (3), 1082-1094.

42. Wang, X. Q.; Xiao, A. Y.; Sheline, C.; Hyrc, K.; Yang, A. Z.; Goldberg, M. P.; Choi, D. W.; Yu, S. P. Apoptotic insults impair Na+, K+-ATPase activity as a mechanism of neuronal death mediated by concurrent ATP deficiency and oxidant stress. *J. Cell Sci.* **2003,** *116* (10), 2099-2110.

43. Bagrov, A. Y.; Shapiro, J. I.; Fedorova, O. V. Endogenous cardiotonic steroids: physiology, pharmacology, and novel therapeutic targets. *Pharmacol. Rev.* **2009,** *61* (1), 9-38.

44. Bagrov, A. Y.; Shapiro, J. I. Endogenous digitalis: pathophysiologic roles and therapeutic applications. *Nat. Clin. Pract. Neph.* **2008,** *4* (7), 378-392.

45. Prassas, I.; Diamandis, E. P. Novel therapeutic applications of cardiac glycosides. *Nat. Rev. Drug Discov.* **2008,** *7* (11), 926-935.

46. Morth, J. P.; Pedersen, B. P.; Toustrup-Jensen, M. S.; Sorensen, T. L. M.; Petersen, J.; Andersen, J. P.; Vilsen, B.; Nissen, P. Crystal structure of the sodium-potassium pump. *Nature* **2007,** *450* (7172), 1043-U6.

47. Lingrel, J. B., The physiological significance of the cardiotonic steroid/ouabain-binding site of the Na,K-ATPase. In *Annu. Rev. Physiol.*, 2010; Vol. 72, pp 395-412.

48. Jimenez, T.; McDermott, J. P.; Sanchez, G.; Blanco, G. Na,K-ATPase alpha 4 isoform is essential for sperm fertility. *Proc. Natl. Acad. Sci. U. S. A.* **2011,** *108* (2), 644-649.

49. Jimenez, T.; Sanchez, G.; McDermott, J. P.; Nguyen, A. N.; Kumar, T. R.; Blanco, G. Increased Expression of the Na,K-ATPase alpha4 Isoform Enhances Sperm Motility in Transgenic Mice. *Biol. Reprod.* **2011,** *84* (1), 153-161.

50. Pierre, S. V.; Xie, Z. J. The Na,K-ATPase receptor complex - Its organization and membership. *Cell Biochem. Biophys.* **2006,** *46* (3), 303-315.

51. Yatime, L.; Laursen, M.; Morth, J. P.; Esmann, M.; Nissen, P.; Fedosova, N. U. Structural insights into the high affinity binding of cardiotonic steroids to the Na(+),K(+)-ATPase. *J. Struct. Biol.* **2011,** *174* (2), 296-306.

52. Ball, W. J.; Tabet, M.; Paula, S. Meeting Abstract: Structure-activity relationship models for cardiac glycoside binding and inhibition of Na,K-ATPase activity. *FEBS J.* **2005,** *272*, 186.

53. Paula, S.; Tabet, M. R.; Ball, W. J. Interactions between cardiac glycosides and sodium/potassium-ATPase: Three-dimensional structure-activity relationship models for ligand binding to the E-2-P-i form of the enzyme versus activity inhibition. *Biochem.* **2005,** *44* (2), 498-510.

54. Cornelius, F.; Mahmmoud, Y. A. Interaction between cardiotonic steroids and Na,K-ATPase. Effects of pH and ouabain-induced changes in enzyme conformation. *Biochem.* **2009,** *48* (42), 10056-10065.

55. Shiratori, O. Growth inhibitory effect of cardiac glycosides and aglycones on neoplastic cells - *in vitro* and *in vivo* studies. *Gann* **1967,** *58* (6), 521-528.

56. Stenkvist, B.; Bengtsson, E.; Eriksson, O.; Holmquist, J.; Nordin, B.; Westmannaeser, S.; Eklund, G. cardiac-glycosides and breast-cancer. *Lancet* **1979,** *1* (8115), 563-563.

57. Stenkvist, B.; Bengtsson, E.; Eklund, G.; Eriksson, O.; Holmquist, J.; Nordin, B.; Westmannaeser, S. Evidence of a modifying influence of heart glucosides on the development of breast-cancer. *Anal. Quant. Cytol. Histol.* **1980,** *2* (1), 49-54.

58. Stenkvist, B.; Bengtsson, E.; Dahlqvist, B.; Eriksson, O.; Jarkrans, T.; Nordin, B. Cardiac-glycosides and breast-cancer, revisted. *New Engl. J. Med.* **1982,** *306* (8), 484-484.

59. Chen, J. Q.; Contreras, R. G.; Wang, R.; Fernandez, S. V.; Shoshani, L.; Russo, I. H.; Cereijido, M.; Russo, J. Sodium/potasium ATPase (Na+, K+-ATPase) and ouabain/related cardiac glycosides: a new paradigm for development of anti-breast cancer drugs? *Breast Cancer Res. Treat.* **2006,** *96* (1), 1-15.

60. Lin, J.; Denmeade, S.; Carducci, M. A. HIF-1 alpha and calcium signaling as targets for treatment of prostate cancer by cardiac glycosides. *Curr. Cancer Drug Targets* **2009,** *9* (7), 881-887.

61. Antczak, C.; Kloepping, C.; Radu, C.; Genski, T.; Mueller-Kuhrt, L.; Siems, K.; de Stanchina, E.; Abramson, D. H.; Djaballah, H. Revisiting old drugs as novel agents for retinoblastoma: in vitro and in vivo antitumor activity of cardenolides. *Invest. Ophthalmol. Vis. Sci.* **2009,** *50* (7), 3065-3073.

62. Gao, H.; Popescu, R.; Kopp, B.; Wang, Z. Bufadienolides and their antitumor activity. *Nat. Prod. Rep.* **2011,** *28* (5), 953-969.

63. Winnicka, K.; Bielawski, K.; Bielawska, A.; Surazynski, A. Antiproliferative activity of derivatives of ouabain, digoxin and proscillaridin a in human MCF-7 and MDA-MB-231 breast cancer cells. *Biol. Pharm. Bull.* **2008,** *31* (6), 1131-1140.

64. Hou, Y. P.; Cao, S. G.; Brodie, P.; Callmander, M.; Ratovoson, F.; Randrianaivo, R.; Rakotobe, E.; Rasamison, V. E.; Rakotonandrasana, S.; TenDyke, K.; Suh, E. M.; Kingston, D. G. I. Antiproliferative cardenolide glycosides of *Elaeodendron alluaudianum* from the Madagascar Rainforest. *Biorg. Med. Chem.* **2009,** *17* (6), 2215-2218.

65. Jensen, M.; Schmidt, S.; Fedosova, N. U.; Mollenhauer, J.; Jensen, H. H. Synthesis and evaluation of cardiac glycoside mimics as potential anticancer drugs. *Biorg. Med. Chem.* **2011,** *19* (7), 2407-2417.

66. Bloise, E.; Braca, A.; De Tommasi, N.; Belisario, M. Pro-apoptotic and cytostatic activity of naturally occurring cardenolides. *Cancer Chemother. Pharmacol.* **2009,** *64* (4), 793-802.

67. Zhao, Q.; Guo, Y. W.; Feng, B.; Li, L.; Huang, C. G.; Jiao, B. H. Neriifolin from seeds of *Cerbera manghas* L. induces cell cycle arrest and apoptosis in human hepatocellular carcinoma HepG2 cells. *Fitoterapia* **2011,** *82* (5), 735-741.

68. Rashan, L. J.; Franke, K.; Khine, M. M.; Kelter, G.; Fiebig, H. H.; Neumann, J.; Wessjohann, L. A. Characterization of the anticancer properties of monoglycosidic cardenolides isolated from *Nerium oleander* and *Streptocaulon tomentosum*. *J. Ethnopharmacol.* **2011,** *134* (3), 781-788.

69. Zhang, H. F.; Qian, D. Z.; Tan, Y. S.; Lee, K.; Gao, P.; Ren, Y. R.; Rey, S.; Hammer, H.; Chang, D.; Pili, R.; Dang, C. V.; Liu, J. O.; Semenza, G. L. Digoxin and other cardiac glycosides inhibit HIF-1 alpha synthesis and block tumor growth. *Proc. Natl. Acad. Sci. U. S. A.* **2008,** *105* (50), 19579-19586.

70. Frese, S.; Frese-Schaper, M.; Andres, A. C.; Miescher, D.; Zumkehr, B.; Schmid, R. A. Cardiac glycosides initiate Apo2L/TRAIL-induced apoptosis in non-small cell lung cancer cells by up-regulation of death receptors 4 and 5. *Cancer Res.* **2006,** *66* (11), 5867-5874.

71. Johnson, P. H.; Walker, R. P.; Jones, S. W.; Stephens, K.; Meurer, J.; Zajchowski, D. A.; Luke, M. M.; Eeckman, F.; Tan, Y. P.; Wong, L.; Parry, G.; Morgan, T. K.; McCarrick, M. A.; Monforte, J. Multiplex gene expression analysis for high-throughput drug discovery: Screening and analysis of compounds affecting genes overexpressed in cancer cells. *Mol. Cancer Ther.* **2002,** *1* (14), 1293-1304.

72. Haas, A.; Wang, H. J.; Tian, J.; Xie, Z. J. Src-mediated inter-receptor cross-talk between the Na+/K+-ATPase and the epidermal growth factor receptor relays the signal from ouabain to mitogen-activated protein kinases. *J. Biol. Chem.* **2002,** *277* (21), 18694-18702.

73. Raghavendra, P. B.; Sreenivasan, Y.; Manna, S. K. Oleandrin induces apoptosis in human, but not in murine cells: Dephosphorylation of Akt, expression of FasL, and alteration of membrane fluidity. *Mol. Immunol.* **2007,** *44* (9), 2292-2302.

74. Xie, Z. J.; Xie, J. The Na/K-ATPase-mediated signal transduction as a target for new drug development. *Front. Biosci.* **2005,** *10*, 3100-3109.

75. Aizman, O.; Aperia, A., Na,K-ATPase as a signal transducer. In *Na,K-ATPase and Related Cation Pumps - Structure, Function, and Regulatory Mechanisms*, Jorgensen, P. L.; Karlish, S. J. D.; Maunsbach, A. B., Eds. 2003; Vol. 986, pp 489-496.

76. Lopez-Lazaro, M. Digitoxin as an anticancer agent with selectivity for cancer cells: possible mechanisms involved. *Expert Opinion on Therapeutic Targets* **2007,** *11* (8), 1043-1053.

77. Bielawski, K.; Winnicka, K.; Bielawska, A. Inhibition of DNA topoisomerases I and II, and growth inhibition of breast cancer MCF-7 cells by ouabain, digoxin and proscillaridin A. *Biol. Pharm. Bull.* **2006,** *29* (7), 1493-1497.

78. Mijatovic, T.; Lefranc, F.; Van Quaquebeke, E.; Van Vynckt, F.; Darro, F.; Kiss, R. UNBS1450: A new hemi-synthetic cardenolide with promising anti-cancer activity. *Drug Dev. Res.* **2007,** *68* (4), 164-173.

79. Juncker, T.; Schumacher, M.; Dicato, M.; Diederich, M. UNBS1450 from *Calotropis procera* as a regulator of signaling pathways involved in proliferation and cell death. *Biochem. Pharmacol.* **2009,** *78* (1), 1-10.

80. Mijatovic, T.; Op de Beeck, A.; Van Quaquebeke, E.; Dewelle, J.; Darro, F.; de Launoit, Y.; Kiss, R. The cardenolide UNBS1450 is able to deactivate nuclear factor kappa B-mediated cytoprotective effects in human non-small cell lung cancer cells. *Mol. Cancer Ther.* **2006,** *5* (2), 391-399.

81. Mekhail, T.; Kaur, H.; Ganapathi, R.; Budd, G. T.; Elson, P.; Bukowski, R. M. Phase 1 trial of Anvirzel (TM) in patients with refractory solid tumors. *Invest. New Drugs* **2006,** *24* (5), 423-427.

82. Staessen, J. A.; Thijs, L.; Stolarz-Skrzypek, K.; Bacchieri, A.; Barton, J.; degli Esposito, E.; de Leeuw, P. W.; Dluzniewski, M.; Glorioso, N.; Januszewicz, A.; Manunta, P.; Milyagin, V.; Nikitin, Y.; Soucek, M.; Lanzani, C.; Citterio, L.; Timio, M.; Tykarski, A.; Ferrari, P.; Valentini, G.; Kawecka-Jaszcz, K.; Bianchi, G. Main results of the Ouabain and Adducin for Specific Intervention on Sodium in Hypertension Trial (OASIS-HT): a randomized placebo-controlled phase-2 dose-finding study of rostafuroxin. *Trials* **2011,** *12*.

83. Ferrari, P. Rostafuroxin: An ouabain-inhibitor counteracting specific forms of hypertension. *Biochimica Et Biophysica Acta-Molecular Basis of Disease* **2010,** *1802* (12), 1254-1258.

84. Platz, E. A.; Yegnasubramanian, S.; Liu, J. O.; Chong, C. R.; Shim, J. S.; Kenfield, S. A.; Stampfer, M. J.; Willett, W. C.; Giovannucci, E.; Nelson, W. G. A Novel Two-Stage, Transdisciplinary Study Identifies Digoxin as a Possible Drug for Prostate Cancer Treatment. *Cancer Discovery* **2011,** *1* (1), 68-77.

85. NIH Digoxin for Recurrent Prostate Cancer. http://clinicaltrials.gov/ct2/show/NCT01162135 (accessed 03-12-2012).

86. Fraga, C. A. M.; Barreiro, E. J. Cardiotonic drugs: history and perspectives of an old and important class of therapeutic agents. *Quim. Nova* **1996,** *19* (2), 182-189.

87. Zhou, M.; O'Doherty, G. The de novo synthesis of oligosaccharides: Application to the medicinal chemistry SAR-study of digitoxin. *Curr. Top. Med. Chem.* **2008,** *8* (2), 114-125.

88. Langenhan, J. M.; Peters, N. R.; Guzei, I. A.; Hoffmann, M.; Thorson, J. S. Enhancing the anticancer properties of cardiac glycosides by neoglycorandomization. *Proc. Natl. Acad. Sci. U. S. A.* **2005,** *102* (35), 12305-12310.

89. Langenhan, J. M.; Engle, J. M.; Slevin, L. K.; Fay, L. R.; Lucker, R. W.; Smith, K. R.; Endo, M. M. Modifying the glycosidic linkage in digitoxin analogs provides selective cytotoxins. *Bioorg. Med. Chem. Lett.* **2008,** *18* (2), 670-673.

90. Kamano, Y.; Yamashita, A.; Nogawa, T.; Morita, H.; Takeya, K.; Itokawa, H.; Segawa, T.; Yukita, A.; Saito, K.; Katsuyama, M.; Pettit, G. R. QSAR evaluation of the Ch'an Su and related bufadienolides against the colchicine-resistant primary liver carcinoma cell line PLC/PRF/51. *J. Med. Chem.* **2002,** *45* (25), 5440-5447.

91. Hagenbuch, B.; Gui, C. Xenobiotic transporters of the human organic anion transporting polypeptides (OATP) family. *Xenobiotica* **2008,** *38* (7-8), 778-801.

92. Maeda, K.; Sugiyama, Y. Impact of genetic polymorphisms of transporters on the pharmacokinetic, pharmacodynamic and toxicological properties of anionic drugs. *Drug Metab. Pharmacok.* **2008,** *23* (4), 223-235.

93. Niemi, M. Role of OATP transporters in the disposition of drugs. *Pharmacogenom.* **2007,** *8* (7), 787-802.

94. Kim, R. B. Organic anion-transporting polypeptide (OATP) transporter family and drug disposition. *Eur. J. Clin. Invest.* **2003,** *33*, 1-5.

95. Lee, W.; Belkhiri, A.; Lockhart, A. C.; Merchant, N.; Glaeser, H.; Harris, E. I.; Washington, M. K.; Brunt, E. M.; Zaika, A.; Kim, R. B.; El-Rifai, W. Overexpression of OATP1B3 confers apoptotic resistance in colon cancer. *Cancer Res.* **2008,** *68* (24), 10315-10323.

96. Wlcek, K.; Svoboda, M.; Thalhammer, T.; Sellner, F.; Krupitza, G.; Jaeger, W. Altered expression of organic anion transporter polypeptide (OATP) genes in human breast carcinoma. *Cancer Biol. Ther.* **2008,** *7* (9), 1452-1457.

97. Hagenbuch, B.; Meier, P. J. Organic anion transporting polypeptides of the OATP/SLC21 family: phylogenetic classification as OATP/SLCO superfamily, new nomenclature and molecular/functional properties. *Pflugers Arch.* **2004,** *447* (5), 653-665.

98. Gui, C.; Obaidat, A.; Chaguturu, R.; Hagenbuch, B. Development of a cell-based high-throughput assay to screen for inhibitors of organic anion transporting polypeptides 1B1 and 1B3. *Curr Chem Genomics* **2010,** *4*, 1-8.

99. Roth, M.; Timmermann, B. N.; Hagenbuch, B. Interactions of green tea catechins with organic anion-transporting polypeptides. *Drug Metab Dispos* **2011,** *39* (5), 920-6.

100. Fuchikami, H.; Satoh, H.; Tsujimoto, M.; Ohdo, S.; Ohtani, H.; Sawada, Y. Effects of herbal extracts on the function of human organic anion-transporting polypeptide OATP-B. *Drug Metab. Dispos.* **2006,** *34* (4), 577-82.

101. Bailey, D. G.; Dresser, G. K.; Leake, B. F.; Kim, R. B. Naringin is a major and selective clinical inhibitor of organic anion-transporting polypeptide 1A2 (OATP1A2) in grapefruit juice. *Clin. Pharmacol. Ther.* **2007,** *81* (4), 495-502.

102. Glaeser, H.; Bailey, D. G.; Dresser, G. K.; Gregor, J. C.; Schwarz, U. I.; McGrath, J. S.; Jolicoeur, E.; Lee, W.; Leake, B. F.; Tirona, R. G.; Kim, R. B. Intestinal drug transporter expression and the impact of grapefruit juice in humans. *Clin. Pharmacol. Ther.* **2007,** *81* (3), 362-70.

103. Dresser, G. K.; Bailey, D. G.; Leake, B. F.; Schwarz, U. I.; Dawson, P. A.; Freeman, D. J.; Kim, R. B. Fruit juices inhibit organic anion transporting polypeptide-mediated drug uptake to decrease the oral availability of fexofenadine. *Clin. Pharmacol. Ther.* **2002,** *71* (1), 11-20.

104. Greenblatt, D. J. Analysis of drug interactions involving fruit beverages and organic anion-transporting polypeptides. *J. Clin. Pharmacol.* **2009,** *49* (12), 1403-1407.

105. Wang, X.; Wolkoff, A. W.; Morris, M. E. Flavonoids as a novel class of human organic anion-transporting polypeptide OATP1B1 (OATP-C) modulators. *Drug Metab. Dispos.* **2005,** *33* (11), 1666-72.

106. Merrifield, R. B. Solid phase peptide synthesis. I. The synthesis of a tetrapeptide. *J. Am. Chem. Soc.* **1963,** *85* (14), 2149-2154.

107. Cano, M.; Balasubramanian, S. From the combinatorial chemistry boom to polymer-supported parallel chemistry: established technologies for drug discovery. *Drugs Future* **2003,** *28* (7), 659-678.

108. Alexandratos, S. D. Ion-exchange resins: a retrospective from industrial and engineering chemistry research. *Ind. Eng. Chem. Res.* **2009,** *48* (1), 388-398.

109. Solinas, A.; Taddei, M. Solid-supported reagents and catch-and-release techniques in organic synthesis. *Synthesis-Stuttgart* **2007,** *16*, 2409-2453.

110. Kennedy, J. P.; Williams, L.; Bridges, T. M.; Daniels, R. N.; Weaver, D.; Lindsley, C. W. Application of combinatorial chemistry science on modern drug discovery. *J. Comb. Chem.* **2008,** *10* (3), 345-354.

111. Applezweig, N.; Ronzone, S. E. Ion exchange process for extracting *Cinchona* alkaloids. *Ind. Eng. Chem.* **1946,** *38* (6), 576-579.

112. Applezweig, N. Cinchona alkaloids prepared by ion exchange. *J. Am. Chem. Soc.* **1944,** *66*, 1990-1990.

113. Herr, D. S. Synthetic Ion exchange resins in the separation, recovery, and concentration of thiamine. *Ind. Eng. Chem.* **1945,** *37* (7), 631-634.

114. Babaev, B.; Abdullaev, N. P.; Shakirov, T. T. Isolation of the alkaloid lidelofine from *Lindelofia anchusoides* by an ion-exchange method. *Chem. Nat. Comp.* **1976,** *12* (1), 109-110.

115. Sayed, H. M.; Desai, H. K.; Ross, S. A.; Pelletier, S. W.; Aasen, A. J. New diterpenoid alkaloids from the roots of *Aconitum septentrionale*: isolation by an Ion exchange method. *J. Nat. Prod.* **1992,** *55* (11), 1595-1606.

116. Vanrensen, I.; Veit, M. Simultaneous Determination of Phenolics and Alkaloids Using Ion Exchange Chromatography for Sample Preparation *Phytochemical Analysis* **1995,** *6* (3), 121-124.

117. Zhao, R. Y.; Yan, Y.; Li, M. X.; Yan, H. S. Selective adsorption of tea polyphenols from aqueous solution of the mixture with caffeine on macroporous crosslinked poly(N-vinyl-2-pyrrolidinone). *Reac. Funct. Pol.* **2008,** *68* (3), 768-774.

118. Tu, Y.; Jeffries, C.; Ruan, H.; Nelson, C.; Smithson, D.; Shelat, A. A.; Brown, K. M.; Li, X.-C.; Hester, J. P.; Smillie, T.; Khan, I. A.; Walker, L.; Guy, K.; Yan, B. Automated high-throughput system to fractionate plant natural products for drug discovery. *J. Nat. Prod.* **2010,** *73* (4), 751-754.

119. Thiericke, R. Drug discovery from Nature: automated high-quality sample preparation. *J. Autom. Methods Manage. Chem.* **2000,** *22* (5), 149-157.

120. Månsson, M.; Phipps, R. K.; Gram, L.; Munro, M. H. G.; Larsen, T. O.; Nielsen, K. F. Explorative solid-phase extraction (E-SPE) for accelerated microbial natural product discovery, dereplication, and purification. *J. Nat. Prod.* **2010,** *73* (6), 1126-1132.

121. Wu, S.; Yang, L.; Gao, Y.; Liu, X.; Liu, F. Multi-channel counter-current chromatography for high-throughput fractionation of natural products for drug discovery. *J. Chromatogr. A* **2008,** *1180* (1-2), 99-107.

122. Araya, J. J.; Montenegro, G.; Mitscher, L. A.; Timmermann, B. N. Application of phase-trafficking methods to natural products research. *J. Nat. Prod.* **2010,** *73* (9), 1568-1572.

123. Flynn, D. L. Phase-trafficking reagents and phase-switching strategies for parallel synthesis. *Med. Res. Rev.* **1999,** *19* (5), 408-431.

124. Houghten, R. A. General-method for the rapid solid-phase synthesis of large numbers of peptides-specificity of antigen-antibody interaction at the level of individual amino-acids. *Proc. Natl. Acad. Sci. U.S.A.* **1985,** *82* (15), 5131-5135.

125. Dowex Marathon WBA engineering information. http://www.dow.com/liquidseps/prod/dx_mar_wba.htm (accessed 03-31-2010).

126. Dowex Mac-3 engineering information. http://www.dow.com/liquidseps/prod/dx_mac3.htm (accessed 03-31-2010).

127. Cordell, G. A.; Quinn-Beattie, M. L.; Farnsworth, N. R. The potential of alkaloids in drug discovery. *Phytotherapy Research* **2001,** *15* (3), 183-205.

128. Djerassi, C.; Shamma, M.; Kutney, J. P. Alkaloid studies 32. Studies on *Skytanthus acutus* Meyen - Structure of monoterpenoid alkaloid Skytanthine. *Tetrahedron* **1962,** *18* (JAN), 183-188.

129. Crozier, A.; Jaganath, I. B.; Clifford, M. N. Dietary phenolics: chemistry, bioavailability and effects on health. *Nat. Prod. Rep.* **2009,** *26* (8), 1001-1043.

130. Mitscher, L. A.; Jung, M.; Shankel, D.; Dou, J. H.; Steele, L.; Pillai, S. P. Chemoprotection: a review of the potential therapeutic antioxidant properties of green tea (*Camellia sinensis*) and certain of its constituents. *Med. Res. Rev.* **1997,** *17* (4), 327-365.

131. Gensler, H. L.; Timmermann, B. N.; Valcic, S.; Wachter, G. A.; Dorr, R.; Dvorakova, K.; Alberts, D. S. Prevention of photocarcinogenesis by topical administration of pure epigallocatechin gallate isolated from green tea. *Nut. Cancer* **1996,** *26* (3), 325-335.

132. Valcic, S.; Timmermann, B. N.; Alberts, D. S.; Wachter, G. A.; Krutzsch, M.; Wymer, J.; Guillen, J. M. Inhibitory effect of six green tea catechins and caffeine on the growth of four selected human tumor cell lines. *Anti-Cancer Drugs* **1996,** *7* (4), 461-468.

133. Valcic, S.; Burr, J. A.; Timmermann, B. N.; Liebler, D. C. Antioxidant chemistry of green tea catechins. New oxidation products of (-)-epigallocatechin gallate and (-)-epigallocatechin from their reactions with peroxyl radicals. *Chem. Res. Toxicol.* **2000,** *13* (9), 801-810.

134. Pharn-Huy, L. A. N.; He, H.; Phamhuy, C. Green tea and health: An overview. *J. Food Agric. Env.* **2008,** *6* (1), 6-13.

135. Afzal, M.; Al-Hadidi, D.; Menon, M.; Pesek, J.; Dhami, M. S. I. Ginger: an ethomedical, chemical and pharmacological review. *Drug Metabol. Drug Interact.* **2001,** *18* (3-4), 159-191.

136. Ali, B. H.; Blunden, G.; Tanira, M. O.; Nemmar, A. Some phytochemical, pharmacological and toxicological properties of ginger (*Zingiber officinale* Roscoe): A review of recent research. *Food Chem. Toxicol.* **2008,** *46* (2), 409-420.

137. Jolad, S. D.; Lantz, R. C.; Solyom, A. M.; Chen, G. J.; Bates, R. B.; Timmermann, B. N. Fresh organically grown ginger (*Zingiber officinale*): composition and effects on LPS-induced PGE(2) production. *Phytochemistry* **2004,** *65* (13), 1937-1954.

138. Jolad, S. D.; Lantz, R. C.; Chen, G. J.; Bates, R. B.; Timmermann, B. N. Commercially processed dry ginger (*Zingiber officinale*): composition and effects on LPS-stimulated PGE(2) production. *Phytochemistry* **2005,** *66* (13), 1614-1635.

139. Funk, J. L.; Frye, J. B.; Oyarzo, J. N.; Timmermann, B. N. Comparative effects of two gingerol-containing *Zingiber officinale extracts on experimental rheumatoid arthritis*. *J. Nat. Prod.* **2009,** *72* (3), 403-407.

140. Lantz, R. C.; Sarihan, M.; Chen, G. J.; Timmermann, B. Sites of action of compounds isolated from ginger. *FASEB J.* **2004,** *18* (4), A99-A99.

141. Wang, D. C.; Xiang, H.; Li, D.; Gao, H. Y.; Cai, H.; Wu, L. J.; Deng, X. M. Purine-containing cucurbitane triterpenoids from *Cucurbita pepo* cv *dayangua*. *Phytochemistry* **2008,** *69* (6), 1434-1438.

142. Rosemeyer, H. The chemodiversity of purine as a constituent of natural products. *Chem. Biodivers.* **2004,** *1* (3), 361-401.

143. Kim, J. S.; Lee, S. I.; Park, H. W.; Yang, J. H.; Shin, T. Y.; Kim, Y. C.; Baek, N. I.; Kim, S. H.; Choi, S. U.; Kwon, B. M.; Leem, K. H.; Jung, M. Y.; Kim, D. K. Cytotoxic components from the dried rhizomes of *Zingiber officinale* Roscoe. *Arch. Pharmacal Res.* **2008,** *31* (4), 415-418.

144. Zhang, Y. G.; Tian, R. R.; Liu, S. C.; Chen, X. L.; Liu, X. Z.; Che, Y. S. Alachalasins A-G, new cytochalasins from the fungus *Stachybotrys charatum* (vol 16, pg 2627, 2008). *Biorg. Med. Chem.* **2009,** *17* (1), 428-428.

145. Yosief, T.; Rudi, A.; Kashman, Y. Asmarines A-F, novel cytotoxic compounds from the marine sponge *Raspailia* species. *J. Nat. Prod.* **2000,** *63* (3), 299-304.

146. Appenzeller, J.; Mihci, G.; Martin, M. T.; Gallard, J. F.; Menou, J. L.; Boury-Esnalllt, N.; Hooper, J.; Petek, S.; Chevalley, S.; Valentin, A.; Zaparucha, A.; Al-Mourabit, A.; Debitus, C. Agelasines J, K, and L from the solomon islands marine sponge *Agelas* cf. *mauritiana*. *J. Nat. Prod.* **2008,** *71* (8), 1451-1454.

147. Wright, A. E.; Roth, G. P.; Hoffman, J. K.; Divlianska, D. B.; Pechter, D.; Sennett, S. H.; Guzman, E. A.; Linley, P.; McCarthy, P. J.; Pitts, T. P.; Pomponi, S. A.; Reed, J. K. Isolation, synthesis, and biological activity of aphrocallistin, an adenine-substituted bromotyramine metabolite from the hexactinellida sponge *Aphrocallistes beatrix*. *J. Nat. Prod.* **2009,** *72* (6), 1178-1183.

148. Araya, J. J.; Zhang, H. P.; Prisinzano, T. E.; Mitscher, L. A.; Timmermann, B. N. Identification of unprecedented purine-containing compounds, the zingerines, from ginger rhizomes (*Zingiber officinale* Roscoe) using a phase-trafficking approach. *Phytochemistry* **2011,** *72* (9), 935-941.

149. Sang, S.; Hong, J.; Wu, H.; Liu, J.; Yang, C. S.; Pan, M.-H.; Badmaev, V.; Ho, C.-T. Increased growth inhibitory effects on human cancer cells and anti-inflammatory potency of shogaols from *Zingiber officinale* relative to gingerols. *J. Agric. Food. Chem.* **2009,** *57* (22), 10645-10650.

150. Hagenbuch, B.; Meier, P. J. The superfamily of organic anion transporting polypeptides. *Biochim. Biophys. Acta* **2003,** *1609* (1), 1-18.

151. Gui, C.; Miao, Y.; Thompson, L.; Wahlgren, B.; Mock, M.; Stieger, B.; Hagenbuch, B. Effect of pregnane X receptor ligands on transport mediated by human OATP1B1 and OATP1B3. *Eur. J. Pharmacol.* **2008,** *584* (1), 57-65.

152. Fevrier, A.; Ferreira, M. E.; Fournet, A.; Yaluff, G.; Inchausti, A.; Rojas de Arias, A.; Hocquemiller, R.; Waechter, A. I. Acetogenins and other compounds from Rollinia emarginata and their antiprotozoal activities. *Planta Med* **1999,** *65* (1), 47-9.

153. Colom, O. A.; Popich, S.; Bardon, A. Bioactive constituents from Rollinia emarginata (Annonaceae). *Nat Prod Res* **2007,** *21* (3), 254-9.

154. Roth, M.; Araya, J. J.; Timmermann, B. N.; Hagenbuch, B. Isolation of modulators of the liver-specific organic anion-transporting polypeptides (OATPs) 1B1 and 1B3 from *Rollinia emarginata* Schlecht (Annonaceae). *J. Pharmacol. Exp. Ther.* **2011,** *339* (2), 624-632.

155. Gui, C.; Miao, Y.; Thompson, L.; Wahlgren, B.; Mock, M.; Stieger, B.; Hagenbuch, B. Effect of pregnane X receptor ligands on transport mediated by human OATP1B1 and OATP1B3. *Eur J Pharmacol* **2008,** *584* (1), 57-65.

156. Gui, C.; Hagenbuch, B. Role of transmembrane domain 10 for the function of organic anion transporting polypeptide 1B1. *Protein science : a publication of the Protein Society* **2009,** *18* (11), 2298-306.

157. Seebacher, W.; Simic, N.; Weis, R.; Saf, R.; Kunert, O. Complete assignments of 1H and 13C NMR resonances of oleanolic acid, 18α-oleanolic acid, ursolic acid and their 11-oxo derivatives. *Magn. Reson. Chem.* **2003,** *41* (8), 636-638.

158. Zhang, X.; Geoffroy, P.; Miesch, M.; Julien-David, D.; Raul, F.; Aoudé-Werner, D.; Marchioni, E. Gram-scale chromatographic purification of [beta]-sitosterol: Synthesis and characterization of [beta]-sitosterol oxides. *Steroids* **2005,** *70* (13), 886-895.

159. Faini, F.; Labbe, C.; Torres, R.; Rodilla, J. M.; Silva, L.; Delle Monache, F. New phenolic esters from the resinous exudate of Haplopappus taeda. *Fitoterapia* **2007,** *78* (7-8), 611-613.

160. Muzitano, M. F.; Tinoco, L. W.; Guette, C.; Kaiser, C. R.; Rossi-Bergmann, B.; Costa, S. S. The antileishmanial activity assessment of unusual flavonoids from *Kalanchoe pinnata*. *Phytochemistry* **2006,** *67* (18), 2071-2077.

161. Aggarwal, B. B.; Shishodia, S. Molecular targets of dietary agents for prevention and therapy of cancer. *Biochem. Pharmacol.* **2006,** *71* (10), 1397-1421.

162. Liu, H. Oleanolic acid and ursolic acid: research perspectives. *J. Ethnopharmacol.* **2005,** *100* (1-2), 92-94.

163. Liu, J. Pharmacology of oleanolic acid and ursolic acid. *J. Ethnopharmacol.* **1995,** *49* (2), 57-68.

164. Khan, N.; Mukhtar, H. Tea polyphenols for health promotion. *Life Sci.* **2007,** *81* (7), 519-533.

165. Jin, X.; Zheng, R. H.; Li, Y. M. Green tea consumption and liver disease: a systematic review. *Liver International* **2008,** *28* (7), 990-996.

166. Kagaya, N.; Tagawa, Y.; Nagashima, H.; Saijo, R.; Kawase, M.; Yagi, K. Suppression of cytotoxin-induced cell death in isolated hepatocytes by tea catechins. *Eur. J. Pharmacol.* **2002,** *450* (3), 231-236.

167. Li, G.; Lin, W.; Araya, J. J.; Chen, T.; Timmermann, B. N.; Guo, G. L. A tea catechin, epigallocatechin-3-gallate, is a unique modulator of the farnesoid X receptor. *Toxicol. Appl. Pharmacol.* **2012,** *258* (2), 268-274.

168. Kadowaki, M.; Sugihara, N.; Tagashira, T.; Terao, K.; Furuno, K. Presence or absence of a gallate moiety on catechins affects their cellular transport. *J. Pharm. Pharmacol.* **2008,** *60* (9), 1189-1195.

169. Zhang, L.; Chow, M. S. S.; Zuo, Z. Effect of the co-occurring components from green tea on the intestinal absorption and disposition of green tea polyphenols in Caco-2 monolayer model. *J. Pharm. Pharmacol.* **2006,** *58* (1), 37-44.

170. Fujiwara, M.; Ando, I.; Arifuku, K. Multivariate analysis for H-1-NMR spectra of two hundred kinds of tea in the world. *Anal. Sci.* **2006,** *22* (10), 1307-1314.

171. Law, W. S.; Huang, P. Y.; Ong, E. S.; Ong, C. N.; Li, S. F. Y.; Pasikanti, K. K.; Chan, E. C. Y. Metabonomics investigation of human urine after ingestion of green tea with gas chromatography/mass spectrometry, liquid chromatography/mass spectrometry and H-1 NMR spectroscopy. *Rapid Commun. Mass Spectrom.* **2008,** *22* (16), 2436-2446.

172. Davis, A. L.; Cai, Y.; Davies, A. P.; Lewis, J. R. H-1 and C-13 NMR assignments of some green tea polyphenols. *Magn. Reson. Chem.* **1996,** *34* (11), 887-890.

173. Pierens, G. K.; Carroll, A. R.; Davis, R. A.; Palframan, M. E.; Quinn, R. J. Determination of analyte concentration using the residual solvent resonance in H-1 NMR spectroscopy. *J. Nat. Prod.* **2008,** *71* (5), 810-813.

174. Wolfender, J.-L.; Marti, G.; Queiroz, E. F. Advances in techniques for profiling crude extracts and for the rapid identification of natural products: dereplication, quality control and metabolomics. *Curr. Org. Chem.* **2010,** *14* (16), 1808-1832.

175. USDA Plants database. http://plants.usda.gov/java/ (accessed 01/25/2011).

176. Konno, K. Plant latex and other exudates as plant defense systems: roles of various defense chemicals and proteins contained therein. *Phytochemistry* **2011,** *72* (13), 1510-1530.

177. Dobler, S.; Petschenka, G.; Pankoke, H. Coping with toxic plant compounds - The insect's perspective on iridoid glycosides and cardenolides. *Phytochemistry* **2011,** *72* (13), 1593-1604.

178. Holzinger, F.; Wink, M. Mediation of cardiac glycoside insensitivity in the Monarch butterfly (Danaus plexippus): Role of an amino acid substitution in the ouabain binding site of Na+,K+-ATPase. *J. Chem. Ecol.* **1996,** *22* (10), 1921-1937.

179. Antoniou, S.; Antoniou, G.; Learney, R.; Granderath, F.; Antoniou, A. The rod and the serpent: history's ultimate healing symbol. *World J. Surg.* **2011,** *35* (1), 217-221.

180. Moerman, D. E., *Native american medicinal plants an ethnobotanical dictionary*. Timber Press, Inc: Portland, Oregon, 2009; p 799.

181. Gaertner, E. E. History and use of milkweed (Asclepias syriaca L.). *Econ. Bot.* **1979,** *33* (2), 119-123.

182. Hallbook, H.; Felth, J.; Eriksson, A.; Fryknas, M.; Bohlin, L.; Larsson, R.; Gullbo, J. Ex vivo activity of cardiac glycosides in acute leukaemia. *Plos One* **2011,** *6* (1).

183. Kindscher, K., *Edible wild plants of the prairie: an ethnobotanical guide*. University Press of Kansas: Lawrence, KS, 1987.

184. Koike, K.; Bevelle, C.; Talapatra, S. K.; Cordell, G. A.; Farnsworth, N. R. Potential anti-cancer agents .5. Cardiac glycosides of *Asclepias albicans* (Asclepiadaceae) *Chem. Pharm. Bull. (Tokyo)* **1980,** *28* (2), 401-405.

185. Piatak, D. M.; Patel, J.; Totten, C. E.; Swenson, R. P.; Brown, P.; Pettit, G. R. Cell-growth inhibitory glycosides from *Asclepias amplexicaulis*. *J. Nat. Prod.* **1985,** *48* (3), 470-471.

186. Ahsan, A. M.; Piatak, D. M.; Sorensen, P. D. Isolation and structure of amplexoside a - new glycoside from *Asclepias amplexicaulis*. *Experientia* **1973,** *29* (7), 788-789.

187. Martin, R. A.; Lynch, S. P.; Schmitz, F. J.; Pordesimo, E. O.; Toth, S.; Horton, R. Y. Cardenolides from *Asclepias asperula* subsp *capricornu* and *A. viridis*. *Phytochemistry* **1991,** *30* (12), 3935-3939.

188. Bartlett, W. R.; Benally, L. H.; Larson, T. R.; Goodtracks, J. B. H.; Bancroft, K. J. cardenolide isolation and characterization from *Asclepias asperula*. *Abs. Papers Am. Chem. Soc.* **1995,** *209*, 245-CHED.

189. Li, J. Z.; Liu, H. Y.; Lin, Y. J.; Hao, X. J.; Ni, W.; Chen, C. X. Six new C-21 steroidal glycosides from *Asclepias curassavica* L. *Steroids* **2008,** *73* (6), 594-600.

190. Li, J. Z.; Qing, C.; Chen, C. X.; Hao, X. J.; Liu, H. Y. Cytotoxicity of cardenolides and cardenolide glycosides from Asclepias curassavica. *Bioorg. Med. Chem. Lett.* **2009,** *19* (7), 1956-1959.

191. Abe, F.; Mori, Y.; Yamauchi, T. 3'-epi-19-Norafroside and 12-beta-hydroxycoroglaucigenin from *Asclepias curassavica*. *Chem. Pharm. Bull. (Tokyo)* **1991,** *39* (10), 2709-2711.

192. Abe, F.; Mori, Y.; Yamauchi, T. Cardenolide glycosides from the seeds of *Asclepias curassavica*. *Chem. Pharm. Bull. (Tokyo)* **1992,** *40* (11), 2917-2920.

193. Cheung, H. T. A.; Watson, T. R.; Seiber, J. N.; Nelson, C. 7-beta,8-beta-Epoxycardenolide glycosides of *Asclepias-eriocarpa*. *J. Chem. Soc., Perkin Trans. 1* **1980,** (10), 2169-2173.

194. Seiber, J. N.; Roeske, C. N.; Benson, J. M. 3 New cardenolides from the milkweeds *Asclepias-eriocarpa* and *Asclepias-labriformis*. *Phytochemistry* **1978,** *17* (5), 967-970.

195. Warashina, T.; Noro, T. Steroidal glycosides and cardenolides from *Asclepias-fruticosa*. *Phytochemistry* **1994,** *37* (1), 217-226.

196. Warashina, T.; Noro, T. Cardenolide glycosides from *Asclepias-fruticosa Phytochemistry* **1994,** *37* (3), 801-806.

197. Abe, F.; Mori, Y.; Okabe, H.; Yamauchi, T. Steroidal constituents from the roots and stems of *Asclepias-fruticosa*. *Chem. Pharm. Bull. (Tokyo)* **1994,** *42* (9), 1777-1783.

198. Abe, F.; Yamauchi, T. 5,11-Epoxymegastigmanes from the leaves of *Asclepias fruticosa*. *Chem. Pharm. Bull. (Tokyo)* **2000,** *48* (12), 1908-1911.

199. Fonseca, G.; Rodriguezhahn, L.; Tablero, M.; Rodriguez, A.; Arreguin, B. Labriformin, a cardiac glucoside from *Asclepias-glaucescens*. *J. Nat. Prod.* **1991,** *54* (3), 860-862.

200. Nishio, S.; Blum, M. S.; Silverton, J. V.; Highet, R. J. Structure of Humistratin - a Novel Cardenolide from the Sandhill Milkweed *Asclepias-humistrata J. Org. Chem.* **1982,** *47* (11), 2154-2157.

201. Warashina, T.; Noro, T. Cardenolide and oxypregnane glycosides from the root of *Asclepias incarnata* L. *Chem. Pharm. Bull. (Tokyo)* **2000,** *48* (4), 516-524.

202. Warashina, T.; Noro, T. Steroidal glycosides from the aerial part of *Asclepias incarnata*. *Phytochemistry* **2000,** *53* (4), 485-498.

203. Rodriguez, L.; Fonseca, G. The cardenolide conetent of *Asclepias-linaria Phytochemistry* **1991,** *30* (12), 3941-3942.

204. Warashina, T.; Noro, T. Acylated-oxypregnane glycosides from the roots of *Asclepias syriaca*. *Chem. Pharm. Bull. (Tokyo)* **2009,** *57* (2), 177-184.

205. Warashina, T.; Noro, T. Cardenolides from Asclepias syriaca L. *Natural Medicines* **2003,** *57* (5), 185-188.

206. Sikorska, M. M., I. Quercetin and its glycosides in the flowers of *Asclepias syriaca* L. *Acta Pol. Pharm.* **2000,** *57* (4), 321-324.

207. Brown, P.; Voneuw, J.; Reichstein, T.; Stockel, K.; Watson, T. R. Cardenolides of *Asclepias-syriaca*-L, probable structure of syrioside and syriobioside glycosides and aglycones.334. *Helv. Chim. Acta* **1979,** *62* (2), 412-441.

208. Gonnet, J. F.; Kozjek, F.; Favrebon.J Flavonols in *Asclepias syriaca*. *Phytochemistry* **1973,** *12* (11), 2773-2775.

209. Mitsuhas.H; Hayashi, K.; Tomimoto, K. Studies on constituents of Asclepiadaceae Plants .28. Components of *Asclepias-syriaca Chem. Pharm. Bull. (Tokyo)* **1970,** *18* (4), 828-&.

210. Jolad, S. D.; Bates, R. B.; Cole, J. R.; Hoffmann, J. J.; Siahaan, T. J.; Timmermann, B. N. Cardenolides and lignan from *Asclepias-subulata*. *Phytochemistry* **1986,** *25* (11), 2581-2590.

211. Warashina, T.; Noro, T. 8,12;8,20-Diepoxy-8,14-secopregnane glycosides from the aerial parts of *Asclepias tuberosa*. *Chem. Pharm. Bull. (Tokyo)* **2010,** *58* (2), 172-179.

212. Warashina, T.; Noro, T. 8,14-Secopregnane glycosides from the aerial parts of Asclepias tuberosa. *Phytochemistry* **2009,** *70* (10), 1294-1304.

213. Abe, F.; Yamauchi, T. Pregnane glycosides from the roots of *Asclepias tuberosa*. *Chem. Pharm. Bull. (Tokyo)* **2000,** *48* (7), 1017-1022.

214. Abe, F.; Yamauchi, T. An androstane bioside and 3'-thiazolidinone derivatives of doubly-linked cardenolide glycosides from the roots of *Asclepias tuberosa*. *Chem. Pharm. Bull. (Tokyo)* **2000,** *48* (7), 991-993.

215. Cheung, H. T. A.; Nelson, C. J.; Watson, T. R. New cardenolide glycosides with doubly linked sugars from *Asclepias-vestita Journal of Chemical Research-S* **1989,** (1), 6-7.

216. Cheung, H. T. A.; Nelson, C. J. Cardenolide glycosides with 5,6-unsaturation from *Asclepias-vestita J. Chem. Soc. [Perkin. 1]*. **1989,** (9), 1563-1570.

217. Hackett, A. J.; Smith, H. S.; Springer, E. L.; Owens, R. B.; Nelsonrees, W. A.; Riggs, J. L.; Gardner, M. B. Two syngeneic cell lines from human breast tissue: aneuploid epithelial (HS578T) and diploid myoepithelial (HS578BST) cell lines. *J. Natl. Cancer Inst.* **1977,** *58* (6), 1795-1806.

218. Araya, J. J.; Kindscher, K.; Timmermann, B. N. Verticillosides A-M: polyoxygenated pregnane glycosides from *Asclepias verticillata* L. *Phytochemistry* **2012,** *Published on-line doi:10.1016/j.phytochem.2012.02.019*.

219. Ye, Y. P.; Li, X. Y.; Sun, H. X.; Chen, F. Y.; Pan, Y. J. Immunomodulating steroidal glycosides from the roots of Stephanotis mucronata. *Helv. Chim. Acta* **2004,** *87* (9), 2378-2384.

220. Gan, H.; Xiang, W. J.; Ma, L.; Hu, L. H. Six new C-21 steroidal glycosides from *Cynanchum bungei* Decne. *Helv. Chim. Acta* **2008,** *91* (12), 2222-2234.

221. Campbell, T. A. Chemical and agronomic evlauation of common milkweed, *Asclepias syriaca*. *Econ. Bot.* **1983,** *37* (2), 174-180.

222. Harry-O'kuru, R. E.; Holser, R. A.; Abbott, T. P.; Weisleder, D. Synthesis and characteristics of polyhydroxy triglycerides from milkweed oil. *Ind. Crops Prod.* **2002,** *15* (1), 51-58.

223. Schlegel, V.; Zbasnik, R.; Gries, T.; Lee, B. H.; Carr, T.; Lee, J. Y.; Weller, C.; Cuppett, S. Characterisation of potential health promoting lipids in the co-products of de-flossed milkweed. *Food Chem.* **2011,** *126* (1), 15-20.

224. Haribal, M.; Renwick, J. A. A. Oviposition stimulants for the monarch butterfly: Flavonol glycosides from *Asclepias curassavica*. *Phytochemistry* **1996,** *41* (1), 139-144.

225. Haribal, M.; Renwick, J. A. A. Identification and distribution of oviposition stimulants for monarch butterflies in hosts and nonhosts. *J. Chem. Ecol.* **1998,** *24* (5), 891-904.

226. Gluchoff-Fiasson, K.; Fiasson, J. L.; Favrebonvin, J. Quercitin glycosides from antartic *Rununculus* species. *Phytochemistry* **1994,** *37* (6), 1629-1633.

227. Matlawska, I. Flavonoid compunds in the flowers of *Kitaibelia vitifolia* Willd. (Malvacae). *Acta Pol. Pharm.* **2001,** *58* (2), 127-131.

228. Kamiya, K.; Tanaka, Y.; Endang, H.; Umar, M.; Satake, T. Chemical constituents of *Morinda citrifolia* fruits inhibit copper-induced low-density lipoprotein oxidation. *J. Agric. Food. Chem.* **2004,** *52* (19), 5843-5848.

229. Takara, K.; Matsui, D.; Wada, K.; Ichiba, T.; Nakasone, Y. New antioxidative phenolic glycosides isolated from Kokuto non-centrifuged cane sugar. *Biosci., Biotechnol., Biochem.* **2002,** *66* (1), 29-35.

230. Liang, S.; Shen, Y.-H.; Tian, J.-M.; Wu, Z.-J.; Jin, H.-Z.; Zhang, W.-D.; Yan, S.-K. Phenylpropanoids from *Daphne feddei* and their inhibitory activities against NO production. *J. Nat. Prod.* **2008,** *71* (11), 1902-1905.

231. Nacef, S.; Ben Jannet, H.; Abreu, P.; Mighri, Z. Phenolic constituents of Convolvulus dorycnium L. flowers. *Phytochem. Lett.* **2010,** *3* (2), 66-69.

232. Ueda, J. Y.; Tezuka, Y.; Banskota, A. H.; Le Tran, Q.; Tran, Q. K.; Sam, I.; Kadota, S. Antiproliferative activity of cardenolides isolated from *Streptocaulon juventas*. *Biol. Pharm. Bull.* **2003,** *26* (10), 1431-1435.

233. Fu, G.; Pang, H.; Wong, Y. H. Naturally occurring phenylethanoid glycosides: potential leads for new therapeutics. *Curr. Med. Chem.* **2008,** *15* (25), 2592-2613.

234. Takeda, Y.; Zhang, H. J.; Masuda, T.; Honda, G.; Otsuka, H.; Sezik, E.; Yesilada, E.; Sun, H. D. Megastigmane glucosides from *Stachys byzantina*. *Phytochemistry* **1997,** *44* (7), 1335-1337.

235. Masuoka, C.; Ono, M.; Ito, Y.; Okawa, M.; Nohara, T. New megastigmane glycoside and aromadendrane derivative from the aerial part of *Piper elongatum*. *Chem. Pharm. Bull. (Tokyo)* **2002,** *50* (10), 1413-1415.

236. Abe, F.; Yamauchi, T.; Honda, K.; Hayashi, N. Conduritol F glucosides and terpenoid glucosides from *Cynanchum liukiuense* and distribution of conduritol F glucosides in several asclepiadaceous plants. *Chem. Pharm. Bull. (Tokyo)* **2000,** *48* (7), 1090-1092.

237. Yasukawa, K. In *Pentacyclic triterpenes as promising agents in cancer*, Nova Science Publishers, Inc.: 2010; pp 127-157.

238. Bai, L.; Wang, L.; Fu, L.; Zhao, M.; Zhang, S.; Kakuta, S.; Sakai, J.-c.; Tang, W.; Bai, Y.; Hasegawa, T.; Ogura, H.; Kataoka, T.; Hirose, K.; Oura, T.; Kasuga, T.; Yasuda, T.; Ando, M. In *Pentacyclic triterpenes as promising agents in cancer*, Nova Science Publishers, Inc.: 2010; pp 89-126.

239. Perazzo, F. F.; Carvalho, J. C. T.; Rodrigues, M.; Morais, E. K. L.; Maciel, M. A. M. Comparative anti-inflammatory and antinociceptive effects of terpenoids and an aqueous extract obtained from *Croton cajucara* Benth. *Rev. Bras. Farmacogn.* **2007,** *17*, 521-528.

240. Pinto, S. A. H.; Pinto, L. M. S.; Guedes, M. A.; Cunha, G. M. A.; Chaves, M. H.; Santos, F. A.; Rao, V. S. Antinoceptive effect of triterpenoid α,β-amyrin in rats on orofacial pain induced by formalin and capsaicin. *Phytomedicine* **2008,** *15*, 630-634.

241. Johansson, S.; Lindholm, P.; Gullbo, J.; Larsson, P.; Bohlin, L.; Claeson, P. Cytotoxicity of digitoxin and related cardiac glycosides in human tumor cells. *Anti-Cancer Drugs* **2001,** *12* (5), 475-483.

242. López-Lázaro, M.; Pastor, N.; Azrak, S. S.; Ayuso, M. J.; Austin, C. A.; Cortés, F. Digitoxin inhibits the growth of cancer cell lines at concentrations commonly found in cardiac patients. *J. Nat. Prod.* **2005,** *68* (11), 1642-1645.

243. Kunert, O.; Rao, V. G.; Babu, G. S.; Sujatha, P.; Sivagamy, M.; Anuradha, S.; Rao, B. V. A.; Kumar, B. R.; Alex, R. M.; Schuhly, W.; Kuhnelt, D.; Rao, G. V.; Rao, A. Pregnane glycosides from *Caralluma adscendens* var. *fimbriata*. *Chem. Biodivers.* **2008,** *5* (2), 239-250.

244. Kunert, O.; Rao, B. V. A.; Babu, G. S.; Padmavathi, M.; Kumar, B. R.; Alex, R. M.; Schuhly, W.; Simic, N.; Kuhnelt, D.; Rao, A. Novel steroidal glycosides from two Indian *Caralluma* species, *C-stalagmifera* and *C-indica*. *Helv. Chim. Acta* **2006,** *89* (2), 201-209.

245. Tsukamoto, S.; Hayashi, K.; Kaneko, K.; Mitsuhashi, H. Studies on the constituents of Asclepiadaceae plants. 65. The optical resolution of D-cymaroses and L-cymaroses. *Chem. Pharm. Bull. (Tokyo)* **1986,** *34* (8), 3130-3134.

246. Nakagawa, T.; Hayashi, K.; Wada, K.; Mitsuhashi, H. Studies on the constituents of asclepiadaceae plants. 52. The structures of 5 glycosides glaucoside-a, glaucoside-b, glaucoside-c, glaucoside-d, and glaucoside e from the Chinese drug Pai-Chien *Cynanchum glaucescens* Hand-Mazz. *Tetrahedron* **1983,** *39* (4), 607-612.

247. Allgeier, H. Structure of pachybiose and asclepobiose. dexoy sugars. 44. *Helv. Chim. Acta* **1968,** *51* (2), 311-&.

248. Jacobs, W. A.; Craig, L. C. The veratrine alkaloids - XXII. On pseudojervine and veratrosine, a companion glycoside in veratrum viride. *J. Biol. Chem.* **1944,** *155* (2), 565-572.

249. Olafsdottir, E. S.; Jaroszewski, J. W.; Seigler, D. S. Natural cyclopentaoid cyanohydrin glycosides. 12. Cyanohydrin glycosides with unusual sugar residues - revised structure of passitrifasciatin. *Phytochemistry* **1991,** *30* (3), 867-869.

250. Perkin, W. H. The magnetic rotation of some polyhydric alcohols, hexoses, and saccharobioses. *J. Chem. Soc.* **1902,** *81*, 177-191.

251. Hudson, C. S.; Johnson, J. M. The isomeric tetracetates of xylose, and observations regarding the acetates of melibiose, trehalose and sucrose. *J. Am. Chem. Soc.* **1915,** *37*, 2748-2753.

252. Nadin, A.; Hattotuwagama, C.; Churcher, I. Lead-oriented synthesis: a new opportunity for synthetic chemistry. *Angew. Chem. Int. Ed.* **2012,** *51* (5), 1114-1122.

253. Hong, J. Y. Role of natural product diversity in chemical biology. *Curr. Opin. Chem. Biol.* **2011,** *15* (3), 350-354.

254. Thomas, G. L.; Johannes, C. W. Natural product-like synthetic libraries. *Curr. Opin. Chem. Biol.* **2011,** *15* (4), 516-522.

255. Galloway, W.; Isidro-Llobet, A.; Spring, D. R. Diversity-oriented synthesis as a tool for the discovery of novel biologically active small molecules. *Nat. Comm.* **2010,** *1*.

256. Dandapani, S.; Marcaurelle, L. A. Current strategies for diversity-oriented synthesis. *Curr. Opin. Chem. Biol.* **2010,** *14* (3), 362-370.

257. Nising, C. F.; Brase, S. Highlights in steroid chemistry: total synthesis versus semisynthesis. *Angew. Chem. Int. Ed.* **2008,** *47* (49), 9389-9391.

258. Danieli, N.; Sondheimer, F.; Mazur, Y. Total synthesis of digitoxigenin. *Bulletin of the Research Council of Israel* **1962,** *A 11* (1), 37-&.

259. Honma, M.; Nakada, M. Enantioselective total synthesis of (+)-digitoxigenin. *Tetrahedron Lett.* **2007,** *48* (9), 1541-1544.

260. Stork, G.; West, F.; Lee, H. Y.; Isaacs, R. C. A.; Manabe, S. The total synthesis of a natural cardenolide: (+)-digitoxigenin. *J. Am. Chem. Soc.* **1996,** *118* (43), 10660-10661.

261. Reddy, M. S.; Zhang, H. X.; Phoenix, S.; Deslongchamps, P. Total synthesis of ouabagenin and ouabain. *Chem. Asian J.* **2009,** *4* (5), 725-741.

262. Templeton, J. F.; Setiloane, P.; Kumar, V. P. S.; Yan, Y. L.; Zeglam, T. H.; Labella, F. S. Pregnanes that bind to the digitalis receptor - synthesis of 14-hydroxy-5-beta,14-beta-pregnane glycosides from digitoxin and digitoxigenin. *J. Med. Chem.* **1991,** *34* (9), 2778-2782.

263. Donovan, S. F.; Avery, M. A.; McMurry, J. E. Synthesis of digitoxigenin by remote functionalization. *Tetrahedron Lett.* **1979,** (35), 3287-3290.

264. Groszek, G.; Kurektyrlik, A.; Wicha, J. Syntheis of a cardenolide, 3-O-mehtyl uzarigenin, with 14-beta-hydroxyanrost-16-ene as key intermidate. *Tetrahedron* **1989,** *45* (7), 2223-2236.

265. Bovicelli, P.; Lupattelli, P.; Fiorini, V.; Mincione, E. Oxyfunctionalization of steroids by dioxiranes - site and steroselective C-14 and C-17 hydroxylation of pregnane and androstane steroids. *Tetrahedron Lett.* **1993,** *34* (38), 6103-6104.

266. Liu, Z.; Meinwald, J. 5-(Trimethylstannyl)-2H-pyran-2-one and 3-(Trimethylstannyl)-2H-pyran-2-one: New 2H-Pyran-2-one Synthons. *J. Org. Chem.* **1996,** *61* (19), 6693-6699.

267. Fell, J. D.; Heathcock, C. H. Oxidative Fragmentation Of Pregna-14,16-dien-20-ones to 14β-hydroxyandrost-15-en-17-ones. *J. Org. Chem.* **2002,** *67* (14), 4742-4746.

268. Zhou, M. Q.; O'Doherty, G. A. De novo approach to 2-deoxy-beta-glycosides: Asymmetric syntheses of digoxose and digitoxin. *J. Org. Chem.* **2007,** *72* (7), 2485-2493.

269. Melero, C. P.; Medarde, M.; San Feliciano, A. A short review on cardiotonic steroids and their aminoguanidine analogues. *Molecules* **2000,** *5* (1), 51-81.

270. Ohe, T.; Miyaura, N.; Suzuki, A. Palladium-catalyzed cross-coupling of organoboron compounds with organic triflates. *J. Org. Chem.* **1993,** *58* (8), 2201-2208.

271. Hilton, P. J.; McKinnon, W.; Gravett, E. C.; Peron, J. M. R.; Frampton, C. M.; Nicholls, M. G.; Lord, G. Selective inhibition of the cellular sodium pump by emicymarin and 14 beta anhydroxy bufadienolides. *Steroids* **2010,** *75* (13-14), 1137-1145.

272. Kabat, M. M.; Kurek, A.; Masnyk, M.; Repke, K. R. H.; Schonfeld, W.; Weiland, J.; Wicha, J. Synthesis of 3-beta-rhamnosyloxy-5-beta, 14-beta-androstan-14-ol and its 17-acetoxy and 17-hydroxy derivates. *J. Chem. Res., Synop* . **1987,** (7), 218-219.

273. Kurti, L.; Czako, B., *Strategic applications of named reactions in organic synthesis*. 1st ed.; Academic Press: San Diego, CA, 2005.

274. Stephenson, L. M.; Speth, D. R. Mechanism of allylic hydroxylation by selenium dioxide. *J. Org. Chem.* **1979,** *44* (25), 4683-4689.

275. Caddick, S.; Fitzmaurice, R. Microwave enhanced synthesis. *Tetrahedron* **2009,** *65* (17), 3325-3355.

276. Santagada, V.; Frecentese, F.; Perissutti, E.; Fiorino, F.; Severino, B.; Caliendo, G. Microwave assisted synthesis: a new technology in drug discovery. *Mini-Rev. Med. Chem.* **2009,** *9* (3), 340-358.

277. Zou, Y.; Chen, C.-H.; Taylor, C. D.; Foxman, B. M.; Snider, B. B. Formal synthesis of (±)-platensimycin. *Org. Lett.* **2007,** *9* (9), 1825-1828.